Faculty of Engineering & Science

Department of Chemical & Energy Engineering

Hydrophobic Modified Honeycomb-like Tubular Biochar with Enhanced Adsorption Capability of Volatile Organic Compounds: Characterization and Kinetic Study

Fanthagiro Rossi Stuard Anak Majing

0000-0002-3583-8618

This thesis is presented for the Degree of

Master of Philosophy (Chemical Engineering)

of Curtin University

June 2023

DECLARATION

To the best of my knowledge and belief this thesis contains no material previously published by any other person except where due acknowledgement has been made.

This thesis contains no material which has been accepted for the award of any other degree or diploma in any university.

Name : Fanthagiro Rossi Stuard Anak Majing

Signature

Date : 19th June 2023

ACKNOWLEDGEMENT

It is a genuine pleasure to express my deep sense of thanks and gratitude to my principal supervisor, Prof. Stephanie Chan Yen San. Her dedication and keen interest, above all her overwhelming attitude to help me had been solely and mainly responsible for completing my work. Her timely advice, meticulous scrutiny, scholarly advice, and scientific approach have helped me to a very great extent to accomplish this task.

Besides my principal supervisor, I would like to thank my supervisory team: Dr. Tan Yie Hua, Dr. Tan Inn Shi, and Dr. Mohd Dinie, for their encouragement, insightful feedback, and valuable advice.

I owe a deep sense of gratitude to the Graduate School and Faculty of Engineering and Science, for providing facilities and support throughout the project.

I am extremely thankful to my peers and family for their mental support, guidance, motivation, and inspirations that make me stay positive, productive, and work harder on this project.

LIST OF PUBLICATION ARISING FROM THE FINAL REPORT

Conference publication

Majing, Fanthagiro Rossi Stuart, Yen San Chan, Inn Shi Tan, Yie Hua Tan, and Mohd Dinie Muhaimin Samsudin. 2023. "Characterization of Valorized Pinewood Sawdust to Engineered Activated Biochar Check for updates." Emerging Technologies for Future Sustainability: Proceedings of the 2nd International Conference on Biomass Utilization and Sustainable Energy; ICoBiomasSE 2022; 20–21 Sept., Malaysia.

Book Chapter

Majing, Fanthagiro Rossi Stuart, Yen San Chan, Inn Shi Tan, Yie Hua Tan, and Mohd Dinie Muhaimin Samsudin. 2023. "Characterization of Valorized Pinewood Sawdust to Engineered Activated Biochar Check for updates." Emerging Technologies for Future Sustainability: Proceedings of the 2nd International Conference on Biomass Utilization and Sustainable Energy; ICoBiomasSE 2022; 20–21 Sept., Malaysia.

Abstract

Volatile organic compounds (VOCs) pose significant environmental and human health risks as they are emitted from various industrial activities such as fossil fuel combustion, chemical and petrochemical manufacturing, and agriculture. Acetone, being one of the significant contributors to VOC emissions, underscores the importance of employing advanced technologies and best practices in industrial processes to minimize its release. Adsorption is a highly effective technique for VOCs emission control due to its simplicity, cost-efficiency, and flexibility. Biochar, known for its high porosity, low-cost, and excellent adsorption capacity, has emerged as a promising adsorbent for environmental remediation. However, pristine biochar exhibits poor surface properties, resulting in limited VOCs adsorption capacity. Furthermore, the presence of water molecules poses a major challenge in achieving efficient biochar adsorption performance under humid conditions, particularly in the separation and purification sector. Therefore, this study aims to develop an effective hydrophobic modified honeycomb-like tubular biochar (HT-B) that exhibits high VOC (acetone) adsorption capacity under humid conditions. In this research, honeycomb-like tubular biochars (HT-Bs) were synthesized by impregnating palm leaves (PL), pinewood sawdust (PWS), and corn stalks (CS) with different concentrations of zinc chloride ($ZnCl_2$) (0.5 M, 1.0 M, and 1.5 M), followed by a hydrophobic coating of polydimethylsiloxane (PDMS). Various characterization techniques and acetone adsorption experiments were conducted at relative humidities (RH) of 50%, 70%, and 90% to determine the physical and chemical properties, and adsorption performance of HT-Bs, as well as the mechanisms involved in the process. The optimization study for impregnation and hydrophobic coating conditions was conducted using one-factor-at-a-time (OFAT) method. Among the synthesized HT-Bs, CS/HT-B impregnated at 1.0 M (CS/HT-B_{1M}) exhibited the highest specific surface areas of 1825.3 m^2 g^{-1} and exhibited a stable honeycomb-like tubular structure with evenly distributed fenestrations on the cellular surface. This indicated that an impregnation concentration of 1.0 M was optimal. The best conditions for coating CS/HT-B_{1M} with PDMS (CS/HT-B_{1M}PDMS) were determined at a mass ratio of 1:25 (CS/HT-B_{1M}: PDMS), a modification temperature at 200°C, and a duration of 1 h. These conditions increased the water contact angle from 0° to 132.8°, indicating enhanced hydrophobicity. When the RH increased from 50% to 90%, the adsorption capacity of CS/HT-B_{1M} significantly decreased by 49.8%, while CS/HT-B_{1M}PDMS decreased only by 28.7%. This indicated that the hydrophobic PDMS coating successfully enhanced the adsorption of acetone by

decreasing the competition between water molecules and acetone. The adsorption efficiency of regenerated CS/HT-B_{1M}PDMS decreased upon the thermal regeneration, however CS/HT-B_{1M}PDMS was still able to perform well compared to CS/HT-B_{1M} at 90% RH. The adsorption kinetics, including isotherm, rate-controlling step, and breakthrough models were utilized to predict the adsorption mechanisms, mass transfer, and breakthrough characteristics of acetone removal. The acetone adsorption onto CS/HT-B_{1M} and CS/HT-B_{1M}PDMS fitted well to Sips model, indicating that the adsorption can be described by a combination of Langmuir and Freundlich models. The rate-controlling steps were intraparticle diffusion, while surface diffusion occurred rapidly. Moreover, the experimental data exhibited good fit to the nonlinear Bohart-Adams (B-A), Thomas, and Yoon-Nelson (Y-N) models. These models exhibited excellent fit to the experimental data, with correlation coefficients (R^2) ranging from 0.997 to 0.999.

Keywords: adsorption, honeycomb-like tubular biochar, humidity, hydrophobic coating, volatile organic compounds

Table of contents

List of Table

List of Figure

ACRONYMS

AC	: Activated carbon
ACF	: Activated carbon fiber
B-A	: Bohart-Adam model
BC	: Biochar
BET	: Brunauer-Emmett-Teller
CNTs	: Carbon nanotubes
CS	: Corn stalks
DSA	: Drop Shape Analyzer
EDS	: Energy Dispersive X-ray Spectroscopy
FTIR	: Fourier-transform infrared spectroscopy
Gr	: Graphene
GC-FID	: Gas Chromatography-Flame Ionization Detector
HT-B	: Honeycomb-like tubular biochar
IPD	: Intraparticle diffusion model
MOFs	: Metal Organic Frameworks
MWCNT	: Multi-walled carbon nanotube
NAAQS	: National Ambient Air Quality Standards
PDMS	: Polydimethylsiloxane
PL	: Palm leaves
PWS	: Pinewood sawdust
rGO	: Reduced graphene oxide
RH	: Relative humidity
SEM	: Scanning electron micrograph
VOC	: Volatile organic compound
XRD	: X-ray diffraction
Y-N	: Yoon-Nelson model

NOMENCLATURE

b	: Adsorption rate
C_e	: Equilibrium concentration of the adsorbate (mg/l)
C	: Constant defined (g/kg)
C_0	: Inlet concentration of the adsorbate (mol L^{-1})
C_t	: Outlet concentration of the adsorbate (mol L^{-1})
K_f	: Adsorption capacity of the adsorbent
$k^{'}$	: Rate constant (min^{-1})
k_p	: Intraparticle diffusion rate constant
P_{ads}	: Probability of adsorption of an adsorbate
q_e	: Equilibrium adsorption capacity
q_{max}	: Adsorption capacity
q_t	: Amount of adsorption at time $t = t$ (g/kg)
q_{ref}	: Adsorption amount at time $t = t_{ref}$ (g/kg)
t	: Time of adsorption (min)
1/n	: Freundlich exponent
π	: Time required for adsorbate breakthrough to reached 50%

CHAPTER 1

INTRODUCTION

1.1 Background

Volatile organic compounds (VOCs) are one of the precursors to the formation of tropospheric ozone (O_3) and secondary organic aerosols (SOA). Their toxic and photochemically sensitive properties pose a significant threat to human health and the environment (Yafei Liu et al. 2020). Common VOCs have an effect on human health, including irritation of the eyes, nose, and skin, nausea, coughing, chest tightness, and even cancer (Ancione et al. 2021; Megías-Sayago et al. 2020; Yuxiu Zhang et al. 2019). As for the environment, VOCs are highly reactive, which enables them to easily react with a variety of compounds in the atmosphere, resulting in photochemical smog, particulate matter, and ozone (Lv et al. 2020; Lomonaco et al. 2020). The primary sources of VOCs emission include industrial activities, such as petroleum refinery, coal-fired power plant, pharmaceutical manufacturing, waste treatment plant, and vehicle exhaust (J. Sun et al. 2019; J. Sun et al. 2019; Z. Liang et al. 2020). Furthermore, in Malaysia, researchers have identified 22 types VOCs, including 14 aldehydes, 5 aromatic hydrocarbons, acetone, trichloroethylene, and tetrachloroethylene from indoor activities such as cooking, material painting and coating, and the used of cleaning and product consumers (Saraga et al. 2023; Y. Huang et al. 2019; Heeley-Hill et al. 2021). Studies indicate that formaldehyde, acetaldehyde, and acetone exhibit the highest concentrations ranged from 99.3±10.7 to 6.8±2.19 μg m^{-3}, from 23.7±13.5 to 5.35±4.57 μg m^{-3}, and from 11±5.95 to 133 μg m^{-3}, respectively. Additionally, indoor concentrations of benzene, toluene, and xylene (BTX) collectively reached 235 μg m^{-3} (Saraga et al. 2023). Notably, acetone and BTX stand out with the highest indoor VOC concentrations, posing a significant risk of contributing to secondary air pollution (Saraga et al. 2023; Vardoulakis et al. 2020). Therefore, it is imperative to implement VOC emission control techniques across various industries. As of now, there is a notable gap in research addressing the adsorption of acetone onto modified biochar under humid conditions.

Various VOCs abatement techniques have been developed to capture or remove the desired VOCs under different process conditions. Among them, adsorption is one of the most economical options and has proven to be an efficient technology due to its wide range of flexibility and facile operation conditions (Vikrant et al. 2020). Besides, desorption process enables VOCs to be recovered and recycled for further applications (Krishnamurthy et al. 2020; Mujan et al. 2019). Recently, adsorption techniques by using highly specific surface area adsorbents are attractive in the removal of VOCs due to their excellent adsorption capability. Porous materials including carbon-based materials, organic polymers, and oxygen-containing materials are commonly used adsorbents to enhance the adsorption of VOCs at low concentration level (<1000 ppm) (Lingli Zhu et al. 2020; Ruofei Chen et al. 2020). Biochar has shown great potential as an adsorbent in environmental remediations due to its high specific surface area, adjustable pore structure, and high adsorption capability (Rajabi et al. 2021; Ziheng Wang et al. 2020). However, due to the nature properties of biomass, biochar synthesized from biomass wastes is mostly hydrophilic. Water vapor is unavoidable in the removal of VOCs due to its high vapor pressure at room temperature (H.-B. Liu et al. 2016; K.-D. Kim et al. 2012). In this case, VOCs and water molecules compete for the adsorption sites on biochar, leading to poor adsorption efficiency for the desired pollutant, which has been reported as low as 50% and remains unresolved (L. Jia et al. 2020). This has become one of the major challenges in VOCs adsorption technology.

In light of the limitations, multiple modifications, including structural and surface modifications are attractive approaches to enhancing the pore structure and surface properties of biochar. A unique honeycomb-like tubular structure has become the key to the high adsorption efficiency of VOCs. Its superior mechanical properties, honeycomb-like and tubular structure result in a high specific surface area, high adsorption capability, and good carrier transport properties (C. Ma et al. 2018; Xiang Xu et al. 2021). Therefore, honeycomb-like tubular biochar (HT-B) could play a significant role in improving the stability of the pore structure and increasing the specific surface area of the biochar at high modification temperatures. Recently, the hydrophobic coating technique has drawn attention as an effective approach for the selective adsorption of VOCs under humid conditions (Xiuquan Li et al. 2020; Z. Xie et al. 2011; M. Kim et al. 2022). Hydrophobic coating by materials with low surface energy, including trimethylchlorosilane (TMCS) and polydimethylsiloxane (PDMS) can decrease the affinity of water by introducing siloxane (Si—O—Si) functional group on the surface of biochar (E.J. Park

et al. 2014; Z. Gao et al. 2020). Studies have reported that this technique maintains the performance of biochar in the adsorption of VOCs under low relative humidity and shows excellent hydrophobicity under high relative humidity (Xiuquan Li et al. 2020; Z. Gao et al. 2020).

In this study, a series of hydrophobic modified honeycomb-like tubular biochars (hydrophobic HT-Bs) were synthesized from palm leaves (PL), pinewood sawdust (PWS), and corn stalks (CS). These raw materials were impregnated with different $ZnCl_2$ concentrations (0.5 M, 1.0 M, and 1.5 M) and then further modified through the hydrophobic coating of PDMS on the surface functional groups of HT-B. The optimization of the impregnation concentration and hydrophobic coating conditions for the development of a great and stable structure of hydrophobic HT-B have been investigated. The hydrophobic HT-B were then used to investigate the performance of VOC (acetone) removal under different relative humidity. The structural properties, morphology, and hydrophobicity of HT-Bs were confirmed by various technique including Brunauer–Emmett–Teller (BET) technique, scanning electron microscopy and energy disperse spectrometry (SEM&EDS), Fourier transform infra-red spectroscopy (FTIR), and drop shape analysis (DSA). Moreover, to investigate the adsorption mechanisms involved and the performance of hydrophobic HT-Bs under different relative humidity conditions, various models such as adsorption isotherm models (Freundlich, Toth, and Sips model), breakthrough models (Borhart-Adams, Thomas, and Yoon-Nelson model), and intraparticle diffusion model were adopted. These models were used to precisely evaluate the influence of water vapor on VOCs adsorption and determine the rate-limiting step of the adsorption. The novelty of this study lies in its ability to fill the gap in the use of hydrophobic HT-B in gas adsorption applications, particularly under humid conditions. The study also provides insights into the optimal conditions for the preparation and modification of hydrophobic HT-B, which can be used to improve the performance of gas adsorption materials.

1.2 Research questions

The main research questions that will be addressed through this study are as follow:

1. Can palm leaves, corn stalks, and pinewood sawdust be used to produce biochars with honeycomb-like tubular structure at different concentration of $ZnCl_2$.

2. What are the best process parameters for the formation of hydrophobic HT-B to achieve the highest VOC adsorption capacity?
3. What is the influence of humidity and its mechanisms for the VOC adsorption on hydrophobic HT-Bs?
4. How does impregnation and hydrophobic modification affect the physical and chemical properties of HT-Bs and hydrophobic HT-Bs?

1.3 Aims and objectives

This research project aims to fulfill the insufficient literature to analyze the potential performance of the biochar to act as an absorbent in VOCs removal under humid environment and proposing effectively modified biochar which can be implemented in the VOCs emission control in industries.

This research project is aimed to achieve the objectives as presented as follow:

1. To examinate the effect of zinc chloride in the formation of honeycomb-like tubular biochars (HT-Bs) from palm leaves, pinewood sawdust, and corn stalks, and to determine the hydrophobic modification by varying the process parameter, such as coating ratio of HT-B to PDMS (HT-B: PDMS), modification temperature (^{o}C), and reaction time (h), for the formation of hydrophobic HT-B to achieve optimum adsorption capacity.
2. To characterize the physical and chemical properties of the HT-Bs and hydrophobic-modified HT-B by using BET, SEM&EDS, FTIR, and DSA.
3. To analyze the adsorption capacity and the gas adsorption kinetics for the removal of VOCs onto hydrophobic HT-B under humid conditions.
4. To evaluate the reusability of hydrophobic-modified HT-B for the adsorption of VOCs under high relative humidity at 90%.

1.4 Significances

1.4.1 Scientific contribution

Although biochar has been widely used in environmental remediations for pollution control, research on selective VOCs adsorption under humid conditions by biochar is still scarce. Hence, this research study draws attention to the beneficial use of the modified biochar as a potential adsorbent for the removal of VOCs under humid conditions. The outcome of this research will provide a better understanding of the effects of metal salts concentration in developing honeycomb-like tubular structure and high porosity of biochar. Moreover, the knowledge on the hydrophobic coating on the surface of biochar could be used to overcome the poor adsorbent adsorption performance at high relative humidity. Besides, this modified biochar could improve the efficiency of the separation and purification processes, thus reducing the VOCs emission in the atmosphere.

Various structural modification methods have been reported, including the metal salts impregnation in developing honeycomb-like tubular structure (Kazemi Shariat Panahi et al. 2020; T. Xie et al. 2015). However, there are still gaps that need to be addressed in order to synthesize a better honeycomb-like tubular structure from biomass wastes for the removal of VOCs. Firstly, lack of research in evaluating the optimum metal salts concentration and the mechanisms involved in the formation of honeycomb-like tubular biochar (HT-B). Next, studies were focusing on the performance of HT-B in the adsorption of heavy metals in wastewater treatment, however the effectiveness of HT-B in the adsorption of VOCs has not been studied. In terms of VOCs adsorption, the presence of water vapor is one of the most significant impact on the adsorption capacity due to its high vapor pressure at room temperature (Jinjin Li et al. 2022; Hunter-Sellars et al. 2020). Thus, the hydrophobic modification of HT-B could enhance the adsorption capacity by increasing the selectivity of desired VOCs (K.-D. Kim et al. 2012; Jiaxing Wang et al. 2021). This brings out the novelty of hydrophobic HT-B to act as an adsorbent in the adsorption of VOCs at high relative humidity. Besides, the mechanisms involved during the adsorption of VOCs by hydrophobic HT-B could offer deep understanding of the interactions between the VOC and the surface functional group of hydrophobic HT-B. This could also be useful knowledge to select a suitable regeneration method to regenerate the adsorbent efficiently.

1.4.2 Practical implementation

The Food and Agriculture Organization (FAO) has reported that global agriculture waste production was approximately 5.9 billion tons in 2020. This includes waste from crop production, livestock farming, and forestry activities. The residues from crop production, such as stalks, leaves, and husks are the largest contributors to agriculture waste up to 80%, while the remaining 20% come from livestock wastes, such as manure and bedding materials. The management of agricultural waste is a significant challenge for sustainable development. The outcomes of this research will be beneficial for the Sustainable Development Goals (SDGs) of biochar through its application in environmental remediation.

The HT-B synthesized from palm leaves, pinewood sawdust, and corn stalks has not been studied. It is essential to investigate the biomass waste properties that influenced the formation of the honeycomb-like tubular structure. Biomass wastes naturally contain lignocellulose, which is composed of different percentages of cellulose, hemicellulose, and lignin. Hence, studying the influence of the lignocellulose content could provide better understanding of the HT-B formation. The use of biochar in this study has the potential to contribute to several SDGs as illustrated in **Figure 1.1**. It is clearly addressed that the greenhouse gas emissions can be reduced by utilizing the biomass wastes into biochar, which indirectly reduces the production cost in industry. Besides, biochar is a promising material to act as an effective adsorbent in air pollution control and wastewater treatment (A. Kumar et al. 2021; Uday et al. 2022). Moreover, the VOCs emission in the urban areas can be reduced, thus leading to cleaner air and healthier cities. The application of biochar also can reduce the negative impact of industrial activities and enhance the waste management in wide range of industry (Neogi et al. 2022; A. Anand et al. 2022).

Figure 1.1: The potential SDGs that contributed by the production and application of biochar in air pollution control technologies (A. Kumar et al. 2021)

1.5 Scope of the study

This research project focuses on the production of honeycomb-like tubular biochar (HT-B), structural and surface modification, and the performance of hydrophobic HT-B in the adsorption of VOCs under different relative humidity (RH). The biomass wastes (PL, PWS, and CS) were pre-treated by metal salts impregnation at different concentrations, and then carbonized at constant conditions of 800 ^{o}C, at heating rate of 3 ^{o}C min^{-1} for 6 h. The effect of metal salts impregnation concentrations was intensively discussed to analyze the surface properties of HT-Bs and obtained the optimum conditions for the formation of great honeycomb-like tubular structure. Hydrophobic modification through PDMS coating was performed to enhance the hydrophobicity of the HT-B. Three optimization parameters of PDMS coating, such as mass ratio of HT-B to PDMS, modification temperature, and reaction time, were comprehensively studied to evaluate the effects of these optimization parameters on the hydrophobicity of HT-B and obtain the optimum conditions for the PDMS coating. Besides, the surface characterizations of the hydrophobic HT-Bs were performed by BET, SEM&EDS, FTIR, and DSA. The Yoon-Nelson model was fitted to the experiment data to investigate the breakthrough curves of the VOCs adsorption by hydrophobic HT-B at RH of 50%, 70%, and 90%. Moreover, the mechanisms

involved during the VOCs adsorption were analyzed by Pseudo first and second order adsorption isotherms. Lastly, the rate-limiting step of the adsorption process was evaluated by intra-particle diffusion model.

1.6 Layout of the report

This report consists of 5 chapters. The first chapter is the introduction to the benefits and contribution on the use of biochar as an adsorbent in the adsorption process. This chapter also comprised of problem statement, aim and objective of the study, significance, and the scope of the study. The second chapter presents the literature review of the study, which includes the VOCs abatement methods, type of porous adsorbents, adsorption mechanisms, modification techniques, adsorption conditions, adsorption kinetic, and the adsorbent regeneration method. In Chapter 3, raw materials and chemicals used in this research were listed under materials. Meanwhile, the preparation of hydrophobic HT-Bs and adsorption procedures were clearly explained under the methodology. Chapter 4 presents the results obtained from the experimental data, characterizations, kinetic study, and comprehensive discussion on the research correlations. Lastly, Chapter 5 consists of the conclusion for the research study, challenges, and recommendation for future reference.

CHAPTER 2

LITERATURE REVIEW

2.1 Overview of volatile organic compounds (VOCs)

Volatile organic compounds (VOCs) are defined as any organic chemical compounds that evaporate easily at room temperature. They are known as common gaseous pollutants in the air, which are toxic and photochemically sensitive (D. Zhou et al. 2022). The major concern of VOCs is their high volatility at standard atmospheric pressure, which increases the potential for human exposure. Generally, VOCs are categorized into groups based on their boiling points, including very volatile organic compounds (< 50℃), volatile organic compounds (50 ~ 260 ℃), semi-volatile organic compounds (260 ~ 400℃), and particulate organic matters (≥ 400℃) (Lingli Zhu et al. 2020; Jinlong Li et al. 2021). In addition, the degree of molecular polarity of VOCs can be divided into polar and nonpolar (Lee et al. 2020; A.J. Li et al. 2021). The classification of VOCs indicates the behavior of VOCs in the atmosphere, which is mainly influenced by the nature, concentration, and emission sources of VOCs (Kamal et al. 2016; Xinmin Zhang et al. 2021). Therefore, the characteristics of VOCs can be better understood through classification. This is because different pollutants have different behaviors and effects on the surrounding environment, especially the environment and human health.

Rapid development and industrialization are major contributors to the growth of VOCs emissions. VOCs are part of essential compounds in our daily life due to their wide range of applications, such as household products, office equipment, agrochemicals, and transportation activities. Some typical examples are paints, disinfecting products, cosmetics, pesticides, fungicides, automotive products, glues, degreasers, and fuel additives (Sha et al. 2021; Mozaffar et al. 2020). Since VOCs can be released into the atmosphere through evaporation, humans are exposed to VOCs in the environment through inhalation, ingestion, and skin contact (Sonne et al. 2022). Certain VOCs can negatively affect human health. For example, carbonyl and aromatic compounds such as benzene, xylene, toluene, formaldehyde (HCHO), and acetaldehyde

(CH_3CHO) are toxic and carcinogenic to human health even at low concentration (below 0.2 mg. m^{-3}), which can cause common discomfort to severe state (Manisalidis et al. 2020; El-Hashemy et al. 2018). Furthermore, drinking water is considered a common source of VOCs exposure due to industrial discharges and disinfection processes. Long-term consumption of drinking water that does not meet the specifications may lead to heart, liver or kidney diseases (S.S. Anand et al. 2014). Moreover, indoor sources of VOCs, including acetone, formaldehyde, acetaldehyde, 1,2-dichloromethanem, and ethyl acetate are commonly produced from furniture, flooring, off-gas of building materials, cleaning and consumer products, cooking, and paint (Saraga et al. 2023; Y. Huang et al. 2019; Heeley-Hill et al. 2021). In contrast to outdoor environments, where exposure to polluted air is limited, individuals predominantly encounter air pollution indoors, given that a significant portion of their time is spent in residences, offices, public buildings, or during commutes (Goldstein et al. 2020; Toyinbo et al. 2022). Prolonged exposure to indoor VOCs poses a heightened risk of causing fatigue (Norbäck et al. 2017). Among most of the VOCs, acetone is relatively less harmful compared to benzene, toluene, ethylbenzene, and xylene. However, despite being less harmful, literature categorizes acetone as a common VOC and an air pollutant. While it may not be as harmful as other VOCs, its classification as an air pollutant underscores its significance. Consequently, acetone serves as an excellent representative of VOCs for lab-scale studies, offering valuable insights into its removal and underlying mechanisms (Rajabi et al. 2021; S.-C. Huang et al. 2021).

Most of the released VOCs play a key role in atmospheric chemistry. The presence of VOCs in the atmosphere can lead to complex photochemical reactions and produce toxic substances, resulting in negative impacts on humans and the environment (Lomonaco et al. 2020). For example, aldehydes in air can trigger atmospheric photolysis and contribute to the formation of airborne particles. Besides, photo-oxidation of benzene, toluene, ethylbenzene, and xylenes produces toxic secondary organic aerosols, which are the air pollutants that cause adverse health effects (Lomonaco et al. 2020; C. Yang et al. 2019). Moreover, studies reported that the condensation and nucleation of oxygenated volatile organic compounds, secondary organic aerosols, and secondary nitric aerosols contributed up to PM2.5 formation (X. Liang et al. 2017; A.J. Li et al. 2021). Formation of these substances can cause impact on air quality, radiation, and cloud microphysics. On the other hand, VOCs can react with atmospheric nitrogen oxides in sunlight to form ground-level ozone. Ozone formation at ground-level is considered hazardous

because they are a combination of harmful air pollutants that can cause a variety of health problems. Some typical VOCs with the highest ozone formation potential that are benzene, toluene, ethylbenzene, and xylenes. They have occupied with a total of up to 30% of VOCs emissions, which leads to 69% of the total ozone production potential (X. Liang et al. 2017; A.J. Li et al. 2021). These lead to serious adverse effects of VOCs on the environment and human health, which has become one of the most significant concerns, especially for sustainable development goals. Hence, appropriate control measures should be taken to reduce the concentration of VOCs in the atmosphere.

2.2 VOCs abatement methods

Various methods have been implemented in VOCs emission control. These methods can be broadly categorized into destruction and recovery techniques, as illustrated in **Figure 2.1** (Lingli Zhu et al. 2020; Xiuquan Li et al. 2020). Destruction methods, such as thermal oxidation, catalytic oxidation, biodegradation, and plasma catalysis, eliminate VOCs through oxidation or biodegradation processes, effectively curbing emissions from industrial processes (Xueyang Zhang et al. 2017a; Xiuquan Li et al. 2020). However, these methods are energy-intensive, expensive, environmentally impactful, have limited applicability, and face regulatory challenges (Krishnamurthy et al. 2020; Gelles et al. 2020).

In contrast, recovery methods are mainly focus on adsorption, absorption, membrane separation and condensation (Krishnamurthy et al. 2020; Xiuquan Li et al. 2020). Recovery methods provide a cost-efficient, environmentally sustainable, flexible, and compliant alternative. This approach involves capturing and reusing or recycling VOCs from industrial processes, making it adaptable to various process conditions and applications while potentially meeting VOCs emission standards (Xin Li et al. 2020; G. Gan et al. 2023). Each recovery method operates on different principles, influencing the process conditions for capturing VOCs (Pirola et al. 2021; C.-C. Chen et al. 2021). **Table 2.1** summarizes the principles, advantages, and disadvantages of recovery methods. It is worth noting that recovery methods offer a promising avenue for reducing VOCs emissions from industrial processes, indirectly promoting resource conservation and cost-effectiveness.

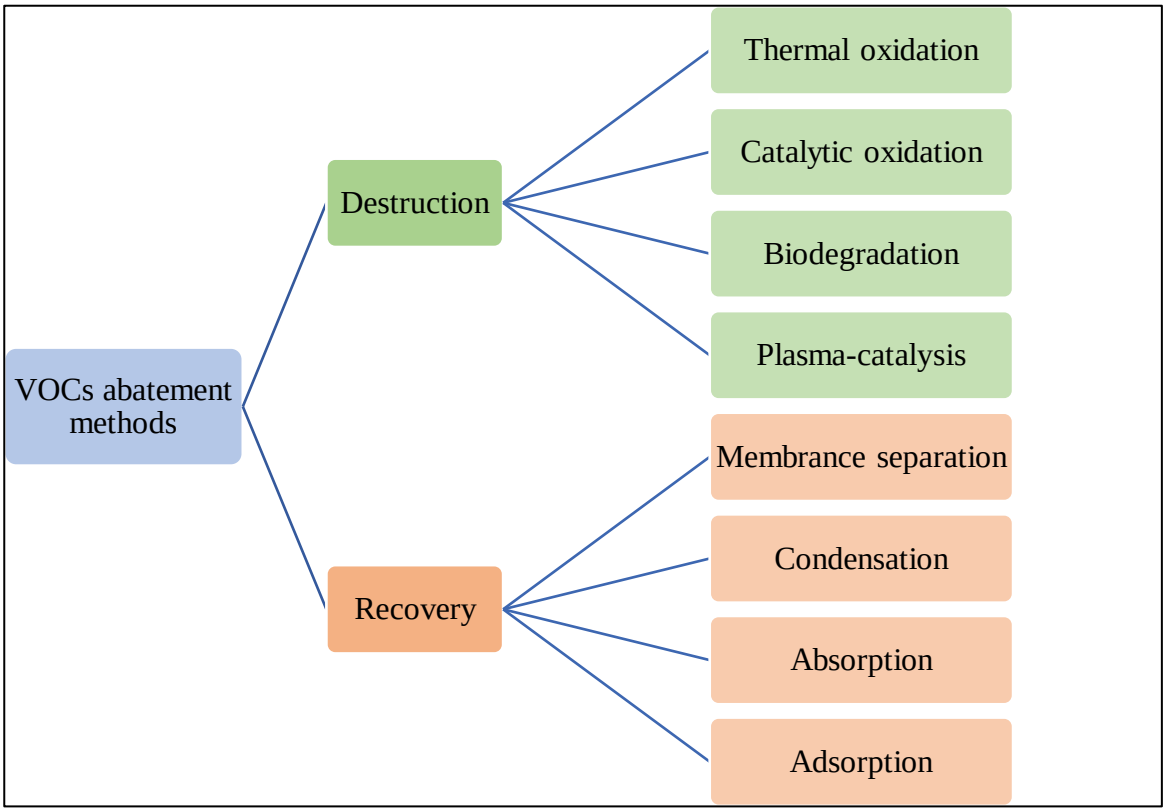

Figure 2.1: VOC abatement methods (Krishnamurthy et al. 2020).

Table 2.1: The advantages and disadvantages of the recovery methods.

Methods	Principles	Energy consumption	VOCs concentration	Efficiency %	Costs	Reuse	Waste generation	Advantages	Disadvantages	References
				Recovery methods						
Membrane separation	Involves concentration of different VOCs, purification, separation process	High	2000-50000 ppm	90-95	Moderate/ High	Yes	Clogged membranes	Flexible operation, high recovery efficiency, high efficiency	High investment cost	(Yujing Liu et al. 2006), (Luengas et al. 2015), (Zhen et al. 2006)
Condensation	VOC is converted to liquid at low temperature	High	>5000 ppm	Moderate	High	Yes	-	High concentration recycles	High energy consumption, high operating cost	(Luengas et al. 2015), (Belaissaoui et al. 2016)
Absorption	VOC absorption in water or chemical solvent	Moderate	500-15000 ppm	90-98	Moderate/ High	Yes	Spent Solvent	Convenient process recycled	Limited data of suitable solvent, limited absorption capacity	(Dumont et al. 2011), (Luengas et al. 2015), (Heymes et al. 2006)
Adsorption	Use porous materials as adsorbents	Moderate	700-10000 ppm	>80	Moderate	Yes	Spent adsorbent	Potential to recycle and reuse both adsorbate and adsorbent, low operating cost, flexible operation	High relative humidity, pore blockage, pollutant load variation, limited adsorption capacity	(Luengas et al. 2015), (L.-q. Li et al. 2012)

2.2.1 Membrane separation

Membrane separation is an innovative technique in which a membrane is utilized for the separation of VOCs for the purpose of recovery. It is highly preferred due to its facile operational procedures and its ability to be implemented in a compact design (G. Gan et al. 2023). Besides, membrane separation is a promising technology for VOCs recovery due to its high selectivity and efficiency (removal rate of over 80%), facile process, and the process can be carried out at normal temperature and pressure without consuming organic solvent (Belaissaoui et al. 2016). The mechanisms involves in membrane separation is the microporous diffusion of porous membrane (Chuah et al. 2018). Microporous diffusion mainly focus on the interaction between gas molecules and the porous membrane, including pore size and surface properties. Thus, the separation efficiency is highly influenced by the membrane properties, such as membrane pores, area, thickness, and separation coefficient (X. Yan et al. 2019) . Commonly used membranes, includes polydimethylsiloxane membrane, glassy polymer membrane, mixed matrix membrane, and liquid membrane (Jinlong Li et al. 2021; B. Shen et al. 2022; Z. Guo et al. 2021). The advantages of using these membranes in the VOCs removal are high removal efficiency, low energy consumption, reusability, and versatility (Yunjia Wang et al. 2022). However, high capital and operating costs are the major drawbacks of membrane separation.

2.2.2 Condensation

The condensation process is one of the promising methods for the recovery of VOCs due to its high concentration recycling, ease of use, requirement of less equipment, and a wide range of applications. The high efficiency of VOC recovery from gas steam into a liquid state have drawn attention due to their economic value (Ding 2019). However, the traditional condensation process for VOC recovery has limitations. Most of the refrigeration systems used a cascade compression refrigeration cycle, which decreased the recovery performance, consumed high energy and had a high operating cost (Molés et al. 2014; Luengas et al. 2015). Therefore, researchers have been exploring new methods to improve the efficiency of the condensation process. Xin Li et al. (2020) developed a novel VOC-DCR that involves turbine expansion refrigeration and two stages of precooling to replace the cascade compression refrigeration and purifier used in the traditional system. The results showed a high recovery rate of up to 99.7% with low energy consumption of 35.67 kW. This new approach represents a significant improvement in the efficiency of the

condensation process, making it a more attractive option for VOC recovery. Despite the advantages of the condensation process, the high energy consumption and operating cost remain significant drawbacks, which limit its use in the separation field (Belaissaoui et al. 2016).

2.2.3 Absorption

Absorption is a recycling process that has gained popularity due to its convenience and effectiveness. It involves the separation of volatile organic compounds (VOCs) from gas streams by adsorbing them onto a suitable solvent (Yingjie Li et al. 2021). This process is categorized into physical and chemical adsorption. Physical adsorption is based on Henry's Law, which describes the physical absorption of VOCs into the solvent. Their regeneration process is typically achieved through the application of heat, pressure reduction, or both (M. Wang et al. 2011). On the other hand, chemical absorption involves the reaction between VOCs and chemical solvents. The chemical reaction forms weak bonded intermediate elements that can be regenerated through heat application. Chemical absorption is particularly useful when the VOCs have low solubility in the solvent or require high energy input for desorption (Dumont et al. 2011). Commonly used solvent, including vegetable oil, dimethyl sulfoxide, silicon oil, and washing oil (Darracq et al. 2010; Yingjie Li et al. 2021). For example. Scholten et al. (2011) conducted a study on the absorption capacity of VOCs onto electrospun polyurethane and found that the Henry's Law constants were the highest for toluene, intermediate for chloroform, and smallest for hexane. This indicated that the fibers had a higher affinity for toluene and chloroform compared to hexane. The study also revealed that electrospun polyurethane fibers had a higher adsorption capacity for VOCs than traditional adsorbents. Despite the benefits of absorption, the technique has some limitations. One of the major limitations is the limited data of suitable solvents for specific VOCs. Additionally, the absorption capacity of the solvent may be limited, leading to low efficiency in separating the VOCs. Nonetheless, absorption is still considered an effective method for separating and recycling VOCs from gas streams.

2.2.4 Adsorption

Adsorption is an efficient and cost-effective approach to control the emission of VOCs, owing to its ability to recycle and reuse adsorbate and adsorbent, as well as its low operating cost and environmental safety (Vikrant et al. 2020; Xiuquan Li et al. 2020). This technique is highly

favorable due to its operational flexibility, high efficiency in adsorption and recovery. The effectiveness of this method relies on various crucial factors, including the selection of adsorbent material, adsorption methods, and the selectivity of adsorbent towards VOCs. Moreover, the operating conditions, including the temperature and humidity of the column, also play a significant role (Asghar et al. 2021; Lingli Zhu et al. 2020).

The selection of adsorbent material is a critical factor in adsorption processes. Porous materials such as activated carbon (AC), graphene, carbon nanotubes (CNTs), metal-organic frameworks (MOFs), and biochar (BC) are commonly used as adsorbents due to their highly porous nature, which provides abundant active adsorption sites, resulting in high adsorption capacity (T. Chen et al. 2021; Bedane et al. 2019; C. Wang et al. 2020; Y. Yang et al. 2022). There are two types of adsorptions: physical (physisorption) and chemical (chemisorption). Physisorption involves the interaction of an adsorbate with a highly porous adsorbent that has a large specific surface area through Van der Waals forces (Huijuan Liu et al. 2019). On the other hand, chemisorption occurs when the adsorbate forms a covalent bond with the surface functional group of the adsorbent (Q. Zhao et al. 2022). These interactions determine the adsorption mechanisms involved and the interaction between adsorbent-adsorbate. For instance, M.-s. Li et al. (2016) observed the adsorption interaction between VOCs and multiwall carbon nanotubes under different relative humidity. The results show that the interactions shifted from hydrogen bond acidity and π-/n-electron pair to hydrogen-bond basicity, polarizationbility /dipolarity, and cavity formation with the increment of relative humidity. This indicated that multiple adsorption mechanisms can occur during the VOCs removal depending on the properties of adsorbent and adsorbate.

In multicomponent adsorption, various VOC molecules compete for the active adsorption sites. The adsorption capacity is influenced by properties of the adsorbent, such as specific surface area, pore structure, and surface functional groups, while adsorbate, such as molecular structure, boiling point, and polarity (Yao et al. 2020; Laskar et al. 2020). Research has shown that VOCs with higher boiling points have a greater tendency to be adsorbed than those with lower boiling points. Furthermore, for stronger interactions, the molecular size of the adsorbate should be slightly smaller than the pore size of the adsorbent. Polar VOCs have a higher affinity to the polar surface of the adsorbent, whereas non-polar VOCs have a greater affinity to the non-polar surface of the

adsorbent (Batur et al. 2022; X. Huang et al. 2023; Virdis et al. 2021). Thus, the characteristics of adsorbent and adsorbate also should be taken into consideration in the removal of VOCs.

Moreover, the effect of adsorption temperature on VOCs adsorption capacity depends on the type of adsorbent used and the specific VOCs being targeted. Studies indicated that increasing the temperature during adsorption can increase the kinetic energy of the VOCs molecules, leading to an increase in the rate of diffusion into the adsorbent pores and an increase in the overall adsorption capacity. However, some adsorbents may exhibit decreased adsorption capacity at higher temperatures due to factors such as desorption or chemical degradation of the adsorbent material (Ruofei Chen et al. 2020; G. Zhang et al. 2019; Laskar et al. 2019; Kutluay et al. 2021). Therefore, it is important to optimize the temperature based on the specific adsorbent and VOCs being targeted to maximize the adsorption capacity.

Furthermore, the presence of water vapor during VOCs adsorption can significantly impact the selectivity of the adsorbent. Water vapor is a polar molecule that has a greater affinity towards the surface functional groups of porous adsorbent, competing with VOCs for adsorption sites through hydrogen bonding (X. Zheng et al. 2020). The surface functional groups of the porous adsorbent play a crucial role in determining the selectivity of VOCs (Huijuan Liu et al. 2022). To enhance the interaction between the desired VOCs and porous adsorbent, surface modifications are typically implemented by introducing appropriate functional groups. Studies has shown that introducing non-polar surface functional groups (such as nitrogen) and low surface energy materials (such as polydimethylsiloxane and trimethylchlorosilane) to the surface of porous adsorbent can increase the selectivity of VOCs and reduce the affinity towards water molecules (R. Wang et al. 2023; S. Zhang et al. 2022; Zhirui Li et al. 2021). Therefore, by introducing suitable surface functional groups, the selectivity of VOCs can be improved.

In conclusion, several VOC removal technologies have been developed to achieve environmentally friendly removal. Membrane separation, condensation, absorption, and adsorption are some of the most common recovery technologies. Among them, adsorption is the most cost-effective and efficient solution, as it allows for the reuse and recycling of both adsorbent and adsorbate and has low operating costs. However, several factors need to be considered to obtain higher VOC adsorption capacity, including adsorbent selection, adsorption method, adsorbent selectivity towards VOCs, and adsorption temperature and humidity. Despite the

advantages of adsorption, certain limitations still exist, such as high relative humidity, pore blockage, pollutant load variation, and limited adsorption capacity (Luengas et al. 2015). These limitations can be addressed by physically and chemically modifying the adsorbent, particularly for porous materials, to enhance the porous structure, pore size, and surface functional groups to increase the selectivity of VOCs removal (Yaashikaa et al. 2020). Therefore, a thorough understanding of the mechanisms involved during VOC adsorption in the presence of water vapor is crucial to perform the necessary modifications on the adsorbent.

2.3 Adsorption mechanisms

The adsorption mechanisms for VOCs can be categorized into two types: physical and chemical adsorption (Lingli Zhu et al. 2020). Physical adsorption occurs when VOC molecules adhere to the surface of an adsorbent material through van der Waals forces, hydrogen bonding, π-π stacking, electrostatic interaction, and hydrophobic interaction (S. Liu et al. 2020). In contrast, chemical adsorption involves the formation of chemical bonds between the VOCs and the surface functional groups of the adsorbent material, which results in a stronger bond than physical adsorption. The polarity of the adsorbent material and adsorbate also influences this type of adsorption (Valdés et al. 2021). Competitive adsorption refers to the scenario where multiple VOCs or the presence of water molecules compete for the available adsorption active sites on the surface of the adsorbent material. Adsorption is a complex process that involves multiple mechanisms that can occur simultaneously and complement each other (C.E.R. Barquilha et al. 2021). These mechanisms play an essential role in determining the effectiveness of the adsorption process and can vary depending on the properties of adsorbent and adsorbate. Understanding and optimizing these mechanisms can lead to more efficient and effective adsorption processes. The adsorption mechanisms of VOCs by biochar are illustrated in **Figure 2.2** and summarized in **Table 2.2**.

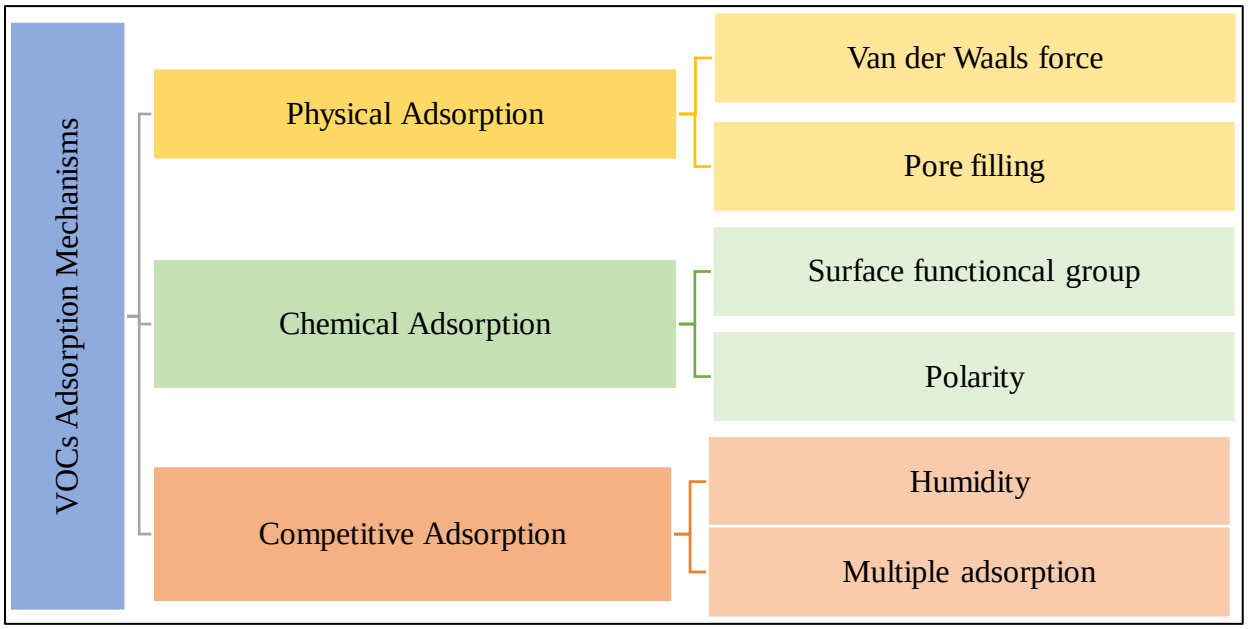

Figure 2.2: The physical and chemical interaction of adsorption mechanisms (Lingli Zhu et al. 2020).

Table 2.2: The summary of gas-phase adsorption mechanisms.

Adsorption Mechanism	Description	Parameter	Advantages	Disadvantages	Reference
Physical	• Intermolecular gravitation known as Van der Waals force • Weak interaction between absorbates and adsorbents • No chemical reaction and low adsorption heat • Involves multilayers	• Specific surface area • Pore structure • Surface properties • Adsorbate properties	• Reversible process • Adsorbents regenerated easily	• Low selectivity	(Xi Yang et al. 2018), (Carter et al. 2011), (Le-Minh et al. 2018), (Lingli Zhu et al. 2020)
Chemical	• Chemical reaction between adsorbates and the surface functional groups of adsorbents • Chemical functional groups provide small contribution to the total surface area • Involved single surface layer	• Surface functional groups	• High selectivity • High temperature accelerated the adsorption rate	• Irreversible process	(Le-Minh et al. 2018), (Lingli Zhu et al. 2020), (Xueyang Zhang et al. 2017)
Competitive	• Competition between adsorbates • Interaction between adsorbent-adsorbate and adsorbate-adsorbate • Involved multi-components gases	• Physical properties • Dipole moment • Affinity • Boiling point • Molecular weight	• High selectivity • High affinity of water molecules	• Complicated mechanisms	(Le-Minh et al. 2018), (Ece et al. 2022), (Lingli Zhu et al. 2020)

2.3.1 Physical adsorption

Physical adsorption is characterized by weak intermolecular attractions, known as van der Waals forces, that do not involve chemical reactions and have low adsorption heat. These interactions are considered relatively weak, ranging from 0.5 to 1 kcal mol^{-1}, and occur due to the attraction between the positive end of one molecule and the negative end of another. This mode of adsorption is primarily employed for gas-phase adsorption onto porous adsorbents. According to studies, physical adsorption can be divided into four stages: (a) convection and dispersion in the gas phase, (b) convection mass transfer, (c) pore diffusion, and (d) adsorption on surfaces, as illustrated in **Figure 2.3**. The rate of physical adsorption mainly relies on the specific surface area, whereas the pore structure and volume are the key factors (Lingli Zhu et al. 2020). In the internal diffusion stage, VOCs vapor enters the internal surface via pore diffusion (Xi Yang et al. 2018). The ratio of micro-, meso-, and macropore volume are the key factors of the adsorption in the equilibrium stage.

Studies have reported that adsorbents with larger pore size, high specific surface area, and pore volume can enhance the efficiency of VOCs adsorption. This indicates that the pore structure of porous adsorbents plays a crucial role in determining their adsorption capacity, and an increase in pore size is generally associated with higher adsorption capacity. For example, Xueyang Zhang et al. (2017) found that micropores (pore diameter <2nm) promote the principle adsorption sites, while mesopores (2nm < pore diameter < 50 nm) improve intra-particle diffusion and reduce adsorption time. Le-Minh et al. (2018) also reported that a larger surface area and well-enhanced pore structure have a positive effect on physical adsorption. Similarly, An et al. (2019) observed that an increase in pore size of activated carbons resulted in higher adsorption capacity for VOCs. However, it should be noted that other factors such as surface properties and adsorbate properties can also influence the adsorption efficiency. For example, Gil et al. (2014) reported that high specific area and pore volume has no direct interaction to achieve great adsorption capacity. Similarly, Y. Guo et al. (2014) indicated the increased of the basic groups in AC treated ammonia results in the increment of adsorption capacity despite the decreased in the microporous surface area. Therefore, it is important to consider multiple factors when evaluating the adsorption efficiency of porous adsorbents for VOC removal.

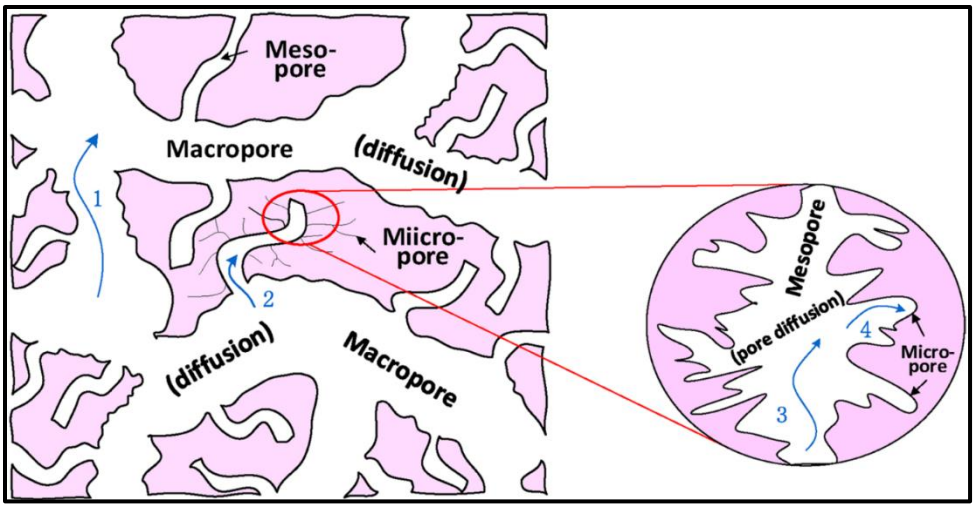

Figure 2.3: Illustration of physical adsorption mechanisms on the porous adsorbent: 1) Convection and dispersion in gas; 2) Convection mass transfer; 3) Pore diffusion; 4) Adsorption on surfaces (Lingli Zhu et al. 2020).

Mesopores are branches of macropores that serve as transport channels for VOC molecules to enter micropores. The contribution of macropores to the total surface area is approximately 5%, which is much lower compared to micro- and mesopores (95%) (Lingli Zhu et al. 2020). Therefore, the adsorption capacity is greatly influenced by micro-, meso-, and macropores of the porous adsorbents. Studies have reported that increased diffusion resistance in narrow pores could lead to low adsorption rates (Xueyang Zhang et al. 2017). In terms of adsorption rates, mesopores provide a faster adsorption rate than micropores due to a higher intra-particle diffusion rate (Y. Qin et al. 2013). G. Shi et al. (2021) prepared AC synthesized from crayfish shells for the adsorption of benzene. They found out that the pore structure of AC was a micro-mesoporous material, which enhances the transportation and diffusion of benzene molecules. Similarly, T. Chen et al. (2021) also observed that the development of mesopores have contributed to easier intraparticle mass transfer and shorten the adsorption time by promoting channel for the faster VOC diffusion. This indicates that shorter adsorption time is desirable because more zones of adsorbent bed could be optimized to achieve the breakthrough point.

Overall, the performance of physical adsorption processes is mainly influenced by the principle of adsorption sites, such as micro-, meso-, and macropores. The microscopic view of adsorbents possesses extremely strong adhesive force, known as Van Der Waals force, towards VOC molecules, which promotes abundant adsorption sites. Porous adsorbents with larger surface

area and well-developed pore structure contribute to higher adsorption capacity due to increased affinity towards VOCs, resulting in better physical adsorption. Mesopores have been shown to provide higher intra-particle diffusion rates, which can accelerate and shorten the adsorption rates. On the macroscopic scale, properties of porous adsorbents such as specific surface area, pore structure, and surface properties, as well as properties of the adsorbate, play a significant role in the physical adsorption process (Xueyang Zhang et al. 2017). Therefore, it is important to consider the characteristics of both the adsorbent and the adsorbate, as multiple factors can affect the performance of the physical adsorption process.

2.3.2 Chemical adsorption

Chemical adsorption, also known as chemisorption, involves chemical reactions that occur between surface functional groups of the adsorbent and adsorbate molecules (Le-Minh et al. 2018). The presence of surface functional groups on porous adsorbents greatly influences the interaction with polar and non-polar adsorbates (H. Ma et al. 2019; S.-J. Park et al. 2003). The oxidation of porous adsorbents increases the concentration of oxygen functional groups on the surface, which tend to adsorb polar volatile organic compounds (VOCs) such as acetone, methanol, and ethanol through hydrogen bonding (Vega et al. 2013). The adsorption capacity of polar adsorbates is mainly influenced by the number of oxygen functional groups, as observed by Ang et al. (2020) in their study on the removal of sevoflurane using oxidized activated carbon. Surface functional groups such as lactone, ether, and carbonyl groups were found to contribute to sevoflurane adsorption through strong hydrogen bonding and polar interactions, while carboxylic acid and hydroxyl groups caused repulsive hydrogen-bond interactions and contributed less to adsorption capacity. In contrast, Lillo-Ródenas et al. (2011) found that the removal of oxygen functional groups from AC increased their adsorption capacities for non-polar VOCs. This indicated that a low content of oxygen functional groups is preferred for achieving higher VOCs adsorption for non-polar adsorbate.

In summary, the use of chemical surface functional groups has been shown to enhance the performance of porous adsorbents in chemical adsorption. However, studies have reported that the contribution of chemical functional groups to the total surface area of adsorbents is relatively low compared to physical properties (Lingli Zhu et al. 2020). Moreover, chemical adsorption is an irreversible process, which is one of its major drawbacks.

2.3.3 Competitive adsorption

Recently, competitive adsorption has gained attention, particularly in gas adsorption applications, where the competition between adsorbates plays a significant role in the adsorption of VOCs onto carbonaceous adsorbents. In competitive adsorption, the adsorption capacity of the adsorbent is limited due to the presence of multiple adsorbates with different affinities. The composition of adsorbates with multiple components having different affinities affects the availability of adsorptive sites, and thus the adsorption capacity is mainly influenced by adsorbent-adsorbate and adsorbate-adsorbate interactions (Baytar et al. 2020; Jinjin Li et al. 2022)

Numerous studies have investigated the adsorption of single and multi-component gases on carbonaceous adsorbents (Lingli Zhu et al. 2020). For instance, Rajabi et al. (2021) reported a reduction in the adsorption of VOCs on biochar by up to 65% due to competitive inhibition in a multi-component adsorption process. Similar to that of Ece et al. (2022) found that the adsorption capacity of toluene-ethylbenzene and toluene-xylene mixtures decreased by up to 45% and 50%, respectively. Studies have shown that gases with higher boiling points have higher adsorption selectivity onto porous adsorbents and greater adsorption capacity compared to those with lower boiling points. Moreover, the chemical and physical properties of the adsorbate molecules, such as dipole moment, affinity, boiling point, and molecular weight, are significant factors in competitive adsorption mechanisms (Ece et al. 2022; Le-Minh et al. 2018).

Furthermore, the competition between water molecules and VOCs is also a significant challenge in practical industrial processes in addition to multi-component VOCs in gas adsorption systems. According to the Dubinin-Serpinsky theory, the adsorption sites in pores may be occupied by water molecules, competing through three ways: 1) surface oxygen functional group reaction, 2) hydrogen bonding, and 3) capillary condensation (Lingli Zhu et al. 2020). H.-B. Liu et al. (2016) reported that the adsorption capacity of benzene onto bare activated carbon decreased by 24% and 51% when the relative humidity increased from a dry condition to 50% and 90%, respectively. Similarly, Yutong Liu et al. (2019) observed that at high relative humidity, the water molecules blocked the adsorption active sites of butane, resulting in low adsorption capacity. Therefore, numerous studies have focused on developing engineered hydrophobic porous adsorbents that perform effectively under high relative humidity. For example, Xiuquan Li et al. (2020) observed that the adsorption capacity of benzene on hydrophobic AC was only reduced by 19.3% for 28.85

minutes. Similar observations have been reported by Yutong Liu and Tian (2019b), where the adsorption capacity of Pd/TiO_2 nanotubes was only reduced by 10% at high relative humidity.

Competitive adsorption is greatly influenced by the physical and chemical properties of porous materials, and adsorbate properties. The polar VOCs exhibited excellent adsorption affinity with polar surface adsorbent, while hydrophobic adsorbent tend to have good affinity toward non-polar VOCs. The selectivity of the adsorption sites prioritizes the VOCs with high boiling point and heavier molecular weight. Hence, hydrophobic modification technologies and removal of hydrophilic surface functional group are facile and imperative methods to implement in enhancing the selectivity of desired VOCs. Further research and understanding of these competitive adsorption mechanisms are crucial for designing efficient adsorbents for VOC removal in practical applications.

2.4 Porous material for VOCs adsorption

This section particularly delves into carbonaceous materials due to their cost-effectiveness and environmentally friendly nature. Lignocellulosic biomass, such as corn stalks, palm leaves, and pinewood sawdust, has gained significant attention as a feedstock for crafting carbonaceous porous materials. Researchers actively explore methods to convert these biomass wastes into activated carbons or porous structures with unique properties. For instance, studies focusing on corn stalks emphasize the optimization of activation conditions to enhance surface area and adsorption capabilities (Jinfeng Li et al. 2021; Nguyen et al. 2023). Investigations into the utilization of corn stalk-derived carbon in composite materials, especially for applications like supercapacitors, gas storage and adsorption, are actively progressing (K. Yu et al. 2020; Nascimento et al. 2023; Yao Li et al. 2021) . Similarly, palm leaves undergo carbonization processes to yield porous carbon materials, with a specific emphasis on tailoring their porous structure for applications in energy storage devices and air pollution remediation (Le et al. 2020; Almanassra et al. 2022; Bumajdad et al. 2023). Pinewood sawdust, as a lignocellulosic material, is under study for the creation of microporous and mesoporous carbons, showcasing potential as catalyst supports and in various applications (Mallakpour et al. 2021; Q. Yan et al. 2021). While specific percentage content of cellulose, hemicellulose, and lignin in pinewood sawdust may vary, typical ranges for these components in wood biomass include cellulose (40%-50%), hemicellulose (20%-30%), and lignin

(20%-30%) (W.-H. Chen et al. 2023; K. Li et al. 2022). Collectively, these studies underscore the versatility of lignocellulosic biomass in developing sustainable and adaptable carbonaceous porous materials, applicable across diverse domains from environmental remediation to energy storage.

2.4.1 Activated carbon

Activated carbon (AC) is part of the big family of carbon with a wide range of categories such as carbon blacks to nuclear graphite and composites to electrode graphite (Marsh et al. 2006). AC is generated from various carbon-rich materials such as wood, lignite, coal, petroleum pitch, and nutshell, whose production cost ranges from \$1000 to 1500 t^{-1} (X. Zhao et al. 2018). Through carbonization and activation processes, AC can be fabricated into powder, granule, pellet or sphere form (Aroldo José Romero-Anaya et al. 2014). AC is considered as one of the most popular adsorbents due to its large specific surface area (600-1400 m^3g^{-1}), high VOCs absorption capability (10-600 mg g^{-1}), and well developed internal pore structure (0.5-1.4 cm^3g^{-1}), which are known as excellent adsorptive properties (X. Zhao et al. 2018). Hence, AC has a wide range of environmental applications such as soil remediation, wastewater treatment, and air purification.

AC has been widely utilized in adsorption for most VOCs abatement, such as alkane, alcohols, aldehydes, aromatics, ethers, esters, and ketones. The adsorption performance of ACs on VOCs removal is heavily influenced by several factors, such as physicochemical properties of the AC and the adsorption condition. Generally, AC has great VOCs adsorption performance under N_2 environment, low or medium VOCs concentration, and at room temperature (Chiang et al. 2001). In addition, AC with a larger specific surface area and total volume can provide positive results on the adsorption capacity for VOCs removal. On the other hand, AC works well with chemisorption mechanism as well due to the presence of chemical function groups on its surface to react with the polar VOCs. However, there are drawbacks of AC that limit its capacity to adsorb VOCs. Firstly, AC is a natively nonpolar adsorbent that constrains the adsorption on the hydrophilic VOCs. Besides, the micropore range of AC's porous structure (pores less than 2 nm) would restrict VOC molecules, particularly those with larger molecular sizes, from entering the pores. This will lead to poor adsorption performance. In addition, AC has irregular pore structure which would lead to greater diffusion resistance, resulted in longer adsorption equilibrium time (Xueyang Zhang et al. 2017). Furthermore, several studies emphasize that AC is capable of

igniting fire due to its flammability properties, especially under the exothermic adsorption process (Jafari et al. 2018).

2.4.2 Graphene

Graphene (Gr) is a two-dimensional atomic crystal that consists of single layer of sp^2 hybridized hexagonal carbon atoms (Fatima et al. 2021). The common Gr production methods include exfoliation, hydrothermal self-assembly, chemical vapor decomposition and nanotube slicing (Mohan et al. 2018). Gr has two typical derivatives, namely graphene oxide (GO) and reduced graphene oxide (rGO). GO can be produced by oxidation/functionalization of Gr with several oxygen-containing groups, such as carboxylic, hydroxyl, and epoxide groups. On the other hand, rGO is a further derivative of GO, where it is fabricated through elimination of functional groups of GO via chemical treatment or thermal annealing (S. Yu et al. 2016).Gr and its derivatives have unique physical and chemical properties, such as superior electrical conductivity, large theoretical surface area, strong mechanical strength, and chemical functionalization. As such, they are widely used in the fields of electronics, energy storage, sensors, photonics, and environment management (L. Yu et al. 2018; Allahbakhsh et al. 2019). Regarding their environmental applications, Gr and its derivatives have received attention in several fields, such as biomedical, electronics, nanotechnologies, adsorption, and wastewater treatment (L. Yu et al. 2018; Mohan et al. 2018; Fatima et al. 2021).

The use of Gr and its derivatives as adsorbents to remove VOCs is novel. As a gas adsorbent, water resistant capability is one of the most important aspects affecting its commercial application. GO exhibits strong hydrophilicity owing to the abundance of oxygen groups on its surface. Hence, the presence of water vapour has a significant negative effect on VOCs removal by GO. Under similar conditions, Gr and rGO that has lesser oxygen groups on its surface would results in better VOCs removal efficiency. This is because Gr and rGO have more defect sites, higher surface area, and posseses hydrophobicity than GO. As a result of the removal of oxygen groups, more sp^2 carbon atoms appeared on the adsorbent, thus weakening the interaction between water vapour and the adsorbent. This makes Gr and rGO have a higher selectivity towards VOCs than water molecules.

It can be concluded that rGO possesses extremely hydrophobic properties due to the high removal of oxygen groups, which promoted better adsorption of nonpolar and weak polar VOCs. The virgin GO shows the lowest adsorption performance among the derivatives due to the presence of water vapour during adsorption process. The drawback of Gr and its derivatives is due to the relatively complicated synthesis and strict aggregation of graphene, which in turn making its industrial applications challenging (L. Yu et al. 2018). In addition, the production cost of graphene is relatively high. It requires large-scale industrial production and high energy consumption (Shadkam et al. 2021; Mu et al. 2021).

2.4.3 Carbon nanotube

Carbon nanotubes (CNTs) are known as graphite sheets with closed ends, which are rolled up like paper in the form of a cylindrical structure (Jain et al. 2021). Some common CNTs fabrication methods are chemical vapor decomposition, arc discharge, and laser vaporization or ablation (Rashed et al. 2021) Generally, the types of CNTs are categorized into single-walled carbon nanotubes (SWCNTs) and multiwalled carbon nanotubes (MWCNTs) based on the arrangement of CNTs (Rathinavel et al. 2021). SWCNTs are formed by rolling a single Gr sheet into a cylinder. In contrast, MWCNTs are defined as a stack of concentric layer cylinders with an interspacing of 0.34 nm that are rolled by at least two graphene sheets (Zare et al. 2015). CNTs have unique properties, such as high tensile strength, thermal conductivity, stability and resilience, and variety of electrical characteristics. Besides, it promotes different types of interactions with organic and inorganic analytes (Herrera-Herrera et al. 2012). In addition, CNTs have large specific surface area, hydrophobic wall, controlled cylindrical hollow structure, and easily functionalized surfaces. This makes CNTs a good adsorbent, especially for organic compounds removal (Gupta et al. 2013).

The adsorption of VOCs by CNTs mainly controlled by physical adsorption in pores, followed by slight chemisorption between surface functional groups and VOC molecules. This is because CNTs are make-up of Gr sheets, which are highly hydrophobic. This makes CNTs have strong adsorption affinities towards aromatic ring VOS. Generally, the primary physical adsorption of CNTs removes nonpolar VOCs due to its hydrophobicity, whereby the chemisorption of CNTs adsorb the polar VOCs, which have been proved by the enthalpy changes and desorption activation energy. Overall, CNTs usually have higher adsorption capacities of organic compounds than AC

and other carbon adsorbents owning to this unique property (Xueyang Zhang et al. 2017). However, the chemistry of CNTs leads to challenges in its industry due to the high number of procedures for the modification of their layers. Besides, CNTs applications are usually limited by the insolubility properties, which are insoluble in most solvents due to the extreme innertube van der Wall interactions (Herrera-Herrera et al. 2012). Furthermore, the adsorption of VOCs onto CNTs could be at a high risk to the environment since CNTs are toxic nanomaterials that possibly transport with the VOCs in atmosphere (M.-s. Li et al. 2016).

2.4.4 Metal organic frameworks

Metal organic frameworks (MOFs) have drawn attention as the most promising materials in adsorption application for the past two decades. The development of these novel hybrid porous materials involved in the combination of organic ligands and metal-containing cluster or metal nodes (Ghanbari et al. 2020). They are constructed from clusters coordinated or metal ions with organic ligands in ordered one, two, or three dimensional frameworks (Lingli Zhu et al. 2020). Most metal and a variety of organic species can be adopted to generate MOFs, which provides different structures and properties. The MOFs are commonly synthesized through diffusion method, evaporation solvent method, ultrasonic, microwave method, and hydrothermal or solvent-thermal method (Lina Zhu et al. 2019). Additionally, the porous structure of MOFs is flexibly controlled by selecting matching organic ligands with excellent properties, such as tailorable pore structure, facile functionalization, ultra-high and surface area up to 3000 m^2g^{-1}, good thermal stability (>400 ºC) (C. Liu et al. 2021; Lingli Zhu et al. 2020). In terms of adsorption application, the open metal sites on the pore surfaces of MOFs are effective to improve the VOCs adsorption process. The MOFs generally maintain their structures and crystalline order with negligible damage and after the regeneration (C.-H. Yu et al. 2012; Y.-T. Zhao et al. 2018).

Many research studies have been generated MOFs, including MIL series, UiO series, and ZIF series to act as an adsorbent in the adsorption of VOCs. Vellingiri et al. (2017) reported that different types of MOFs influenced the adsorption capacity of toluene under ambient conditions. The adsorption capacities of ZIF-67, UiO-66, MOF-199, and MIL-101 were 244, 166, 159, and 98.3 mg g^{-1}, respectively. The results show that ZIF-67 has the highest adsorption capacity might be due to the large surface area of 1404 m^2g^{-1}. Most recent studies have modified MOFs depending on the adsorption conditions to upgrade the VOCs adsorption efficiency. observed that bio-MOF-

11 composed of abundant exposed nitrogen atoms and amino groups, which promotes the adsorption of toluene, benzene, acetone, and methanol (polar adsorbates) with the adsorption capacity of 2.65, 1.86, 1.17, and 0.79 mmol g^{-1}, respectively. M. Zhu et al. (2017) reported that hydrophobic MIL(Cr)-Z1 material exhibited high adsorption capacity and selectivity for benzene series VOCs through grafting naphthalene dicarboxylic acid as the ligand. Similarly, Xiaodong Zhang et al. (2019) observed that enhance UiO-66 material possessed high adsorption performance of gaseous toluene.

In summary, the unique properties of MOFs provide a larger range of applications in industry, such as sensors, catalysts, gas storage, biomedical, and particularly for VOCs adsorption. Studies reported that the adsorption capacity of MOFs on VOCs is higher compared to that of conventional adsorbents. Additionally, the adsorption efficiency of MOFs could be enhanced by modification technologies to increase their hydrophobicity and selectivity. Nonetheless, several drawbacks are reported, such as weak dispersive force, insufficient open metal sites beneficial for coordination and catalysis (Lina Zhu et al. 2019; D. Wang et al. 2018). High preparation cost required for the utilization of MOF for the adsorption of VOCs is the biggest drawback (Sampieri et al. 2018).

2.4.5 Biochar

Biochar (BC) is a group of carbon materials that is being considered as a possible replacement for commercial AC because of its cheap and abundant feedstocks, and low production cost. BC is usually synthesized by slow pyrolysis under inert atmosphere and temperature below 700℃ (Dissanayake et al. 2020). For the production of BC, a variety of abundant carbon-rich materials can be employed, such as wood materials, agriculture and forestry waste, and fruit byproducts. The physicochemical properties of biochar are mainly influenced by the type of biomass feedstock used and synthesis condition during its production (Kumar and Bhattacharya 2021). Generally, biomass feedstock that contains high lignin and mineral content has a high tendency to generate a high yield of biochar. However, increasing pyrolysis temperature and time may result in a decrease in the mineral content, which leads to lower yield (Suliman et al. 2016). In addition, high production rate of agricultural waste promotes wide applications of biochar (Inyang et al. 2014), such as CO_2 sequestration, pollution remediation, soil fertility improvement, and conversion of syngas into biodiesel (Xueyang Zhang et al. 2017). Although biochar has wide

applications in environmental remediation, the use of biochar as an adsorbent for VOCs abatement is still scarce. Besides, BC has distinct differences from AC despite of similar raw material and production method. Firstly, the production temperature that BC requires is smaller than 700℃, which is lower than AC. Moreover, the activation step is not necessary for the synthesis of BC, but is essential for the production of AC. Lastly, the production cost of BC is far cheaper than AC (Ahmad et al. 2012; Ahmad et al. 2014).

The type of feedstock for BC production has significant influence on its physicochemical properties, which further affects its adsorption performance. By varying the feedstocks, BCs with different surface areas can be produced, even under the same synthesis condition. Feedstocks, including crop residue, woody biomass, and organic wastes contain high lignocellulosic content that plays a significant role in biochar production (Ben Salem et al. 2021; Ji et al. 2022). Besides, the pyrolysis temperature also plays a crucial role in affecting the performance of biochar on the VOC adsorption. The change of pyrolysis temperature directly affects the morphological structure and surface chemical functional groups of BC. Generally, the surface area and pore size of BC increase with increasing pyrolysis temperature. Suitable pyrolysis temperature should be traded off as BC with large surface area and small pore size is more favorable for VOCs removal. In addition, high pyrolysis temperature facilitates the removal of oxygen containing groups on the surface of BC during its production. This leads to enhanced aromaticity of BC, which in turn facilitates adsorption of hydrophobic VOCs (Xueyang Zhang et al. 2017). However, BC has drawbacks that are similar to AC, such as high hygroscopicity that lead to pore blocking, and high flammability. Further research on the use of BC for VOC adsorption is needed to facilitate the implementation of BC in VOC abatement technologies.

2.5 Key factor affecting VOC adsorption by biochar

The adsorption process of VOCs by biochar is a complex phenomenon that is affected by various factors such as the characteristics of the adsorbent and adsorbate, and the operational conditions of the abatement process. To make appropriate decisions concerning the design and functioning of adsorption systems for efficient and effective VOCs control, it is crucial to comprehend the influence of these variables. The upcoming sections provide a summary of the available information regarding the key factors that affect the adsorption of VOCs by biochar.

2.5.1 Adsorbent

2.5.1.1 Specific surface area

The specific surface area of biochar is one of its primary properties, whereas the specific surface area of an adsorbent refers to the total surface area per unit mass. It is commonly calculated using the Brunauer-Emmett-Teller (BET) method, which includes the internal and external area of biochar (L. Leng et al. 2021; Xiuquan Li et al. 2020). Adsorbents with large specific surface area generally have large adsorption capacity, which led to better adsorption performance (X. Ma et al. 2021; Huidong Liu et al. 2020). This is because the specific surface area of an adsorbent is related to the number of active sites, which provide a space for the adsorption of VOCs to take place (Xueyang Zhang et al. 2021). Several studies reported that biochar with higher specific surface area has greater adsorption capacity. For instance, both Cao et al. (2022) and Xiang et al. (2022) disclosed that modified biochar that has a larger specific surface area exhibits greater adsorption capacity, which complies with the discussion above. This indicates that specific surface area should be taken into consideration to obtain high VOCs adsorption capacity.

In addition, by fitting the adsorption coefficient to the physical properties of the adsorbent feedstock, the relationship between adsorption efficiency and specific surface area can be studied (Jianlong Wang et al. 2020). The adsorption coefficient indicates the positive correlation with the specific surface area, which is also known as t-Plot method (X. Ma et al. 2018). For example, Ruofei Chen et al. (2020) investigate the relationship of acetone adsorption capacity with the total pore volume, micropore volume, and specific surface area of activated carbon (AC) by using BET and t-plot method. They found out that the adsorption capacity of AC is linearly proportional to its specific surface area, where adsorbent with higher specific surface area has a greater adsorption efficiency on the VOC molecules. It can be summarized that specific surface area plays a crucial role in the adsorption of VOCs by carbon-based materials. As biochar is categorized as a carbon-based material, they have mutual characteristics in terms of specific surface area. The higher the specific surface area of biochar, the higher the adsorption efficiency of VOCs. However, specific surface area of biochar is not the only factor affecting the VOCs adsorption efficiency. The complex interactions that occur during the adsorption of VOCs to biochar indicate that other factors are involved, which are discussed below.

2.5.1.2 Pore size

The formation of biochar pore structures involves the carbonization and activation processes. During these processes, adsorbent pore structures with different size ranges are formed, which play different roles in the VOCs adsorption process. Pore size can be categorized into three: micropores (<2 nm), mesopores (2-50 nm), and macropores (>50 nm) (Palliyarayil et al. 2021). Micropores serve as adsorption sites for VOCs removal, whereby mesopores and macropores increase the kinetic process of VOCs adsorption and provide the diffusion transport channels for VOCs (D. Li et al. 2022). The combination of these pores facilitates excellent intra-particle diffusion, thereby shortening the adsorption time for VOCs adsorption.

Recent studies have highlighted that VOCs are mainly adsorbed in the micropores of adsorbents due to intermolecular gravitation, namely Van der Waals force toward VOCs (C. Su et al. 2020; X. Ma et al. 2021; Ruofei Chen et al. 2020). Hence, the volume of micropores is the main factor affecting the adsorption capacity of biochar for VOCs. Generally, macropores are only present on the external surface of porous adsorbents, and they serve as the inlet for VOCs to enter the internal part of the adsorbent. Then, mesopores act as transport channels for VOCs to reach micropores. When the micropores are saturated, capillary condensation occurs in the mesopores, resulting in high VOCs adsorption capacity (Tang et al. 2020; X. Huang et al. 2022; Shengyong Lu et al. 2021). Therefore, the larger the volume of mesopores, the higher the VOCs diffusion leading to high VOCs adsorption capacity.

Generally, adsorbents have micro- and mesopores that account for 95% of the surface area, while macropores contribute little (~5%) to the surface area, which is beneficial for VOCs adsorption. However, it should be noted that excessively small micropores (size 0.7 nm) could increase diffusion resistance, resulting in low diffusion rates (Le-Minh et al. 2018; Xueyang Zhang et al. 2017; Lingli Zhu et al. 2020). On the other hand, too high pyrolysis temperatures can cause the deformation, collapse, and blockage of micropores, leading to pore widening and a decrease in the specific surface area of the adsorbent, ultimately resulting in poor VOCs adsorption capacity (R. Zhu et al. 2021). For example, F. Gan et al. (2021) reported that walnut shell-derived hierarchical biochar with narrower micropores and well-developed mesopores exhibited higher toluene adsorption. Similarly, Y. Yang et al. (2022) found that the pyrolysis temperature of activated biochar above 800 ºC effectively enhanced the micropores, mesopores, and macropores

structures, resulting in higher toluene adsorption. However, not all biomasses will form a good pore structure at high pyrolysis temperatures due to their natural properties, such as lignocellulosic. For instance, Mazlan et al. (2016) showed that high pyrolysis temperatures (>700 ºC) resulted in a volume increment of mesopores and macropores of the porous adsorbent, which decreased the specific surface area of the adsorbent and led to poor VOCs adsorption capacity.

In summary, well-developed micropores, mesopores, and macropores are essential for achieving adequate adsorption capacity for VOCs. The synthesis conditions, such as biomass type and pyrolysis temperature, can affect the pore structure of the biochar, and excessively small or wide micropores can hinder the diffusion rate and reduce the adsorption capacity. Thus, the optimized adsorbent synthesis temperature could provide excellent pore sizes (nm), which generates many active sites for higher VOCs adsorption capacity.

2.5.1.3 Surface functional group

The surface functional groups of an adsorbent are responsible for the chemical adsorption of VOCs (Rajabi et al. 2021). The chemical interaction between biochar and VOCs is significantly influenced by the functional groups on the surface of biochar. Several factors can affect the surface functional groups of biochar, including biomass composition, pyrolysis conditions, and different pre-treatment and activation methods, leading to different adsorption properties (J. Li et al. 2019). Besides, the functional groups distributed on the surface of biochar are commonly verified by Fourier transform infrared (FT-IR), near-edge X-ray absorption fine structure spectroscopy (NEXAFS), and X-ray photoelectron spectroscopy (XPS) (W. Gao et al. 2022; Xiang et al. 2020).

Biochar contains multiple surface functional groups that can be categorized as oxygen (O)- and nitrogen (N)-containing groups, which lead to different chemical characteristics, such as acidity, alkalinity, reduction, oxidation, hydrophilicity, and hydrophobicity (J. Xiong et al. 2021). The O-containing surface functional groups promote surface polarity, known as hydrophilicity, which tends to adsorb polar VOCs, such as methane, ethanol, and acetone, through the formation of hydrogen bonds (Fan et al. 2018). In contrast, reduced O-containing functional groups on the surface of biochar (hydrophobic) promote better adsorption selectivity toward non-polar VOCs, such as benzene, ethylbenzene, and toluene, due to dispersive interactions between biochar and non-polar VOCs (X.-F. Tan et al. 2021). Ke Zhou et al. (2019) achieved a higher methanol adsorption capacity with ZnO-AC than acetone and toluene because of the polarity of the

adsorbates; acetone and methanol are polar species, while toluene is non-polar. However, the polarity of methanol is stronger than acetone, resulting in more methanol molecules being captured by the oxygen-containing groups on the surface of ZnO-AC. Additionally, ball-milled biochar was prepared by Xiang et al. (2020) for the adsorption of acetone, ethanol, chloroform, cyclohexane, and toluene. Ball-milled biochar exhibits good adsorption towards polar acetone, ethanol, and chloroform because of the abundant oxygen-containing groups on the surface of the biochar, which provide the adsorption active sites for polar VOCs, such as carboxyl and hydroxyl functional groups. Moreover, Jin et al. (2020) observed that N-containing functional groups on the surface of N-doped biochar enhance its hydrophobicity, resulting in an increased affinity for toluene. Therefore, the introduction of oxygen-containing groups promotes the hydrophilicity of biochar for polar VOCs, while nitrogen-containing groups increase the hydrophobicity of carbon-based adsorbents, thus strengthening dispersive forces towards non-polar VOCs.

The adsorption of VOCs by biochar is primarily influenced by its physical and chemical properties, such as specific surface area, pore structure, and surface functional groups. However, the properties of the VOCs themselves, including boiling, molecular structure, and polarity, also play a crucial role in achieving higher adsorption efficiency.

2.5.2 Adsorbate

2.5.2.1 Boiling point

The physical adsorption of gases onto biochar is analogous to vapor-liquid phase transitions. During this process, adsorbates with higher boiling points are preferentially adsorbed because of their stronger intermolecular forces compared to those with lower boiling points. For instance, Xueyang Zhang et al. (2019) investigated the adsorption of cyclohexane and acetone on highly porous hydrochar and observed that cyclohexane had a higher adsorption capacity than acetone due to its higher boiling point (80.74°C) compared to acetone (56.53°C). Similar findings have been reported for biochar, activated carbon (AC), and metal-organic frameworks (MOFs), where VOCs with higher boiling points exhibit higher saturation adsorption capacity (Xueyang Zhang et al. 2021; Ruofei Chen et al. 2020; Dobre et al. 2014).

Moreover, high boiling point VOCs show a strong affinity towards adsorbents, enabling them to outcompete lower boiling point VOCs in competitive adsorption processes. Jahandar

Lashaki et al. (2023) noted that adsorbates with high boiling point, such as n-decane, 1,2,4-trimethylbenzene, and 2,2-dimethylpropylbenzene, tend to displace less strongly adsorbed adsorbates like 1-butanol, n-butylacetate, 2-heptanone, and 2-butoxyethanol because of their lower volatility. Although high boiling point VOCs tend to have a higher adsorption capacity on biochar, their desorption is complicated because of their strong affinity towards biochar, which leads to the formation of permanent bonds. Batur et al. (2022) discovered that these bonds make it challenging to fully remove VOCs during the desorption or regeneration process. Therefore, a higher desorption temperature is necessary to break these bonds and release the VOCs from the biochar.

2.5.2.2 Molecular structure

The adsorption capacity of VOCs on biochar is influenced by the molecular structure of the VOCs, particularly their molecular size. Adsorbents with a pore size similar to or larger than the molecular diameter of VOCs could potentially become effective adsorption sites, thereby improving the removal rate of VOCs. On the contrary, pores that are too small or much larger than the molecular diameter of VOCs will lead to weak adsorption between the adsorbent and the adsorbate, which is not conducive to the removal of VOCs.

Theoretically, the optimal ratio of the pore size to VOCs molecular size should be between 1.7 - 3.0, which has been shown to result in excellent adsorption performance (Lingli Zhu et al. 2020). For example, X. Shen et al. (2020) demonstrated that banana peel-derived biochar, which had micropores with a size similar to toluene (0.67 nm), had a higher adsorption capacity for toluene than benzene. This was due to the strong interaction between the biochar surface and the toluene molecules, resulting from the specific micropore size of the biochar being closer to the molecular size of toluene than benzene (0.58 nm). Furthermore, the dispersion and molecular interaction forces of toluene were stronger than those of benzene, leading to a greater adsorption force. In addition, X. Zhao et al. (2018) found that coconut shell-derived biochar, with a specific micropore size of 0.8 nm, had excellent adsorption performance for chlorobenzene (0.78 nm) but less so for toluene (0.67 nm), which suggests that the specific micropore size of the adsorbent and the molecular size of the VOCs must be considered when attempting to efficiently remove specific pollutants. Thus, the molecular size (nm) of the VOCs and the size of the micropores (nm) of the biochar must be closely matched to achieve effective VOC removal.

2.5.2.3 Polarity

The efficiency of VOC adsorption by biochar can be significantly influenced by the polarity of the adsorbate. Polar VOCs such as alcohols, aldehydes, and ketones tend to have a stronger interaction with polar functional groups such as hydroxyl (-OH) and carboxyl (-COOH) on the surface of biochar, resulting in higher adsorption capacity. Conversely, nonpolar VOCs such as benzene and toluene preferentially interact with nonpolar functional groups such as alkyl and aromatic groups (F. Meng et al. 2019; Lingli Zhu et al. 2020). For instance, Ece et al. (2022) reported that carbon nanotubes (CNTs) had the highest adsorption capacity for xylene compared to ethylbenzene and toluene, which is attributed to the higher dipole moment of xylene resulting in a stronger adsorption affinity with non-polar CNTs. Similarly, Rajabi et al. (2021) reported that non-polar biochar had excellent adsorption capacity for toluene compared to hexane, attributed to the high affinity of toluene towards hydrophobic carbon surface with fewer O-containing functional group (non-polar) and greater porosity. This trend has also been observed with other adsorbents such as AC and MOFs (Z. Chen et al. 2023; Jurkiewicz et al. 2022). Thus, the polarity of both the adsorbent and adsorbate should be considered in designing efficient VOC adsorption processes.

In a humid system, the polar water molecules have a higher affinity towards the surface functional groups of biochar, occupying the adsorption sites by forming hydrogen bonds. The polarity of water is higher than that of VOCs, resulting in a stronger interaction between water molecules and the polar surface of biochar. This competitive adsorption phenomenon leads to pore filling, which reduces the adsorption capacity of VOCs as the relative humidity (RH) increases. Thus, chemical agents containing significant functional groups are often introduced on its surface to reduce the O-containing functional groups, resulting in improved adsorption efficiency towards VOCs under humid conditions. In such systems, the hydrophobicity of biochar is the primary factor that determines selectivity for VOC molecules and reduces the affinity for water molecules at high RH. This was demonstrated by T. Cheng et al. (2022) modified biomass-derived AC by using K_2CO_3, which increased the content of non-polar surface functional groups, such as ether, ester, and alkyl groups and reduced the hydroxyl and carboxyl groups (polar), thereby making the surface of biochar hydrophobic and improving its adsorption efficiency towards toluene and ethyl acetate under humid conditions. Similarly, Xiuquan Li et al. (2020) loaded Si-O-Si groups onto the surface of AC through a hydrophobic coating of polydimethylsiloxane (PDMS), which

increased the selectivity of benzene at high RH and stabilized its adsorption at low RH. Hence, decreasing the polar surface functional groups could increase the selectivity of desired VOCs by reducing the affinity for water molecules. In conclusion, various interactions, such as polar and non-polar VOC interactions, hydrophilic and hydrophobic interactions, play crucial roles in the adsorption of VOCs by biochar.

In summary, the physical and chemical properties of biochar, including its specific surface area, pore structure, and functional groups, are the primary factors that affect the adsorption of VOCs. In addition, the properties of the VOCs, such as their boiling point, molecular structure, and polarity, should also be taken into consideration to achieve higher VOCs adsorption. However, a direct relationship between these properties and the adsorption capacity of VOCs has not yet been reported. This may be due to the fact that these properties do not work in isolation and can be influenced by other factors, such as adsorption conditions.

2.5.3 Adsorption conditions

2.5.3.1 Temperature

Temperature is one of the adsorption conditions that influenced the adsorption efficiency due to the endothermic or exothermic reaction involved upon the elevation of adsorption temperature (Xueyang Zhang et al. 2017). With the increases of adsorption temperature, the VOCs adsorption capacity increased until a specific temperature, then decreased at elevated temperature due to the desorption process (Soliman et al. 2020). Thus, depending on the adsorption temperature, the adsorption exhibits an endothermic or exothermic process. Endothermic adsorption involves increases of temperature that promote VOCs adsorption efficiency, this may attribute to their strong interaction with adsorbent active sites (L. Sun et al. 2020). Whereas exothermic adsorption results in the decreases of VOCs adsorption capacity with the increases of adsorption temperature due to the weak interaction between VOC molecules and adsorbent active sites (S. Wang et al. 2021). For instance, Qian et al. (2015) investigated the effect of adsorption temperatures on AC for the removal of chloromethanes. Chloromethane adsorption capacities decreased by 46.2% and 47.4% when adsorption temperature increased from 20 ºC to 60 ºC. Elevation of the adsorption temperature resulting in negative values of the enthalpy of adsorption due to weak forces between the AC and chloromethanes. In addition, Davarpanah et al. (2022) points out that the increasing of adsorption temperature does not affect the adsorption capacity up

to 30 ºC, however decreased at higher temperature. Similar observations have been reported for the adsorption of acetone, alkane, toluene, and aromatic vapors by carbon-based adsorbent (S. Wang et al. 2021; Kutluay et al. 2019). Thus, the adsorption temperature should be kept below 30 ºC to maintain the adsorption efficiency.

In the presence of humidity, increasing adsorption temperature reduced relative humidity due to an increase in the equilibrium water vapor pressure (Kutluay et al. 2019). The water vapor adsorption isotherm on carbon-based adsorbent follows the type V isotherm. According to the type V isotherm, the adsorption is negligible at low relative humidity, followed by drastic increases in the amount of adsorbed before achieving a plateau at high relative humidity. These scenarios are also known as the interfering region to a non-interfering region by controlling the relative humidity value in a short period. For example, Davarpanah et al. (2022) evaluated the effect of adsorption temperature on the relative humidity and adsorption efficiency of 1,2,4-trimethylbenzene (TMB) on AC. The TMB removal exhibits excellent adsorption when the adsorption temperature increases from 22 ºC to 27-30 ºC. Such results are also attributed to decreasing relative humidity in the inlet gas, which decreases with the transition from an interfering to a non-interfering value (adjusting the relative humidity in the inlet gas). Further increasing the adsorption temperature to 50 ºC, the removal efficiency was reduced due to the decreased equilibrium adsorption capacity of AC towards TMB, and the decrease in relative humidity to 20%. To efficiently adsorb VOCs at different adsorption temperatures under humid conditions, the optimum adsorption temperature and inlet gas relative humidity should be considered.

It can be summarized that the adsorption temperature is important in the removal of VOCs because it contributes to the exothermic reaction that results in a negative value of enthalpy, lowering the adsorption capacity of VOCs. Besides, the elevation of the adsorption temperature is related to economic and environmental cost, attributed to energy consumption and greenhouse gas emissions. As a result, the optimal adsorption temperature is critical for striking a balance between an environmentally friendly adsorption process and an economical cost. In a humid system, the adsorption temperature and inlet gas relative humidity have a significant impact on VOC adsorption efficiency. Hence, it could be beneficial to understand the adsorption mechanisms of VOCs under humid conditions.

2.5.3.2 Humidity

Humidity is a significant challenge in the adsorption of VOCs onto porous adsorbents. The presence of water vapor during the VOCs adsorption process leads to the competitive adsorption mechanisms of VOCs on biochar. Water vapors compete with VOC molecules and occupied the adsorption sites to form water clusters through hydrogen bonding, resulting in a decrease in adsorption capacity (Laskar et al. 2019; Xiuquan Li et al. 2020). Studies have shown that the adsorption capacity of porous adsorbents can decrease by up to 50% when relative humidity exceeds 60% (Kawamoto 2022; Yin et al. 2022). The adsorption of VOCs in high relative humidity environments is influenced by various factors, such as pore size distribution, surface functional groups, and hydrophobicity of the biochar. Narrower micropores (<0.7 nm) exhibit higher resistance to water vapor, and a lower content of surface oxygen-containing groups increases the selectivity of desired VOC molecules, resulting in higher VOCs adsorption capacity at high relative humidity (Jinjin Li et al. 2022; Oh et al. 2019).

Studies have developed engineered hydrophobic porous adsorbents to overcome this challenge. For example, Yu Zhang et al. (2022) developed a PDMS-coated highly porous metal-organic framework with superhydrophobic surface properties and a high specific surface area and pore volume that exhibit excellent adsorption towards toluene. Similarly, Xiuquan Li et al. (2020) demonstrated that PDMS-coated AC for benzene adsorption only decreased by 19.3% at high relative humidity of 90% compared to Bare-AC (55%) due to the Si-O-Si groups attached to the surface of AC, which increased its hydrophobicity and the selectivity of benzene. This approach could be applied to biochar, as carbon-based and MOF materials exhibit similar characteristics in terms of their behavior on the adsorption of VOCs in humid environments. Therefore, pore size distribution, selection of suitable surface functional groups, and the hydrophobicity of carbon-based adsorbent should all be considered when overcoming the water vapor under humid conditions.

The relative humidity (P_{water}/P_{air}) is one of the key factors in controlling the adsorption of water vapor on the porous adsorbent, which can be categorized into low relative humidity (P_{water}/P_{air} = 0.0-0.6) and high relative humidity (P_{water}/P_{air} = 0.7-1.0). According to Dubinin-Serpinsky theory, the adsorption sites of a biochar could be occupied by water molecules competitively via three ways: surface O-containing functional group reactions, hydrogen bonding,

and capillary condensation (Lingli Zhu et al. 2020). Besides, the characteristics of water adsorption in microporous carbon-based adsorbents follow an isotherm of type V, which aligns with the Dubinin-Astakhov (D-A) model. Studies reported that at low relative humidity, a small amount of water vapor was adsorbed. This is due to the water clusters self-accumulating based on the number of hydrophilic sites in the biochar and occupied the hydrophilic sites via hydrogen bonding. In contrast, great amounts of water vapor were adsorbed under high relative humidity. According to Shuangchun Lu et al. (2021), the increasing relative humidity that leads to pore filling is due to the high polarity of water molecules, which exhibits higher affinity to the surface O-containing functional group. Besides, T. Chen et al. (2021) point out that the aggregation of water molecules occupied the adsorption sites via hydrogen bonding to form large-size water clusters followed by capillary condensation. This reduces the accessibility of VOC molecules to adsorption sites and shortens the breakthrough time (Y. Yang et al. 2020). Thus, water vapors greatly decrease the adsorption capacity of VOCs under high relative humidity, and the mechanisms involved under these conditions should be taken into consideration.

It is clearly demonstrated that humidity is a critical factor in VOCs removal technology as the presence of water vapor in the VOC-laden air stream can significantly affect the performance of biochar. The characteristics of biochar, such as specific surface area, pore structure, and surface functional groups, as well as the properties of VOCs, including boiling point, molecular structure, and polarity, all play a crucial role in enabling effective VOCs adsorption under humid conditions. To overcome this limitation, adsorbents are commonly modified by promoting narrower micropores, introducing suitable surface functional groups, hydrophobicity for higher selectivity of desired VOCs, and reducing the affinity of water molecules (W. Zhang et al. 2022).

2.6 Biochar modification technology for VOCs adsorption under humid conditions

The behavior of biochar in adsorption applications is significantly influenced by its physicochemical and textural properties. Additionally, the presence of water vapor and the characteristics of VOCs can also affect its performance. However, the use of biochar in some industries is limited due to a lack of adsorption selectivity, high temperature sensitivity, and hydrophilicity (W. Zhang et al. 2022). These limitations can be overcome by implementing

modification technologies, such as physical and chemical modifications. Physical modification methods, including CO_2 and steam activation, typically require a high temperature range of 700-1000°C. On the other hand, chemical modification methods, such as acid and alkali treatment, nitrogen doping, metal/metal oxide impregnation, and organic polymer, involve in the use of chemical agents (C. Xu et al. 2018; Gang et al. 2021). Chemical modification has a short production cycle, flexible operation, and low energy consumption compared to physical activation methods (Lobato-Peralta et al. 2021). However, physical modification is considered environmentally friendly since it does not involve corrosive or harmful chemical agents(Lingli Zhu et al. 2020).

2.6.1 Structural modification

2.6.1.1 Spherical biochar

The use of spherical biochar has become widespread in various applications, including energy generation, storage, and environmental applications such as gaseous, aqueous, and soil phases due to its high mechanical strength, wear resistance, good adsorption performance, high micropores volume, and adjustable pore structure (Wickramaratne et al. 2013; Aroldo José Romero-Anaya et al. 2014). Spherical biochar (SBC) is a carbon-rich material that is micro-scale in size and has a spherical shape derived from spherical materials. SBC is generally derived from sugar sources, such as glucose, sucrose, and xylose, through hydrothermal carbonization (HTC) and pyrolysis at different temperatures without using any activating chemical agents, making it more cost-efficient than spherical activated carbon (SAC) (Aroldo José Romero-Anaya et al. 2014; Binh et al. 2018).

Numerous studies have shown the effectiveness of SBC in water treatment to remove contaminants, including heavy metals and aromatic pollutants, due to its large specific surface area, high total pore volume, well-developed internal pore structure, and excellent removal of water contaminants (Tran et al. 2020; Sajjadi et al. 2018; X. Liu et al. 2021). For gaseous adsorption, SAC has been evaluated for CO_2 removal, and due to its high mechanical strength, low dusting properties, good spherical form with a diameter of up to 1.5 mm, and high porosity, it exhibits excellent CO_2 removal efficiency (N. Sun et al. 2013). Moreover, A. J. Romero-Anaya et al. (2014) prepared activated SAC with a high specific surface area and narrow micropore volume of activated SAC leading to high toluene adsorption capacity. This characteristic can also be

applied to SBC as they have similar controllable pore size distribution. It is observed that the higher porosity of spherical carbon could be a promising adsorbent in the adsorption of VOCs under humid conditions.

A two-stage process: hydrothermal carbonization and pyrolysis are the most common method in synthesizing spherical carbon (C. Qin et al. 2020). Wan et al. (2020) indicates that carbon-rich SBC could be achieved through hydrothermal carbonization of sugar sources or biomass wastes, attributed to dehydration, condensation, or aromatization and polymerization reactions. In addition, Tran et al. (2018) point out that the spherical hydrochar exhibits low specific surface area, however upon the pyrolysis process at high carbonization temperatures, the porosity of SBC were greatly enhanced. At high pyrolysis temperature (>500 ºC), the SBC possessed great porosity characteristics than that of non-spherical biochar. In contrast, poor porosity of SBC was observed at low pyrolysis temperature (<500 ºC), which slightly similar to non-spherical biochar (F. Yang et al. 2018; Weisheng Chen et al. 2021). Moreover, studies reported that higher pyrolysis temperature more than 900 ºC results in collapsed of the micropore structure of biochar, and further leading to sintering effect, followed by a shrinkage of biochar and could possibly destroyed the surface O-containing functional groups (Xiang Yang et al. 2018; Weisheng Chen et al. 2021). Hence, pyrolysis temperature should take into consideration in developing good structure of SBC, narrower micropores volume, and higher specific surface area.

Furthermore, the main functional groups present on the surface of SBC could affect its performances for the adsorption of VOCs under humid condition. Similar to AC, the SBC consist of hydrophilic sites associated to high concentration of reactive O-containing functional groups and hydrophobic adsorption sites related to the condensed aromatic nucleus (Y. Shen et al. 2021; B. Song et al. 2019). Studies highlighted that SBC possessed abundant surface O-containing functional group for the adsorption of water contaminants, however, poor performance in the adsorption of VOCs under humid condition. This is attributed to the O-containing functional group increasing the affinity for water molecules and decreased the selectivity of VOC molecules.

It can be concluded that the pyrolysis temperature is a crucial key factor in synthesizing excellent structure of SBC. Similar to the development of non-spherical biochar, the optimized pyrolysis temperature is required to achieve narrower micropores, larger specific surface area, and high total pore volume of SBC. Due to abundant O-containing functional groups on the surface of

SBC, it potentially exhibits poor adsorption performance under high relative humidity. This could be enhanced by introducing aromatic functional groups to increase the selectivity of VOC molecules via surface modification.

2.6.1.2 Honeycomb-like tubular biochar

Honeycomb-like tubular biochar (HT-B) is a unique structure and had become a very effective host matrix to dope and load substances, attributed to its significant honeycomb-like and tubular structure. The characteristics of HT-B, such as large specific surface area, superior porosity, good adsorption performance, and high conductivity have become a key attraction in a wide range of applications. Commonly, the HT-B is widely used in water treatment, energy storage devices, soil remediation, and CO_2 capture (Eshun et al. 2019; Heaney et al. 2018; Xiangping Li et al. 2021). Although HT-B is still in its research stages, its beneficial to widen its applications, particularly in the removal of VOCs are still worth to explore.

The HT-B can be synthesized through the impregnation of metal oxide (ZnO, Fe_3O_2, MnO, and CuO) or metal salts ($ZnCl_2$, $FeCl_3$, and $CoCl_2$) to act as a pore-forming agents and treat the raw material before the carbonization (Z. Xu et al. 2020; Gopalan et al. 2022). In terms of surface modification, the impregnation loading of metal oxide or metal salts plays a crucial role in providing sufficient amount of metal ions attached on the surface of biochar, potentially developing a honeycomb-like tubular structure. Karimnezhad et al. (2014) prepared treated AC derived from the walnut shell using $ZnCl_2$ with different impregnation ratio of 0.5:1, 1:1, 1.5:1, and 2:1 ($ZnCl_2$: walnut shell) wt/wt. They reported a significant increase in the specific surface area of the treated activated carbons with an increasing impregnation ratio. Similarly, Lei et al. (2020) prepared AC impregnated by CuO with loading ranged 0.1-0.8 wt.% for the adsorption of toluene. Upon the increases of CuO loading, the specific surface area of AC reduced from 1038.5 $m^2\ g^{-1}$ (bare AC) to 946.7 $m^2\ g^{-1}$ (AC impregnated with 0.8 wt.%). Such results implied due to the blockage and collapse of the pores, including micro-, meso-, and macropores at high CuO loading leading to smaller specific surface area and intense reaction between the biochar and metal ions. Nevertheless, AC impregnated with 0.3 wt.% exhibits the highest adsorption capacity of 701.8 mg g^{-1} with specific surface area of 985.2 $m^2\ g^{-1}$, attributed to the sufficient amount of CuO attached on the surface of AC and created adsorption active sites resulting high adsorption of toluene. Hence, the higher impregnation ratio fosters a more vigorous reaction between the activation agent

and the carbon material. This occurs because a greater amount of activation agent is incorporated into the precursor matrices, leading to pore expansion. In addition, the porosity of biochar improved with the impregnation of metal oxide or metal salts at optimum impregnation loading, which could potentially enhanced the adsorption efficiency of VOCs (Adeniyi et al. 2022; L. Yan et al. 2020; D. Zhang et al. 2021; S. Cheng et al. 2022). Moreover, this could apply to construct a honeycomb-like structure as it mainly involved in pores forming and requires optimum impregnation loading of metal oxide or metal salts to produce well-developed HT-B.

Furthermore, the selection of pore-forming agents also correlated with the formation of honeycomb-like structure. C. Ma et al. (2018) prepared HT-B derived from fargesia leaves and impregnated with 1 mol L^{-1} of $ZnCl_2$, $FeCl_3$, and $CoCl_2$. They observed that HT-B treated with $ZnCl_2$ exhibits excellent structure of honeycomb-like, which constructed from abundant amount of biochar tubes and uniform distributed fenestration on the surface of biochar. While, incomplete and irregular honeycomb-like structure was observed in HT-B treated with $FeCl_3$ and $CoCl_2$. During the carbonization stage, $ZnCl_2$ played a role in making pores on the surface of biochar and improved the breakage of organic matter in the biochar. Then, effectively recombined the solid matrix to construct a uniform honeycomb-like tubular structure. Thus, $ZnCl_2$ with optimum impregnation loading could perform well in developing a honeycomb-like tubular biochar.

Moreover, the formation of HT-B firstly occurred on macropores, where the arrangement is formed by thin carbon walls with a gap distance ranged from 10-40 µm. These walls are associated with cellulose, hemi-cellulose, and lignin from biomass materials. Among them, lignin is the hardest molecule to decompose, which maintains the cell wall structure until a certain temperature is achieved. Hence, the structure of honeycomb-like tubular is well-developed at certain ranged of pyrolysis temperature. B. Zhao et al. (2018) indicated that the HT-B constructed from stable and great amount of honeycomb-like macropores structure with specific surface area of 384.1 m^2 g^{-1} at pyrolysis temperature of 700 ºC with heating rate of 1 ºC min^{-1} for 10 min, as illustrated in **Figure 2.4(a)**. They also reported that the temperature lower than 700 ºC, resulted in incomplete formation of honeycomb. In addition, heating rate below 20 ºC min^{-1} and reaction time more than 60 mins resulted in the development of the pore structure and higher surface area. Besides, Bataillou et al. (2022) observed similar results, however collapsed of the pores for honeycomb structure pyrolyzed at 900 ºC, attributed to the decreases of its specific surface area

by 72% (136 m^2 g^{-1}) resulting in lost ordered of honeycomb structure, as presented in **Figure 2.4(b)-(c)**. Moreover, C. Ma et al. (2018) successfully created a honeycomb tubular biochar with a specific surface area of 461.9 m^2 g^{-1} using a pyrolysis temperature of 800 ºC, a heating rate of 3 ºC min-1, and a duration of 6 h, as shown in **Figure 2.4(d)**. This demonstrates that pyrolysis temperatures ranging from 700 to 800 ºC, heating rates between 1 and 20 ºC min^{-1}, and reaction times from 1 to 6 h have the potential to develop well-structured honeycomb tubular biochar. Apart from that, pyrolysis temperature possessed a great effect on the hydrophilic or hydrophobic characteristics of HT-B, which is generally investigated by water contact angles. Studies reported that the increases of pyrolysis temperature also decrease its hydrophobicity with lower water contact angles due to the decomposition of lignin that could increase the wettability of the HT-B. Thus, pyrolysis temperature, heating rate, and reaction time should take into account to develop a honeycomb-like tubular structure with high hydrophobicity that could be used in VOCs adsorption under humid conditions.

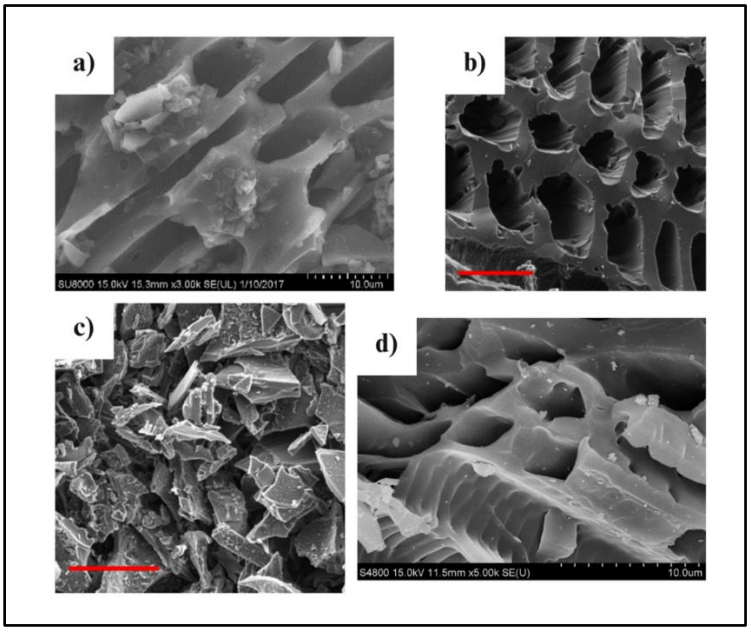

Figure 2.4: SEM images of the related studies.

Similar to synthetic SBC, the preparation of honeycomb-like tubular biochar are also mainly influenced by the shape and structure of biomass raw material (C. Qin et al. 2020). Studies showed that suitable biomass raw materials are favorable to develop low cost and green honeycomb-like tubular biochar. Besides, plant in nature evolve with various microstructure in

different parts due to variety of pore sizes and morphologies (Z. Su et al. 2022; Bi et al. 2019; Yi Wang et al. 2020). Biomass material with vascular bundle and fiber can be found in vascular plants or parts of the plant that contain vascular bundle, such as bamboo, palm leaves, corn stalks, and other plant species (Boch et al. 2021; Boumediri et al. 2019). C. Ma et al. (2018) point out that vascular bundle and fiber can act as template for the development of honeycomb-like AC derived from fargesia leaves due to its superior tubular and pore structure. Upon the pre-treatment and carbonization, the HT-B exhibits a larger specific surface area, good adsorption capacity, excellent carrier transportation properties and stable honeycomb-like tubular structure, as illustrated in **Figure 2.5(d)**. In addition, other biomass wastes have been reported in the literature for the development of honeycomb-like pore structure via only activation, such as cedar wood, bagasse, spruce (softwood), coconut shell, rice husk, and rapeseed stem (Bataillou et al. 2022; Kamran et al. 2020; Kang et al. 2022). Their findings showed that the honeycomb-like structure was constructed from micropores cubic block and interconnected cylindrical holes of meso- and macropores. Besides, the specific surface area and total pore volume of honeycomb-like pore structure was ranged from 223-484 $m^2 g^{-1}$ and 0.33-0.41 $cm^3 g^{-1}$, respectively, which was slightly similar to the HT-B synthesized via biomass template (462 $m^2 g^{-1}$ and 0.41 $cm^3 g^{-1}$). Thus, the HT-B can be produced via two ways: biomass materials act as templates followed by activation or only by activation, and both promotes larger specific surface area for higher adsorption sites (L. Leng et al. 2021).

It can be concluded that the shape and structure of biomass materials are one of the key factors in regulating the pore structure of biochar. Biomass materials with high lignin content and consist of vascular bundle and fiber are the crucial characteristics in the development of honeycomb-like tubular structure. Besides, it is beneficial to inherit the excellent structure of its raw materials. The optimized pyrolysis temperature plays an important role in constructed well-developed spherical and honeycomb-like tubular structure. However, the HT-B promotes higher value of specific surface area and total pore volume compared with SBC. In terms of adsorption process, specific surface area is crucial factor in providing adsorption active sites, adsorption capability, and interaction between adsorbent and contaminant (R. Li et al. 2020; Mahmoud et al. 2020). Moreover, the large number of pores in the tube wall extremely increase the specific surface are of HT-B, which further promotes great matrix for supporting other materials and promotes higher area of contact on the surface of HT-B for other substances, especially for surface

modification (Tao et al. 2018). Thus, the surface modification on HT-B is worth exploring to wider its application on gaseous adsorption and enhance its performance under humid conditions.

2.6.2 Surface modification

2.6.2.1 CO_2 activation

The CO_2 activation is a widely used physical activation that involves using a typical activation gas to develop an engineered biochar at high temperatures. CO_2 is considered as the preferred gas for activation due to its cleanliness and convenient handling. Besides, CO_2 has been selected as the activation gas on the laboratory scale because it enables the control of the activation process due to the slow reaction rate at high temperatures (T. Zhang et al. 2004). In addition, the mechanism involved in the formation of micropores structure during the CO_2 activation is the development of char-CO_2 gasification, which CO_2 act as activating agent during the reaction known as Boudouard reaction (Zhikai Li et al. 2020). The mechanisms of oxygen exchange developed by Ergun have been widely adopted to describe the reactions involved. Firstly, CO_2 is attached on the free carbon active site (C_f) on the surface of biochar and detached to form a reactive carbon-oxygen complex (C(O)) and a molecule of carbon monoxide (**Eq. (2.1)**). Next, the reaction surface oxide transformed solid to gas phase resulting in the removal of a carbon atom from the biochar and generates a new adsorption active site (**Eq. (2.2)**). These reactions are shown as follows (Shafawi et al. 2021):

$$C_f + CO_2 \leftrightarrow C(O) + CO \quad \textbf{(2.1)}$$

$$C(O) + C \leftrightarrow CO + C_f \quad \textbf{(2.2)}$$

This activation process promotes the formation of micropores, attributed to hot corrosion between the biochar and CO_2 at high temperature leading to high specific surface area, which is more desired for VOCs adsorption (Dissanayake et al. 2020).

The parameters that affect CO_2 activation include activation temperature, holding time, and CO_2 flow rate (Jiang et al. 2020). Among these, activation temperature is the most crucial factor that affects the physicochemical properties, porous structure, and VOC adsorption efficiency of biochar (Khuong et al. 2021). Besides, CO_2 activation promotes narrower micropores for higher adsorption capacity of VOCs and small mesopores to enhance the diffusion of VOC molecules

into the pores of biochar (Manyà et al. 2020). Studies have reported that high CO_2 activation temperatures up to 950 ºC have a significant impact on the specific surface area and porosity of biochar. On the other hand, lower activation temperatures result in an incomplete pore structure, and less endothermic reaction between biochar and CO_2 interferes with the porosity development, especially at holding times less than 60 min (Lang et al. 2017; Z. Xiong et al. 2013). For instance, Rashidi et al. (2019) prepared activated carbon derived from palm kernel shell exhibits high specific surface area and micropore volume with the increases of temperatures from 750 to 950 ºC leading to high CO_2 adsorption. Similarly, Ogungbenro et al. (2018) highlighted that the specific surface area and micropores volume of activated carbon synthesized from date seeds was enhanced with the increases of activation temperature from 600 to 800 ºC. However, the collapse of the pores was observed upon further increase of the temperature to 900 ºC, attributed to the widening of the pores at high temperature. Nevertheless, at a temperature of 900 ºC, holding time of 60 min, and CO_2 flow rate of 150 ml/min, the activated carbon possessed a higher specific surface area and micropore volume of, resulting in a higher CO2 adsorption capacity. This also could be a promising biochar activation that can be applied in VOCs adsorption application as biochar and activated carbon have similar porosity development characteristics. Thus, the activation temperature, holding time, and CO_2 flowrate should be taken into consideration in this activation.

Apart from that, activation temperature impacts the surface functional groups of biochar, which is similar to the effect of pyrolysis temperature. High CO_2 activation temperature results in the decreases of the polar functional groups, such as -OH and C=O, which further reduced the polarity index and hydrophilicity of biochar (Adhikari et al. 2022; Zornoza et al. 2016). This indicates that at high CO_2 activation temperature the biochar possessed more hydrophobicity, which enhance the interaction with non-polar VOC molecules and higher selectivity for its adsorption due to lower content of -OH functional group, and low H/C and O/C ratios. Besides, higher hydrophobicity also could increase the selectivity of VOC molecules in the presence of water molecules (Shafawi et al. 2021). Hence, CO_2 activation could be beneficial in developing biochar with excellent hydrophobic behavior and high selectivity of desired VOC molecules under humid conditions.

In summary, it is worth noting that the increases of CO_2 activation temperature not always have a positive result for specific surface area and micropores volume. The holding time and CO_2

flow rate also play a role in developing porosity of biochar. The optimum conditions could promote well-developed pores structure of biochar with higher specific surface area and micropores volume. Moreover, it is crucial to have a balance the relationship between specific surface area with surface functional groups and hydrophobicity. Higher activation temperatures result in high specific surface area and micropores volume, additionally it also results in reducing of O-containing functional groups, which increases the hydrophobicity of biochar. This hydrophobic biochar could become a promising adsorbent for the adsorption of VOCs under humid conditions.

2.6.2.2 Nitrogen doping

Nitrogen doping (N-doping) is a method to introduce N-containing functional groups on the surface of biochar to alter its surface chemical properties (M. Song et al. 2021). N-containing functional groups, including amide, pyridinic, imide, pyrrolic, graphitic, and lactam groups are commonly used to increase the surface basicity of biochar, which favor the adsorption of VOCs in the presence of water molecules (Q. Zhou et al. 2018). N-doping techniques can be categorized into two types of N sources: natural N source within biomass and impregnation with nitrogen containing reagent or ammonia purging. Among these, ammonia purging is suitable method to produced biochar with high hydrophobicity due to the thermal reforming of biomass at high temperature. Xiong Zhang et al. (2014) point out that ammonia purging successfully introduced some of N-containing functional group, attributed to ammonia dissociated to form NH_2, NH, and H at high temperature, then react with surface oxides and active sites to form N-containing functional groups. This similar to the mechanisms that was proposed by Wei Chen et al. (2016). The ammonia reacted with carboxyl groups on the surface of biochar via Mailard reaction to form C-NH_2 and C-NH and accompanied by H_2 production to promote N-doping as expressed in **Eq. (2.3)**. Then, further converted into pyridinic N and graphitic N. Thus, ammonia purging produced microporous structure by removing the oxygen containing functional groups. This reaction as shown as follows:

$$(C)_{Biomass} + NH_3 \rightarrow C\text{-}NH_2 + C\text{-}NH + H_2 \quad \textbf{(2.3)}$$

Among the N-containing functional groups, graphitic-N are the most effective in enhancing the hydrophobicity of biochar, attributed to π-π interactions with the VOCs and weaken the electrostatic interaction with water molecules (C. Zheng et al. 2017). Jinjin Li et al. (2022) prepared N-doped resin-based activated carbon with high specific surface area and micropores

volume of 1583 m^2 g^{-1} and 0.77 cm^3 g^{-1}, respectively, thereby superior adsorption capacity of toluene at high RH. Such results implied due to the formation of pyridinic-N, pyrrolic-N, and graphitic-N. However, graphitic-N exhibits dominant contributor to increase the selectivity of weak polar toluene and decrease the affinity for water molecules. In addition, F. Meng et al. (2019) indicated that the introduction of N-containing functional groups can enhance the hydrophobic property of the biochar surface by eliminating the O-containing functional groups to promote high adsorption capacity of non-polar VOCs. On the other hand, Yuan et al. (2020) highlighted that pyridinic-N and pyrrolic-N species make the dominant contribution to water adsorption capacity due to the strong polarization on the surface of porous carbon occurs in pyridinic-N and pyrrolic-N. These species promote strong electrostatic interactions with water molecules, thus high adsorption of water uptake. Hence, N-containing functional groups provides different surface chemical characteristics of biochar, which could be implemented depending on the VOCs adsorption conditions. In the system with humidity, graphitic-N species are highly required.

Apart from that, the activation temperature and holding time play an important role in determining the porosity development and the content of graphitic-N in the biochar. For instance, W. Yu et al. (2018) evaluated the effect of activation temperature and holding time of ammonia purging ranged 600-800 ºC and 1-3 h, respectively. The increases of activation temperature and holding time leading to positive results, which N-doped biochar exhibits larger specific surface area (418.7 m^2 g^{-1}) and high content of graphitic-N (46.4 %). This attributed to the pyridinic-N or pyrrolic-N was converted into graphitic-N with the increases of activation temperature and holding time. In addition, Lian et al. (2016) indicates that extremely narrow micropores structure with pores smaller than 2.0 nm and some ultra-micropores (<1.0 nm) were formed at high activation temperature over 800 ºC and longer holding time. Therefore, N-doped biochar could potentially improve the adsorption of VOCs under humid conditions and the characteristics of N-doped biochar could be altered by controlling the operational conditions. It is worth noting that the optimum conditions of N-doped with larger specific surface area, narrow micropores, and high hydrophobicity are constructed at activation temperature over 800 ºC and holding time more than 2h.

2.6.2.3 Organic polymer coating

Organic polymer coating is also known as hydrophobic coating, which has been implemented in the selective adsorption of VOCs under humid conditions. Hydrophobic coating technique is a modification process with the used of low surface energy materials, such as polydimethylsiloxane (PDMS), trimethylchlorosilane (TMCS), polyacrylonitrile (PAN), and poly furfuryl alcohol (PFA) (H.-B. Liu et al. 2016). Among these, PDMS has been widely explored to graft thin film on the surface of porous materials by thermal evaporation process (Eduok et al. 2017). The heat applied during the modification allows PDMS deposited a hydrophobic coating on the surface of biochar to increase the selectivity of desired VOC molecules under high RH and maintains the performance of biochar under low RH (Xiuquan Li et al. 2020). This attributed to the relatively low surface energies of PDMS thin film with reduced wetness (Kobayashi et al. 2012) . Thus, PDMS coating has been utilized in various protective coating systems for industrial substrates, however it is beneficial to widen its application in VOCs adsorption technology.

The hydrophobic films form an extremely stable chemical bond on the surface of biochar and the silica content in the PDMS constructed silica (─Si─O─) network, which allows the biochar being incorporated with VOC molecules under high RH (Eduok et al. 2017). Xiuquan Li et al. (2020) performed PDMS coating on walnut shell-derived activated carbon for the adsorption of benzene at RH ranged 0-90 %. The adsorption capacity of benzene on PDMS-coated activated carbon was only decreased by 19.3 %, while bare activated carbon exhibits significantly decreased on benzene adsorption capacity by 55.6 % at high RH of 90 %. This due to the surface of activated carbon was coated with Si─O─Si groups resulting in the increases of its surface hydrophobicity, which reduced the affinity for water molecules. In addition, E.J. Park et al. (2014) indicated that the effect of water molecules presents at high RH on the adsorption efficiency was reduced due to the continuous siloxane chains in PDMS on the surface of mesoporous silica leading to high water resistant. As biochar is categorized under porous materials, which similar to activated carbon and mesoporous silica, this also could apply to biochar as they have similar physical characteristics. Besides, the changes in hydrophobicity of biochar can be verified by water contact angle measurement and fitted by Young-Laplace equation (Akbari et al. 2021). Generally, water contact angle more than 90 º is considered to be hydrophobic, and conversely hydrophilic. Studies reported that the PDMS coating can be range from hydrophobic (>90 º) to super-hydrophobic (≥150 º), which depending on the thickness of PDMS coated on the surface of biochar (Xiuquan Li et al.

2020; E.J. Park et al. 2014; Z. Gao et al. 2020; J. Liu et al. 2019). Thus, the sufficient thickness of PDMS should be taken into consideration to promote high hydrophobicity of biochar for higher adsorption of desired VOC molecules.

Modification temperature is one of the factors that affecting the thickness film of PDMS coated on biochar. As reported in the literature, the heating temperature of PDMS coating was positively correlated with water contact angles (Eduok et al. 2017). H.-B. Liu et al. (2016) reported that PDMS-coated activated carbon at 250 ºC exhibits super-hydrophobic with water contact angle of 159.2º, while 133.4, 137.0, and 147.3º were observed for PDMS-coated activated carbon at 80, 150, and 200 ºC, respectively. Similar to Lan et al. (2016), they observed that PDMS-coated biochar at 300 ºC has superior hydrophobic property with water contact angle of 165º. However, further increased the modification temperature to 600 and 900 ºC, the water contact angle reduced to 150 and 145 º, attributed to the degradation of the organic groups (CH_2 and C─C) at high temperature, while Si─O groups maintained it film on the surface of biochar as FTIR spectra showed unchanged sharp peak of Si─O groups. Thus, biochar still maintained its hydrophobic property at high temperature. Despite the positive results on the water contact angle with the increases of modification temperature up to 300 ºC, negative correlation was reported for the specific surface area. H.-B. Liu et al. (2016) observed that the specific surface area of activated carbon was reduced from 868 $m^2 g^{-1}$ (bare activated carbon) to 811 $m^2 g^{-1}$ (PDMS-coated activated carbon) with the increases of temperature up to 250 ºC. The decrease was not significant between the bare activated carbon and PDMS-coated activated carbon. However, Xiuquan Li et al. (2020) reported that the specific surface area of bare activated carbon and PDMS-coated activated carbon were greatly reduced from 1553.89 $m^2 g^{-1}$ to 1232.71 $m^2 g^{-1}$ as the temperature increase up to 250 ºC, respectively. Such results implied due to the PDMS being deposited on the surface of biochar, including micro-, meso-, and macropores. With the increases of temperature, the PDMS film getting thicker, and more pores were filled, which resulting in the decreasing of specific surface area of porous materials, including biochar. Nevertheless, studies indicate that PDMS-coated porous materials at temperature ranged of 200-250 ºC with larger specific surface area exhibits lesser effect on the adsorption capacity of VOCs in the present of water molecules (H.-B. Liu et al. 2016; Xiuquan Li et al. 2020). Therefore, PDMS coating temperature crucially affects the thickness of the PDMS film on the surface of biochar, which further affects the water contact angle and specific surface area of biochar. Furthermore, the optimum condition for the PDMS coating

on biochar should take into consideration to sufficiently coated the surface of biochar and maintains its textural properties to initial materials, particularly for specific surface area.

In summary, most of the biomass-derived biochar is naturally hydrophilic, which has become a drawback to VOCs adsorption technology under humid conditions (Xian et al. 2015). Besides, structural modification could be applied follows by hydrophobic modification on the surface of biochar to enhance the porosity development and selectivity of VOC molecules in the present of water molecule, thereby increase the adsorption efficiency. The honeycomb-like structure promotes larger specific surface area and higher area of contact on the surface of HT-B for other substances, such as surface modification compared to SBC. In terms of surface modification, PDMS coating could be a promising technique to increase the hydrophobicity of HT-B, attributed to the potential of producing HT-B with super-hydrophobic property. Compared to CO_2 activation and nitrogen doping, PDMS coating required lower modification temperature and the PDMS thickness on the surface of HT-B is only controlled by modification temperature. While CO_2 activation required a high activation temperature of 900 ºC, which could cause collapsed of the honeycomb-like structure as HT-B is well-developed at 800 ºC. Moreover, N-doped biochar contained different amounts of O-containing functional groups resulting in complication to evaluate the role of N-containing functional groups separately through experiment data. Thus, PDMS coating is eco-friendly and facile modification that could be applied to HT-B. Besides, PDMS-coated HT-B could be a promising adsorbent to provides abundant adsorption sites and reduced the affinity for water molecules for the higher VOCs adsorption efficiency.

2.7 Regeneration of adsorbent

The regeneration of biochar is a reverse process of adsorption. Biochar regenerations are classified into two principles: adsorbate desorption and adsorbate decomposition (Dai et al. 2019). For industrial applications, it is important for an ideal adsorbent to exhibit good recycling and reusability, particularly to reduce the cost of biochar through repetitive sorption-desorption cycles (Ifthikar et al. 2018; Bamdad et al. 2018). Studies have shown that the biochar can retain between 50 and 95% of the adsorbed chemicals at temperatures of 50-60 ºC (Xiang et al. 2020). This demonstrates the reliability of biochar for managing adsorbed volatile chemicals, even under extreme operating conditions (Rajabi et al. 2021). In addition, the regeneration and cost-efficient

of biochar could be achieved by implementing different regeneration technologies depending on the properties of biochar (Dai et al. 2019). There are several biochar regeneration techniques, including chemical, microwaves irradiation, and thermal regeneration, each designed for specific applications related to the adsorption process.

2.7.1 Chemical regeneration

Chemical regeneration is a technique that involves the use of chemical agents to recover the adsorption capability of biochar that has reached saturation with pollutants, including VOCs. Various chemical regeneration methods such as steam stripping, solvent extraction, and chemical oxidation to desorb the pollutants from the surface of biochar (T. Dutta et al. 2019). Solvent extraction involves the use of solvent to dissolve and eliminate the adsorbed VOCs from the biochar. Steam stripping involves passing steam through the biochar to desorb the VOCs, whereas chemical oxidation uses an oxidizing agent to transform the adsorbed VOCs into less harmful byproducts (W. Zhang et al. 2022).

The solvent extraction can be categorized into inorganic and organic solvent regeneration. Inorganic chemicals can be regenerated through acid-base regeneration methods, which involve the use of inorganic acids (HCl and H_2SO_4) or alkalis (NaOH) to remove the VOCs from the surface of the biochar (RongPing Chen et al. 2014). While, organic solvent regeneration using solvents, such as acetone, benzene, and methanol to extract the VOCs from biochar (Makoś-Chełstowska 2023). For example, El Gamal et al. (2018) regenerated biochar adsorbed with high concentrations of phenol using a NaOH solution, which recovered the desorbed phenol in the form of sodium phenolate. Recently, a novel technology involving ultrasound cultivation and ethanol extraction co-processing has been developed by Y. Ma et al. (2021) to regenerate KOH + Fe/Zn-BBC. They reported that this method was effective in maintaining a high adsorption capacity of up to 96.1% of the fresh biochar, even after five reuse cycles, whereas H_2O washing resulted in a capacity of only 10.2% of the fresh adsorbent after five cycles. Additionally, maintaining an equimolar mixture of acid and base is essential for achieving optimal regeneration. A study conducted by Han et al. (2015) exemplifies this principle, where they regenerated HKUST-1 using a combination of HCl and NaOH at various ratios. Their findings indicated successful regeneration of HKUST-1 when the amount of base was less than 1 equimolar compared to the acid. However, adding more than 1 equimolar base led to unsuccessful regeneration of HKUST-1. This suggests

that adjusting the equimolar ratio or concentrations of the acid and base solution is crucial in expanding the regeneration capacity. Furthermore, the choice of organic solution (acetone, benzene, methanol, ethanol, and chloroform) in the regeneration process significantly influences the surface functional groups of the adsorbent. It is crucial to select the appropriate organic solution based on the polarity of the adsorbent. Research indicates that polar solvents are not suitable for regenerating non-polar adsorbents due to alterations in surface functional groups (Reguyal et al. 2017; Ani et al. 2020). Therefore, careful consideration of the organic solvent selection is necessary when regenerating specific adsorbents. Apart from that, the use of inorganic and organic solvents in adsorbent regeneration poses challenges, as these solvents are corrosive and have a high potential to create secondary pollution during the regeneration process (P.-J. Lu et al. 2011). This situation has caused an environmental footprint attributed to the production of large amount of waste solvents. This environmental impact stands as a major drawback of this regeneration technique (T. Dutta et al. 2019).

2.7.2 Thermal regeneration

Thermal regeneration is a technique used to restore the adsorption capability of a carbonaceous adsorbent that has become saturated with VOCs (Salvador et al. 2015). This process can be categorized into traditional and non-traditional techniques. Commonly used non-traditional techniques, such as using microwave, while traditional techniques, including utilizing hot inert gases and steam (temperature-swing adsorption (TSA) and temperature-programmed desorption (TPD)) (Salvador et al. 2015; Xueyang Zhang et al. 2017).

Microwave regeneration is a technique used to induce polarization in polar substance molecules in an adsorbent, which can then be converted into heat energy through an electromagnetic field (Dai et al. 2019). This method is particularly effective for heating materials containing mobile electric charges, such as polar solvents and conducting ions in solids. Several of carbon materials, commonly AC, and BC from various of industry applications adsorbed with toluene, phenol, high molecular weight VOCs, and xylose were successfully regenerated using microwave technique of heating (Nigar et al. 2015; Lv et al. 2020). This is because the VOCs adsorbed in the adsorbent is heated and volatilized, and microwave heating can uniformly heat both the inside and outside of the adsorbent (Y. Jia et al. 2016; Zubrik et al. 2022). Microwave regeneration is attractive due to the quick start-up and stopping, short heating rate, contactless

heating, selectivity, low energy consumption, and effective volume heating process (Kumar N et al. 2020). The microwave regeneration of adsorbents consists of two techniques: direct heating of adsorbent containing the VOCs and microwave-assisted solvent desorption (Zubrik et al. 2022). The first technique involved the attachment of VOCs molecules on the surface of the biochar and thermally degraded. In terms of physiosorbed, pore-blocking species, including water, hydrocarbons, and other volatile compounds, the desorption process requires low energy compared to chemisorbed species, such as pharmaceutical product, dyes, and other reactive organic compounds (Kumar N et al. 2020; A.J. Shah et al. 2022). For example, A.J. Shah et al. (2022) performed microwave regeneration of BC derived from corn stalk for the desorption of 4-chlorophenol at power ranged from 400 to 800 W. They observed that at low microwave power ranged from 400 to 500 W, the adsorbates are removed effectively, and deformation of the pores occurred at high temperature. Similarly, Lv et al. (2020) performed regeneration of zeolite by microwave regeneration technique. They observed that the modified zeolite and hybrid adsorbent shows good recycling performance at the first and after several rapid microwave regenerations.

The second technique is microwave-assisted solvent desorption, where the adsorbate is desorbed from the adsorbent using a solvent that is heated by microwave irradiation (W. Zhang et al. 2022). In this technique, the adsorbent is first saturated with the solvent, and then microwave energy is applied to the system. The microwave energy heats the solvent and the adsorbent, causing the VOC molecules to desorb from the surface of the biochar and dissolve in the solvent. The solvent is then removed from the system, leaving behind a regenerated adsorbent that can be reused (Peyravi et al. 2022). This technique is particularly effective for desorbing chemisorbed species, such as pharmaceutical products, dyes, and other reactive organic compounds, which require higher energy for desorption. For example, Q.B. Meng et al. (2013) and Q.B. Meng et al. (2012) reported that polymer adsorbent and MOF exhibits higher microwave-assisted desorption efficiency of benzene. They also indicated that microwave-assisted desorption is favorable for hydrophilic adsorbents. This is because the adsorbent tends to adsorb water and other polar molecules that can be removed efficiently with low-energy microwave radiation (Junfeng Li et al. 2022). Hence, microwave-assisted solvent desorption is a suitable method for hydrophilic adsorbents due to its energy efficiency and effectiveness in removing polar adsorbates. Nevertheless, the drawback of this technique is similar to chemical regeneration due to the amount of solvent or chemical waste, which is not eco-friendly approach.

In TSA, the process involves heating the adsorbent at temperature less than 300 ^{o}C for 1 to 3 h to achieve complete desorption of VOCs from the surface of adsorbent. Subsequently, the system is cooled with an inert gas supply for purging purposes (nitrogen (N_2) or argon (Ar)), resulting in the complete removal of adsorbed VOCs through desorption. The effectiveness of TSA is influenced by specific parameters, such as the type of adsorbent and operating conditions. Certain adsorbents like carbonaceous materials and zeolites exhibit high-temperature resistance, enabling the complete desorption of VOCs at high regeneration temperature. Conversely, some polymers have low-temperature resistance, making them unstable at temperatures exceeding 350°C (W. Zhang et al. 2022). For example, Gabruś et al. (2022) reported that HS zeolite maintained its porous structure after regenerated at temperature of 800 ^{o}C for 1 h, however exhibited poor regeneration efficiency due to incomplete desorption of hexane. Similarly, Hongli Liu et al. (2022) observed incomplete desorption of ethyl acetate at temperature of 150 ^{o}C for 1 h attributed to strong interaction between ethyl acetate and MIL-101. This indicated that adsorbents containing benzene rings in their microporous carbon or material are challenging to desorb due to π-π stacking interactions. While these interactions offer superior selectivity and stronger bonding forces for VOCs, desorption can only occur with higher temperature. On the other hand, hydrophobic adsorbents, such as porous silica required low regeneration temperature due to the weak interaction, which is hydrogen bonding between VOC molecules and the surface of silica. For instance, Ramzy et al. (2014) reported that silica gel achieves maximum desorption efficiency at a regeneration temperature ranging between 90 to 95°C. Similarly, J. Chen et al. (2020) indicated that the pure silica regenerated by thermal treatment at 80 ^{o}C exhibited good desorption efficiency of toluene. This shows that conducting a thermal analysis of the adsorbent, such as through thermogravimetric analysis (TGA), can assess the thermal conditions and determine the optimal regeneration temperature. This approach ensures higher regeneration efficiency while preserving the physicochemical properties of the adsorbent (L. Tan et al. 2022; T. Dutta et al. 2019). Therefore, it is important to take into account both the desorption efficiency and the characteristics of the adsorbent when determining the optimal desorption temperature. However, thermal regeneration may require a significant amount of energy to generate higher temperature to complete the desorption process for certain adsorbents, which could result in high operating costs (Zijian Wang et al. 2023; Yadong Li et al. 2023). Compared to chemical regeneration, thermal regeneration is eco-friendlier as it requires energy and inert gas for the desorption process, while

chemical regeneration produced large amounts of chemical or solvent wastes that required a proper disposal.

2.8 Adsorption kinetic study

Adsorption kinetic study is aimed to investigate the rate and mechanism of adsorption. It involves measuring the rate at which a VOC is taken up by biochar over time, under specific conditions such as temperature, pressure, and concentration. The kinetic study usually involves determining the amount of adsorbate adsorbed by the adsorbent at different time intervals, and then using this data to calculate the rate of adsorption. The results of the kinetic study can provide important information regarding the adsorption process, such as the mechanism of adsorption by isotherms, breakthrough models, and rate-limiting models. This information can be used to optimize the design and operation of adsorption processes for various applications, such as wastewater treatment, air pollution control, and gas separation.

2.8.1 Isotherm models

2.8.1.1 Brunauer-Emmet-Teller (BET) model

Brunauer, Emmet, and Teller (BET) proposed an adsorption isotherm model in 1938, which was based on the multimolecular adsorption theory for gaseous substances. The model included five different types of isotherms, each of which represented a distinct behavior of the adsorbate-adsorbent system (Abu-Alsoud et al. 2020). They accounted for two pressure regions in the adsorption process, and the isotherms showed a concave shape at low pressures and a convex shape at high pressures, particularly near the point of condensation (S. Zhou et al. 2019).

The convex shape of isotherms at high pressures is likely due to the presence of liquid molecules that have condensed within the tiny capillaries of the adsorbent, occurring at a molecular scale. This phenomenon is called capillary condensation and leads to the formation of a multimolecular adsorption layer in systems where non-polar molecules act as adsorbates and ionic adsorbents are used. The surface layer of the adsorbent induces electrical dipoles in the first layer of adsorption, which in turn polarizes the subsequent layers (Adebayo et al. 2020; Buttersack 2019). Several variations of the BET isotherm have been proposed in the literature, with the most widely used version described by Alyousef et al. (2020) in **Eq. (2.4)** as follows:

$$q_e = \frac{q_{mBET} C_{BET} C_e}{(C_{s,BET} - C_e)\left[1 + (C_{BET} - 1)\left(\frac{C_e}{C_{s,BET}}\right)\right]} \quad \textbf{(2.4)}$$

Where q_{mBET} (mg g^{-1}) is the maximum adsorption capacity, $C_{s,BET}$ is the monolayer saturation concentration, C_{BET} (L mg^{-1}) is the BET adsorption constant, and C_e is the equilibrium concentration. The relative pressure (P/P_0) of the BET model ranges from 0.05 to 0.3.

Recently, the BET isotherm has been shown to be effective in predicting the adsorption behavior of organic compounds on soil (vapor-solid), as evidenced by the excellent fit of experimental data to the model (R. Zhang et al. 2022). In addition, Ogungbenro et al. (2018) reported that BET isotherm exhibits the best fit to predict the relationship between VOCs and nanoparticles with high specific surface area (P25-TiO_2) under humid conditions. This is because the BET isotherm assumes that the surface of the adsorbent consists of a series of homogeneous sites, each of which can adsorb one molecule. This model also takes into account the multilayer adsorption phenomenon, which is important in understanding the adsorption of VOCs under humid conditions where water vapor may also be present. Moreover, the BET isotherm has been shown to accurately describe the adsorption of VOCs by various types of porous adsorbents, including activated carbon, zeolites, and silica gel. This is due to the fact that the BET isotherm considers the specific surface area of the adsorbent, which is an important factor in determining the adsorption capacity for gas molecules.

In summary, BET isotherm is one of the best techniques in predicting the relationship between the desired VOC and porous adsorbent. Furthermore, it is important to note that the suitability of the BET isotherm to predict the behavior of VOCs adsorbed into a porous adsorbent under humid conditions can vary depending on the specific adsorbent and VOC being studied, as well as the experimental conditions. Other isotherm models, such as the Toth, Freundlich, and Sips isotherm, may also be suitable for humidity systems.

2.8.1.2 Toth model

The Toth isotherm model is effective to describe the adsorption of a gaseous adsorbate by a porous adsorbent in heterogeneous systems. This semi-empirical equation accurately predict the adsorption phenomena that involve sub-monolayer coverage (Rajahmundry et al. 2021). The Toth model incorporates both the Langmuir adsorption model and Henry's law and can be simplified to

either model depending on the conditions. Specifically, the Toth model can be simplified to the Langmuir model when the adsorption exponent approaches 1, indicating that the adsorption process is homogeneous. Conversely, the Toth model can be represented by Henry's law when the adsorbate concentration approaches zero, indicating that the adsorption process is heterogenous (Serafin et al. 2023; K.V. Kumar et al. 2021) . Additionally, the Toth model assumes that the distribution of quasi-Gaussian energy is asymmetrical, and that many active sites have adsorption energies that are smaller than the maximum value, which contributes to the high accuracy of the model. The Toth isotherm equation can be expressed in **Eq. (2.5)** as follows (Jianlong Wang et al. 2020):

$$q_e = \frac{q_{m,TO} C_e}{\left(K_{TO} + C_e^{z_{TO}}\right)^{1/z_{TO}}} \quad \textbf{(2.5)}$$

where $q_{m,TO}$ is the maximum adsorption capacity (mg g^{-1}), K_{TO} is the constant model, and Z_{TO} is the dimensionless parameter, which represents the inhomogeneity of the adsorbent surface (Z_{TO} <1). The Toth model converted to Langmuir model when Z_{TO} is equal to 1, indicating homogeneous adsorption.

This model is widely used in investigating the behavior of heterogeneous adsorbent-adsorbate systems due to its ease of fitting experimental data. Recent studies by S. Huang et al. (2020) and Adebayo et al. (2020) have shown that the Toth isotherm model was highly effective in describing the adsorption of various VOCs such as n-hexane, cyclohexane, toluene, 1-hexene, 2-methylpentane, 3-methylpentane, 2,2-dimethylbutane, acetone, butanone, and 2-pentanone by activated carbon. Compared to Langmuir, Dual-Site Langmuir (DSL), and Dual-Site Sips (DSS) isotherms, the Toth model provided the best fit to the experimental data, indicating its superiority in describing the adsorption behavior of these VOCs by activated carbon. Furthermore, Yingshu Liu et al. (2023) conducted research on the hydrophobicity of zeolites for VOCs adsorption under humid conditions. Their findings suggest that the Toth isotherm model can be effectively used to study the water uptake mechanisms of zeolites, with the parameter t serving as an index to represent surface heterogeneity. A value closer to 1 indicates more homogeneous adsorption, while a value closer to 0 indicates heterogeneous adsorption. Hence, the Toth isotherm model can be used to analyze the mechanisms involved in the removal of VOCs under humid conditions.

It can be concluded that the Toth isotherm model is an effective method for investigating the behavior of heterogeneous adsorbent-adsorbate systems and gaining insights into the

mechanisms involved in VOCs adsorption by porous adsorbents. The surface heterogeneity parameter (t) indicates the distribution of quasi-Gaussian energy and the proportion of active sites with adsorption energies smaller than the maximum value. A value of t closer to 1 indicates more homogeneous adsorption, while a value closer to 0 represents heterogeneous adsorption. Therefore, the Toth isotherm model is a highly valuable tool for investigating VOCs adsorption and gaining an understanding of the underlying mechanisms involved.

2.8.1.3 Freundlich model

The Freundlich isotherm was originally proposed as an empirical model and has since become a widely used tool for characterizing the adsorption of VOCs onto porous materials with heterogeneous or variable affinities for the adsorbate (Zou et al. 2019). The heterogeneity of the adsorption sites can arise from variations in the adsorption energies, which are influenced by several factors, including the interactions between the VOCs and the porous materials and intermolecular interactions among the VOCs themselves. In particular, multilayer adsorption can lead to complex interactions between the adsorbate molecules and the adsorbent surface, as the adsorbate molecules form layers on top of each other (Bedane et al. 2019). The Freundlich isotherm equation can be expressed in **Eq. (2.6)** as follows (Jianlong Wang et al. 2020):

$$q = K_F \cdot C^{1/n} \quad \textbf{(2.6)}$$

Where q is the amount of VOCs adsorbed per unit mass of adsorbent, C is the equilibrium concentration of VOCs in the humid gas phase, K_F is the Freundlich constant, and n is the Freundlich exponent.

This model consists of two parameters: the Freundlich constant K_F, which represents the adsorption capacity of the adsorbent for the VOCs, and the exponent n, which describes the adsorption process. When n=1, the process is linear; when n<1, it is chemical; and when n>1, it is physical adsorption (Ammendola et al. 2017). For example, S. Huang et al. (2020) synthesized a zeolite and evaluated its performance in adsorbing toluene under humid conditions. They found that the synthesized zeolite had a higher K_F value, indicating a greater adsorption capacity for toluene. Furthermore, the Freundlich exponent n was found to be less than 0.5, indicating that the toluene was primarily adsorbed onto the synthesized zeolite by chemical adsorption processes. However, Pei et al. (2012) reported that the Freundlich isotherm is not suitable for describing the

adsorption mechanism of low VOC concentrations under humid conditions, as the process does not obey Henry's Law, resulting in poor fits to experimental data. Moreover, the model has less agreement at low temperatures and high pressures but shows good agreement at intermediate pressure ranges. Therefore, while the Freundlich isotherm is a useful tool for characterizing VOC adsorption, its limitations must be considered when interpreting experimental results.

Adsorption of VOCs under humid conditions is often challenging because the presence of water vapor in the gas phase can compete with the VOCs for adsorption sites on the porous adsorbent. The Freundlich isotherm can still be used to model the adsorption of VOCs in these conditions. Overall, the Freundlich isotherm provides a useful framework for understanding and predicting the adsorption behavior of VOCs on porous adsorbents under humid conditions, which is relevant for applications such as air pollution control and indoor air quality improvement.

2.8.1.4 Sips model

The Sips isotherm model, first proposed by Sips in 1948, is a hybrid of the Langmuir and Freundlich isotherm models (Sips 1948). This three-parameter model has been widely regarded as the most effective in predicting monolayer adsorption in both homogeneous and heterogeneous systems. Its superiority over the Freundlich model lies in its ability to overcome the limitations associated with high concentrations of the adsorbate (Jianlong Wang et al. 2020). This makes it a valuable tool in various fields of research, including environmental remediation and separation processes. The equation for the Sips isotherm model is as follows (X. Chen et al. 2022):

$$q_e = \frac{q_{m,SP} K_{SP} C_e^{n_{SP}}}{1 + K_{SP} C_e^{n_{SP}}} \quad \textbf{(2.7)}$$

where $q_{m,SP}$ is the maximum adsorption capacity (mg g^{-1}), K_{SP} is the Sips isotherm constant (L mg^{-1}), n_{SP} is the Sips isotherm model exponent (heterogeneity factor). Similar to Toth isotherm, when n_{SP} =1, it is homogeneous adsorption, while n_{SP} >1 the adsorption is heterogeneous.

The Sips model can be converted into Langmuir model to describe the monolayer adsorption (n_{SP} =1). At low VOCs concentrations, it becomes Freundlich model, which does not follow Henry's Law (Jianlong Wang et al. 2020; Feyzbar-Khalkhali-Nejad et al. 2021). This hybrid model offers higher accuracy in predicting the adsorption process, as it incorporates both Langmuir and Freundlich models, providing a better fit to experimental data. Several studies have

demonstrated that the Sips model provides the best fit for describing the adsorption of toluene, 2-butanone, ethanol, xylene, ethylbenzene, and benzene on various porous adsorbents under humid conditions, when compared to Langmuir, Freundlich, and Dubinin-Astakhov (DA) models (Hunter-Sellars et al. 2020; Verma et al. 2019; Uddin et al. 2020). These studies have also suggested that the adsorption processes were heterogeneous, involving multiple interactions, which can be attributed to the presence of multiple surface functional groups on the adsorbent materials. Hence, Sips model is suitable to describe VOCs adsorption under humid conditions because it is a three-parameter hybrid model that combines the Langmuir and Freundlich models. It provides a better fit to experimental data by incorporating both monolayer and multilayer adsorption processes and accounts for heterogeneity in adsorption sites due to the presence of multiple surface functional groups on the adsorbent materials.

Overall, several isotherm models are favorable to investigate the mechanisms involves in the adsorption of VOCs under humid conditions. The selection of isotherm model is crucially depending on the adsorption conditions, the properties of adsorbent and adsorbate. In this study, the VOCs adsorption by biochar was involved with multilayer and heterogenous adsorption due to the present of water vapor (humidity). Thus, Toth, Freundlich, and Sips model are selected in describing the process of VOCs adsorption by biochar due to their assumptions are appropriate for the present study process.

2.8.2 Breakthrough models

2.8.2.1 Bohart-Adam model

The Bohart-Adams model is widely used in the field of chemical engineering to study the behavior of adsorbents in a fixed bed. This model has found applications in various fields such as water purification, air pollution control, and gas separation processes (Hu et al. 2021). The model operates under the assumption that adsorption reactions are not instantaneous and that the rate of adsorption depends on the remaining adsorption capacity of the adsorbent and the concentration of the adsorbate. This assumption is grounded in the surface nature of adsorption, where adsorbate molecules must come into contact with the surface of adsorbent to be adsorbed (Chu 2020). The **Eq. (2.8)** represents the mathematical expression of the Bohart-Adams model, which is widely used in the industry to predict the performance of fixed-bed adsorption systems (Ang et al. 2020). This equation is derived from the mass balance equations that describe the transport of adsorbate

molecules through the adsorbent bed and simplified version of Bohart-Adams model is expressed as follow (Apiratikul et al. 2021):

$$\frac{c}{c_0} = \frac{1}{1 + exp\left[k_{BA}c_0\left(\frac{a_0 x}{uc_0} - t\right)\right]} \quad \textbf{(2.8)}$$

where C_0 and C are defined as the inlet and outlet concentration of the adsorbate (mg L^{-1}), K_{BA} is defined as kinetic constant, a_0 is defined as the adsorption capacity per unit volume of the reactor bed (kg m^{-3}), x is defined as column bed depth (m), and u_0 is defined as inflow gas linear velocity (m min^{-1}).

2.8.2.2 Thomas model

The Thomas model is a widely used mathematical model in the field of adsorption, which takes into account the maximum adsorption capacity of an adsorbent at equilibrium. The model employs the Langmuir isotherm for equilibrium and second-order reversible reaction kinetics, as proposed by Thomas in 1948. The simplified Thomas model is presented as follows (Bai et al. 2022):

$$\frac{c}{c_0} = \frac{1}{1 + exp\left[k_T c_0\left(\frac{q_0 m}{\nu c_0} - t\right)\right]} \quad \textbf{(2.9)}$$

where K_T is defined as kinetic constant, q_0 is defined as adsorption capacity (mg g^{-1}), m is defined as adsorbent mass (g), and ν is defined as volumetric flow rate (m^3 min^{-1}), and t is defined as total flow time (min).

2.8.2.3 Yoon-Nelson model

The Yoon-Nelson model, developed in 1984, offers a straightforward approach for predicting the adsorption and breakthrough of volatile or gaseous adsorbates on adsorbents. The model is based on the premise that the rate of decrease in the probability of adsorption by an adsorbate is proportional to its probability for breakthrough, as evidenced by the changes in breakthrough concentration over time (Yoon et al. 1984). Compared to other models, the Yoon-Nelson model is less complex and requires minimal inputs related to the characteristics of adsorbate, the type of adsorbent, or the physical properties of the adsorption bed (Salehi et al. 2020). This makes the model particularly attractive and an effective tool for predicting

breakthrough and designing adsorption processes. The model is expressed by **Eq. (2.10)** (Gómez-Avilés et al. 2021):

$$\frac{c}{c_0} = \frac{1}{1 + \exp[k_{YN}(\tau - t)]} \quad \textbf{(2.10)}$$

where k_{YN} is the rate constant (min^{-1}), τ is the time required for adsorbate breakthrough to reached 50%, and t is the time of adsorption (min). The inlet concentration, C_0 is assumed to achieve the adsorption breakthrough when the concentration of the adsorbate, C reached 10%. Then, assumed that the adsorption saturation is achieved when C reached 95%.

Overall, simplified models, including the Bohart-Adams, Thomas, and Yoon-Nelson models, have been developed based on the principles of mass transfer in adsorption systems. These models provide a simplified framework for predicting the performance of adsorption processes, and are widely used for practical design purposes. The Bohart-Adams model assumes that the adsorption reaction is not instantaneous, and that the rate of adsorption is dependent on the remaining adsorption capacity of the adsorbent and the concentration of the adsorbate. The Thomas model, on the other hand, assumes that the adsorbate concentration in the adsorption bed decreases exponentially with time, and that the rate of adsorption is proportional to the remaining adsorption capacity of the adsorbent. The Yoon-Nelson model assumes that the probability of adsorption by an adsorbate decreases at a rate proportional to its probability of breakthrough. Despite their simplicity, these models have been shown to provide satisfactory predictions of experimental data for most practical design purposes.

2.8.3 Rate-limiting adsorption mechanisms

Diffusional models are commonly used to explain the adsorption of gas pollutants onto biochar. These models are built on the assumption that the transport of adsorbate molecules from the gas phase to the biochar surface occurs more slowly than the actual adsorption process (Largitte et al. 2016). As such, diffusion is typically considered the rate-limiting step in the overall adsorption process. Three main diffusional models are often used: interparticle diffusion, intraparticle diffusion and Boyd's film-diffusion model. These models allow for accurate predictions of the rate-limiting step involved in the adsorption of VOCs onto biochar.

2.8.3.1 Interparticle diffusion models

The interparticle diffusion model proposes that interparticle diffusion is the rate-limiting step in the adsorption process. In practice, this model often assumes that particles are roughly spherical in shape, which allows for an explanation of the diffusion mechanism in a spherical coordinate system (Kudahi et al. 2017). By considering an equivalent sphere, this approximation simplifies the mathematical representation of interparticle diffusion. The model is expressed as follows (Goel et al. 2021):

$$\frac{dq}{dt} = D_c\left(\frac{\partial^2 q}{\partial r^2} + \frac{2}{r}\frac{\partial q}{\partial r}\right) \quad \textbf{(2.11)}$$

Then the boundary condition are $q(r,0) = q_0$', $q(r_c,t) = q_0$, $(\frac{\partial q}{\partial r})_{r=0} = 0$, giving the following solution:

$$\frac{q_t}{q_e} = 1 - \frac{6}{\pi^2}\sum_{n=1}^{\infty}\frac{1}{n^2}e^{\left(-\frac{n^2\pi^2 D_c t}{r_p^2}\right)} \quad \textbf{(2.12)}$$

where Dc is defined as the diffusivity in the adsorbent, r_p is defined as the radius of the particles. From the experimental q_t/q_e, the diffusion time constant $t_D = D_c/r^2_p$ (min^{-1}) can be obtained by **Eq. (2.11)**. Specifically, when the value of q_t/q_e exceeds 70%, the higher terms in the summation can be considered negligible and **Eq. (2.12)** can be reduced to only the first term:

$$1 - \frac{q_t}{q_e} \approx \frac{6}{\pi^2}exp\left(-\frac{\pi^2 D_c t}{r_p^2}\right) \quad \textbf{(2.13)}$$

When interparticle diffusion is the rate-controlling resistance, the adsorption process approaches equilibrium over a long time period. At this stage, a plot of ln(1 − qt/qe) versus t should be linear, with a slope of $-D_c/r^2_p$. This slope can be used to calculate the diffusion time constant. Furthermore, the intercept of this plot should be $\ln(6/\pi^2)$. If the plot does not follow this pattern, it suggests that other factors are controlling the adsorption process.

2.8.3.2 Boyd's films-diffusion model

The Boyd's film-diffusion models primarily focus on the mass transfer from the bulk gas phase to the surface of biochar, and it is assumed to be the slowest step in the process attributed to the diffusion of adsorbate through the boundary layer (Ece et al. 2022). This is also known as

external resistance to mass transfer. The Boyd's model is generally used to describe the diffusion of adsorbate through a boundary layer. This model expressed as follows (Raganati et al. 2019):

$$F = 1 - \frac{6}{\pi^2} \sum_{n=1}^{\infty} \frac{1}{n^2} exp(-n^2 B_t) \quad \textbf{(2.14)}$$

where F is defined as the fractional uptake at given time (q_t/q_e), B_t is a mathematical function of F based on:

when F more than 0.85,

$$B_t = f(F) = -0.4977 - \ln(1 - F) \quad \textbf{(2.15)}$$

when F less than 0.85,

$$B_t = f(F) = \left(\sqrt{\pi} - \sqrt{\pi - \left(\frac{\pi^2 F}{3} \right)} \right)^2 \quad \textbf{(2.16)}$$

Plotting B_t against time can provide insight into the mechanism governing the adsorption process, specifically whether it is controlled by film diffusion or intraparticle diffusion. If the resulting plot is a straight line that passes through the origin, the adsorption rate is primarily governed by intraparticle diffusion. Conversely, if the plot deviates from a straight line or does not pass through the origin, it indicates that the adsorption rate is influenced by film diffusion (Goel et al. 2021).

2.8.3.3 Intraparticle diffusion models

The intraparticle diffusion model describes the mass transfer within the interior of the particles and can be expressed using the intraparticle diffusion coefficient. The intraparticle diffusion model (IP) was developed by Weber-Morris and has been widely adopted for the analysis of adsorption kinetics (Bernal et al. 2020). In this model, the mass transfer inside the adsorbent particles is described by the intraparticle diffusion coefficient, which is a measure of how easily the adsorbate molecules can diffuse into the interior of the adsorbent particles. The relationship between the operating time and the amount of adsorption in the IPD model can be expressed as follows (G. Zhang et al. 2019):

$$q_t = k_p t^{\frac{1}{2}} + C \quad \textbf{(2.17)}$$

where q_t is the adsorption capacity at time t (mg g^{-1}), k_p is the IPD rate constant (min^{-1}), t is adsorption time (min), and C is related to the boundary layer thickness. A plot of q_t against $t^{0.5}$ should result in a straight line with a slope of k_P, when interparticle (IP) diffusion is the rate-limiting step. However, if other factors come into play, C will have a non-zero value and the plot will not pass through the origin. In such cases, it can be concluded that IP diffusion is not the only rate-limiting step.

The rate-limiting adsorption mechanisms can be described by interparticle, Boy's film, and intraparticle diffusion models. Among these models, the intraparticle diffusion model is the most commonly used to accurately describe the mass transfer within the interior pores of biochar. In summary, several adsorption kinetic models are beneficial for the study of adsorption mechanisms, the performance of biochar, and rate-limiting step of the VOCs adsorption under humid condition, as tabulated in **Table 2.3**. The selection of the most appropriate kinetic model depends on the specific conditions of the adsorption process and the properties of the adsorbent and adsorbate. The use of these models can aid in understanding the adsorption mechanisms and performance of biochar for VOCs removal under humid conditions.

Table 2.3: Summary of the adsorption kinetics models.

Model	Equation	Reference
Isotherm		
Brunauer, Emmet, and Teller (BET)	$q_e = \frac{q_{mBET} C_{BET} C_e}{(C_{s,BET} - C_e)\left[1 + (C_{BET} - 1)\left(\frac{C_e}{C_{s,BET}}\right)\right]}$	(Al-Ghouti et al. 2020)
Toth	$q_e = \frac{q_{m,TO} C_e}{\left(K_{TO} + C_e^{z_{TO}}\right)^{1/z_{TO}}}$	(Jianlong Wang et al. 2020)
Freundlich	$q = K_F \,.\, C^{1/n}$	(Jianlong Wang et al. 2020)
Sips	$q_e = \frac{q_{m,SP} K_{SP} C_e^{n_{SP}}}{1 + K_{SP} C_e^{n_{SP}}}$	(X. Chen et al. 2022)
Breakthrough		
Bohart-Adam	$\frac{c}{c_0} = \frac{1}{1 + exp\left[k_{BA} c_0 \left(\frac{a_0 x}{u c_0} - t\right)\right]}$	(Apiratikul et al. 2021)
Thomas	$\frac{c}{c_0} = \frac{1}{1 + exp\left[k_T c_0 \left(\frac{q_0 m}{\nu c_0} - t\right)\right]}$	(Bai et al. 2022)
Yoon-Nelson	$\frac{c}{c_0} = \frac{1}{1 + \exp[k_{YN}(\tau - t)]}$	(Shiue et al. 2011; Zhirui Li et al. 2021)
Diffusional		
Interparticle	$1 - \frac{q_t}{q_e} \approx \frac{6}{\pi^2} exp\left(-\frac{\pi^2 D_c t}{r_p^2}\right)$	(Goel et al. 2021)
Boyd's firm	$F = 1 - \frac{6}{\pi^2} \sum_{n=1}^{\infty} \frac{1}{n^2} exp(-n^2 B_t)$	(Raganati et al. 2019)

Table 2.3 *(Continue)*

Model	Equation	Reference
Diffusional		
Intraparticle diffusion	$q_t = k_p t^{\frac{1}{2}} + C$	(Bernal et al. 2020)

In conclusion, adsorption is the most favorable technology for the removal of VOCs due to its low operating cost, environmental safety, and ability to recycle and reuse adsorbent and adsorbate compared to other available technologies (P.S. Kumar et al. 2019; Chai et al. 2021; Bushra et al. 2021). The adsorption process can be categories into physisorption and chemisorption, which describes the interactions between VOC molecules and surface of biochar. The selection of porous adsorbent is crucial for adsorption application. Commonly used porous adsorbent including activated carbon (AC), graphene, carbon nanotubes (CNTs), metal-organic frameworks (MOFs), and biochar. Among them, biochar is a promising adsorbent for the removal of VOCs due to its highly porous, low-cost, and abundant feedstocks. The characteristics of biochar, as well as properties of VOCs and operating conditions, significantly influence the performance of biochar for VOCs adsorption. To date, only a few literatures study the performance of biochar for VOCs adsorption under humid conditions. By structural and surface modification, the pore structure, specific surface area, and surface functional groups of biochar can be altered to provide honeycomb-like tubular structure, higher specific surface area, and introduce polydimethylsiloxane (PDMS) on the surface of biochar for higher VOCs selectivity under humid conditions. Several regeneration techniques, including chemical, microwave, and thermal regeneration, can be used to desorb the adsorbed VOCs from the biochar. The importance of biochar regeneration lies in promoting cost-effectiveness, environmental sustainability, improved efficiency, extended lifespan, and versatility, which are beneficial for various industrial fields.

In addition, to study the adsorption mechanisms and performance of biochar under humid conditions, various models, such as adsorption isotherm models (BET, Freundlich, Toth, and Sips models), breakthrough models (Borhart-Adams, Thomas, and Yoon-Nelson models), and diffusion models (interparticle, Boyd's film, and intraparticle models) can be used to describe the mechanisms involved. These models are useful in accurately assessing the effect of water vapor on VOCs adsorption and determining the rate-limiting step of the adsorption process.

Therefore, the development of hydrophobic modified honeycomb-like tubular biochar (hydrophobic HT-B) aims to address the gaps in VOCs adsorption under humid conditions. Hydrophobic HT-B has a high specific surface area, honeycomb-like tubular structure, and high VOCs selectivity, making it capable of promoting higher VOCs adsorption under humid conditions.

CHAPTER 3

RESEARCH METHODOLOGY

3.1 Research experiment flowchart

The research methodology in this study consists of four stages: 1) preparation of honeycomb-like tubular biochar (HT-B), 2) surface modification of HT-B and parametric optimization of polydimethylsiloxane (PDMS) coating, 3) acetone adsorption, and 4) regeneration of PDMS-coated HT-B, as shown in **Figure 3.1**. Stage 1 described the formation of HT-Bs synthesized from palm leaves (PL), pinewood sawdust (PWS), and corn stalks (CS). The preparation of HT-Bs include the impregnation of $ZnCl_2$ at different concentrations (0.5 M, 1.0 M, and 1.5 M), and then carbonized under inert condition (argon gas) at 800 ^{o}C for 6 h. This stage was repeated with different raw materials. Stage 2 illustrates the PDMS coating via the thermal evaporation method. Three optimization parameters, such as coating ratio (HT-B: PDMS), modification temperature, and reaction time were studied to obtain the optimum conditions for the formation of hydrophobic HT-B through water contact angle. Next, the optimized hydrophobic HT-B was used for acetone adsorption at different relative humidities of 50%, 70%, and 90%. Lastly, the hydrophobic HT-B was regenerated via thermal regeneration to evaluate its reusability in the acetone adsorption application. The regeneration process was repeated until the final cycles. The bare biochars, HT-Bs, and hydrophobic HT-Bs were characterized via BET, SEM&EDS, FTIR, and DSA to evaluate the changes in its physicochemical properties and were replicates with average three times.

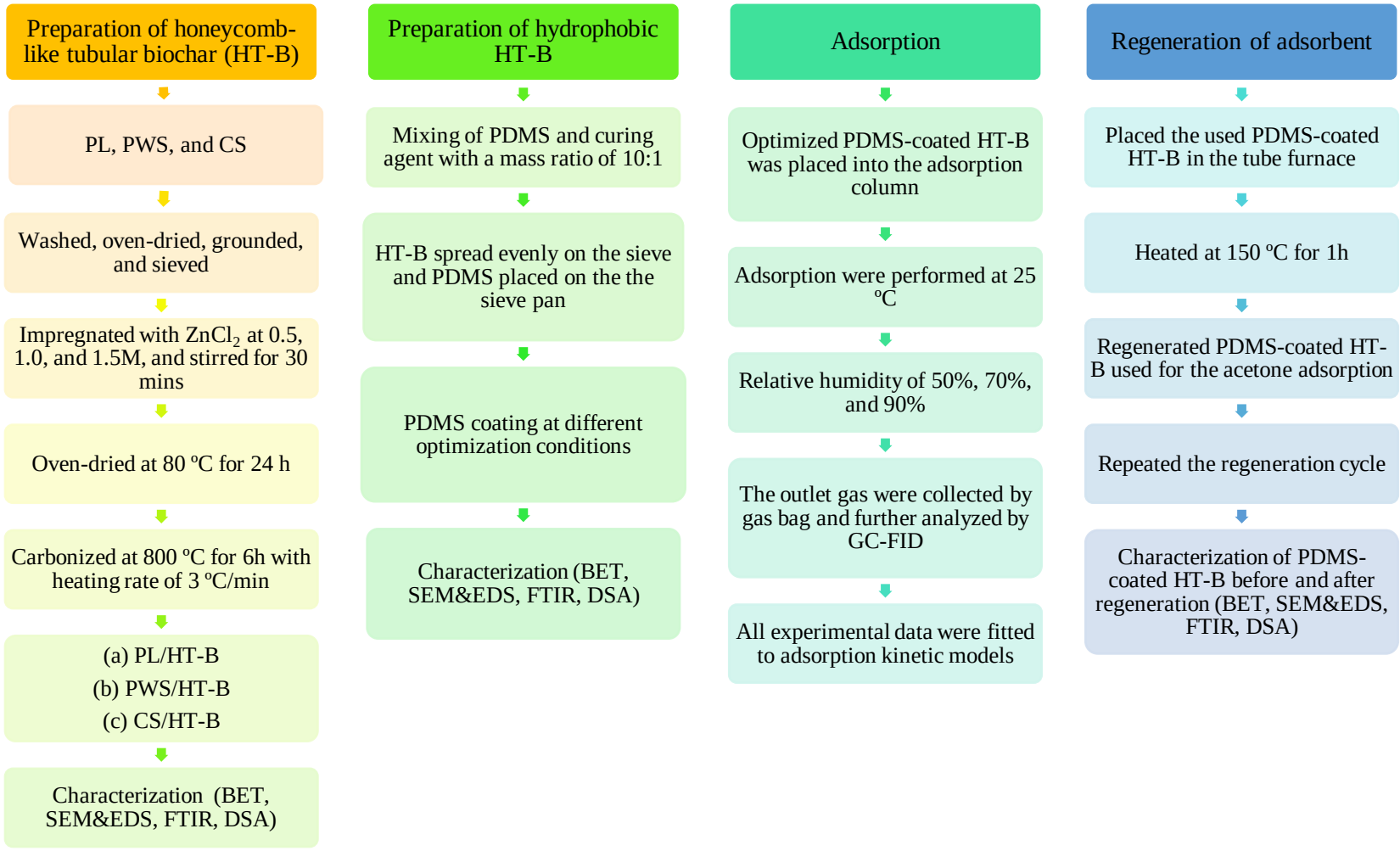

Figure 3.1: The flow chart of the experimental.

3.2 Materials

The $ZnCl_2$ (CAS No. 108816.0250-250g), acetone (CAS No. 67-64-1-2.5L), hydrochloric acid (CAS No. 7647-01-0), and PDMS (CAS No. 761036) were purchased from Sigma-Aldrich. The corn stalks were collected from the supermarket waste, palm leaves were supplied by Woodman Sdn. Bhd., and pinewood sawdust were provided by Alex Metalwork Sdn. Bhd. in Miri, Sarawak (Lat: 4° 23´ N, Long: 113° 59´ E).

3.3 Preparation of honeycomb-like tubular biochar

The preparation of HT-B is illustrated in **Figure 3.2.** First, the PL were washed, oven-dried at 80 ºC for 24 h, grounded using miller analytical, and sieved into a power form (100-200 mesh). Then, 5 g of PL powder was weighted and impregnated at different concentrations of $ZnCl_2$ (0.5, 1.0, and 1.5 M) under magnetic stirring condition for 30 min. Next, the pre-treated PL powder was oven-dried at 80 ºC for 24 h. After that, 2 g of pre-treated PL powder was weighed and placed in a ceramic boat, then was carbonized under an inert atmosphere at 800 ºC for 6 h with a heating rate of 3 ºC min^{-1} in a tube furnace. After cooling, the PL/HT-B was refluxed by dilute hydrochloric acid (HCl) at 80 ºC for 2 h, followed by excessive washing with deionized water and oven-dried overnight at 105 ºC. This procedure was repeated for PWS and CS. Then, the HT-Bs were labelled as HT-B follows by the impregnated concentration as shows in **Table 3.1.**

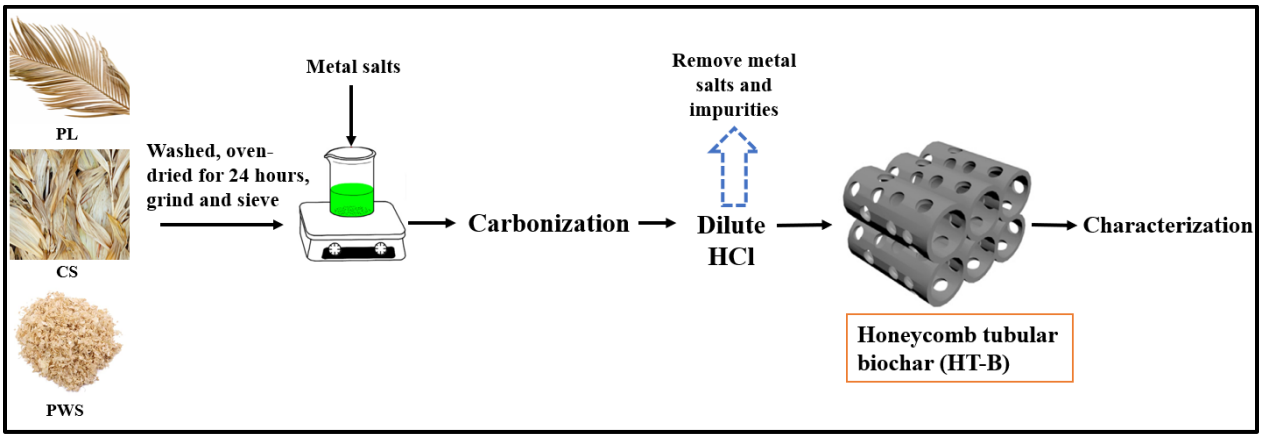

Figure 3.2: Schematic diagram of HT-B preparation (C. Ma et al. 2018)

Table 3.1: The label name of the HT-Bs.

$ZnCl_2$ concentration (M)	Samples	Label name
0.5	PL	PL/HT-$B_{0.5M}$
	PWS	PWS/HT-$B_{0.5M}$
	CS	CS/HT-$B_{0.5M}$
1.0	PL	PL/HT-B_{1M}
	PWS	PWS/HT-B_{1M}
	CS	CS/HT-B_{1M}
1.5	PL	PL/HT-$B_{1.5M}$
	PWS	PWS/HT-$B_{1.5M}$
	CS	CS/HT-$B_{1.5M}$

3.4 Surface modification of HT-B and parametric optimization of the PDMS coating

The optimization study was conducted by using the one-factor-at-a-time (OFAT) method and the optimization parameters are tabulated in **Table 3.2**. The three main optimization parameters for the PDMS coating are coating ratio, modification temperature, and reaction time. The range of these parameters were determined based on recent studies (Xiuquan Li et al. 2020; E.J. Park et al. 2014; Lan et al. 2016). The coating was performed by weighing 25 g of PDMS and placed on the stainless-steel sieve pan, then the stainless-steel sieve with a pore measurement of 100-200 mesh was placed over it, as shown in **Figure 3.3**. Next, 1 g of CS/HT-B_{1M} was placed evenly on the sieve, and finally the sieve was sealed and heated in the furnace at modification temperature of 200 ºC for 1 h (Xiuquan Li et al. 2020). The HT-B coated with PDMS was cooled down at room temperature, collected and closed storage for the next applications. This procedure was repeated at different optimization conditions. Then, the yields were labelled as CS/HT-B_{1M}PDMS.

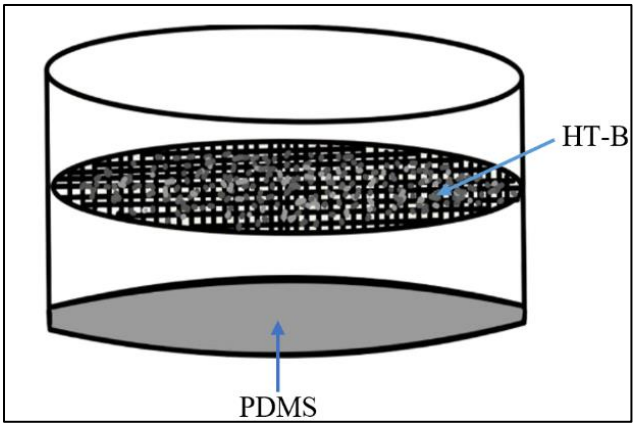

Figure 3.3: Schematic diagram of PDMS-coated HT-B preparation

Table 3.2: Optimization parameters for the formation of CS/HT-B_{1M}PDMS

No	Parameter	Unit	Range
1	Coating ratio (HT-B: PDMS)	g	1:15, 1:20, 1:25, 1:30
2	Modification temperature	ºC	150, 200, 250, 300
3	Reaction time	h	0.5, 1, 1.5, 2

3.5 Characterization

The specific surface area, pore volume, and average pore diameter of the bare biochars, HT-Bs, and hydrophobic HT-Bs were analyzed by Brunauer-Emmett-Telle (BET), with Sorptometric 1990 Series. The samples were degassed at 300 ºC for 8 h. Their surface morphology and chemical compositions were studied by using a Scanning electron micrograph (SEM-EDS), with Thermo Scientific Quattro S, which operated at 12.5-15 kV.

The surface functional groups of the bare biochars, HT-Bs, and hydrophobic HT-Bs were analyzed by the Attenuated total reflection infrared spectroscopy (ATR-IR) technique with transmission mode between 650-4000 cm^{-1} using a Fourier transform infrared spectroscopy (FTIR), with Cary 630.

The hydrophobicity of the bare biochars, HT-Bs, and hydrophobic HT-Bs were evaluated by water contact angle using a drop shape analyzer (DSA), with Kruss DSA 100B. The biochar was fixed with double-sided tape and flattened on a glass slide. Then, approximately 3µL of

deionized water was pipetted on the surface of each biochar at 3 different sites, and the average water contact angle from different sites were used as the results and Young-Laplace equation was adopted to determine the water contact angle measurement.

3.6 Acetone adsorption

Figure 3.4 illustrates the acetone adsorption set-up that consists of three sub-systems. The first sub-system is the gas generation which composed of air compressor as a carrier gas, and acetone and water vapors were produced by bubbler. The carrier gas transport acetone and water vapors to the adsorption column sub-system, where the U-shape tube with a measurement of 127 mm in height and 10 mm inner diameter was placed in the water bath to maintain the adsorption temperature at 25 °C. The CS/HT-B_{1M}PDMS was weighted at 1 g and placed at the bottom of the U-shape tube, then both sides of the opening tubes were closed. The flow of carrier gas was detected by a gas flowmeter of 25 ml min^{-1}. The acetone vapors were maintained at concentration of 8 ml g^{-1} and the relative humidity of 50%, 70%, and 90% were detected by humidity hygrometer (Xiuquan Li et al. 2020). The last sub-system involves analysis by gas chromatography (GC-FID), with Agilent 8890 and computer for data storage. The inlet and outlet concentration of acetone in gas stream were constantly measured by GC-FID and the results were labeled as C_0 and C_t.

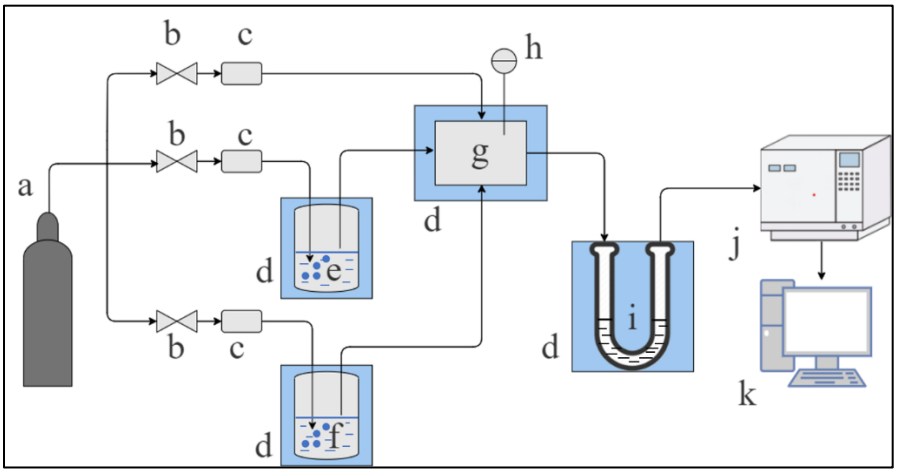

Figure 3.4: Scheme of acetone adsorption: a. gas cylinder (compressed air); b. valve; c. mass flowmeter; d. water bath; e. acetone; f. deionized water; g. mixer; h. humidity hygrometer; i. adsorption column; j. gas chromatography; k. data collector (Yin et al. 2020)

3.7 Adsorption kinetic

3.7.1 Isotherm model

The Toth, Freundlich, and Sips models were used to describe the mechanisms of the acetone adsorption onto CS/HT-B_{1M}PDMS under humid condition. The Toth model expression is shown in **Eq. (3.1)** (Jianlong Wang et al. 2020):

$$q_e = \frac{q_{m,TO} C_e}{\left(K_{TO} + C_e^{Z_{TO}}\right)^{1/Z_{TO}}} \quad \textbf{(3.1)}$$

where $q_{m,TO}$ is the maximum adsorption capacity (mg g^{-1}), K_{TO} is the constant model, and Z_{TO} is the dimensionless parameter, which represents the inhomogeneity of the adsorbent surface (Z_{TO} <1). The Toth model converted to Langmuir model when Z_{TO} is equal to 1, indicating homogeneous adsorption.

The Freundlich equation is shown in **Eq. (3.2):**

$$q = K_F \, . \, C^{1/n} \quad \textbf{(3.2)}$$

where q is the amount of VOCs adsorbed per unit mass of adsorbent, C is the equilibrium concentration of VOCs in the humid gas phase, K_F is the Freundlich constant, and n is the Freundlich exponent.

The Sips model expression as shown in **Eq. (3.3)**

$$q_e = \frac{q_{m,SP} K_{SP} C_e^{n_{SP}}}{1 + K_{SP} C_e^{n_{SP}}} \quad \textbf{(3.3)}$$

where q_{ms} is the maximum adsorption capacity (mg g^{-1}), K_s is the Sips isotherm constant (L mg^{-1}), n_s is the Sips isotherm model exponent (heterogeneity factor). Similar to Toth isotherm, when n_s=1, it is homogeneous adsorption, while n_s<1 the adsorption is heterogeneous.

3.7.2 Breakthrough model

Fixed bed adsorption is applied in the gas adsorption kinetic of the adsorbent to identify the characteristics of the acetone adsorption onto CS/HT-B_{1M}PDMS at different relative humidity. The

breakthrough models are adopted and assumed by using Bohart-Adam (B-A), Thomas, and Yoon-Nelson models (Y-N). The Bohart-Adam equation is expressed as follows (Apiratikul et al. 2021):

$$\frac{c}{c_0} = \frac{1}{1 + exp\left[k_{BA}c_0\left(\frac{a_0 x}{uc_0} - t\right)\right]} \quad \textbf{(3.4)}$$

where C_0 and C are defined as the inlet and outlet concentration of the adsorbate (mg L^{-1}), K_{BA} is defined as kinetic constant, a_0 is defined as the adsorption capacity per unit volume of the reactor bed (kg m^{-3}), x is defined as column bed depth (m), and u_0 is defined as inflow gas linear velocity (m min^{-1}).

The Thomas equation is shown in **Eq. (3.5)** (Bai et al. 2022):

$$\frac{c}{c_0} = \frac{1}{1 + exp\left[k_T c_0\left(\frac{q_0 m}{\nu c_0} - t\right)\right]} \quad \textbf{(3.5)}$$

where K_T is defined as kinetic constant, q_0 is defined as adsorption capacity (mg g^{-1}), m is defined as adsorbent mass (g), and ν is defined as volumetric flow rate (m^3 min^{-1}), and t is defined as total flow time (min).

The Yoon-Nelson expression as shown in **Eq. (3.6)** (Zhirui Li et al. 2021):

$$\frac{c}{c_0} = \frac{1}{1 + \exp[k_{YN}(\tau - t)]} \quad \textbf{(3.6)}$$

where C_0 and C are the inlet and outlet concentration of the adsorbate (mg L^{-1}), π is the time required for adsorbate breakthrough to reach 50%, K_{YN} is the rate constant (min^{-1}) and t is the time of adsorption (min). The inlet concentration, C_0 is assumed to achieve the adsorption breakthrough when the concentration of the adsorbate, C reached 10%. Then, assumed that the adsorption saturation is achieved when inlet concentration, C_0 reached 90%.

The adsorption capacity of acetone with CS/HT-B_{1M}PDMS under humid conditions can be calculated by using the following equation (Xiuquan Li et al. 2020):

$$q = \frac{F.C_0}{M}\left(T_s - \frac{1}{C_0}\int_0^{T_s} C_t . dT_s\right) \quad \textbf{(3.7)}$$

where q is the adsorbed molecule amount mg g^{-1}, C_0 and C_t are the inlet and outlet concentration (mg L^{-1}), M is the mass of adsorbent (g) and T_s is the saturation time that can be obtained from the breakthrough curves.

3.7.3 Intraparticle diffusion model

The intraparticle diffusion model (IPD) developed by Weber and Morris has been widely adopted for the analysis of the rate-limiting step in the adsorption process. The relationship between operating time and the amount of adsorption can be expressed as follow (Bernal et al. 2020):

$$q_t = k_p t^{\frac{1}{2}} + C \quad \textbf{(3.8)}$$

where q_t is the adsorption capacity at time t (mg g^{-1}), k_p is the IPD rate constant (min^{-1}), t is adsorption time (min), and C is related to the boundary layer thickness. A plot of q_t against $t^{0.5}$ should result in a straight line with a slope of k_P, when interparticle (IP) diffusion is the rate-limiting step.

3.8 Regeneration of biochar

The hydrophobic HT-B was regenerated in a tube furnace at 150 ºC for 1 h with a constant flow of inert gas (argon) to desorb the adsorbed acetone and water molecules. Then, the regenerated hydrophobic HT-B was again used as an adsorbent for the acetone adsorption at relative humidity of 90% to evaluate its reusability. The regeneration was repeated until the final cycle, where the regenerated hydrophobic HT-B shows a constant acetone adsorption capacity.

CHAPTER 4

RESULTS AND DISCUSSION

The characteristics of adsorbent play a crucial role in the adsorption of VOCs under humid conditions. Honeycomb-like structure of biochar could enhance the reaction rate, increase the specific surface area, and providing abundant adsorption active sites for the adsorption of VOCs (L. Yan et al. 2020). Various metal salts such as $CoCl_3$, $FeCl_3$, $CaCl_2$, and $ZnCl_2$ (Lingli Zhu et al. 2020) have been studied to enhance the pore structures. Among, $ZnCl_2$ is the most favorable in forming a honeycomb-like structure due to its low melting point of 420 ºC (Adeniyi et al. 2022). The hydrophilic nature of HT-B can be modified by coating surface functional groups such as trimethylchlorosilane (TMCS), polyacrylonitrile (PAN), and polydimethylsiloxane (PDMS) to improve the adsorption capacity of VOCs in humid condition. In this section, the physicochemical changes and its VOC adsorption performance of the hydrophobic modified HT-B are evaluated and discussed.

4.1 Morphology of the micropores on selected biomasses and its respective HT-B

The microstructure of the biochars synthesized under different conditions were analyzed using scanning electron microscopy (SEM). The SEM images provide information about the surface morphology of the synthesized biochar and its features such as the pore structures, and pore size.

The morphology and structure of the bare biochar and their respective HT-Bs derived from palm leave (PL), pinewood sawdust (PWS), corn stalk (CS) are illustrated in **Figure 4.1 – Figure 4.3**. The SEM images show significant difference between the surface morphology of the bare biochar and their respective HT-Bs treated at different concentration of $ZnCl_2$. Generally, the bare biochars show fewer and smaller pores, rougher surface, and demonstrates heterogeneity compared

to their respective HT-Bs. The nature of the selected biomasses (PL, PWS, and CS) consist of vascular bundles and fiber which were attributed to the tubular structure. These characteristics serve as a template for the formation of honeycomb-like tubular structures. The tubular structure that consists of abundant adsorption active sites further enhanced the attachment of $ZnCl_2$ for the formation of HT-Bs (C. Ma et al. 2018).

Generally, the impregnated HT-Bs at 0.5 M $ZnCl_2$ show the formation of incomplete and asymmetric honeycomb-like tubes, in contrast, at 1.5 M, the pores are collapsed and widened. The widening of pores occur due to the high concentration of metal ion adsorbed into the precursor matrix and intensified during the carbonization process, whereas lower concentration results in insufficient amount of metal ions to develop a complete pore structure (F. Zhao et al. 2021; Cai et al. 2022). The HT-Bs that were treated at 1.0 M exhibit uniformly distributed fenestrations on the cellular surface and a more stable honeycomb-like tubular structure. Similar to C. Ma et al. (2018) and Karapınar (2021), who discovered that activated carbon treated at 1.0 M of $ZnCl_2$ exhibited high specific surface area with abundant adsorption active sites, and showed well-developed honeycomb-like tubular structure. Hence, 1.0 M of $ZnCl_2$ is used for the formation of HT-Bs for the subsequent studies.

Among the HT-Bs, HT-B derived from CS exhibited superior honeycomb-like tubular structure with high porosity and better homogeneity compared to PL and PWS. This is mainly attributed to the lignocellulosic compositions of CS with cellulose, hemicellulose and lignin content at 27.8%, 10.1%, and 34.1% respectively. CS has a higher lignin content than that of PL (27.1%) and PWS (25.6%), which promoted the formation of honeycomb-like tubular structure (X. Lu et al. 2022; Syarifah et al. 2021; Jiong Wang et al. 2022). Hence, it was selected for further studies. The formation of tubular structure first occurs in macropores, where the arrangement is formed by thin carbon walls with a gap distance ranging from 10-40 μm (S. Dutta et al. 2014). These walls are associated with percentage of cellulose, hemicellulose, and lignin content from the biomasses. Lignin helps to maintain the tubular cell wall structure because of its tough biopolymeric structure and only decomposes at a high temperature (Tian et al. 2020; F. Shi et al. 2021). Then, the pores are formed from the evaporation of metal chloride, leaving a vacant space and resulted in the pores widening in accordance with the structure of lignin (Thue et al. 2017). The low melting point of metal chloride favors the formation of HT-B with high specific surface

area because it evaporates rapidly during the carbonization process. As a result, at 800 °C, CS impregnated at 1.0 M of $ZnCl_2$ successfully synthesized a well-developed HT-B, as show in **Figure 4.3 (c)**. This indicated that melting point of metal chloride plays a significant role in the development of micropores structure (Xiaohu Yang et al. 2016; Thue et al. 2017; Özhan et al. 2014). Moreover, the pore diameter of the HT-Bs does not follow a consistent trend with the increase in $ZnCl_2$ concentration from 0.5 to 1.5 M. This outcome aligns with the findings of Xueyang Zhang et al. (2022), who observed a similar inconsistency in pore diameter trends as the impregnation ratio increased. The irregularities were attributed to the formation of micropores from lignin during the carbonization process. They also further noted that the augmentation of micropore volume led to a reduction in pore diameter. These observations are consistent with the BET analysis of the HT-Bs, as presented in **Table 4.1** in **Section 4.3**.

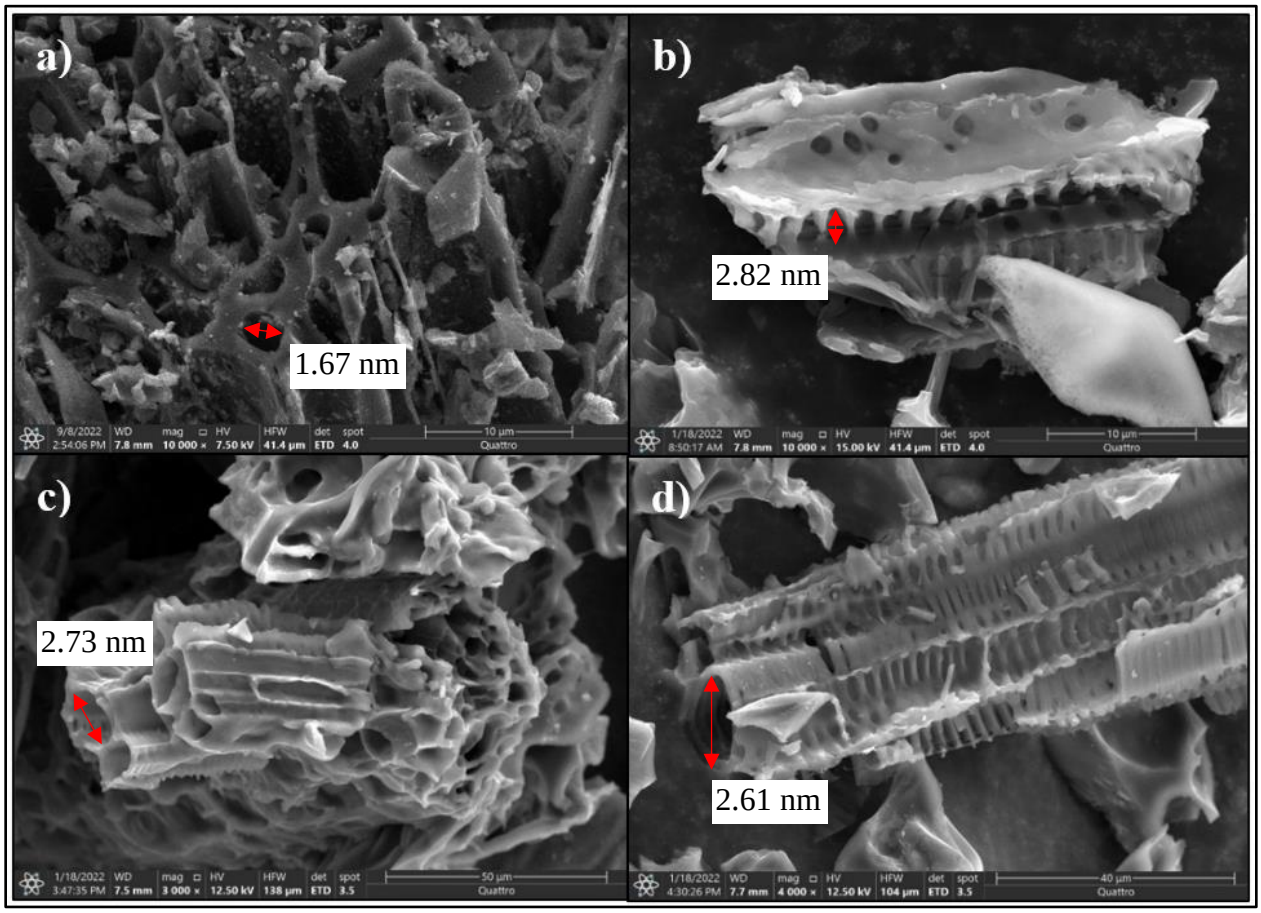

Figure 4.1: SEM micrographs of a) PL/BC and treated with $ZnCl_2$ at b) 0.5 M, c) 1.0 M, and d) 1.5 M

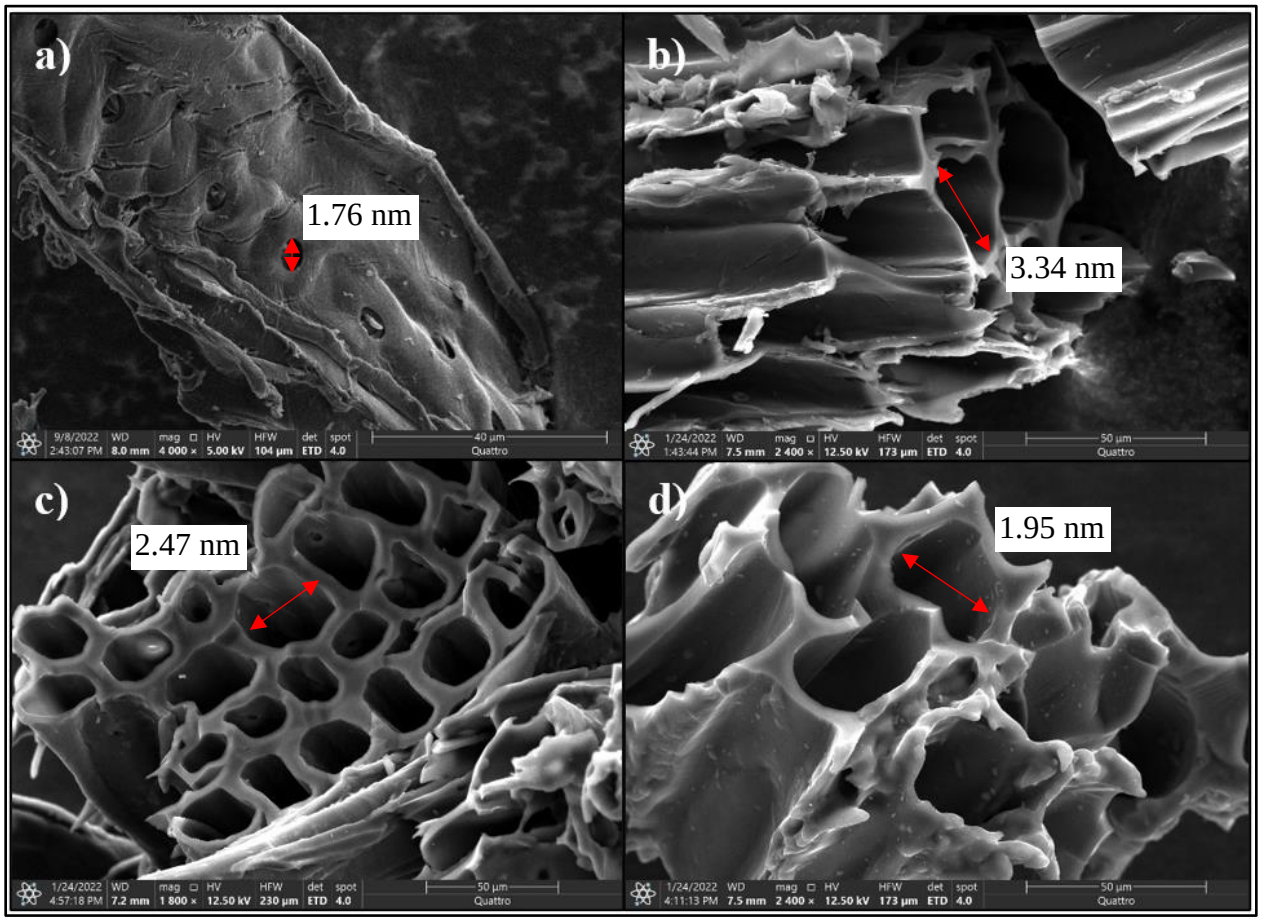

Figure 4.2: SEM micrographs of a) PWS/BC and treated with $ZnCl_2$ at b) 0.5 M, c) 1.0 M, and d) 1.5 M

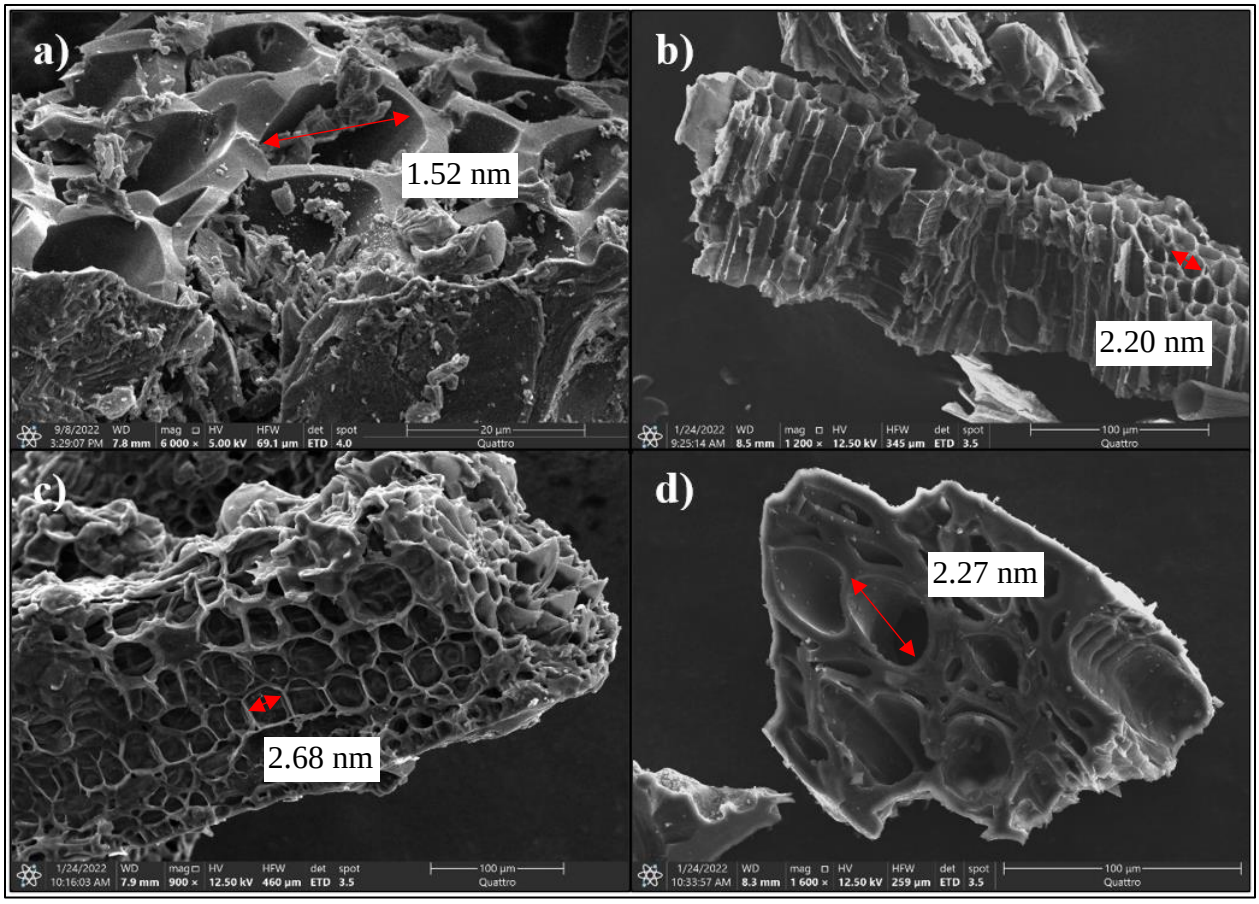

Figure 4.3: SEM micrographs of a) CS/BC and treated with $ZnCl_2$ at b) 0.5 M, c) 1.0 M, and d) 1.5 M

4.2 Surface modification of HT-B and parametric optimization of CS/HT-B_{1M}PDMS

Humidity is one of the challenges to be resolved for the adsorption of VOCs in the industry, particularly in the separation process (Yin et al. 2020). In order to overcome the challenge, the hydrophobicity of the adsorbent plays an important role. The synthesized HT-Bs that have high porosity requires further modifications to cater for such condition. In general, HT-Bs are hydrophilic in nature leading to poor VOCs adsorption performance due to the presence of water molecules. The water molecules compete with VOCs for the adsorption active sites, which decreased the selectivity of VOCs. Thus, changing the hydrophobicity of the HT-Bs could increase the adsorption capacity at high relative humidity (Jiaxing Wang et al. 2021; Hunter-Sellars et al.

2020). In this study, HT-Bs were coated with PDMS, and the water contact angels were analyzed as an indication of the modified hydrophobicity.

The water contact angles of the HT-Bs were tested to identify the changes in their surface properties. Prior to the PDMS coating, the CS/BC and CS/HT-B_{1M} adsorbed the water droplet as soon as the water dropped on the surface of the samples. This indicated that the CS/BC and CS/HT-B_{1M} are super hydrophilic, which have a high affinity for water molecules (Xiuquan Li et al. 2020). Hence, surface modification is essential to improve the adsorption capacity under humid conditions.

The optimization of CS/HT-B_{1M}PDMS was performed by using One-Factor-At-a-Time (OFAT) method to investigate the optimum parameters for the formation of CS/HT-B_{1M}PDMS that have promotes high selectivity of acetone that increase the adsorption capacity at high relative humidity. Three parameters were selected, which include coating ratio, modification temperature, and reaction time for the PDMS coating. These parameters significantly affect the water contact angle of CS/HT-B_{1M}PDMS, which indicates the hydrophobicity of the coated CS/HT-B_{1M} as illustrated in **Figure 4.4─Figure 4.6**.

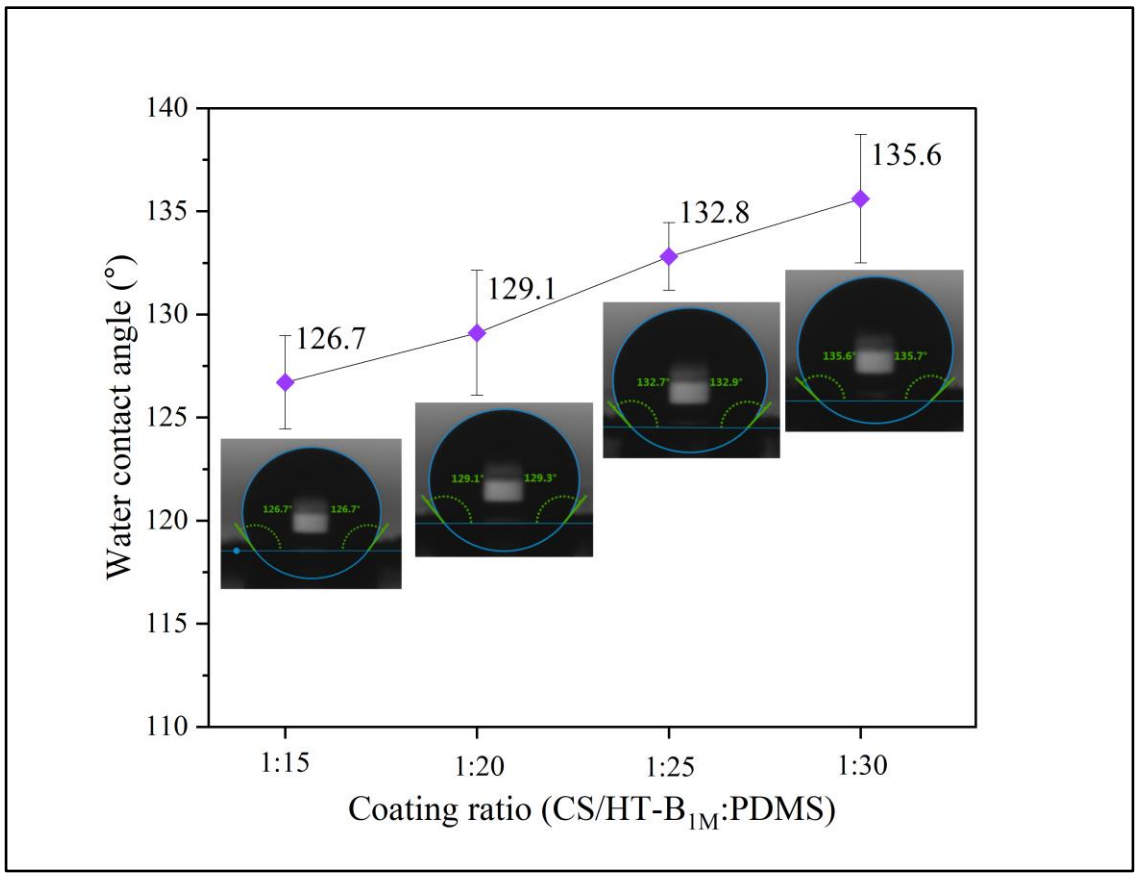

Figure 4.4: Effects of the coating ratio (CS/HT-B_{1M}:PDMS) on the water contact angle at 200°C, 1 hour

Based on **Figure 4.4**, the water contact angle increased by 1.5%, 2.9%, and 2.1% as the coating ratios increased from 1:15 to 1:20, 1:20 to 1:25, and 1:25 to 1:30 (CS/HT-B_{1M}: PDMS), respectively. This result implies that the more PDMS deposited on the surface of CS/HT-B_{1M}, the higher is the hydrophobicity. The increased in the water contact angle which corresponding to the hydrophobicity also correlated to the thickness of the PDMS film coated on the surface of CS/HT-B_{1M} (H.-B. Liu et al. 2016). Thus, the higher the coating ratio, the thicker the PDMS film, thereby increasing the hydrophobicity. Notably, the coating ratio of 1:25 exhibited the most significant increase in the water contact angle compared to other ratios. This finding suggests that a 1:25 ratio represents the optimal condition for hydrophobic coating. Additionally, using a lesser amount of PDMS at this ratio proves to be more economical due to the expensive nature of the material. This observation is further supported by the EDS mapping reported in **Figure 4.16**, where the sample shown to fully coated with Si─O─Si element from PDMS and hence 1:25 coating ratio is selected.

To date, there has been a lack of studies evaluating the effect of coating ratio on the properties of biochar. Therefore, this study provides insight into how the coating ratio influences the characteristics of biochar, particularly its water contact angle.

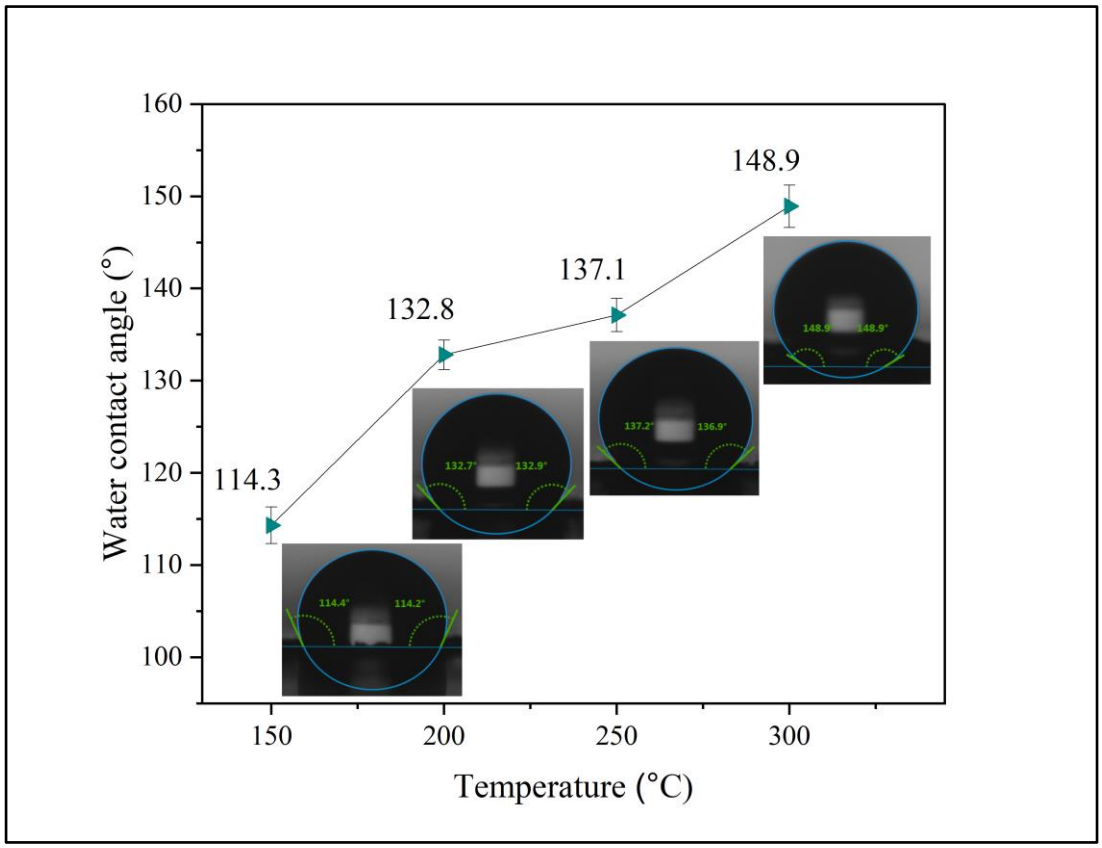

Figure 4.5: Effects of the modification temperature on the water contact angle at 1:25 CS/HT-B_{1M}: PDMS coating ratio, 1hour

The modification temperatures of PDMS coating were investigated, as illustrated in **Figure 4.5**. Similar to coating ratio, the water contact angle increases as the PDMS modification temperature increases from 150 to 300 ºC. The water contact angle increased by 16.2%, 3.2%, and 8.6% from 150 to 200 ºC, 200 to 250 ºC, and 250 to 300 ºC, respectively. The low water contact angle of 114.3º is obtained at modification temperature of 150 ºC. It might be attributed to less amount of PDMS deposited on the surface of CS/HT-B_{1M} (Lv et al. 2020). This is due to insufficient heat for the PDMS to evaporate and deposit on the surface of CS/HT-B_{1M}. At higher temperature above 200 ºC the PDMS is shown to be successfully deposited on the surface of CS/HT-B_{1M} by providing a higher water contact angle. A heating temperature of 300 ºC has the

highest water contact angle of 148.9 º, which was considered as super hydrophobic compared to 132.8º and 137.1º. However, H.-B. Liu et al. (2016) and Xiuquan Li et al. (2020) reported that at higher PDMS coating temperature (above 250 ºC) may resulting collapses and blockages in the pores of activated carbon (AC), particularly micropores. This is attributed to the changes of the pore structure in the AC, hence decreases the specific surface area. As biochar has mutual porosity characteristics with AC, it could potentially exhibit similar behavior upon exposure to the high modification temperature during the PDMS coating process. This indicated that the modification temperature above 250 ºC is not favorable for the PDMS coating process. Moreover, the water contact angle at 200 ºC shows the highest increment by 16.2 % compared to other modification temperatures. Furthermore, the S_{BET} value of CS/HT-B_{1M}PDMS reduced only by 10.4%, indicating that the pore structure of CS/HT-B_{1M} was maintained. Therefore, 200 ºC was selected as the modification temperature for PDMS coating.

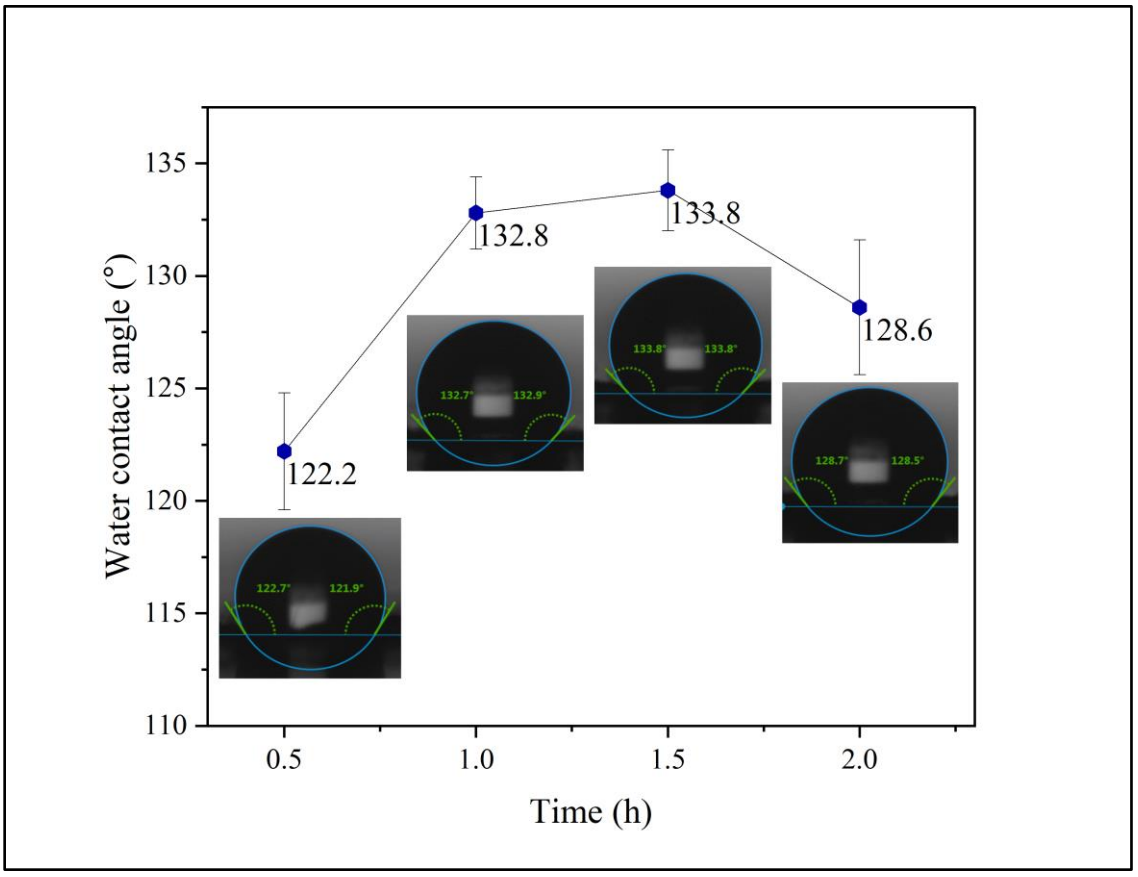

Figure 4.6: Effects of the reaction time on the water contact angle at 1:25 CS/HT-B_{1M}: PDMS coating ratio, 200 ºC

The duration of the PDMS coating has shown a significant effect on the water contact angle, as illustrated in **Figure 4.6**. The water contact angle increased when the reaction time increased from 0.5 to 1.5 h, then decreased as it reached 2 h. This might be due to the decomposition of PDMS at longer coating period. Thus, it is worth mentioning that the favorable duration for the PDMS coating is ranged from 1─1.5 h, indicating that 1 h is sufficient for the complete coating of PDMS (Xiuquan Li et al. 2020). In addition, the coating period of 1 h has the highest increment in water contact angle (8.2 %) than that of 1.5 h (0.8 %), and higher water contact angle compared to 0.5 h. Hence, 1 h was selected as the optimum time for the PDMS coating. Besides, the PDMS coating with lower heating temperature and shorter coating duration is favorable as it is energy efficient. Therefore, the optimum PDMS coating conditions are determined at 1:25 (CS/HT-B_{1M}: PDMS), 200 ºC for 1h to successfully surface modified the hydrophobicity of the CS/HT-B_{1M}.

The surface morphology of the CS/HT-B_{1M}PDMS synthesized under optimum conditions is further analyzed using SEM. **Figure 4.7** shows the morphological and structural transformation of CS/BC, CS/HT-B_{1M} and CS/HT-B_{1M}PDMS. The coating of PDMS on the surface of CS/HT-B_{1M} was done through thermal evaporation vapor decomposition method. This method of depositing a thin layer of PDMS onto biochar surface through the process of thermal evaporation. The PDMS is first heated to its boiling point (<200 ºC), causing it to vaporize. The PDMS vapor is then directed towards the surface of biochar, where it decomposes and forms a thin layer of Si-O-Si bonds on the surface (Y.-W. Cheng et al. 2020). The PDMS was coated on the surface of CS/HT-B_{1M} at the optimum conditions. **Figure 4.7(a)-(d)** shows that there were no significant changes in the pore structure of CS/HT-B_{1M}PDMS upon the coating of PDMS. The smooth surface shown in **Figure 4.7(c)** demonstrated the coating of PDMS thin layer on the surface of CS/HT-B_{1M} (**Figure 4.7(b)**). However, the PDMS layer filled some of the pores of the CS/HT-B_{1M}, resulting in a decrease in porosity, as shown in **Figure 4.7(d)**. This can be attributed to the increase in coating ratio, modification temperature, and reaction time, as more PDMS was deposited on the surface of CS/HT-B_{1M}, leading to the blockage and collapse of pores (X. Zheng et al. 2020). According to BET results of CS/HT-B_{1M}PDMS, the S_{BET} only decreased by 10.4%, which indicates that the optimum coating conditions are considered acceptable. This observation is further supported by the EDS mapping analysis, where it shows that the atomic percent of Si (silicon) and O (oxygen) on the surface of CS/HT-B_{1M}PDMS increased from 3.1% to 6.7%.

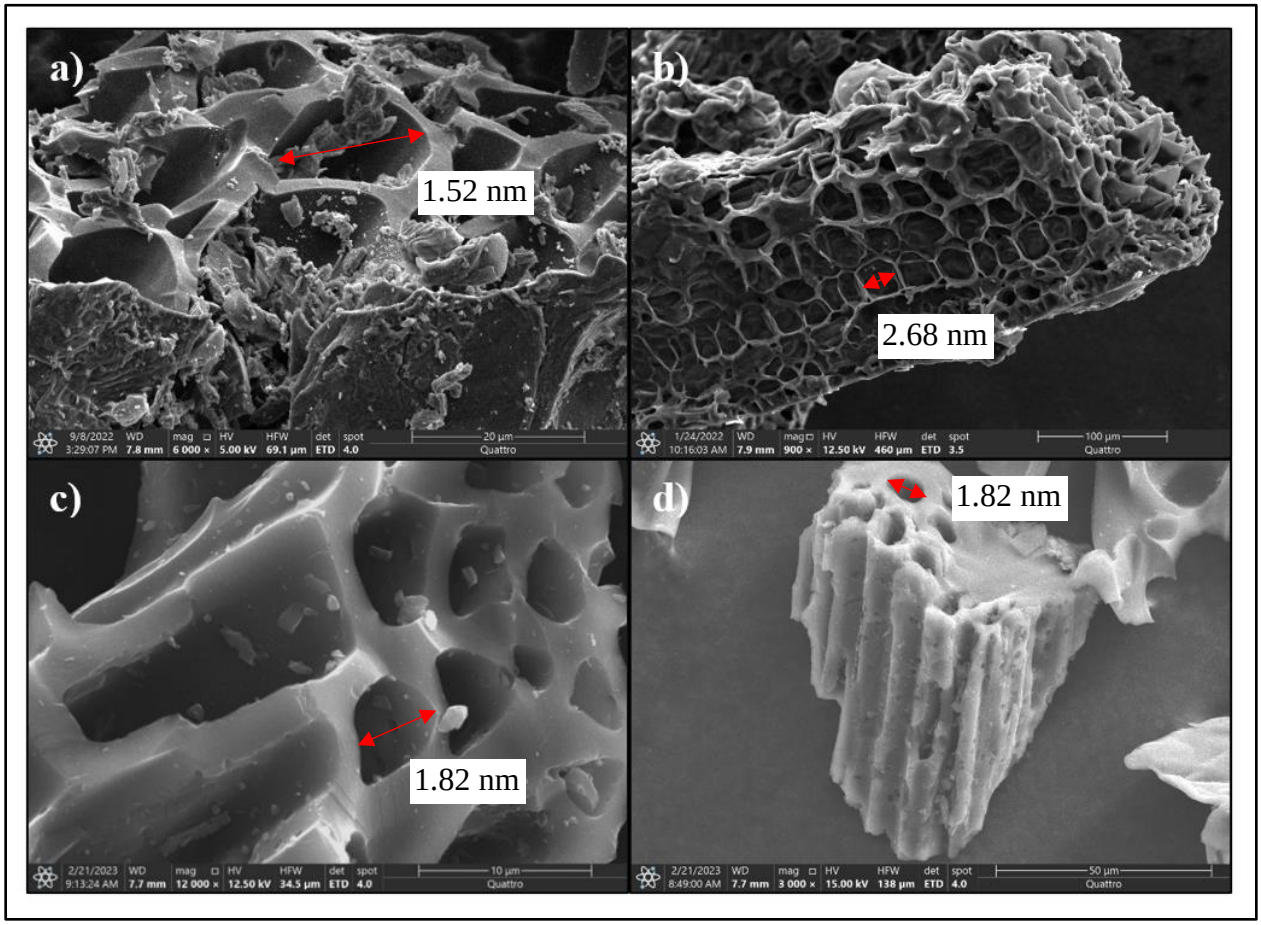

Figure 4.7: SEM images of a) CS/BC, b) CS/HT-B_{1M}, and c-d) CS/HT-B_{1M}PDMS

4.3 Microporosity study

The pore structure properties of bare biochars, HT-Bs, and CS/HT-B_{1M}PDMS were analyzed by Brunauer-Emmett-Teller (BET) analysis, and presented in **Table 4.1**. It is observed that the concentration of $ZnCl_2$ has significant effects on the porosity development of HT-Bs. The biochar synthesized from PL, PWS, and CS have low specific surface area (S_{BET}) compared to HT-Bs due to the nature properties of these biomasses. Upon the impregnation, the S_{BET} of PL/HT-Bs and PWS/HT-Bs gradually increased from 726.59 to 1376.94 $m^2\ g^{-1}$ and 1024.39 to 1890.25 $m^2\ g^{-1}$ as the $ZnCl_2$ concentration increases from 0.5 to 1.5 M, respectively. The total pore volumes (V_{total}) of PL/HT-Bs and PWS/HT-Bs follows the same trend, where it increased from 0.30 to 0.59

$cm^3\ g^{-1}$ and 0.42 to 0.77 $cm^3\ g^{-1}$, respectively. The increase in S_{BET} and V_{total} are attributed to the higher cross-linked of metal ions with the functional groups of the biomasses and evaporated during the carbonization leaving the vacant space on the surface of biochar (Thue et al. 2017). In contrast, the S_{BET} of CS/HT-Bs decreases at 1.5 M of $ZnCl_2$ which may be due to the deposition of $ZnCl_2$ on the surface of biochar (Lei et al. 2020). This phenomenon leading to the blockage of the pores and clogged the main channels for the transportation of VOCs to micropores during the adsorption process (Zubbri et al. 2020). Thus, metal salts concentration capable to act as an adjustable parameter to regulate the pore structure properties of the biochar (Karimnezhad et al. 2014; F. Zhao et al. 2021). Among HT-Bs, although PWS/HT-$B_{1.5M}$ has the highest S_{BET} of 1890.25 $m^2\ g^{-1}$, the SEM images shown in **Figure 4.3(c)**, indicated that CS/HT-B_{1M} exhibits better honeycomb-like tubular structure compared to PWS/HT-$B_{1.5M}$ where it is postulated to have higher adsorption capacity. Hence, CS/HT-B_{1M} with reasonably high S_{BET} is selected for the hydrophobic study.

Surface modification of CS/HT-B_{1M} through PDMS coating led to a decrease in S_{BET} from 1825.279 to 1335.567 $m^2\ g^{-1}$. This decrease was attributed to the PDMS coating conditions, including coating ratio, modification temperature, and reaction time, as discussed in **Section 4.2**. These parameters significantly influenced the deposition of PDMS on the surface of CS/HT-B_{1M}. A higher coating ratio, modification temperature, and reaction time resulted in more PDMS deposited on the surface, leading to a higher water contact angle. However, excessive PDMS layer on the surface of CS/HT-B_{1M} also resulted in pore blockage and collapse of the micropores due to a higher modification temperature. The results of this study are consistent with those of Haider et al. (2020) and Mohd Azmi et al. (2022), who reported that the S_{BET} of MOFs and membranes were decreased significantly as the modification temperature and reaction time of PDMS coating increased. Compared to recent studies, the CS/HT-B_{1M}PDMS prepared in this study has a competitive S_{BET} value, which suggests that it can achieve a high VOCs adsorption capacity. Additionally, despite the decrease in S_{BET} value, CS/HT-B_{1M}PDMS exhibited significant hydrophobicity when compared to non-coated HT-Bs. Consequently, CS/HT-B_{1M}PDMS has the potential to perform effectively in VOC adsorption, especially under humid conditions.

Table 4.1: The porous structural properties of biochars, HT-Bs, and CS/HT-B_{1M}PDMS

Sample	S_{BET} [a] ($m^2 g^{-1}$)	V_{total} [b] ($cm^3 g^{-1}$)	$S_{t\text{-}plot}$ [c] ($m^2 g^{-1}$)	S_{micro} [d] (t-plot)	V_{micro} [e] (t-plot)	D_p [f] (nm)
PL/BC	469.430	0.197	514.461	412.837	0.163	1.675
PWS/BC	587.908	0.259	643.976	486.134	0.193	1.761
CS/BC	528.318	0.201	516.984	493.383	0.192	1.523
PL/HT-$B_{0.5M}$	726.538	0.300	719.009	644.065	0.254	2.820
PL/HT-$B_{1.0M}$	1253.212	0.517	1242.537	1102.220	0.536	2.730
PL/HT-$B_{1.5M}$	1376.940	0.587	1375.654	1085.719	0.437	2.608
PWS/HT-$B_{0.5M}$	1024.394	0.424	1013.572	891.836	0.352	3.340
PWS/HT-$B_{1.0M}$	1392.305	0.588	1381.977	1156.545	0.459	2.467
PWS/HT-$B_{1.5M}$	1890.252	0.770	1889.234	1550.067	0.621	1.954
CS/HT-$B_{0.5M}$	1111.215	0.473	1104.440	838.760	0.336	2.203
CS/HT-$B_{1.0M}$	1825.279	0.803	1832.585	1370.300	0.557	2.683
CS/HT-$B_{1.5M}$	1518.570	0.738	1545.847	672.249	0.304	2.267
CS/HT-B_{1M}PDMS	1335.567	0.608	1051.987	981.543	0.512	1.822

[a] BET surface area; [b] Total pore volume; [c] BET surface area plot; [d] Micropores surface area; [e] Micropores volume; [f] pore diameter.

4.4 Surface functional groups

The FTIR analysis was performed to study the changes of the surface functional groups of HT-Bs before and after the impregnation at different $ZnCl_2$ concentrations, as well as after the surface modifications. The FTIR spectra of the bare biochars, HT-Bs, and CS/HT-B_{1M}PDMS are shown in **Figure 4.8**. As can be seen from the FTIR results, the bare biochars and HT-B(s) have similar surface functional groups. The broad peaks that appeared at around 3300-3347 cm^{-1} indicates the presence of the ─OH bond of the hydroxyl group due to the dehydration process in the biomass during the carbonization (Lin et al. 2021). The PL/HT-Bs, PWS/HT-Bs, and CS/HT-Bs have significant difference in their ─OH group upon the increases in the impregnation concentration. Based on **Figure 4.8(a),** the PL/HT-$B_{1.5M}$ shows boarder ─OH stretching vibration due to the formation of more stable zinc hydroxide oxide (ZnO─OH) crystalline form derived from hydrolyzation of $Zn(OH)_3^-$ and $Zn(OH)_2$ (Hadroug et al. 2022). While, the disappearance of the ─OH in PWS/HT-Bs is due to the removal of oxygen content during the carbonization process

(Tomin et al. 2021). In contrast, CS/HT-Bs maintains its ─OH group even at high impregnation concentration, indicates a complete carbonization process (F. Li et al. 2020).

The narrow peaks observed around 1500-1576 cm^{-1}, corresponding to the C=C stretching bonds, are attributed to the stretching of the C─O bond (Khoshnood Motlagh et al. 2021; H.-B. Liu et al. 2016). Weak and broad peaks are observed at around 1319-1330 cm^{-1} and 1006-1077 cm^{-1}, which are related to the CH_3 bend and C─O stretching due to the formation of aromatic structure and the occurrence of deoxygenation reaction, respectively (Khoshnood Motlagh et al. 2021). The disappearance of the CH_3 bend as the impregnation concentration increases is attributed to the success of the $ZnCl_2$ impregnation process (Luo et al. 2019). In addition, weak peaks observed at around 700-685 cm^{-1} can be ascribed to the Zn─O bond that only appeared in HT-Bs due to the decomposition of $ZnCl_2$ during the carbonization process (Jung et al. 2016; T. Yang et al. 2021). The following reactions were occurred during the carbonization process of HT-Bs (Lin et al. 2021):

$$ZnCl_2.\ 6H_2O \rightarrow ZnCl_2.\ 2H_2O + 4H_2O \quad \textbf{(4.1)}$$

$$ZnCl_2\ .\ 2H_2O \rightarrow Zn(OH)Cl + H_2O + HCl \quad \textbf{(4.2)}$$

$$Zn(OH)Cl \rightarrow ZnO + HCl \quad \textbf{(4.3)}$$

Similarly, C. Ma et al. (2018) observed that the Zn-O bond appeared around 400-500 cm^{-1}, while T. Yang et al. (2021) reported that the metal-oxygen stretching (Fe-O and Zn-O) have strong peaks at around 500-700 cm^{-1}.

Upon the PDMS coating on the surface of CS/HT-B_{1M}, the asymmetric and symmetric Si─O─Si stretching is observed at 779 and 1028 cm^{-1} due to the introduction of PDMS. Based on **Figure 4.8(d)**, the CH_3 peak of the CS/HT-B_{1M}PDMS is sharper than that CS/HT-B_{1M} which is attributed to the asymmetric stretching of Si─O─Si. These observations are further supported by the EDS mapping results of CS/HT-B_{1M}PDMS in **Section 4.8**. Similarly, H.-B. Liu et al. (2016) and Xiuquan Li et al. (2020) observed similar surface functional groups on the surface of AC upon the PDMS coating (asymmetric and symmetric Si─O─Si stretching) with the increases in atomic percent of Si and O.

In summary, the appearance of the significant peaks, particularly Zn-O and Si─O─Si could draw a conclusion that the CS/HT-B_{1M}PDMS was successfully synthesized, impregnated with $ZnCl_2$, and coated with PDMS. It is worth mentioning that the impregnation of $ZnCl_2$ is significantly influenced the oxygenic surface functional group and the pore structure of the biochar. While PDMS improves the hydrophobicity of the CS/HT-B_{1M} by the introduction of siloxane functional group on the surface of CS/HT-B_{1M}.

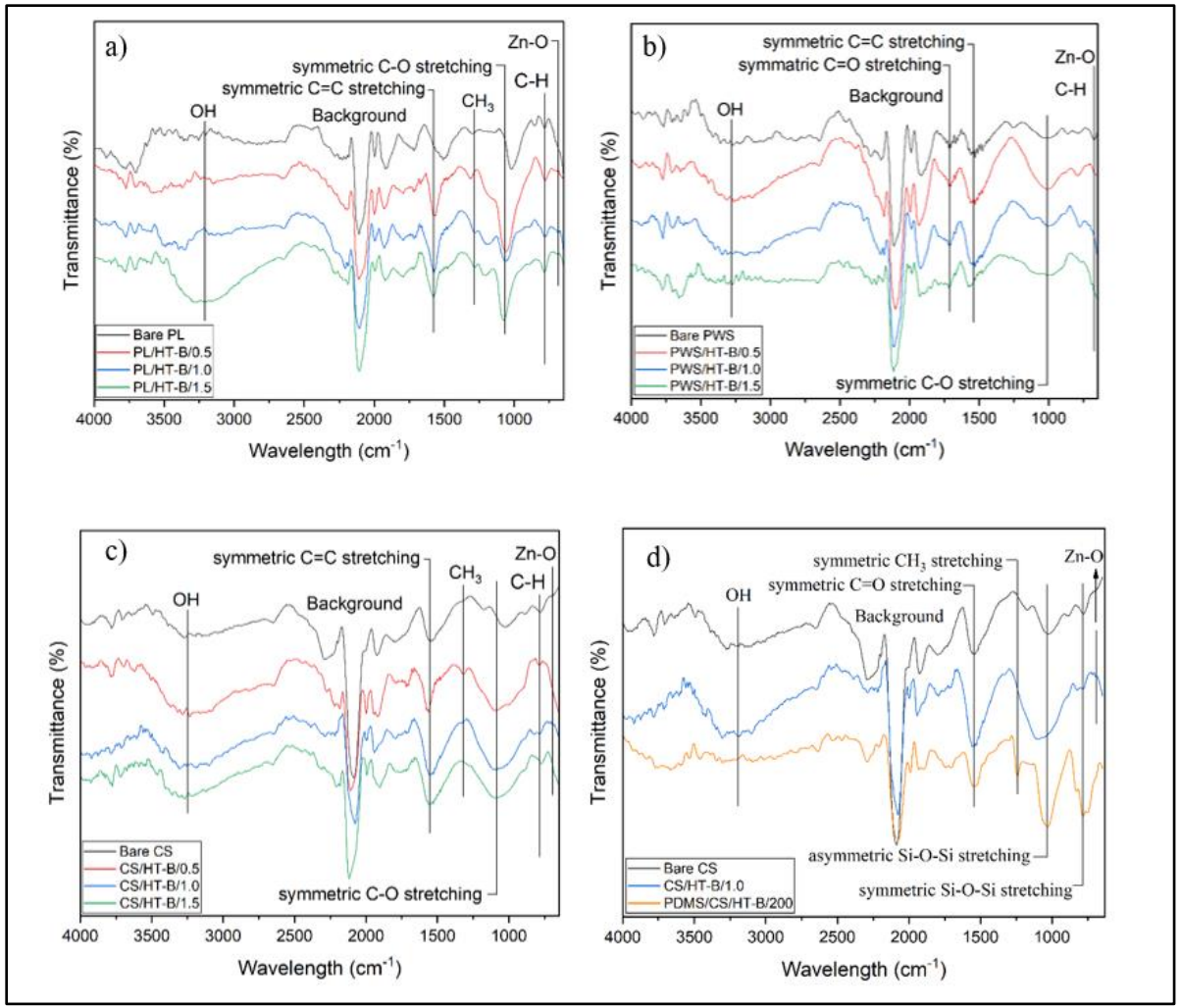

Figure 4.8: FTIR spectra for a) PL/HT-B, b) PWS/HT-B, c) CS/HT-B, and d) CS/HT-B_{1M}PDMS

4.5 Elemental study

The elemental analysis on the surface of HT-Bs and CS/HT-B_{1M}PDMS were performed using EDS analysis to investigate the chemical reactions involved during the structural and surface modifications. The EDS spectra and chemical compositions of HT-Bs are tabulated in **Table 4.2**. The EDS analyses show the main elements on the surface of HT-Bs are C, O, Zn, and Cl (F. Zhao et al. 2021). This result is similar to that of Xiuquan Li et al. (2020), who investigated the chemical compositions of AC treated with KOH, where C, O, Cl, and K were reported. Besides, a high atomic percent of C is observed, indicating the high purity of biochar. In addition, naturally biomass contains a number of removable O fractions, which valorized during the carbonization process, leaving a small amount of O remains in the biochar (Bagheri et al. 2020). Moreover, trace small amounts of Zn and Cl elements might be derived from the $ZnCl_2$ and HCl used during the structural modification and the washing process (Xiuquan Li et al. 2020). Similarly, Bagheri et al. (2020) observed traces of P and Cl in the biochar impregnated with H_3PO_4 and upon washing using HCl. This indicated that the slight deposition of metal salts and impurities from the washing processes. Similarly, in this study, traces of Zn and Cl are observed, where it is further confirmed by FTIR spectra with a weak peak of Zn-O around 685-700 cm^{-1}.

During the carbonization process, metal elements present in biomass can undergo thermal decomposition and produce metal oxides that can act as pore-forming agents, resulting in the creation of pores in the resulting biochar (E. Leng et al. 2022; Nzihou et al. 2019; Gopalan et al. 2022). This process is similar to the one that occurs when biomass is impregnated with metal salts, where the metal ions are reduced and converted into metal oxides during carbonization (Gopalan et al. 2022). Metal elements commonly found in biomass include zinc, sulfur, copper, manganese, nickel, and cobalt (Giudicianni et al. 2021). However, in this study, the biomasses used were found to contain only small amounts of zinc (<0.04%), which were not sufficient to develop HT-B as evidenced by the SEM and BET analyses in **Sections 4.1** and **4.3** (Emmanuel Onoja et al., 2017). Therefore, the impregnation of $ZnCl_2$ was performed to promote higher S_{BET} for the development of HT-Bs. Moreover, PL has a high amount of Si content (9.2%), which could contribute to its physicochemical properties. Silicon is known to improve the thermal stability, mechanical

strength, and adsorption capacity of biochar (Q. Liu et al. 2018; Xiaoyun Xu et al. 2019). The presence of Si in PL/HT-Bs could have contributed to its high S_{BET} value.

The surface modification of CS/HT-B_{1M} by PDMS coating leads to significant changes in the atomic percent of HT-Bs. The atomic percent of C, Cl, and Zn decreased from 92.7% to 88.9%, 1.6% to 0.5%, and 0.3% to 0%, respectively, upon the coating of PDMS, due to the increase in the atomic percent of Si and O. The increased atomic ratio of Si (3.8%) and O (6.7%) for CS/HT-B_{1M}PDMS are close to 1: 1.1, indicating the formation of an ultrathin PDMS film on the surface of CS/HT-B_{1M}. Other studies have reported that an increase in the atomic ratio close to 1:1.5 and 1:1.2 is considered an ultrathin PDMS film, and a slight increase in the atomic ratio could be due to incomplete oxidation of silicon dioxide (SiO_2) H.-B. Liu et al. (2016) and Xiuquan Li et al. (2020). They also indicate that the atomic percent of Si is correlated with the thickness of PDMS deposited on the surface of the carbon-based materials, where the higher the atomic percent of Si, the thicker the PDMS film coated on the surface. Furthermore, the EDS mapping image shown in **Figure 4.16** of **Section 4.8** indicates that the surface of CS/HT-B_{1M}PDMS is fully covered by the Si element. Therefore, both impregnation of $ZnCl_2$ and PDMS coating induce significant effects on the elemental atomic percent of the biochars.

Table 4.2: The summary of the atomic percent of the HT-Bs and CS/HT-B_{1M}PDMS

Sample	EDS Analysis (wt%)					
	C	**O**	**Zn**	**Cl**	**Si**	**S**
PL/HT-B						
0.5M	89.7	7.0	0.65	8.2	0.26	0.33
1.0M	92.4	7.2	0.3	0.8	1.1	0.78
1.5M	91.5	12.4	0.9	0.3	0.4	0.3
CS/HT-B						
0.5M	87.7	6.3	0.5	2.6	-	-
1.0M	92.7	3.1	0.3	1.6	-	0.1
1.5M	84.7	6.3	3.7	4.1	-	0.4
PWS/HT-B						
0.5M	90.8	3.8	-	3.3	-	-
1.0M	91.4	5.7	-	5.9	-	-
1.5M	88.3	3.9	-	1.2	-	-
CS/HT-B_{1M}PDMS	88.9	6.7	-	0.5	3.8	-

4.6 Isotherms and surface diffusion of acetone adsorption onto CS/HT-B_{1M} and CS/HT-B_{1M}PDMS

The adsorption behavior of acetone onto CS/HT-B_{1M} and CS/HT-B_{1M}PDMS was studied at different relative humidity (RH) of 50%, 70%, and 90%. To analyze the data, three nonlinear isotherm models were employed, namely Freundlich, Toth, and Sips models. The adsorption isotherms of CS/HT-B_{1M} and CS/HT-B_{1M}PDMS are presented in **Figure 4.9**, and relevant parameters are tabulated in **Table 4.3**. The Toth and Sips models showed better fitting with the experimental adsorption data than the Freundlich model, as indicated by the R^2 values above 0.997. The Sips model had the best fit, with R^2 values above 0.999 compared to the Toth model. This outcome suggested that the adsorption of acetone onto CS/HT-B_{1M} and CS/HT-B_{1M}PDMS at different RH levels could be described by a combination of Langmuir and Freundlich models,

indicating heterogeneous surface adsorption (Deng et al. 2020). The heterogeneity factor (n_s) of the Sips models was greater than 1, supporting the hypothesis of a heterogeneous surface. This heterogeneity could be attributed to the different affinities of acetone and water molecules toward CS/HT-B_{1M} and CS/HT-B_{1M}PDMS, as well as competitive inhibition between acetone and water molecules at higher humidity.

CS/HT-B_{1M} has a hydrophilic surface that interacts with water molecules via hydrogen bonding at low RH. As the RH increases, the adsorption effectiveness of acetone is reduced due to pore-filling phenomena caused by the build-up of large water clusters (B. Liu et al. 2021). At high RH, multi-layer adsorption occurs due to competitive inhibition between acetone and water molecules. In contrast, the heterogeneity factor of Freundlich, Toth, and Sips models for CS/HT-B_{1M}PDMS decreased as the RH increased. This decrease indicates that the heterogeneous adsorption active sites of the CS/HT-B_{1M}PDMS were reduced (Deng et al. 2020). The introduction of Si-O-Si surface functional groups by PDMS coating transformed the hydrophilic surface of CS/HT-B_{1M} to a hydrophobic one, resulting in reduced affinity towards water molecules. Consequently, its affinity towards acetone increased, and the interaction occurred via van der Waals forces and π-π interaction, leading to a higher acetone adsorption capacity (Mohd Azmi et al. 2022).

The Weber-Morris (W-M) intraparticle diffusion model (IPD) was utilized to predict the rate-controlling steps for acetone adsorption on CS/HT-B_{1M} and CS/HT-B_{1M}PDMS, as well as to analyze the impact of water molecules on acetone diffusion at different RH of 50%, 70%, and 90%. The W-M IPD kinetic plots of acetone adsorption on both adsorbents are presented in **Figure 4.10**, and the fitting parameters are listed in **Table 4.4**. The entire adsorption process can be divided into three stages: external surface, intraparticle diffusion, and adsorption equilibrium (Shuangchun Lu et al. 2021). Moreover, these three linear kinetic stages do not pass through the origin point, indicating the complex adsorption process of acetone onto CS/HT-B_{1M} and CS/HT-B_{1M}PDMS, which involves chemisorption interactions and surface diffusion (D. Chen et al. 2022). The fitting results indicate that the rate-controlling step for the acetone adsorption process on both adsorbents was intraparticle diffusion, while surface diffusion was a fast step. The values of the pore and surface diffusivity constants (k_P and C_P) decrease with increasing RH for both CS/HT-B_{1M} and CS/HT-B_{1M}PDMS. This can be attributed to the presence of water molecules, which limit the

intraparticle diffusion of acetone due to competitive diffusion between acetone and water molecules, with water clusters blocking the adsorption active sites for acetone (Jinjin Li et al. 2023). CS/HT-B_{1M}PDMS exhibits higher k_P than CS/HT-B_{1M} due to its low affinity towards water molecules, which increases the diffusion of acetone. This suggests that the mesopores and macropores of CS/HT-B_{1M}PDMS provide sufficient channels for faster intraparticle diffusion (Jinjin Li et al. 2022). Therefore, the presence of water molecules primarily affects the intraparticle diffusion process, resulting in a negative impact on acetone adsorption.

Overall, the Sips model provides a good description of the adsorption behavior of acetone onto CS/HT-B_{1M} and CS/HT-B_{1M}PDMS at varying RH, suggesting that adsorption occurs on heterogeneous surfaces. The hydrophilic surface of CS/HT-B_{1M} was found to preferentially interact with water molecules even at low RH, leading to a significant reduction in acetone adsorption capacity due to pore-blocking by large water clusters. Conversely, the presence of Si-O-Si surface functional groups in CS/HT-B_{1M}PDMS increased its affinity towards acetone over water molecules, resulting in good performance in adsorbing acetone that remained effective even at high RH. Moreover, the rate-controlling steps for acetone adsorption on both adsorbents was intraparticle diffusion, while surface diffusion was a fast step. CS/HT-B_{1M}PDMS provided faster channels for acetone diffusion compared to CS/HT-B_{1M} due to its high hydrophobicity.

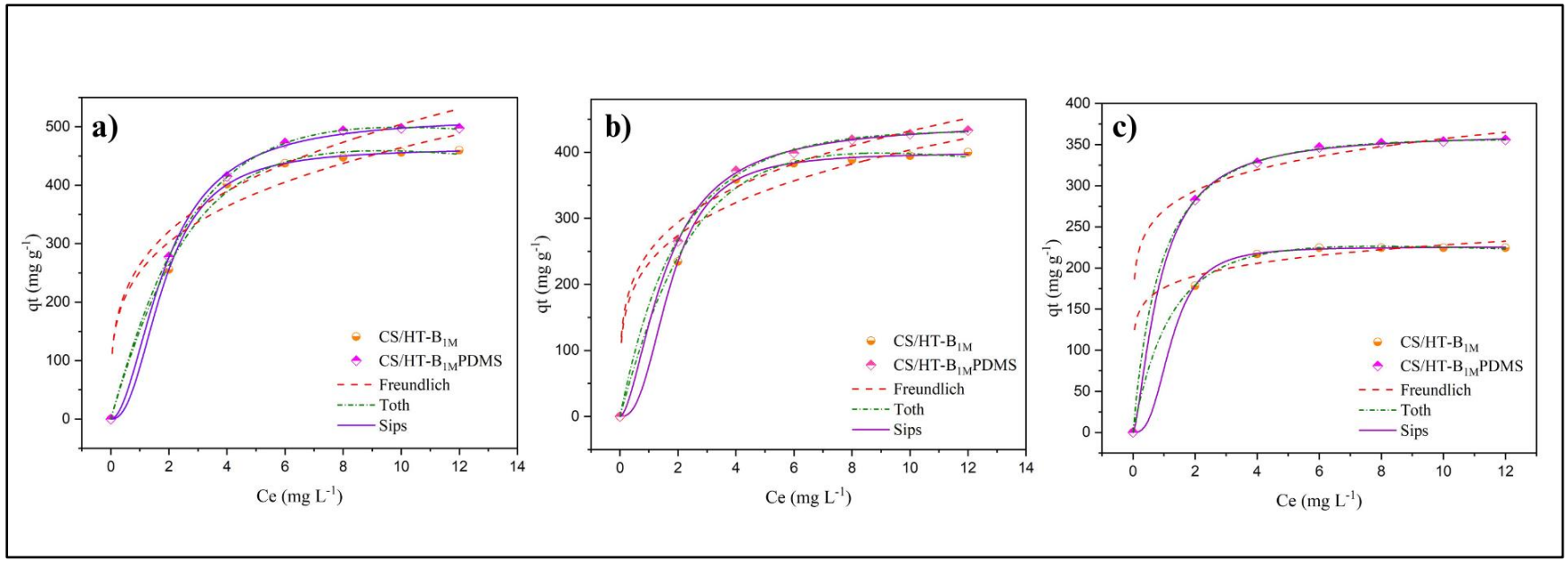

Figure 4.9: Nonlinear isotherms kinetic plots for acetone adsorption on CS/HT-B_{1M} and CS/HT-B_{1M}PDMS at a) 50 RH%, b) 70 RH%, and c) 90 RH%

Table 4.3: Adsorption isotherm parameters of acetone on CS/HT-B_{1M} and CS/HT-B_{1M}PDMS across varying RH.

Adsorbent	RH	Freundlich			Toth				Sips			
	(%)	K_F[a]	n_F[b]	R^2	$q_{m,TO}$[c]	K_{TO}[d]	Z[b]	R^2	$q_{m,SP}$[c]	K_{SP}[e]	n_{SP}[b]	R^2
CS/HT-B_{1M}	50	251.535	4.422	0.817	1196.952	0.198	1.42	0.997	463.572	0.236	2.381	0.999
	70	232.006	4.162	0.796	997.353	0.222	1.384	0.997	399.693	0.238	2.58	0.999
	90	175.966	8.903	0.745	409.995	0.523	1.181	0.999	225.606	0.523	2.851	0.999
CS/HT-B_{1M}PDMS	50	264.016	3.559	0.857	1264.952	0.195	1.395	0.999	517.108	0.302	1.926	0.999
	70	249.124	4.179	0.891	795.849	0.317	1.195	0.999	445.876	0.457	1.695	0.999
	90	270.023	1.232	0.893	479.564	0.904	1.066	0.999	364.129	1.241	1.475	0.999

[a]Freundlich constant; [b] homogeneity factor; [c] maximum adsorption capacity (mg g^{-1}); [d] Toth constant; [e] Sips constant.

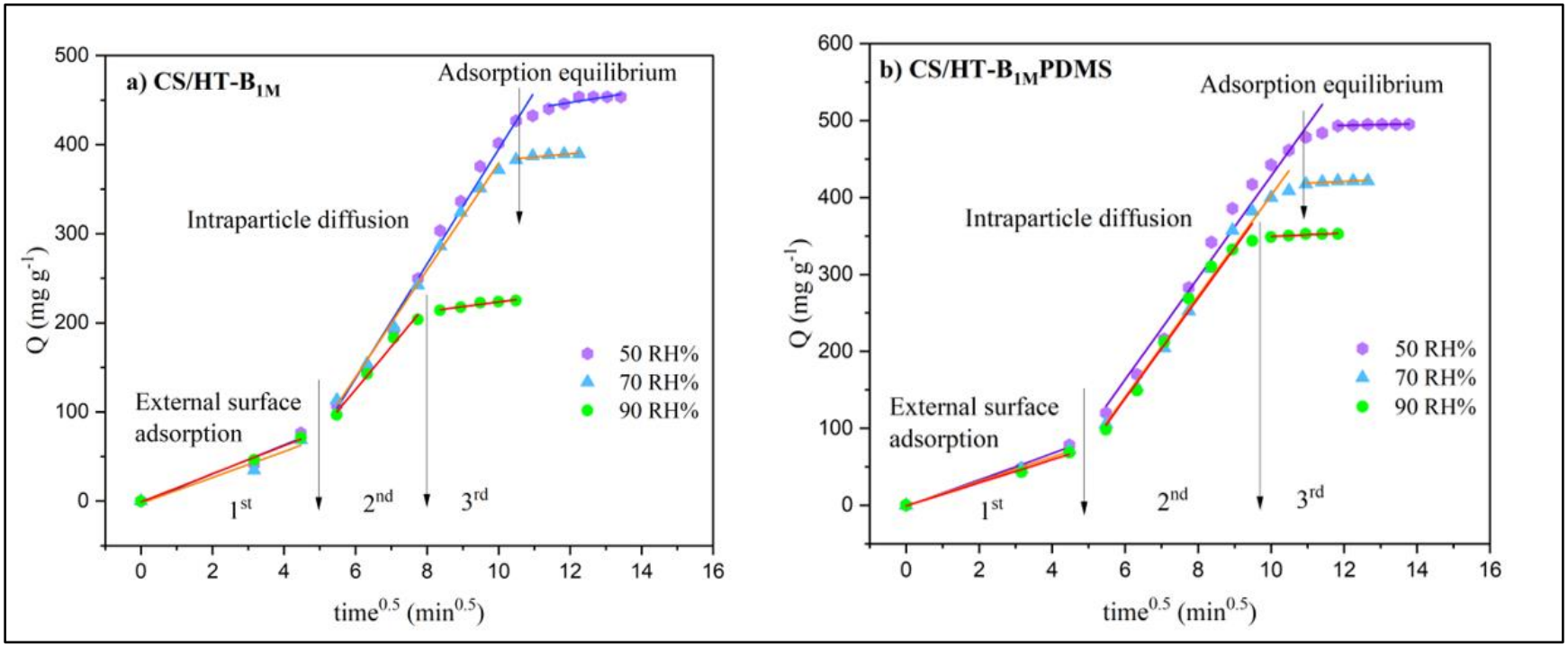

Figure 4.10: The IPD kinetic plot for acetone adsorption onto a) CS/HT-B_{1M} and b) CS/HT-B_{1M}PDMS at 50, 70, and 90 RH%

Table 4.4: IPD model parameters for the adsorption of acetone on CS/HT-B_{1M} and CS/HT-B_{1M}PDMS.

Adsorbent	**RH**	**k_P (mg g^{-1})[a]**			**C_P (mg g^{-1})[b]**			**R^2**		
	(%)	1st	2nd	3rd	1st	2nd	3rd	1st	2nd	3rd
CS/HT-B_{1M}	50	16.341	64.3	6.423	-2.344	-248.236	370.21	0.965	0.988	0.725
	70	14.564	60.034	3.644	-2.609	-221.01	346.101	0.946	0.995	0.817
	90	14.612	42.122	5.053	0	-89.202	175.556	1	0.99	0.948
CS/HT-B_{1M}PDMS	50	17.106	66.149	0.956	-1.26	-223.395	482.298	0.99	0.975	0.722
	70	15.843	65.492	2.172	-0.714	-251.997	394.81	0.996	0.983	0.734
	90	15.005	65.324	2.301	-0.94	-253.547	326.242	0.993	0.877	0.803

[a] IPD rate constant; [b] boundary later thickness.

4.7 Adsorption capacity and dynamic kinetic models of acetone adsorption onto CS/HT-B_{1M} and CS/HT-B_{1M}PDMS

Figure 4.11 shows the acetone adsorption capacity of CS/HT-B_{1M} and CS/HT-B_{1M}PDMS at varying relative humidity (RH) of 50%, 70%, and 90%. The results indicate a reduction in acetone adsorption capacity for both adsorbents as RH increased from 50% to 90%. This suggests that the presence of water molecules has a significant impact on acetone adsorption. The acetone adsorption capacity of CS/HT-B_{1M} decreased by 24.3% and 49.8% when RH increased from 50% to 70% and 90%, respectively. This can be attributed to the increased amount of water clusters, which block and compete with acetone for the adsorption active sites. The results of DSA indicated that CS/HT-B_{1M} has a hydrophilic surface, which means water molecules occupy the adsorption active sites more easily than acetone, leading to poor adsorption performance at high RH. In contrast, the acetone adsorption capacity of CS/HT-B_{1M}PDMS decreased only by 15.1% and 28.7% when RH increased from 50% to 70% and 90%, respectively, indicating that the presence of water molecules has a lesser effect on acetone adsorption at high RH. Furthermore, CS/HT-B_{1M}PDMS exhibited a hydrophobic surface with a water contact angle of 132.8º. The hydrophobicity of CS/HT-B_{1M}PDMS reduced the affinity of water molecules and increased the selectivity of acetone adsorption. As a result, CS/HT-B_{1M}PDMS showed excellent acetone adsorption performance at high RH.

The breakthrough curves of acetone adsorption onto CS/HT-B_{1M} and CS/HT-B_{1M}PDMS were investigated using three nonlinear breakthrough models, such as Bohart-Adams (B-A), Thomas, and Yoon-Nelson (Y-N) model. To determine the values of the parameters, a logistic equation was used and expressed as follow (Plata-Gryl et al. 2022):

$$\frac{C_t}{C_0} = \frac{1}{1+\exp\,(a-bt)} \qquad \textbf{(4.4)}$$

Fundamentally, the abovementioned models are the same and only difference are their parameters, *a* and *b*. Both parameters can be represent as a logistic growth function (Chu 2020). The parameters *a* and *b* for the B-A, Thomas, and Y-N models are presented in **Table 4.5**.

Table 4.5: The logistic growth function of the models.

Model	Expression	Logistic growth function	
		a	b
Yoon-Nelson	$\frac{c}{c_0} = \frac{1}{1+\exp[k_{YN}(\tau - t)]}$	$k_{YN}\tau$	k_{YN}
Thomas	$\frac{c}{c_0} = \frac{1}{1+exp\left[k_T c_0\left(\frac{q_0 m}{F c_0} - t\right)\right]}$	$\frac{k_T q_0 m}{F}$	$k_T c_0$
Bohart-Adams	$\frac{c}{c_0} = \frac{1}{1+\exp\left[k_{BA}\, c_0(\frac{N_0 L}{u c_0} - t)\right]}$	$\frac{k_{BA} N_0 L}{u}$	$k_{BA} c_0$

Table 4.6 displays the results of fitting a logistic growth function model and the associated parameters for the B-A, Thomas, and Y-N models. The experimental breakthrough data for CS/HT-B_{1M} and CS/HT-B_{1M}PDMS demonstrated a strong agreement with the logistic growth equations derived from Eq. (9) with a high fitting correlation coefficient of R^2 above 0.998. In principle, applying the logistic equation to breakthrough data is adequate to determine the two fundamental parameters, which can then be employed to calculate the respective values for the three fixed bed models. Moreover, recent research has mathematically demonstrated the equivalence of these abovementioned models, resulting in a similar level of fit quality [60]. Consequently, these findings align with the fitting of breakthrough curves observed in this study, as shown in **Figure 4.12**. Moreover, the rate constants (K_{BA}, K_T, and K_{YN}) for both adsorbents increased as RH increased, and there is no significant difference between both adsorbents. The rate constants value represents the steepness of the breakthrough curve, a larger value indicates a steeper breakthrough curve (B. He et al. 2020). However, based on the 50% breakthrough time (τ), CS/HT-B_{1M}PDMS exhibited longer period to reach breakthrough when RH increased from 50% to 70% and 90%, this indicated that it performed well under high RH in comparison to CS/HT-B_{1M}, resulted in higher acetone adsorption capacity. This observation is consistent with the increase in q_0 and N_0 values of B-A and Thomas models obtained in this study. Such results implied due to the CS/HT-B_{1M}PDMS exhibited hydrophobic surface properties, which maintained its performance at low RH and reduced the affinity of water molecules, which provided more

adsorption active sites for acetone at high RH (Jiaxing Wang et al. 2021). Consequently, CS/HT-B_{1M}PDMS showed better adsorption performance for acetone than CS/HT-B_{1M}, as demonstrated in **Figure 4.11**.

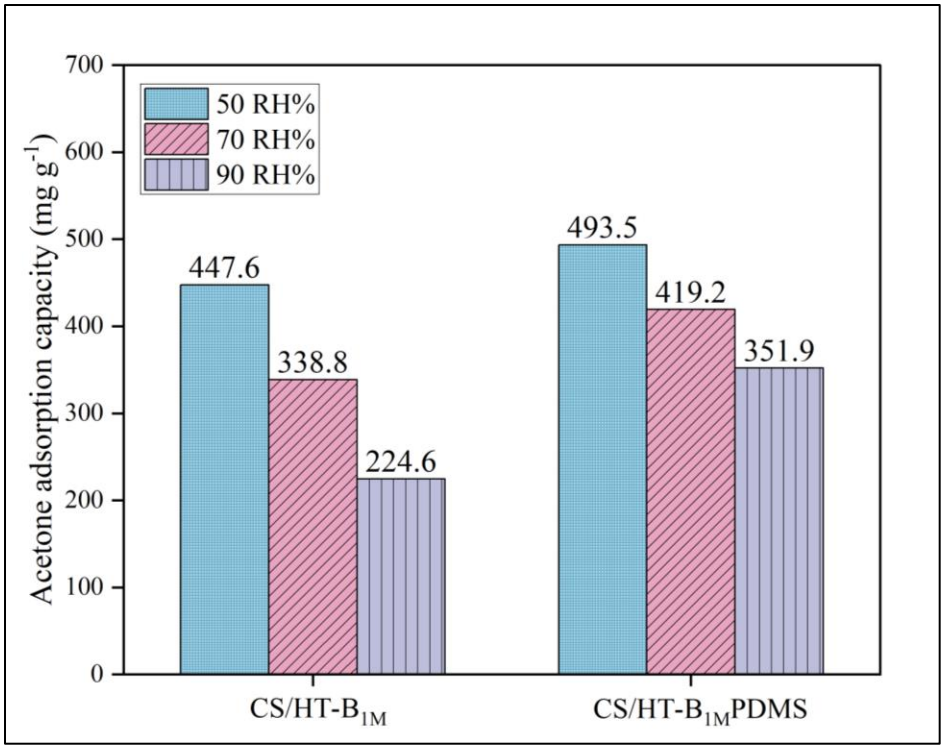

Figure 4.11: Acetone adsorption capacity of CS/HT-B_{1M} and CS/HT-B_{1M}PDMS at 50, 70, and 90 RH%

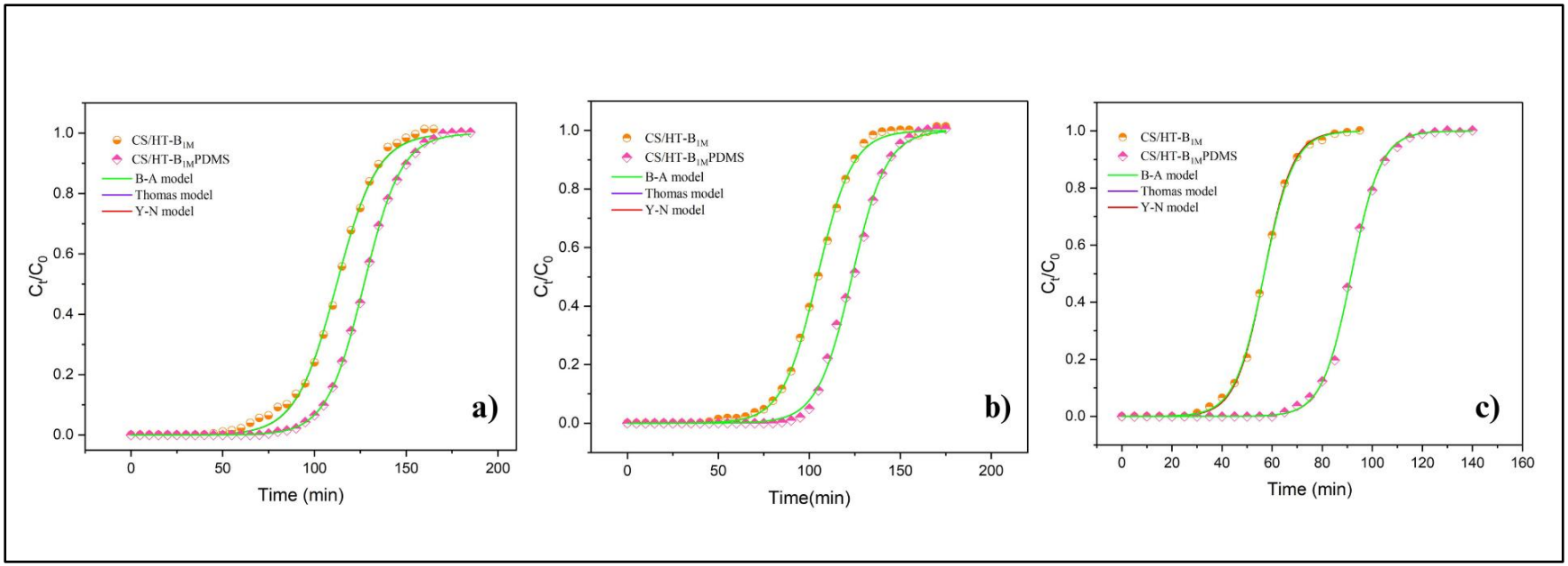

Figure 4.12: Breakthrough curves of acetone adsorption onto CS/HT-B_{1M} and CS/HT-B_{1M}PDMS at a) 50 RH% b) 70 RH%, and c) 90 RH%

Table 4.6: Breakthrough kinetic parameters of acetone adsorption onto CS/HT-B_{1M} and CS/HT-B_{1M}PDMS.

Adsorbent	**RH (%)**	**Logistic growth function**		**Y-N**				**Thomas**			**B-A**		
		a	b	k_{YN}[a]	τ[b]	τ_{exp}[c]	R^2	k_T[a]	q_0[d]	R^2	k_{AB}[a]	N_0[e]	R^2
				min^{-1}	min	min		$cm^3\ mg^{-1}\ min^{-1}$	mg g^{-1}		$cm^3\ mg^{-1}\ min^{-1}$	mg cm^{-3}	
CS/HT-B_{1M}	50	10.0	0.089	0.089	112.1	112.3	0.998	11.1	0.339	0.998	11.1	0.096	0.998
	70	10.8	0.104	0.104	104.4	104.5	0.999	13.0	0.313	0.999	13.0	0.088	0.999
	90	9.96	0.175	0.175	56.7	56.8	0.999	21.1	0.171	0.999	21.1	0.050	0.999
CS/HT-B_{1M}PDMS	50	12.4	0.098	0.098	127.0	127.2	0.999	12.2	0.381	0.999	12.2	0.108	0.999
	70	13.0	0.105	0.105	123.5	123.6	0.998	13.1	0.370	0.998	13.1	0.105	0.998
	90	15.6	0.171	0.171	91.7	91.9	0.999	21.3	0.275	0.999	21.3	0.078	0.999

[a] rate constant of the model; [b] 50% breakthrough time; [c] experimental 50% breakthrough time; [d] adsorption capacity; [e] adsorption capacity per unit volume of bed reactor.

4.8 Regeneration of CS/HT-B_{1M}PDMS

The regeneration was carried out to evaluate the reusability of CS/HT-B_{1M}PDMS as an efficient adsorbent for the removal of acetone under high relative humidity (RH). The breakthrough curves and the adsorption capacity of regenerated CS/HT-B_{1M}PDMS at 90% RH are presented in **Figure 4.13** and **Figure 4.14**, respectively. The data obtained from the acetone adsorption experiments on the regenerated CS/HT-B_{1M}PDMS showed a good fit to the B-A, Thomas, and Y-N models, with a high fitting correlation coefficient (R^2) exceeding 0.997. The breakthrough acetone adsorption capacity of regenerated CS/HT-B_{1M}PDMS decreased sharply in the second cycle by 23.7%, and gradually decreased in third and fourth cycles by 6% and 2%, respectively. The decreased in the adsorption capacity in the second cycle is more than 10%, might be attributed to the strong interaction between acetone molecules and Si─O─Si bond of PDMS. These interactions may be led to the formation of some permanent bonds between acetone molecules and Si─O─Si bond, which blocked the adsorption active sites for the next regeneration cycle (Rong et al. 2023; Y. Yang et al. 2021).

The regeneration of biochar is related to the adsorption mechanisms and the characteristics of the VOCs being adsorbed (Z. Zhao et al. 2022). In the present study, competitive adsorption occurred, where multiple adsorption mechanisms were involved, including physical and chemical adsorption. Acetone interacted with the surface functional group of biochar (Si-O-Si bond) via hydrogen bonding, π-π interaction, and weak van der Waal forces, while water molecules interacted with hydrophilic sites through hydrogen bonding at low RH and water cluster formation resulting in pore filling at high RH. This is consistent with the observations by Mohd Azmi et al. (2022) and H.-B. Liu et al. (2016). Furthermore, studies have reported that increasing the thermal regeneration temperature to a certain range more than 200 ^{o}C can reduce the S_{BET} value and destroy the surface functional groups of the biochar, particularly the PDMS film (Zhirui Li et al. 2021; Pi et al. 2017). Thus, the CS/HT-B_{1M}PDMS was regenerated at 150 ^{o}C for 1h for four regeneration cycles; however, a significant decrease in efficiency was observed after regeneration. Consequently, higher thermal regeneration temperature or a longer regeneration duration might be required to break the bonds or interactions between the adsorbed acetone and siloxane functional group of CS/HT-B_{1M}PDMS. The boiling point of water molecules is 100°C, which means that

water molecules readily evaporate at temperatures of 150°C and higher. Therefore, further investigation is recommended to determine the optimal conditions for regenerating CS/HT-B_{1M}PDMS for competitive adsorption under humid conditions.

The characterizations of the CS/HT-B_{1M}PDMS before and after the regeneration were also carried out to investigate the changes in their physicochemical properties. The morphology and structure of CS/HT-B_{1M}PDMS before and after the regeneration are illustrated in **Figure 4.15**. It can be observed that the pore structure of CS/HT-B_{1M}PDMS collapsed, shrank, and expanded upon the fourth cycle regeneration. These observations are consistent with the slight decrease in the S_{BET} results of CS/HT-B_{1M}PDMS after the regeneration from 1335.567 to 1307.904 $m^2\ g^{-1}$. This slight decrease indicates that the regeneration conditions do not significantly affect the porosity of CS/HT-B_{1M}PDMS; however, the regeneration temperature and duration are not favorable for desorbing that adsorbed acetone from CS/HT-B_{1M}PDMS. Based on the EDS mapping results before and after regeneration as shown in **Figure 4.16-4.17**, the atomic percent of Si and O elements were reduced by 10.5% and 19.4% at the fourth cycle regeneration of CS/HT-B_{1M}PDMS, respectively. These observations were consistent with the appearance of weak peaks of Si─O─Si bond and CH_3 stretching of FTIR results, as shown in **Figure 4.18**. As the atomic percent of Si and O elements were reduced, the water contact angle of regenerated CS/HT-B_{1M}PDMS was also decreased from 132.8 º to 123.4 º.

The results suggest that the regeneration conditions for CS/HT-B_{1M}PDMS were not optimal, possibly due to the strong interaction between the adsorbed acetone and the Si-O-Si bond of PDMS or the formation of permanent bonds during regeneration, leading to a reduced amount of active sites for adsorption in subsequent cycles. However, even after regeneration, CS/HT-B_{1M}PDMS still performed well at 90% RH compared to CS/HT-B_{1M}. To improve the regeneration process, it may be necessary to increase the thermal regeneration temperature and duration. A method combining low-temperature and high-temperature regeneration has been proposed for chemical adsorption, which can maintain the integrity of the biochar and achieve optimal regeneration conditions (Zeng et al. 2021). Therefore, further studies on the optimal conditions for the regeneration of biochar for competitive adsorption are needed, which could have significant applications in the field of separation and purification.

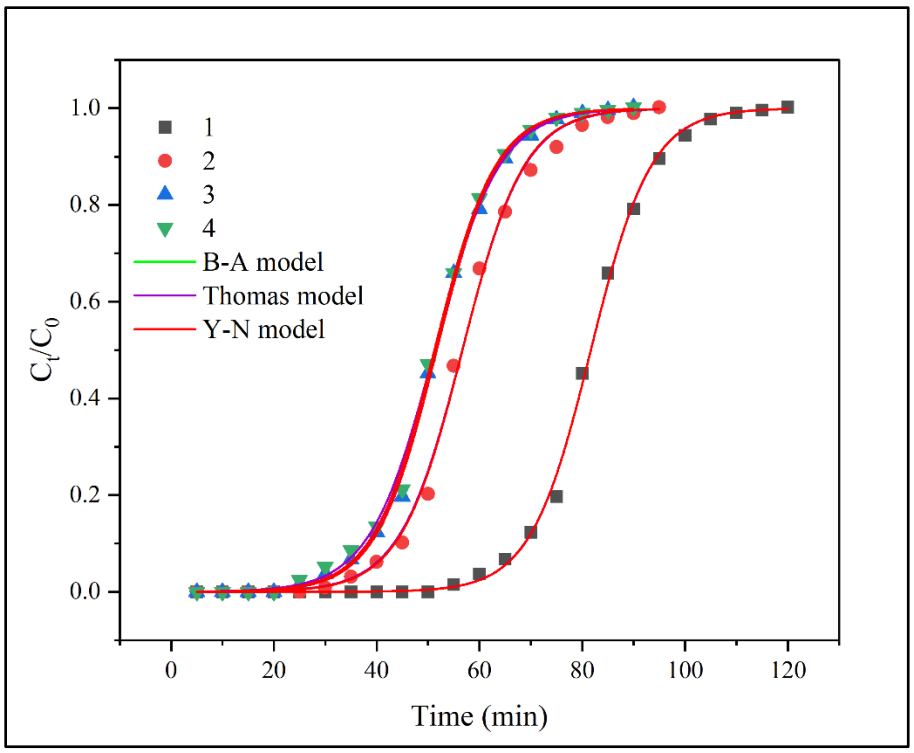

Figure 4.13: Breakthrough curves of regenerated CS/HT-B_{1M}PDMS at 90 RH% for 4 cycles

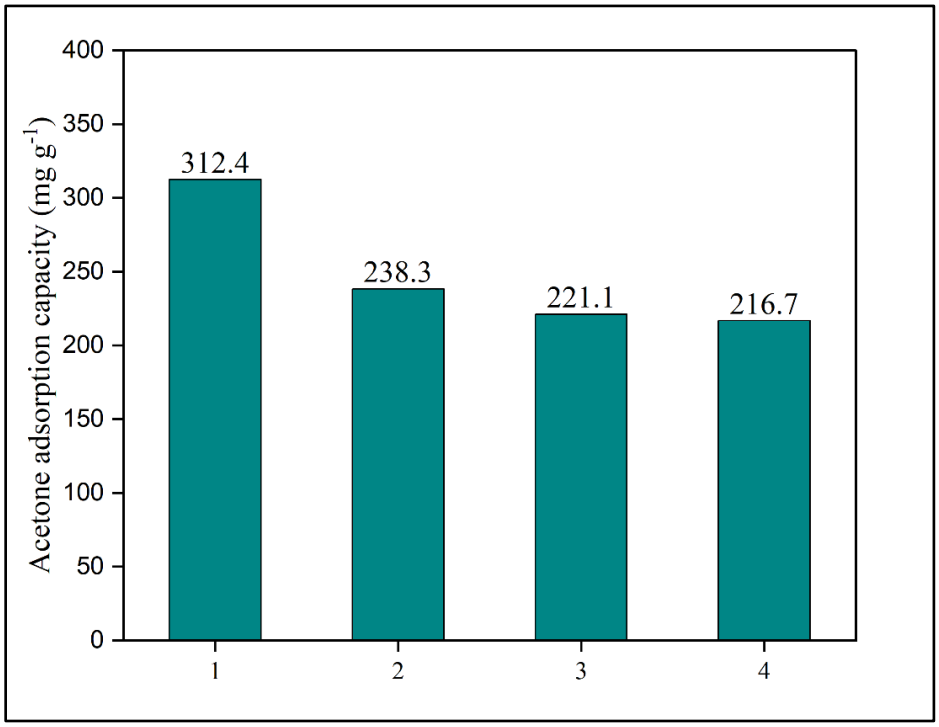

Figure 4.14: Acetone adsorption capacity of regenerated CS/HT-B_{1M}PDMS at 90 RH% for 4 cycles

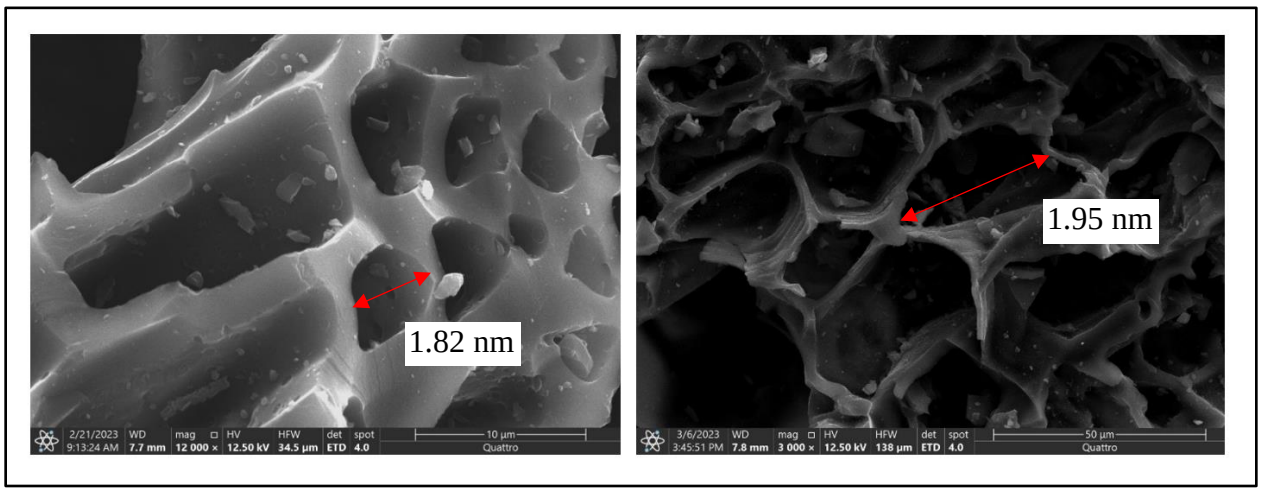

Figure 4.15: SEM images of CS/HT-B_{1M}PDMS before and after regeneration

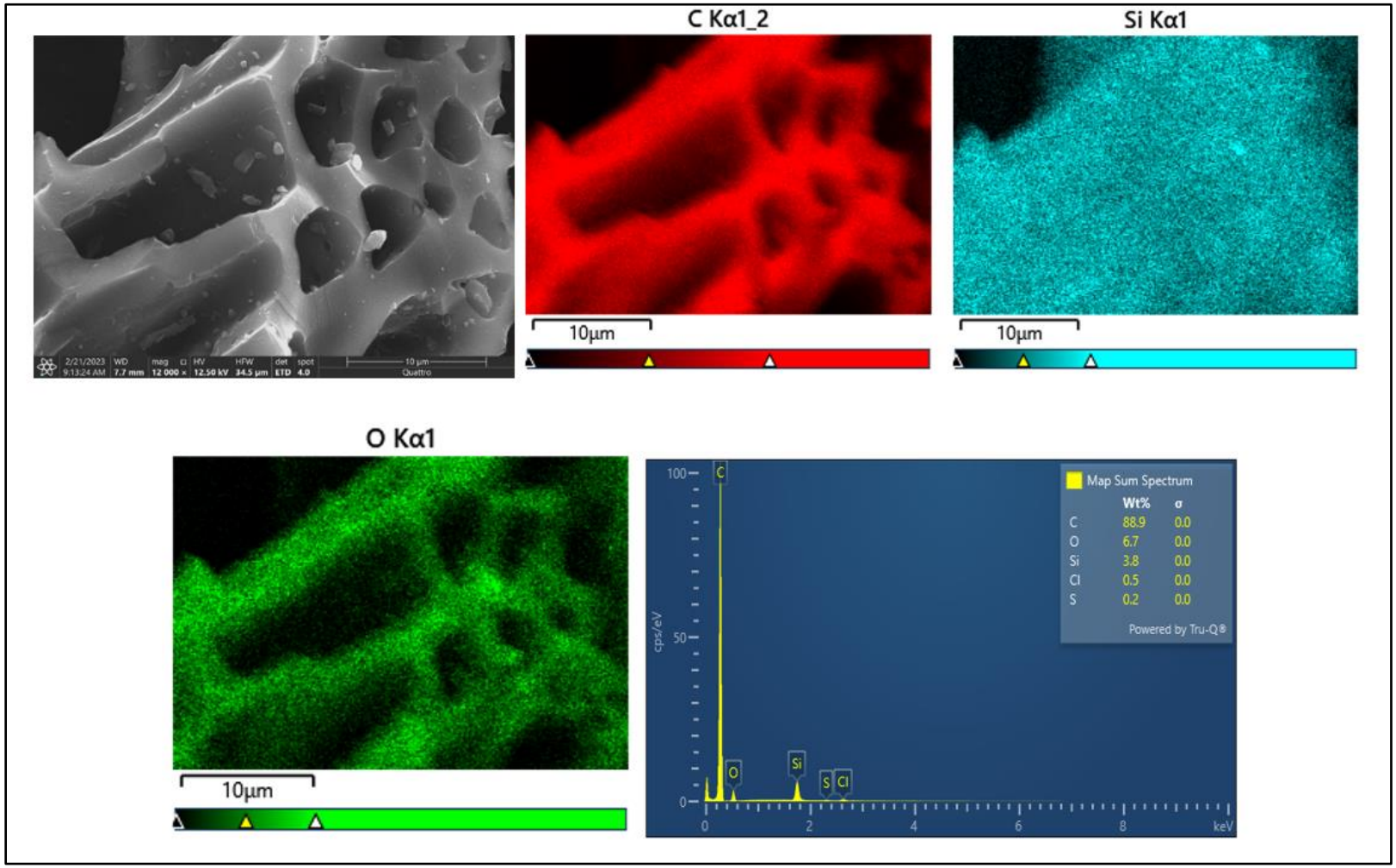

Figure 4.16: EDS mapping images and spectra of CS/HT-B_{1M}PDMS

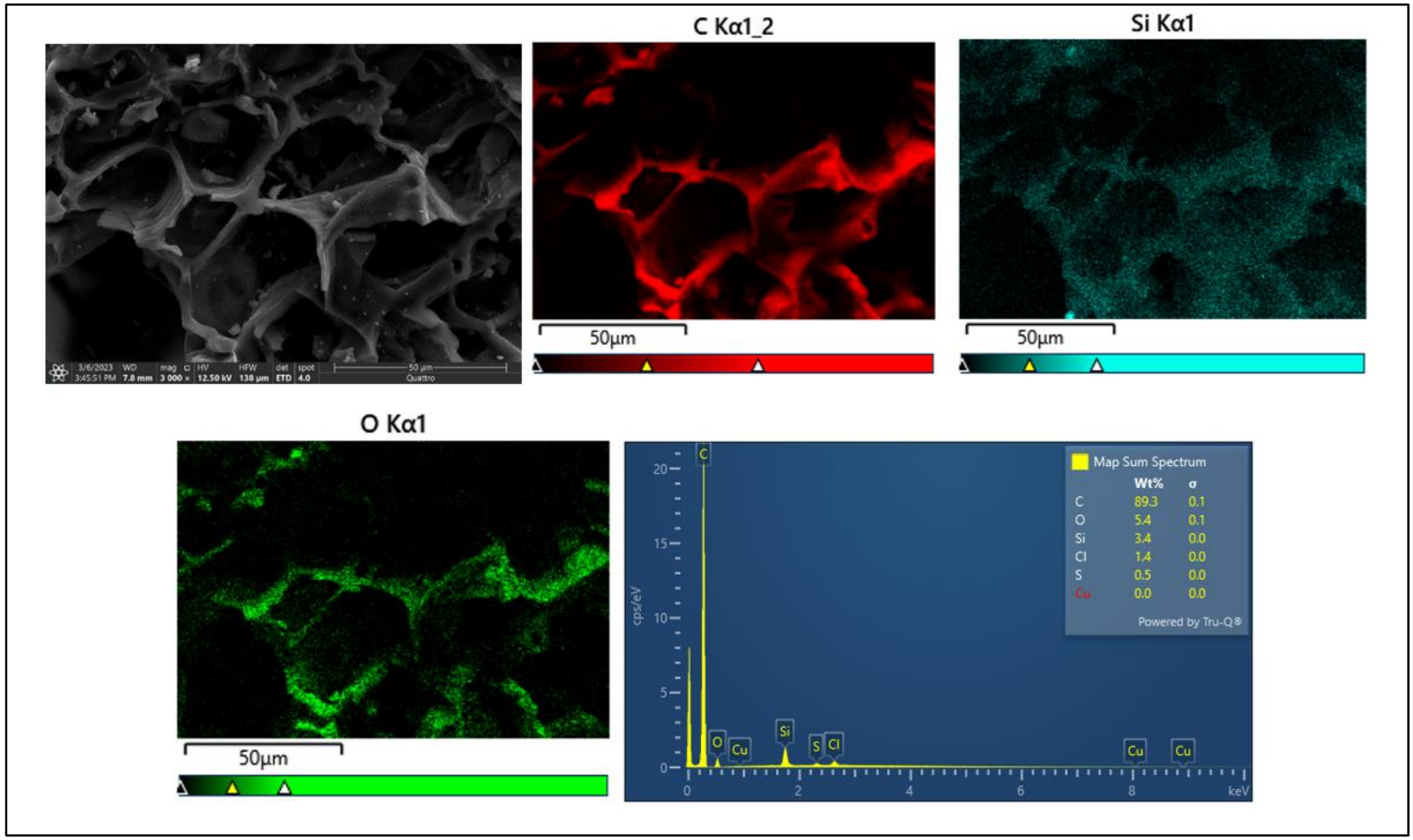

Figure 4.17: EDS mapping images and spectra of regenerated CS/HT-B_{1M}PDMS

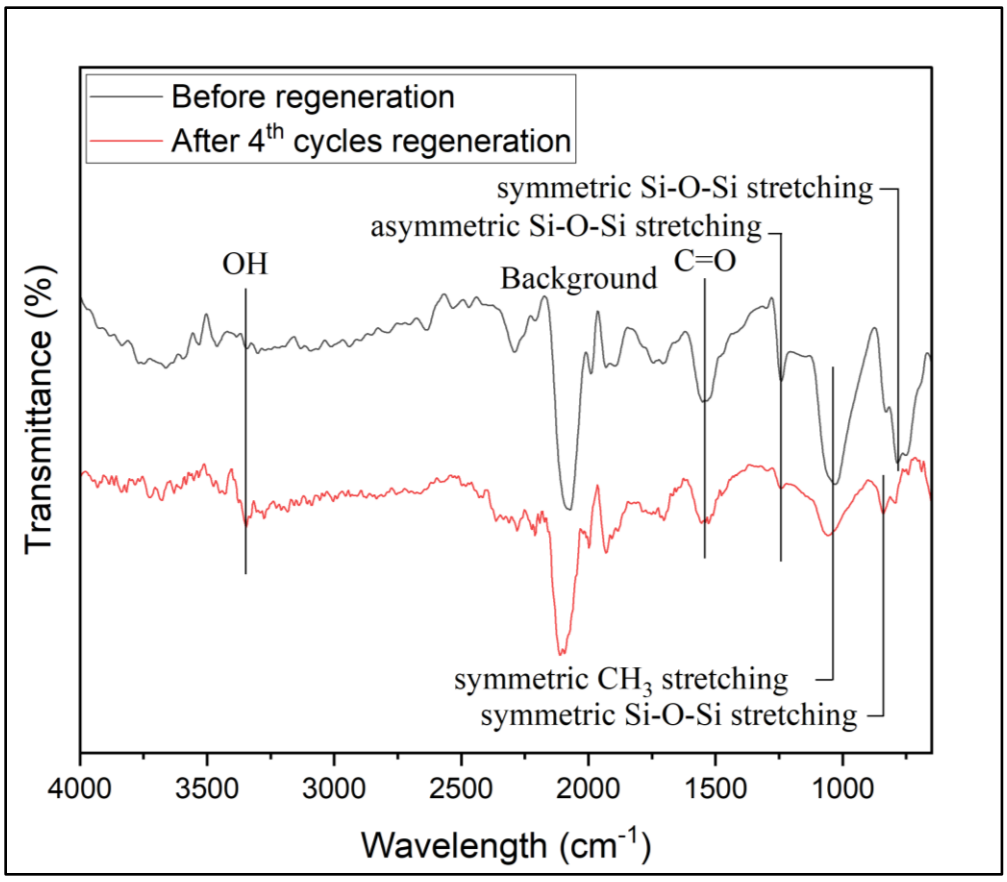

Figure 4.18: FTIR spectra of CS/HT-B_{1M}PDMS before and after regeneration

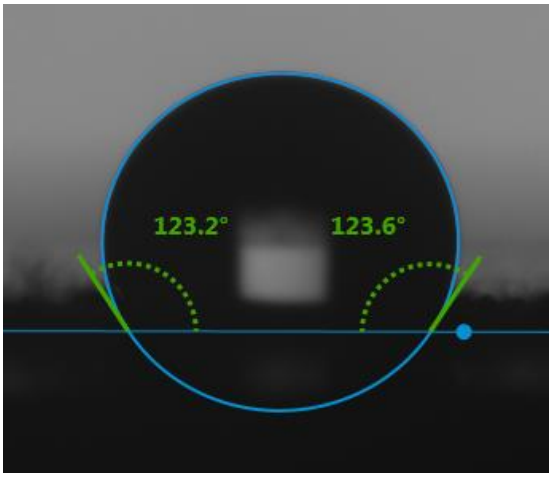

Figure 4.19: Water contact angle of CS/HT-B_{1M}PDMS after regeneration

CHAPTER 5

CONCLUSION, CHALLENGES AND LIMITATIONS, AND RECOMMENDATIONS

Conclusion

In summary, this study successfully synthesized hydrophobic honeycomb-like tubular biochar (hydrophobic HT-B) from corn stalks (CS) with an impregnation ratio of 1.0 M $ZnCl_2$, resulting in a good structure of HT-B that exhibited a high specific surface area (S_{BET}) of 1825.279 $m^2\ g^{-1}$ compared to palm leaves (PL) and pinewood sawdust (PWS). The concentration of 1.0 M was found to be optimal for the development of HT-B. Additionally, the hydrophobicity of CS impregnated with 1.0 M (CS/HT-B_{1M}) was increased by coating it with hydrophobic polydimethylsiloxane (PDMS) via thermal evaporation for the introduction of siloxane (Si-O-Si) surface functional groups on CS/HT-B_{1M}. The optimization parameters for PDMS coating, including coating ratio (CS/HT-B_{1M}: PDMS), modification temperature, and reaction time. These parameters played a crucial role in ensuring that a sufficient amount of PDMS was deposited on the surface of CS/HT-B_{1M}. The CS/HT-B_{1M} coated at coating ratio of 1:25 (CS/HT-B1M: PDMS), heated at 200 ºC for 1 h (CS/HT-B_{1M}PDMS) was found to be the optimum condition for PDMS coating with water contact angle rose from 0 to 132.8 º.

The adsorption of acetone onto CS/HT-B_{1M} and CS/HT-B_{1M}PDMS under different relative humidity (RH) conditions reveals the significant impact of water molecules on acetone adsorption. At high RH levels, the presence of water clusters obstructs the adsorption active sites, leading to competition between water molecules and acetone for adsorption. CS/HT-B_{1M}, with its hydrophilic surface, exhibits strong affinity for water molecules through hydrogen bonding, resulting in poor performance in acetone adsorption. On the other hand, CS/HT-B_{1M}PDMS, with its hydrophobic surface and Si-O-Si bonds, demonstrates enhanced acetone adsorption performance by reducing

the selectivity of water molecules and providing more available adsorption sites for acetone. Consequently, CS/HT-B_{1M}PDMS exhibits a higher capacity for acetone adsorption compared to CS/HT-B_{1M}.

The adsorption isotherm of acetone onto CS/HT-B_{1M} and CS/HT-B_{1M}PDMS exhibited a Sips model, which combines Langmuir-Freundlich models and indicates heterogeneous surface adsorption. In order to analyze the rate-controlling step of acetone adsorption, intraparticle diffusion (IPD) was assessed using the Weber-Morris model (W-M). The findings revealed that the mass transfer during acetone adsorption on both adsorbents primarily occurred through a diffusion-based process involving three consecutive steps: external surface adsorption, intraparticle diffusion, and adsorption equilibrium. The fitting results of the W-M IPD model demonstrated that intraparticle diffusion was the rate-controlling step for the acetone adsorption process on both adsorbents, while surface diffusion occurred rapidly. Additionally, the experimental data exhibited good fit to the nonlinear Bohart-Adams (B-A), Thomas, and Yoon-Nelson (Y-N) models. These three models exhibited high fitting correlation coefficients (R^2) above 0.998, confirming their ability to accurately predict the breakthrough curves of acetone adsorption onto CS/HT-B_{1M} and CS/HT-B_{1M}PDMS.

The regeneration of CS/HT-B_{1M}PDMS showed a decreased in performance after the first cycle; however, it still exhibited better performance compared to CS/HT-B_{1M}, particularly at 90% RH. This decrease could be attributed to the strong interaction between acetone and the Si-O-Si bond of PDMS, or the formation of permanent bonds that limit the availability of adsorption active sites for subsequent cycles. Acetone interacts with the Si-O-Si bond through various forces, including van der Waals forces, hydrogen bonding, and π-π interactions. Hydrogen bonding and π-π interactions are particularly strong attractions that require high temperatures for bond breaking during regeneration.

Challenges and limitations

The project encountered several challenges and limitations. The primary challenge was the impact of the pandemic. In certain states, there was a significant increase in Covid-19 cases, leading to restrictions on working conditions, domestic flights, courier services, and business hours. These

restrictions resulted in delays in the delivery of purchased experimental items, especially chemicals, which took longer than usual to arrive. Consequently, the research progress was affected.

Recommendation and further research study

There are several recommendations for further research studies that are worth exploring to enhance the performance of CS/HT-B_{1M}PDMS in VOCs adsorption under humid conditions. The regeneration of CS/HT-B_{1M}PDMS can be further improved by utilizing a combination of low-temperature and high-temperature regeneration methods, which have been proposed for chemical adsorption. This approach can preserve the integrity of the biochar and achieve optimal regeneration conditions. Furthermore, it is crucial to gain a deeper understanding of the mechanisms underlying the interactions between VOCs and the Si-O-Si bond of PDMS. Exploring these interactions will provide insights into the adsorption process and guide the development of more effective regeneration strategies. By implementing these improvements, it is possible to enhance the regeneration efficiency and extend the lifespan of CS/HT-B_{1M}PDMS as an effective adsorbent for VOC removal under humid conditions.

REFERENCES

Abu-Alsoud, Ghadeer F., Kelly A. Hawboldt, and Christina S. Bottaro. 2020. "Comparison of Four Adsorption Isotherm Models for Characterizing Molecular Recognition of Individual Phenolic Compounds in Porous Tailor-Made Molecularly Imprinted Polymer Films." *ACS Applied Materials & Interfaces* 12 (10): 11998-12009. https://doi.org/10.1021/acsami.9b21493. https://doi.org/10.1021/acsami.9b21493.

Adebayo, Busuyi O., Anirudh Krishnamurthy, Ali A. Rownaghi, and Fateme Rezaei. 2020. "Toluene Abatement by Simultaneous Adsorption and Oxidation over Mixed-Metal Oxides." *Industrial & Engineering Chemistry Research* 59 (30): 13762-13772. https://doi.org/10.1021/acs.iecr.0c02550. https://doi.org/10.1021/acs.iecr.0c02550.

Adeniyi, Adewale George, Sulyman A. Abdulkareem, Kingsley O. Iwuozor, Samuel Ogunniyi, Maryam T. Abdulkareem, Ebuka Chizitere Emenike, and Patience A. Sagboye. 2022. "Effect of salt impregnation on the properties of orange albedo biochar." *Cleaner Chemical Engineering* 3: 100059. https://doi.org/https://doi.org/10.1016/j.clce.2022.100059. https://www.sciencedirect.com/science/article/pii/S2772782322000572.

Adhikari, Sirjana, Wendy Timms, and M. A. Parvez Mahmud. 2022. "Optimising water holding capacity and hydrophobicity of biochar for soil amendment – A review." *Science of The Total Environment* 851: 158043. https://doi.org/https://doi.org/10.1016/j.scitotenv.2022.158043. https://www.sciencedirect.com/science/article/pii/S0048969722051427.

Ahmad, Mahtab, Sang Soo Lee, Xiaomin Dou, Dinesh Mohan, Jwa-Kyung Sung, Jae E. Yang, and Yong Sik Ok. 2012. "Effects of pyrolysis temperature on soybean stover-and peanut shell-derived biochar properties and TCE adsorption in water." *Bioresource technology* 118: 536-544.

Ahmad, Mahtab, Anushka Upamali Rajapaksha, Jung Eun Lim, Ming Zhang, Nanthi Bolan, Dinesh Mohan, Meththika Vithanage, Sang Soo Lee, and Yong Sik Ok. 2014. "Biochar as a sorbent for contaminant management in soil and water: a review." *Chemosphere* 99: 19-33.

Akbari, Raziyeh, and Carlo Antonini. 2021. "Contact angle measurements: From existing methods to an open-source tool." *Advances in Colloid and Interface Science* 294: 102470. https://doi.org/https://doi.org/10.1016/j.cis.2021.102470. https://www.sciencedirect.com/science/article/pii/S0001868621001111.

Al-Ghouti, Mohammad A., and Dana A. Da'ana. 2020. "Guidelines for the use and interpretation of adsorption isotherm models: A review." *Journal of Hazardous Materials* 393: 122383. https://doi.org/https://doi.org/10.1016/j.jhazmat.2020.122383. https://www.sciencedirect.com/science/article/pii/S030438942030371X.

Allahbakhsh, Ahmad, and Mohammad Arjmand. 2019. "Graphene-based phase change composites for energy harvesting and storage: State of the art and future prospects." *Carbon* 148: 441-480. https://doi.org/https://doi.org/10.1016/j.carbon.2019.04.009. https://www.sciencedirect.com/science/article/pii/S0008622319303264.

Almanassra, Ismail W., Anjaneyulu Chatla, Yahya Zakaria, Viktor Kochkodan, Abdallah Shanableh, Tahar Laoui, and Muataz Ali Atieh. 2022. "Palm leaves based biochar: advanced material characterization and heavy metal adsorption study." *Biomass*

Conversion and Biorefinery. https://doi.org/10.1007/s13399-022-03590-y. https://doi.org/10.1007/s13399-022-03590-y.

Alyousef, Haifa, Mohamed Ben Yahia, and Fatma Aouaini. 2020. "Statistical physics modeling of water vapor adsorption isotherm into kernels of dates: Experiments, microscopic interpretation and thermodynamic functions evaluation." *Arabian Journal of Chemistry* 13 (3): 4691-4702. https://doi.org/https://doi.org/10.1016/j.arabjc.2019.11.004. https://www.sciencedirect.com/science/article/pii/S1878535219301376.

Ammendola, P., F. Raganati, and R. Chirone. 2017. "CO2 adsorption on a fine activated carbon in a sound assisted fluidized bed: Thermodynamics and kinetics." *Chemical Engineering Journal* 322: 302-313. https://doi.org/https://doi.org/10.1016/j.cej.2017.04.037. https://www.sciencedirect.com/science/article/pii/S1385894717305648.

An, Yaxiong, Qiang Fu, Donghui Zhang, Yayan Wang, and Zhongli Tang. 2019. "Performance evaluation of activated carbon with different pore sizes and functional groups for VOC adsorption by molecular simulation." *Chemosphere* 227: 9-16. https://doi.org/https://doi.org/10.1016/j.chemosphere.2019.04.011. https://www.sciencedirect.com/science/article/pii/S0045653519306575.

Anand, Abhijeet, Vivek Kumar, and Priyanka Kaushal. 2022. "Biochar and its twin benefits: Crop residue management and climate change mitigation in India." *Renewable and Sustainable Energy Reviews* 156: 111959. https://doi.org/https://doi.org/10.1016/j.rser.2021.111959. https://www.sciencedirect.com/science/article/pii/S1364032121012247.

Anand, S. S., B. K. Philip, and H. M. Mehendale. 2014. "Volatile Organic Compounds." In *Encyclopedia of Toxicology (Third Edition)*, edited by Philip Wexler, 967-970. Oxford: Academic Press.

Ancione, Giuseppa, Roberto Lisi, and Maria Francesca Milazzo. 2021. "Human health risk associated with emissions of volatile organic compounds due to the ship-loading of hydrocarbons in refineries." *Atmospheric Pollution Research* 12 (2): 432-442. https://doi.org/https://doi.org/10.1016/j.apr.2020.12.004. https://www.sciencedirect.com/science/article/pii/S1309104220303469.

Ang, Teck Nam, Brent R. Young, Matthew Taylor, Rob Burrell, Mohamed Kheireddine Aroua, Wei-Hsin Chen, and Saeid Baroutian. 2020. "Enrichment of surface oxygen functionalities on activated carbon for adsorptive removal of sevoflurane." *Chemosphere* 260: 127496. https://doi.org/https://doi.org/10.1016/j.chemosphere.2020.127496. https://www.sciencedirect.com/science/article/pii/S0045653520316908.

Ani, J. U., K. G. Akpomie, U. C. Okoro, L. E. Aneke, O. D. Onukwuli, and O. T. Ujam. 2020. "Potentials of activated carbon produced from biomass materials for sequestration of dyes, heavy metals, and crude oil components from aqueous environment." *Applied Water Science* 10 (2): 69. https://doi.org/10.1007/s13201-020-1149-8. https://doi.org/10.1007/s13201-020-1149-8.

Apiratikul, Ronbanchob, and Khim Hoong Chu. 2021. "Improved fixed bed models for correlating asymmetric adsorption breakthrough curves." *Journal of Water Process Engineering* 40: 101810. https://doi.org/https://doi.org/10.1016/j.jwpe.2020.101810. https://www.sciencedirect.com/science/article/pii/S2214714420306875.

Asghar, Usama, Sikander Rafiq, Adeel Anwar, Tanveer Iqbal, Ashfaq Ahmed, Farrukh Jamil, M. Shahzad Khurram, Majid Majeed Akbar, Abid Farooq, Noor S. Shah, and Young-Kwon Park. 2021. "Review on the progress in emission control technologies for the abatement

of CO2, SOx and NOx from fuel combustion." *Journal of Environmental Chemical Engineering* 9 (5): 106064. https://doi.org/https://doi.org/10.1016/j.jece.2021.106064. https://www.sciencedirect.com/science/article/pii/S2213343721010411.

Bagheri, Afrouz, Emmanuel Abu-Danso, Jibran Iqbal, and Amit Bhatnagar. 2020. "Modified biochar from Moringa seed powder for the removal of diclofenac from aqueous solution." *Environmental Science and Pollution Research* 27 (7): 7318-7327. https://doi.org/10.1007/s11356-019-06844-x. https://doi.org/10.1007/s11356-019-06844-x.

Bai, Shuqin, Jiaxin Li, Wei Ding, Shuxuan Chen, and Ru Ya. 2022. "Removal of boron by a modified resin in fixed bed column: Breakthrough curve analysis using dynamic adsorption models and artificial neural network model." *Chemosphere* 296: 134021. https://doi.org/https://doi.org/10.1016/j.chemosphere.2022.134021. https://www.sciencedirect.com/science/article/pii/S0045653522005148.

Bamdad, Hanieh, Kelly Hawboldt, and Stephanie MacQuarrie. 2018. "Nitrogen Functionalized Biochar as a Renewable Adsorbent for Efficient CO2 Removal." *Energy & Fuels* 32 (11): 11742-11748. https://doi.org/10.1021/acs.energyfuels.8b03056. https://doi.org/10.1021/acs.energyfuels.8b03056.

Barquilha, Carlos E. R., and Maria C. B. Braga. 2021. "Adsorption of organic and inorganic pollutants onto biochars: Challenges, operating conditions, and mechanisms." *Bioresource Technology Reports* 15: 100728. https://doi.org/https://doi.org/10.1016/j.biteb.2021.100728. https://www.sciencedirect.com/science/article/pii/S2589014X21001067.

Barquilha, Carlos ER, and Maria CB %J Bioresource Technology Reports Braga. 2021. "Adsorption of organic and inorganic pollutants onto biochars: challenges, operating conditions, and mechanisms." 15: 100728.

Bataillou, Gregory, Carine Lee, Virginie Monnier, Tony Gerges, Andrei Sabac, Christian Vollaire, and Naoufel Haddour. 2022. "Cedar Wood-Based Biochar: Properties, Characterization, and Applications as Anodes in Microbial Fuel Cell." *Applied Biochemistry and Biotechnology* 194 (9): 4169-4186. https://doi.org/10.1007/s12010-022-03997-3. https://doi.org/10.1007/s12010-022-03997-3.

Batur, Ebru, and Sinan Kutluay. 2022. "Dynamic adsorption behavior of benzene, toluene, and xylene VOCs in single- and multi-component systems by activated carbon derived from defatted black cumin (Nigella sativa L.) biowaste." *Journal of Environmental Chemical Engineering* 10 (3): 107565. https://doi.org/https://doi.org/10.1016/j.jece.2022.107565. https://www.sciencedirect.com/science/article/pii/S2213343722004389.

Baytar, Orhan, Ömer Şahin, Sabit Horoz, and Sinan Kutluay. 2020. "High-performance gas-phase adsorption of benzene and toluene on activated carbon: response surface optimization, reusability, equilibrium, kinetic, and competitive adsorption studies." *Environmental Science and Pollution Research* 27 (21): 26191-26210. https://doi.org/10.1007/s11356-020-08848-4. https://doi.org/10.1007/s11356-020-08848-4.

Bedane, Alemayehu H., Tian-xiang Guo, Mladen Eić, and Huining Xiao. 2019. "Adsorption of volatile organic compounds on peanut shell activated carbon." *The Canadian Journal of Chemical Engineering* 97 (1): 238-246. https://doi.org/https://doi.org/10.1002/cjce.23330. https://doi.org/10.1002/cjce.23330.

Belaissaoui, Bouchra, Yann Le Moullec, and Eric Favre. 2016. "Energy efficiency of a hybrid membrane/condensation process for VOC (Volatile Organic Compounds) recovery from air: A generic approach." *Energy* 95: 291-302. https://doi.org/https://doi.org/10.1016/j.energy.2015.12.006. https://www.sciencedirect.com/science/article/pii/S0360544215016485.

Ben Salem, Imen, Maisa El Gamal, Manish Sharma, Suhaib Hameedi, and Fares M. Howari. 2021. "Utilization of the UAE date palm leaf biochar in carbon dioxide capture and sequestration processes." *Journal of Environmental Management* 299: 113644. https://doi.org/https://doi.org/10.1016/j.jenvman.2021.113644. https://www.sciencedirect.com/science/article/pii/S0301479721017060.

Bernal, Valentina, Liliana Giraldo, and Juan Carlos Moreno-Piraján. 2020. "A new methodology to determine the effect of the adsorbate-adsorbent interactions on the analgesic adsorption onto activated carbon using kinetic and calorimetry data." *Environmental Science and Pollution Research* 27 (29): 36639-36650. https://doi.org/10.1007/s11356-020-09725-w. https://doi.org/10.1007/s11356-020-09725-w.

Bi, Zhihong, Qingqiang Kong, Yufang Cao, Guohua Sun, Fangyuan Su, Xianxian Wei, Xiaoming Li, Aziz Ahmad, Lijing Xie, and Cheng-Meng Chen. 2019. "Biomass-derived porous carbon materials with different dimensions for supercapacitor electrodes: a review." *Journal of Materials Chemistry A* 7 (27): 16028-16045. https://doi.org/10.1039/C9TA04436A. http://dx.doi.org/10.1039/C9TA04436A.

Binh, Quach An, and Puangrat Kajitvichyanukul. 2018. "Adsorption mechanism of dichlorvos onto coconut fibre biochar: the significant dependence of H-bonding and the pore-filling mechanism." *Water Science and Technology* 79 (5): 866-876. https://doi.org/10.2166/wst.2018.529. https://doi.org/10.2166/wst.2018.529.

Boch, Steffen, Yasemin Kurtogullari, Eric Allan, Malie Lessard-Therrien, Nora Simone Rieder, Markus Fischer, Gerard Martínez De León, Raphaël Arlettaz, and Jean-Yves Humbert. 2021. "Effects of fertilization and irrigation on vascular plant species richness, functional composition and yield in mountain grasslands." *Journal of Environmental Management* 279: 111629. https://doi.org/https://doi.org/10.1016/j.jenvman.2020.111629. https://www.sciencedirect.com/science/article/pii/S0301479720315541.

Boumediri, Haithem, Abderrezak Bezazi, Gilberto Garcia Del Pino, Abdelkrim Haddad, Fabrizio Scarpa, and Alain Dufresne. 2019. "Extraction and characterization of vascular bundle and fiber strand from date palm rachis as potential bio-reinforcement in composite." *Carbohydrate Polymers* 222: 114997. https://doi.org/https://doi.org/10.1016/j.carbpol.2019.114997. https://www.sciencedirect.com/science/article/pii/S0144861719306575.

Bumajdad, A., and P. Hasila. 2023. "Surface modification of date palm activated carbonaceous materials for heavy metal removal and CO2 adsorption." *Arabian Journal of Chemistry* 16 (1): 104403. https://doi.org/https://doi.org/10.1016/j.arabjc.2022.104403. https://www.sciencedirect.com/science/article/pii/S1878535222007195.

Bushra, Rani, Sharifah Mohamad, Yatimah Alias, Yongcan Jin, and Mehraj Ahmad. 2021. "Current approaches and methodologies to explore the perceptive adsorption mechanism of dyes on low-cost agricultural waste: A review." *Microporous and Mesoporous Materials* 319: 111040. https://doi.org/https://doi.org/10.1016/j.micromeso.2021.111040. https://www.sciencedirect.com/science/article/pii/S1387181121001669.

Buttersack, Christoph. 2019. "Modeling of type IV and V sigmoidal adsorption isotherms." *Physical Chemistry Chemical Physics* 21 (10): 5614-5626.

Cai, Guanjing, and Zhi-long Ye. 2022. "Concentration-dependent adsorption behaviors and mechanisms for ammonium and phosphate removal by optimized Mg-impregnated biochar." *Journal of Cleaner Production* 349: 131453. https://doi.org/https://doi.org/10.1016/j.jclepro.2022.131453. https://www.sciencedirect.com/science/article/pii/S0959652622010757.

Cao, Danyang, Yuxiang Ji, Li Liu, Long Li, Licheng Li, Xin Feng, Jiahua Zhu, Xiaohua Lu, and Liwen Mu. 2022. "A facile and green strategy to synthesize N/P co-doped bio-char as VOCs adsorbent: Through efficient biogas slurry treatment and struvite transform." *Fuel* 322: 124156. https://doi.org/https://doi.org/10.1016/j.fuel.2022.124156. https://www.sciencedirect.com/science/article/pii/S0016236122010134.

Carter, Ellison M., Lynn E. Katz, Gerald E. Speitel, and David Ramirez. 2011. "Gas-Phase Formaldehyde Adsorption Isotherm Studies on Activated Carbon: Correlations of Adsorption Capacity to Surface Functional Group Density." *Environmental Science & Technology* 45 (15): 6498-6503. https://doi.org/10.1021/es104286d. https://pubs.acs.org/doi/abs/10.1021/es104286d.

Chai, Wai Siong, Jie Ying Cheun, P. Senthil Kumar, Muhammad Mubashir, Zahid Majeed, Fawzi Banat, Shih-Hsin Ho, and Pau Loke Show. 2021. "A review on conventional and novel materials towards heavy metal adsorption in wastewater treatment application." *Journal of Cleaner Production* 296: 126589. https://doi.org/https://doi.org/10.1016/j.jclepro.2021.126589. https://www.sciencedirect.com/science/article/pii/S095965262100809X.

Chen, Chun-Chi, Yen-Hui Huang, Shih-Min Hung, Chiaying Chen, Chi-Wen Lin, and Hsi-Hsien Yang. 2021. "Hydrophobic deep eutectic solvents as attractive media for low-concentration hydrophobic VOC capture." *Chemical Engineering Journal* 424: 130420. https://doi.org/https://doi.org/10.1016/j.cej.2021.130420. https://www.sciencedirect.com/science/article/pii/S1385894721020064.

Chen, Donghang, Qianxi Tang, Wei Deng, Soamwadee Chaianansutcharit, and Limin Guo. 2022. "Comparative studies on the toluene sorption performance over silicalite-1 zeolites with different morphologies." *Microporous and Mesoporous Materials* 346: 112275. https://doi.org/https://doi.org/10.1016/j.micromeso.2022.112275. https://www.sciencedirect.com/science/article/pii/S1387181122005935.

Chen, Junjie, Chao Sun, Zhen Huang, Feng Qin, Hualong Xu, and Wei Shen. 2020. "Fabrication of Functionalized Porous Silica Nanocapsules with a Hollow Structure for High Performance of Toluene Adsorption–Desorption." *ACS Omega* 5 (11): 5805-5814. https://doi.org/10.1021/acsomega.9b03982. https://doi.org/10.1021/acsomega.9b03982.

Chen, RongPing, YinLong Zhang, AiJun Ma, and WeiMin %J JOURNAL OF NANJING FORESTRY UNIVERSITY Jiang. 2014. "Study on the modification of humic acid and its adsorption to cadmium." 57 (04): 102.

Chen, Ruofei, Ning Han, Liqing Li, Shaobin Wang, Xiancheng Ma, Chunhao Wang, Hailong Li, Haoyang Li, and Lin Zeng. 2020. "Fundamental understanding of oxygen content in activated carbon on acetone adsorption desorption." *Applied Surface Science* 508: 145211. https://doi.org/https://doi.org/10.1016/j.apsusc.2019.145211. https://www.sciencedirect.com/science/article/pii/S0169433219340280.

Chen, Ruofei, Zhengxin Yao, Ning Han, Xiancheng Ma, Liqing Li, Shaomin Liu, Hongqi Sun, and Shaobin Wang. 2020. "Insights into the Adsorption of VOCs on a Cobalt-Adeninate Metal–Organic Framework (Bio-MOF-11)." *ACS Omega* 5 (25): 15402-15408. https://doi.org/10.1021/acsomega.0c01504. https://doi.org/10.1021/acsomega.0c01504.

Chen, Tao, Chenchong Fu, Yaqian Liu, Feng Pan, Feng Wu, Zhixiong You, and Jinjun Li. 2021. "Adsorption of volatile organic compounds by mesoporous graphitized carbon: Enhanced organophilicity, humidity resistance, and mass transfer." *Separation and Purification Technology* 264: 118464. https://doi.org/https://doi.org/10.1016/j.seppur.2021.118464. https://www.sciencedirect.com/science/article/pii/S1383586621001660.

Chen, Tao, Yuanfeng Wei, Weijian Yang, and Chengbin Liu. 2021. "Highly efficient As(III) removal in water using millimeter-sized porous granular MgO-biochar with high adsorption capacity." *Journal of Hazardous Materials* 416: 125822. https://doi.org/https://doi.org/10.1016/j.jhazmat.2021.125822. https://www.sciencedirect.com/science/article/pii/S030438942100786X.

Chen, Wei-Hsin, C. Naveen, Praveen Kumar Ghodke, Amit Kumar Sharma, and Prakash Bobde. 2023. "Co-pyrolysis of lignocellulosic biomass with other carbonaceous materials: A review on advance technologies, synergistic effect, and future prospectus." *Fuel* 345: 128177. https://doi.org/https://doi.org/10.1016/j.fuel.2023.128177. https://www.sciencedirect.com/science/article/pii/S0016236123007901.

Chen, Wei, Haiping Yang, Yingquan Chen, Xu Chen, Yang Fang, and Hanping Chen. 2016. "Biomass pyrolysis for nitrogen-containing liquid chemicals and nitrogen-doped carbon materials." *Journal of Analytical and Applied Pyrolysis* 120: 186-193. https://doi.org/https://doi.org/10.1016/j.jaap.2016.05.004. https://www.sciencedirect.com/science/article/pii/S0165237015303399.

Chen, Weisheng, Baolong Zhao, Yiping Guo, Yujie Guo, Zhihong Zheng, Tannaz Pak, and Guoting Li. 2021. "Effect of hydrothermal pretreatment on pyrolyzed sludge biochars for tetracycline adsorption." *Journal of Environmental Chemical Engineering* 9 (6): 106557. https://doi.org/https://doi.org/10.1016/j.jece.2021.106557. https://www.sciencedirect.com/science/article/pii/S2213343721015347.

Chen, Xinyu, Md Faysal Hossain, Chengyu Duan, Jian Lu, Yiu Fai Tsang, Md Shoffikul Islam, and Yanbo Zhou. 2022. "Isotherm models for adsorption of heavy metals from water - A review." *Chemosphere* 307: 135545. https://doi.org/https://doi.org/10.1016/j.chemosphere.2022.135545. https://www.sciencedirect.com/science/article/pii/S0045653522020380.

Chen, Zihan, and Ren He. 2023. "Competitive adsorption characteristics of gasoline evaporated VOCs in microporous activated carbon by molecular simulation." *Journal of Molecular Graphics and Modelling* 121: 108444. https://doi.org/https://doi.org/10.1016/j.jmgm.2023.108444. https://www.sciencedirect.com/science/article/pii/S1093326323000426.

Cheng, Song, Saidan Zhao, Hui Guo, Baolin Xing, Yongzhi Liu, Chuanxiang Zhang, and Mingjie Ma. 2022. "High-efficiency removal of lead/cadmium from wastewater by MgO modified biochar derived from crofton weed." *Bioresource Technology* 343: 126081. https://doi.org/https://doi.org/10.1016/j.biortech.2021.126081. https://www.sciencedirect.com/science/article/pii/S0960852421014231.

Cheng, Tangying, Jinjin Li, Xiuwei Ma, Lei Zhou, Hao Wu, and Linjun Yang. 2022. "Alkylation modified pistachio shell-based biochar to promote the adsorption of VOCs in high

humidity environment." *Environmental Pollution* 295: 118714. https://doi.org/https://doi.org/10.1016/j.envpol.2021.118714. https://www.sciencedirect.com/science/article/pii/S026974912102296X.

Cheng, Yu-Wei, Chia-Wei Hsiao, Zi-Ling Zeng, Wei-Lin Syu, and Ting-Yu Liu. 2020. "The interparticle gap manipulation of Au-Ag nanoparticle arrays deposited on flexible and atmospheric plasma-treated PDMS substrate for SERS detection." *Surface and Coatings Technology* 389: 125653. https://doi.org/https://doi.org/10.1016/j.surfcoat.2020.125653. https://www.sciencedirect.com/science/article/pii/S0257897220303224.

Chiang, Yu-Chun, Pen-Chi Chiang, and Chin-Pao Huang. 2001. "Effects of pore structure and temperature on VOC adsorption on activated carbon." *Carbon* 39 (4): 523-534. https://doi.org/https://doi.org/10.1016/S0008-6223(00)00161-5. https://www.sciencedirect.com/science/article/pii/S0008622300001615.

Chu, Khim Hoong. 2020. "Breakthrough curve analysis by simplistic models of fixed bed adsorption: In defense of the century-old Bohart-Adams model." *Chemical Engineering Journal* 380: 122513. https://doi.org/https://doi.org/10.1016/j.cej.2019.122513. https://www.sciencedirect.com/science/article/pii/S1385894719319163.

Chuah, Chong Yang, Kunli Goh, Yanqin Yang, Heqing Gong, Wen Li, H. Enis Karahan, Michael D. Guiver, Rong Wang, and Tae-Hyun Bae. 2018. "Harnessing Filler Materials for Enhancing Biogas Separation Membranes." *Chemical Reviews* 118 (18): 8655-8769. https://doi.org/10.1021/acs.chemrev.8b00091. https://doi.org/10.1021/acs.chemrev.8b00091.

Dai, Yingjie, Naixin Zhang, Chuanming Xing, Qingxia Cui, and Qiya Sun. 2019. "The adsorption, regeneration and engineering applications of biochar for removal organic pollutants: A review." *Chemosphere* 223: 12-27. https://doi.org/https://doi.org/10.1016/j.chemosphere.2019.01.161. https://www.sciencedirect.com/science/article/pii/S0045653519301778.

Dai, Yingjie, Naixin Zhang, Chuanming Xing, Qingxia Cui, and Qiya %J Chemosphere Sun. 2019. "The adsorption, regeneration and engineering applications of biochar for removal organic pollutants: a review." 223: 12-27.

Darracq, Guillaume, Annabelle Couvert, Catherine Couriol, Abdeltif Amrane, and Pierre Le Cloirec. 2010. "Kinetics of toluene and sulfur compounds removal by means of an integrated process involving the coupling of absorption and biodegradation." *Journal of Chemical Technology & Biotechnology* 85 (8): 1156-1161. https://doi.org/https://doi.org/10.1002/jctb.2414. https://doi.org/10.1002/jctb.2414.

Davarpanah, Morteza, Keivan Rahmani, Samineh Kamravaei, Zaher Hashisho, David Crompton, and James E. Anderson. 2022. "Modeling the effect of humidity and temperature on VOC removal efficiency in a multistage fluidized bed adsorber." *Chemical Engineering Journal* 431: 133991. https://doi.org/https://doi.org/10.1016/j.cej.2021.133991. https://www.sciencedirect.com/science/article/pii/S1385894721055649.

Deng, Hua, Tingting Pan, Yan Zhang, Lian Wang, Qinming Wu, Jinzhu Ma, Wenpo Shan, and Hong He. 2020. "Adsorptive removal of toluene and dichloromethane from humid exhaust on MFI, BEA and FAU zeolites: An experimental and theoretical study." *Chemical Engineering Journal* 394: 124986. https://doi.org/https://doi.org/10.1016/j.cej.2020.124986. https://www.sciencedirect.com/science/article/pii/S1385894720309785.

Ding, Yong. 2019. "Volatile Organic Compound Liquid Recovery by the Dead End Gas Separation Membrane Process: Theory and Process Simulation." *Industrial & Engineering Chemistry Research* 58 (12): 5008-5017. https://doi.org/10.1021/acs.iecr.9b00586. https://doi.org/10.1021/acs.iecr.9b00586.

Dissanayake, Pavani Dulanja, Siming You, Avanthi Deshani Igalavithana, Yinfeng Xia, Amit Bhatnagar, Souradeep Gupta, Harn Wei Kua, Sumin Kim, Jung-Hwan Kwon, Daniel C. W. Tsang, and Yong Sik Ok. 2020. "Biochar-based adsorbents for carbon dioxide capture: A critical review." *Renewable and Sustainable Energy Reviews* 119: 109582. https://doi.org/https://doi.org/10.1016/j.rser.2019.109582. http://www.sciencedirect.com/science/article/pii/S1364032119307907.

Dobre, Tănase, Oana C. Pârvulescu, Gustav Iavorschi, Marta Stroescu, and Anicuţa Stoica. 2014. "Volatile Organic Compounds Removal from Gas Streams by Adsorption onto Activated Carbon." *Industrial & Engineering Chemistry Research* 53 (9): 3622-3628. https://doi.org/10.1021/ie402504u. https://doi.org/10.1021/ie402504u.

Dumont, Eric, Guillaume Darracq, Annabelle Couvert, Catherine Couriol, Abdeltif Amrane, Diane Thomas, Yves Andrès, and Pierre Le Cloirec. 2011. "VOC absorption in a countercurrent packed-bed column using water/silicone oil mixtures: Influence of silicone oil volume fraction." *Chemical Engineering Journal* 168 (1): 241-248. https://doi.org/https://doi.org/10.1016/j.cej.2010.12.073. https://www.sciencedirect.com/science/article/pii/S138589471100009X.

Dutta, Saikat, Asim Bhaumik, and Kevin C. W. Wu. 2014. "Hierarchically porous carbon derived from polymers and biomass: effect of interconnected pores on energy applications." *Energy & Environmental Science* 7 (11): 3574-3592. https://doi.org/10.1039/C4EE01075B. http://dx.doi.org/10.1039/C4EE01075B.

Dutta, Tanushree, Taejin Kim, Kowsalya Vellingiri, Daniel C. W. Tsang, J. R. Shon, Ki-Hyun Kim, and Sandeep Kumar. 2019. "Recycling and regeneration of carbonaceous and porous materials through thermal or solvent treatment." *Chemical Engineering Journal* 364: 514-529. https://doi.org/https://doi.org/10.1016/j.cej.2019.01.049. https://www.sciencedirect.com/science/article/pii/S1385894719300579.

Ece, Mehmet Şakir, and Sinan Kutluay. 2022. "Comparative and competitive adsorption of gaseous toluene, ethylbenzene, and xylene onto natural cellulose-modified Fe3O4 nanoparticles." *Journal of Environmental Chemical Engineering* 10 (2): 107389. https://doi.org/https://doi.org/10.1016/j.jece.2022.107389. https://www.sciencedirect.com/science/article/pii/S2213343722002627.

Eduok, Ubong, Omar Faye, and Jerzy Szpunar. 2017. "Recent developments and applications of protective silicone coatings: A review of PDMS functional materials." *Progress in Organic Coatings* 111: 124-163. https://doi.org/https://doi.org/10.1016/j.porgcoat.2017.05.012. https://www.sciencedirect.com/science/article/pii/S0300944016306464.

El-Hashemy, Mohammed A., and Hazim M. Ali. 2018. "Characterization of BTEX group of VOCs and inhalation risks in indoor microenvironments at small enterprises." *Science of The Total Environment* 645: 974-983. https://doi.org/https://doi.org/10.1016/j.scitotenv.2018.07.157. https://www.sciencedirect.com/science/article/pii/S0048969718326470.

El Gamal, Maisa, Hussein A Mousa, Muftah H El-Naas, Renju Zacharia, Simon %J Separation Judd, and Purification Technology. 2018. "Bio-regeneration of activated carbon: A comprehensive review." 197: 345-359.

Eshun, John, Lijun Wang, Emmanuel Ansah, Abolghasem Shahbazi, Keith Schimmel, Vinayak Kabadi, and Shyam Aravamudhan. 2019. "Characterization of the physicochemical and structural evolution of biomass particles during combined pyrolysis and CO2 gasification." *Journal of the Energy Institute* 92 (1): 82-93. https://doi.org/https://doi.org/10.1016/j.joei.2017.11.003. https://www.sciencedirect.com/science/article/pii/S1743967117300879.

Fan, Qinya, Jianxiong Sun, Lei Chu, Liqiang Cui, Guixiang Quan, Jinlong Yan, Qaiser Hussain, and Muhammad Iqbal. 2018. "Effects of chemical oxidation on surface oxygen-containing functional groups and adsorption behavior of biochar." *Chemosphere* 207: 33-40. https://doi.org/https://doi.org/10.1016/j.chemosphere.2018.05.044. https://www.sciencedirect.com/science/article/pii/S0045653518308865.

Fatima, Nabira, Umair Yaqub Qazi, Asim Mansha, Ijaz Ahmad Bhatti, Rahat Javaid, Qamar Abbas, Nimra Nadeem, Zulfiqar Ahmad Rehan, Saima Noreen, and Muhammad Zahid. 2021. "Recent developments for antimicrobial applications of graphene-based polymeric composites: A review." *Journal of Industrial and Engineering Chemistry* 100: 40-58. https://doi.org/https://doi.org/10.1016/j.jiec.2021.04.050. https://www.sciencedirect.com/science/article/pii/S1226086X21002550.

Feyzbar-Khalkhali-Nejad, Farshad, Ehsan Hassani, Ali Rashti, and Tae-Sik Oh. 2021. "Adsorption-based CO removal: Principles and materials." *Journal of Environmental Chemical Engineering* 9 (4): 105317. https://doi.org/https://doi.org/10.1016/j.jece.2021.105317. https://www.sciencedirect.com/science/article/pii/S2213343721002943.

Gabruś, Elżbieta, Piotr Tabero, and Tomasz Aleksandrzak. 2022. "A study of the thermal regeneration of carbon and zeolite adsorbents after adsorption of 1-hexene vapor." *Applied Thermal Engineering* 216: 119065. https://doi.org/https://doi.org/10.1016/j.applthermaleng.2022.119065. https://www.sciencedirect.com/science/article/pii/S1359431122009978.

Gan, Fengli, Bowen Cheng, Ziheng Jin, Zhongde Dai, Bangda Wang, Lin Yang, and Xia Jiang. 2021. "Hierarchical porous biochar from plant-based biomass through selectively removing lignin carbon from biochar for enhanced removal of toluene." *Chemosphere* 279: 130514. https://doi.org/https://doi.org/10.1016/j.chemosphere.2021.130514. https://www.sciencedirect.com/science/article/pii/S0045653521009851.

Gan, Guoqiang, Shiying Fan, Xinyong Li, Zhongshen Zhang, and Zhengping Hao. 2023. "Adsorption and membrane separation for removal and recovery of volatile organic compounds." *Journal of Environmental Sciences* 123: 96-115. https://doi.org/https://doi.org/10.1016/j.jes.2022.02.006. https://www.sciencedirect.com/science/article/pii/S100107422200064X.

Gang, Daniel, Zaki Uddin Ahmad, Qiyu Lian, Lunguang Yao, and Mark E. Zappi. 2021. "A review of adsorptive remediation of environmental pollutants from aqueous phase by ordered mesoporous carbon." *Chemical Engineering Journal* 403: 126286. https://doi.org/https://doi.org/10.1016/j.cej.2020.126286. https://www.sciencedirect.com/science/article/pii/S1385894720324141.

Gao, Wenran, Zixiang Lin, Haoran Chen, Shanshan Yan, Haonan Zhu, Hong Zhang, Hongqi Sun, Shu Zhang, Shoujun Zhang, and Yinlong Wu. 2022. "Roles of graphitization degree and surface functional groups of N-doped activated biochar for phenol adsorption." *Journal of Analytical and Applied Pyrolysis* 167: 105700. https://doi.org/https://doi.org/10.1016/j.jaap.2022.105700. https://www.sciencedirect.com/science/article/pii/S0165237022002704.

Gao, Zhimin, Guoshuai Song, Xuemin Zhang, Qian Li, Shuang Yang, Tieqiang Wang, Yunong Li, Liying Zhang, Lei Guo, and Yu Fu. 2020. "A facile PDMS coating approach to room-temperature gas sensors with high humidity resistance and long-term stability." *Sensors and Actuators B: Chemical* 325: 128810. https://doi.org/https://doi.org/10.1016/j.snb.2020.128810. https://www.sciencedirect.com/science/article/pii/S0925400520311576.

Gelles, Teresa, Anirudh Krishnamurthy, Busuyi Adebayo, Ali Rownaghi, and Fateme Rezaei. 2020. "Abatement of gaseous volatile organic compounds: A material perspective." *Catalysis Today* 350: 3-18. https://doi.org/https://doi.org/10.1016/j.cattod.2019.06.017. https://www.sciencedirect.com/science/article/pii/S0920586119302950.

Ghanbari, Taravat, Faisal Abnisa, and Wan Mohd Ashri Wan Daud. 2020. "A review on production of metal organic frameworks (MOF) for CO2 adsorption." *Science of The Total Environment* 707: 135090. https://doi.org/https://doi.org/10.1016/j.scitotenv.2019.135090. https://www.sciencedirect.com/science/article/pii/S004896971935082X.

Gil, R. R., B. Ruiz, M. S. Lozano, M. J. Martín, and E. Fuente. 2014. "VOCs removal by adsorption onto activated carbons from biocollagenic wastes of vegetable tanning." *Chemical Engineering Journal* 245: 80-88. https://doi.org/https://doi.org/10.1016/j.cej.2014.02.012. https://www.sciencedirect.com/science/article/pii/S1385894714001405.

Giudicianni, Paola, Valentina Gargiulo, Corinna Maria Grottola, Michela Alfè, Ana Isabel Ferreiro, Miguel Abreu Almeida Mendes, Massimo Fagnano, and Raffaele Ragucci. 2021. "Inherent Metal Elements in Biomass Pyrolysis: A Review." *Energy & Fuels* 35 (7): 5407-5478. https://doi.org/10.1021/acs.energyfuels.0c04046. https://doi.org/10.1021/acs.energyfuels.0c04046.

Goel, Chirag, Sooraj Mohan, and P. Dinesha. 2021. "CO2 capture by adsorption on biomass-derived activated char: A review." *Science of The Total Environment* 798: 149296. https://doi.org/https://doi.org/10.1016/j.scitotenv.2021.149296. https://www.sciencedirect.com/science/article/pii/S0048969721043692.

Goldstein, Allen H, William W Nazaroff, Charles J Weschler, and Jonathan Williams. 2020. "How do indoor environments affect air pollution exposure?" *Environmental science & technology* 55 (1): 100-108.

Gómez-Avilés, A., M. Peñas-Garzón, C. Belver, J. J. Rodriguez, and J. Bedia. 2021. "Equilibrium, kinetics and breakthrough curves of acetaminophen adsorption onto activated carbons from microwave-assisted FeCl3-activation of lignin." *Separation and Purification Technology* 278: 119654. https://doi.org/https://doi.org/10.1016/j.seppur.2021.119654. https://www.sciencedirect.com/science/article/pii/S1383586621013629.

Gopalan, Jayaprina, Archina Buthiyappan, and Abdul Aziz Abdul Raman. 2022. "Insight into metal-impregnated biomass based activated carbon for enhanced carbon dioxide

adsorption: A review." *Journal of Industrial and Engineering Chemistry* 113: 72-95. https://doi.org/https://doi.org/10.1016/j.jiec.2022.06.026. https://www.sciencedirect.com/science/article/pii/S1226086X22003501.

Guo, Dongsheng, Qiantao Shi, Binbin He, and Xiaoying %J Journal of hazardous materials Yuan. 2011. "Different solvents for the regeneration of the exhausted activated carbon used in the treatment of coking wastewater." 186 (2-3): 1788-1793.

Guo, Yangyang, Yuran Li, Jian Wang, Tingyu Zhu, and Meng Ye. 2014. "Effects of activated carbon properties on chlorobenzene adsorption and adsorption product analysis." *Chemical Engineering Journal* 236: 506-512. https://doi.org/https://doi.org/10.1016/j.cej.2013.10.017. https://www.sciencedirect.com/science/article/pii/S1385894713013351.

Guo, Zhenji, Zhongyuan Liu, Kai Zhang, Wenwen Wang, Jia Pang, Zongge Li, Zixi Kang, and Dongfeng Zhao. 2021. "Stable metal-organic frameworks based mixed matrix membranes for Ethylbenzene/N2 separation." *Chemical Engineering Journal* 416: 129193. https://doi.org/https://doi.org/10.1016/j.cej.2021.129193. https://www.sciencedirect.com/science/article/pii/S1385894721007841.

Gupta, Vinod Kumar, Rajeev Kumar, Arunima Nayak, Tawfik A. Saleh, and M. A. Barakat. 2013. "Adsorptive removal of dyes from aqueous solution onto carbon nanotubes: a review." *Advances in colloid and interface science* 193: 24-34.

Hadroug, Samar, Salah Jellali, Ahmed Amine Azzaz, Marzena Kwapinska, Helmi Hamdi, James J. Leahy, Mejdi Jeguirim, and Witold Kwapinski. 2022. "Valorization of salt post-modified poultry manure biochars for phosphorus recovery from aqueous solutions: investigations on adsorption properties and involved mechanism." *Biomass Conversion and Biorefinery* 12 (10): 4333-4348. https://doi.org/10.1007/s13399-021-02099-0. https://doi.org/10.1007/s13399-021-02099-0.

Haider, Bilal, Muhammad Rizwan Dilshad, Muhammad Atiq ur Rehman, Muhammad Sarfraz Akram, and Malte Kaspereit. 2020. "Highly permeable innovative PDMS coated polyethersulfone membranes embedded with activated carbon for gas separation." *Journal of Natural Gas Science and Engineering* 81: 103406. https://doi.org/https://doi.org/10.1016/j.jngse.2020.103406. https://www.sciencedirect.com/science/article/pii/S1875510020302602.

Han, Seungwan, and Myoung Soo Lah. 2015. "Simple and Efficient Regeneration of MOF-5 and HKUST-1 via Acid–Base Treatment." *Crystal Growth & Design* 15 (11): 5568-5572. https://doi.org/10.1021/acs.cgd.5b01218. https://doi.org/10.1021/acs.cgd.5b01218.

He, Bojun, Jinglei Liu, Ying Zhang, Shengzhong Zhang, Peng Wang, and Hong Xu. 2020. "Comparison of structured activated carbon and traditional adsorbents for purification of H2." *Separation and Purification Technology* 239: 116529. https://doi.org/https://doi.org/10.1016/j.seppur.2020.116529. https://www.sciencedirect.com/science/article/pii/S1383586619334240.

He, Dan, Jianfu Wu, Chenglong Yu, Bichun Huang, Xiang Tu, Danping Li, Xuehui Jia, Junhui Dan, Zheng Fang, and Zhenhua Dai. 2023. "Synthesis of corncob biochar with high surface area by KOH activation for VOC adsorption: effect of KOH addition method." *Journal of Chemical Technology & Biotechnology* 98 (8): 2051-2064.

Heaney, Natalie, Mufidat Mamman, Hajara Tahir, Ahmed Al-Gharib, and Chuxia Lin. 2018. "Effects of softwood biochar on the status of nitrogen species and elements of potential toxicity in soils." *Ecotoxicology and Environmental Safety* 166: 383-389.

https://doi.org/https://doi.org/10.1016/j.ecoenv.2018.09.112. https://www.sciencedirect.com/science/article/pii/S0147651318309862.
Heeley-Hill, Aiden C, Stuart K Grange, Martyn W Ward, Alastair C Lewis, Neil Owen, Caroline Jordan, Gemma Hodgson, and Greg Adamson. 2021. "Frequency of use of household products containing VOCs and indoor atmospheric concentrations in homes." *Environmental Science: Processes & Impacts* 23 (5): 699-713.
Herrera-Herrera, Antonio V., Miguel Ángel González-Curbelo, Javier Hernández-Borges, and Miguel Ángel Rodríguez-Delgado. 2012. "Carbon nanotubes applications in separation science: A review." *Analytica Chimica Acta* 734: 1-30. https://doi.org/https://doi.org/10.1016/j.aca.2012.04.035. https://www.sciencedirect.com/science/article/pii/S0003267012006307.
Heymes, Frédéric, Peggy Manno-Demoustier, Françoise Charbit, Jean L. Fanlo, and Philippe Moulin. 2006. "A new efficient absorption liquid to treat exhaust air loaded with toluene." *Chemical Engineering Journal* 115 (3): 225-231. https://doi.org/https://doi.org/10.1016/j.cej.2005.10.011. https://www.sciencedirect.com/science/article/pii/S1385894705004092.
Hu, Qili, Shuyue Pang, Dan Wang, Yuhang Yang, and Hengyuan Liu. 2021. "Deeper Insights into the Bohart–Adams Model in a Fixed-Bed Column." *The Journal of Physical Chemistry B* 125 (30): 8494-8501. https://doi.org/10.1021/acs.jpcb.1c03378. https://doi.org/10.1021/acs.jpcb.1c03378.
Huang, Show-Chu, Tsair-Wang Chung, and Hung-Ta Wu. 2021. "Effects of Molecular Properties on Adsorption of Six-Carbon VOCs by Activated Carbon in a Fixed Adsorber." *ACS Omega* 6 (8): 5825-5835. https://doi.org/10.1021/acsomega.0c06260. https://doi.org/10.1021/acsomega.0c06260.
Huang, Shushu, Wei Deng, Long Zhang, Dengyao Yang, Qiang Gao, Zhengfang Tian, Limin Guo, and Tatsumi Ishihara. 2020. "Adsorptive properties in toluene removal over hierarchical zeolites." *Microporous and Mesoporous Materials* 302: 110204. https://doi.org/https://doi.org/10.1016/j.micromeso.2020.110204. https://www.sciencedirect.com/science/article/pii/S1387181120302079.
Huang, Xinlei, Hongxian Li, Ling Wang, Minghui Tang, and Shengyong Lu. 2022. "Removal of toluene and SO2 by hierarchical porous carbons: a study on adsorption selectivity and mechanism." *Environmental Science and Pollution Research* 29 (19): 29117-29129. https://doi.org/10.1007/s11356-021-18380-8. https://doi.org/10.1007/s11356-021-18380-8.
Huang, Xinlei, Minghui Tang, Hongxian Li, Ling Wang, and Shengyong Lu. 2023. "Adsorption of multicomponent VOCs on various biomass-derived hierarchical porous carbon: A study on adsorption mechanism and competitive effect." *Chemosphere* 313: 137513. https://doi.org/https://doi.org/10.1016/j.chemosphere.2022.137513. https://www.sciencedirect.com/science/article/pii/S0045653522040061.
Huang, Yu, Ting Su, Liqin Wang, Nan Wang, Yonggang Xue, Wanting Dai, Shun Cheng Lee, Junji Cao, and Steven Sai Hang Ho. 2019. "Evaluation and characterization of volatile air toxics indoors in a heavy polluted city of northwestern China in wintertime." *Science of The Total Environment* 662: 470-480. https://doi.org/https://doi.org/10.1016/j.scitotenv.2019.01.250. https://www.sciencedirect.com/science/article/pii/S0048969719302785.

Hunter-Sellars, Elwin, J. J. Tee, Ivan P. Parkin, and Daryl R. Williams. 2020. "Adsorption of volatile organic compounds by industrial porous materials: Impact of relative humidity." *Microporous and Mesoporous Materials* 298: 110090. https://doi.org/https://doi.org/10.1016/j.micromeso.2020.110090. https://www.sciencedirect.com/science/article/pii/S1387181120300937.

Ifthikar, Jerosha, Xiang Jiao, Audrey Ngambia, Ting Wang, Aimal Khan, Ali Jawad, Qiang Xue, Lei Liu, and Zhuqi Chen. 2018. "Facile One-Pot Synthesis of Sustainable Carboxymethyl Chitosan – Sewage Sludge Biochar for Effective Heavy Metal Chelation and Regeneration." *Bioresource Technology* 262: 22-31. https://doi.org/https://doi.org/10.1016/j.biortech.2018.04.053. https://www.sciencedirect.com/science/article/pii/S0960852418305662.

Jafari, Saeed, Farshid Ghorbani-Shahna, Abdulrahman Bahrami, and Hossein Kazemian. 2018. "Adsorptive removal of toluene and carbon tetrachloride from gas phase using Zeolitic Imidazolate Framework-8: Effects of synthesis method, particle size, and pretreatment of the adsorbent." *Microporous and Mesoporous Materials* 268: 58-68. https://doi.org/https://doi.org/10.1016/j.micromeso.2018.04.013. https://www.sciencedirect.com/science/article/pii/S1387181118301926.

Jahandar Lashaki, Masoud, Samineh Kamravaei, Zaher Hashisho, John H. Phillips, David Crompton, James E. Anderson, and Mark Nichols. 2023. "Adsorption and desorption of a mixture of volatile organic Compounds: Impact of activated carbon porosity." *Separation and Purification Technology* 314: 123530. https://doi.org/https://doi.org/10.1016/j.seppur.2023.123530. https://www.sciencedirect.com/science/article/pii/S1383586623004380.

Jain, Nidhi, and Nand Jee Kanu. 2021. "The potential application of carbon nanotubes in water Treatment: A state-of-the-art-review." *Materials Today: Proceedings* 43: 2998-3005. https://doi.org/https://doi.org/10.1016/j.matpr.2021.01.331. https://www.sciencedirect.com/science/article/pii/S221478532100420X.

Ji, Mengyuan, Xiaoxia Wang, Muhammad Usman, Feihong Liu, Yitong Dan, Lei Zhou, Stefano Campanaro, Gang Luo, and Wenjing Sang. 2022. "Effects of different feedstocks-based biochar on soil remediation: A review." *Environmental Pollution* 294: 118655. https://doi.org/https://doi.org/10.1016/j.envpol.2021.118655. https://www.sciencedirect.com/science/article/pii/S0269749121022375.

Jia, Lijuan, Jialu Shi, Chao Long, Fei Lian, and Baoshan Xing. 2020. "VOCs adsorption on activated carbon with initial water vapor contents: Adsorption mechanism and modified characteristic curves." *Science of The Total Environment* 731: 139184. https://doi.org/https://doi.org/10.1016/j.scitotenv.2020.139184. https://www.sciencedirect.com/science/article/pii/S0048969720327017.

Jia, Y, Q Zong, M Zhang, ZM Wang, and LH %J Bull. China Ceram. Soc Zhang. 2016. "Research progress in regeneration technology of activated carbon from flue gas desulfurization." 35: 815-818.

Jiang, Changle, Gunes A. Yakaboylu, Tugrul Yumak, John W. Zondlo, Edward M. Sabolsky, and Jingxin Wang. 2020. "Activated carbons prepared by indirect and direct CO2 activation of lignocellulosic biomass for supercapacitor electrodes." *Renewable Energy* 155: 38-52. https://doi.org/https://doi.org/10.1016/j.renene.2020.03.111. https://www.sciencedirect.com/science/article/pii/S0960148120304432.

Jin, Ziheng, Bangda Wang, Liang Ma, Pengbo Fu, Lingling Xie, Xia Jiang, and Wenju Jiang. 2020. "Air pre-oxidation induced high yield N-doped porous biochar for improving toluene adsorption." *Chemical Engineering Journal* 385: 123843. https://doi.org/https://doi.org/10.1016/j.cej.2019.123843. https://www.sciencedirect.com/science/article/pii/S1385894719332589.

Jung, Kyung-Won, Brian Hyun Choi, Tae-Un Jeong, and Kyu-Hong Ahn. 2016. "Facile synthesis of magnetic biochar/Fe3O4 nanocomposites using electro-magnetization technique and its application on the removal of acid orange 7 from aqueous media." *Bioresource Technology* 220: 672-676. https://doi.org/https://doi.org/10.1016/j.biortech.2016.09.035. https://www.sciencedirect.com/science/article/pii/S0960852416312925.

Jurkiewicz, Martyna, Marlena Musik, and Robert Pełech. 2022. "Competitive Adsorption of a Binary VOC Mixture from the Gas Phase onto Activated Carbon Modified with Malic Acid." *Industrial & Engineering Chemistry Research* 61 (32): 11947-11952. https://doi.org/10.1021/acs.iecr.2c01621. https://doi.org/10.1021/acs.iecr.2c01621.

Kamal, Muhammad Shahzad, Shaikh A. Razzak, and Mohammad M. Hossain. 2016. "Catalytic oxidation of volatile organic compounds (VOCs) – A review." *Atmospheric Environment* 140: 117-134. https://doi.org/https://doi.org/10.1016/j.atmosenv.2016.05.031. https://www.sciencedirect.com/science/article/pii/S1352231016303727.

Kamran, Urooj, and Soo-Jin Park. 2020. "MnO2-decorated biochar composites of coconut shell and rice husk: An efficient lithium ions adsorption-desorption performance in aqueous media." *Chemosphere* 260: 127500. https://doi.org/https://doi.org/10.1016/j.chemosphere.2020.127500. https://www.sciencedirect.com/science/article/pii/S0045653520316945.

Kang, Fuyan, Cai Shi, Weici Li, Malin Eqi, Zeshun Liu, Xiaogang Zheng, and Zhanhua Huang. 2022. "Honeycomb like CdS/sulphur-modified biochar composites with enhanced adsorption-photocatalytic capacity for effective removal of rhodamine B." *Journal of Environmental Chemical Engineering* 10 (1): 106942. https://doi.org/https://doi.org/10.1016/j.jece.2021.106942. https://www.sciencedirect.com/science/article/pii/S2213343721019199.

Karapınar, Hacer Sibel. 2021. "Adsorption performance of activated carbon synthesis by ZnCl2, KOH, H3PO4 with different activation temperatures from mixed fruit seeds." *Environmental Technology*: 1-19. https://doi.org/10.1080/09593330.2021.1968507. https://doi.org/10.1080/09593330.2021.1968507.

Karimnezhad, Leila, Mohammad Haghighi, and Esmaeil Fatehifar. 2014. "Adsorption of benzene and toluene from waste gas using activated carbon activated by ZnCl2." *Frontiers of Environmental Science & Engineering* 8 (6): 835-844. https://doi.org/10.1007/s11783-014-0695-4. https://doi.org/10.1007/s11783-014-0695-4.

Kawamoto, Katsuya. 2022. "Adsorption characteristics of the carbonaceous adsorbents for organic compounds in a model exhaust gas from thermal treatment processing." *Journal of the Air & Waste Management Association* 72 (5): 463-473. https://doi.org/10.1080/10962247.2022.2053244. https://doi.org/10.1080/10962247.2022.2053244.

Kazemi Shariat Panahi, Hamed, Mona Dehhaghi, Yong Sik Ok, Abdul-Sattar Nizami, Benyamin Khoshnevisan, Solange I. Mussatto, Mortaza Aghbashlo, Meisam Tabatabaei, and Su Shiung Lam. 2020. "A comprehensive review of engineered biochar: Production,

characteristics, and environmental applications." *Journal of Cleaner Production* 270: 122462. https://doi.org/https://doi.org/10.1016/j.jclepro.2020.122462. https://www.sciencedirect.com/science/article/pii/S0959652620325099.

Khoshnood Motlagh, Eisa, Neda Asasian-Kolur, Seyedmehdi Sharifian, and Azadeh Ebrahimian Pirbazari. 2021. "Sustainable rice straw conversion into activated carbon and nano-silica using carbonization-extraction process." *Biomass and Bioenergy* 144: 105917. https://doi.org/https://doi.org/10.1016/j.biombioe.2020.105917. https://www.sciencedirect.com/science/article/pii/S0961953420304505.

Khuong, Duy Anh, Hong Nam Nguyen, and Toshiki Tsubota. 2021. "Activated carbon produced from bamboo and solid residue by CO2 activation utilized as CO2 adsorbents." *Biomass and Bioenergy* 148: 106039. https://doi.org/https://doi.org/10.1016/j.biombioe.2021.106039. https://www.sciencedirect.com/science/article/pii/S0961953421000763.

Kim, Kwang-Dae, Eun Ji Park, Hyun Ook Seo, Myung-Geun Jeong, Young Dok Kim, and Dong Chan Lim. 2012. "Effect of thin hydrophobic films for toluene adsorption and desorption behavior on activated carbon fiber under dry and humid conditions." *Chemical Engineering Journal* 200-202: 133-139. https://doi.org/https://doi.org/10.1016/j.cej.2012.06.044. https://www.sciencedirect.com/science/article/pii/S1385894712007656.

Kim, Minjae, Jae Won Lee, Seonggon Kim, and Yong Tae Kang. 2022. "CO2 adsorption on zeolite 13X modified with hydrophobic octadecyltrimethoxysilane for indoor application." *Journal of Cleaner Production* 337: 130597. https://doi.org/https://doi.org/10.1016/j.jclepro.2022.130597. https://www.sciencedirect.com/science/article/pii/S0959652622002384.

Kobayashi, Motoyasu, Yuki Terayama, Hiroki Yamaguchi, Masami Terada, Daiki Murakami, Kazuhiko Ishihara, and Atsushi Takahara. 2012. "Wettability and Antifouling Behavior on the Surfaces of Superhydrophilic Polymer Brushes." *Langmuir* 28 (18): 7212-7222. https://doi.org/10.1021/la301033h. https://doi.org/10.1021/la301033h.

Krishnamurthy, Anirudh, Busuyi Adebayo, Teresa Gelles, Ali Rownaghi, and Fateme Rezaei. 2020. "Abatement of gaseous volatile organic compounds: A process perspective." *Catalysis Today* 350: 100-119. https://doi.org/https://doi.org/10.1016/j.cattod.2019.05.069. https://www.sciencedirect.com/science/article/pii/S0920586119302676.

Krishnamurthy, Anirudh, Busuyi Adebayo, Teresa Gelles, Ali Rownaghi, and Fateme %J Catalysis Today Rezaei. 2020. "Abatement of gaseous volatile organic compounds: A process perspective." 350: 100-119.

Kudahi, Saeed Nazari, Ali Reza Noorpoor, and Niyaz Mohammad Mahmoodi. 2017. "Determination and analysis of CO2 capture kinetics and mechanisms on the novel graphene-based adsorbents." *Journal of CO2 Utilization* 21: 17-29. https://doi.org/https://doi.org/10.1016/j.jcou.2017.06.010. https://www.sciencedirect.com/science/article/pii/S2212982017300161.

Kumar, Abhishek, and Tanushree Bhattacharya. 2021. "Biochar: a sustainable solution." *Environment, Development and Sustainability* 23 (5): 6642-6680. https://doi.org/10.1007/s10668-020-00970-0. https://doi.org/10.1007/s10668-020-00970-0.

Kumar, K. Vasanth, Srinivas Gadipelli, Christopher A. Howard, Witold Kwapinski, and Dan J. L Brett. 2021. "Probing adsorbent heterogeneity using Toth isotherms." *Journal of Materials Chemistry A* 9 (2): 944-962. https://doi.org/10.1039/D0TA08150G. http://dx.doi.org/10.1039/D0TA08150G.

Kumar N, Sasi, Denys Grekov, Pascaline Pré, and Babu J. Alappat. 2020. "Microwave mode of heating in the preparation of porous carbon materials for adsorption and energy storage applications – An overview." *Renewable and Sustainable Energy Reviews* 124: 109743. https://doi.org/https://doi.org/10.1016/j.rser.2020.109743. https://www.sciencedirect.com/science/article/pii/S136403212030040X.

Kumar, Prashanth Suresh, Leon Korving, Mark C. M. van Loosdrecht, and Geert-Jan Witkamp. 2019. "Adsorption as a technology to achieve ultra-low concentrations of phosphate: Research gaps and economic analysis." *Water Research X* 4: 100029. https://doi.org/https://doi.org/10.1016/j.wroa.2019.100029. https://www.sciencedirect.com/science/article/pii/S2589914719300660.

Kutluay, Sinan, Orhan Baytar, and Ömer Şahin. 2019. "Equilibrium, kinetic and thermodynamic studies for dynamic adsorption of benzene in gas phase onto activated carbon produced from elaeagnus angustifolia seeds." *Journal of Environmental Chemical Engineering* 7 (2): 102947. https://doi.org/https://doi.org/10.1016/j.jece.2019.102947. https://www.sciencedirect.com/science/article/pii/S2213343719300703.

Kutluay, Sinan, and Farabi Temel. 2021. "Silica gel based new adsorbent having enhanced VOC dynamic adsorption/desorption performance." *Colloids and Surfaces A: Physicochemical and Engineering Aspects* 609: 125848. https://doi.org/https://doi.org/10.1016/j.colsurfa.2020.125848. https://www.sciencedirect.com/science/article/pii/S0927775720314412.

Lan, Yongqiang, Ning Yan, and Weihong Wang. 2016. "Application of PDMS pervaporation membranes filled with tree bark biochar for ethanol/water separation." *RSC Advances* 6 (53): 47637-47645. https://doi.org/10.1039/C6RA06794H. http://dx.doi.org/10.1039/C6RA06794H.

Lang, Xian-Dong, Xing He, Zheng-Ming Li, and Liang-Nian He. 2017. "New routes for CO2 activation and subsequent conversion." *Current Opinion in Green and Sustainable Chemistry* 7: 31-38. https://doi.org/https://doi.org/10.1016/j.cogsc.2017.07.001. https://www.sciencedirect.com/science/article/pii/S245222361730041X.

Largitte, L., and R. Pasquier. 2016. "A review of the kinetics adsorption models and their application to the adsorption of lead by an activated carbon." *Chemical Engineering Research and Design* 109: 495-504. https://doi.org/https://doi.org/10.1016/j.cherd.2016.02.006. https://www.sciencedirect.com/science/article/pii/S0263876216000691.

Laskar, Imranul I., and Zaher Hashisho. 2020. "Insights into modeling adsorption equilibria of single and multicomponent systems of organic and water vapors." *Separation and Purification Technology* 241: 116681. https://doi.org/https://doi.org/10.1016/j.seppur.2020.116681. https://www.sciencedirect.com/science/article/pii/S1383586619353535.

Laskar, Imranul I., Zaher Hashisho, John H. Phillips, James E. Anderson, and Mark Nichols. 2019. "Competitive adsorption equilibrium modeling of volatile organic compound (VOC) and water vapor onto activated carbon." *Separation and Purification Technology*

212: 632-640. https://doi.org/https://doi.org/10.1016/j.seppur.2018.11.073. https://www.sciencedirect.com/science/article/pii/S1383586618334609.
---. 2019. "Modeling the Effect of Relative Humidity on Adsorption Dynamics of Volatile Organic Compound onto Activated Carbon." *Environmental Science & Technology* 53 (5): 2647-2659. https://doi.org/10.1021/acs.est.8b05664. https://doi.org/10.1021/acs.est.8b05664.
Le-Minh, Nhat, Eric C. Sivret, Ari Shammay, and Richard M. Stuetz. 2018. "Factors affecting the adsorption of gaseous environmental odors by activated carbon: A critical review." *Critical Reviews in Environmental Science and Technology* 48 (4): 341-375. https://doi.org/10.1080/10643389.2018.1460984. https://doi.org/10.1080/10643389.2018.1460984.
Le, Phuoc-Anh, Van-Truong Nguyen, Sumanta Kumar Sahoo, Tseung Yuen Tseng, and Kung-Hwa Wei. 2020. "Porous carbon materials derived from areca palm leaves for high performance symmetrical solid-state supercapacitors." *Journal of Materials Science* 55 (24): 10751-10764. https://doi.org/10.1007/s10853-020-04693-5. https://doi.org/10.1007/s10853-020-04693-5.
Lee, Jung Eun, Yong Sik Ok, Daniel C. W. Tsang, JiHyeon Song, Sang-Chul Jung, and Young-Kwon Park. 2020. "Recent advances in volatile organic compounds abatement by catalysis and catalytic hybrid processes: A critical review." *Science of The Total Environment* 719: 137405. https://doi.org/https://doi.org/10.1016/j.scitotenv.2020.137405. https://www.sciencedirect.com/science/article/pii/S0048969720309153.
Lei, Bingman, Biyan Liu, Huijun Zhang, Libei Yan, Hongmei Xie, and Guilin Zhou. 2020. "CuO-modified activated carbon for the improvement of toluene removal in air." *Journal of Environmental Sciences* 88: 122-132. https://doi.org/https://doi.org/10.1016/j.jes.2019.07.001. https://www.sciencedirect.com/science/article/pii/S1001074219300312.
Leng, Erwei, Yilin Guo, Jingwei Chen, Shuai Liu, Jiaqiang E, and Yuan Xue. 2022. "A comprehensive review on lignin pyrolysis: Mechanism, modeling and the effects of inherent metals in biomass." *Fuel* 309: 122102. https://doi.org/https://doi.org/10.1016/j.fuel.2021.122102. https://www.sciencedirect.com/science/article/pii/S0016236121019785.
Leng, Lijian, Qin Xiong, Lihong Yang, Hui Li, Yaoyu Zhou, Weijin Zhang, Shaojian Jiang, Hailong Li, and Huajun Huang. 2021. "An overview on engineering the surface area and porosity of biochar." *Science of The Total Environment* 763: 144204. https://doi.org/https://doi.org/10.1016/j.scitotenv.2020.144204. https://www.sciencedirect.com/science/article/pii/S0048969720377354.
Li, Adela Jing, Vineet Kumar Pal, and Kurunthachalam Kannan. 2021. "A review of environmental occurrence, toxicity, biotransformation and biomonitoring of volatile organic compounds." *Environmental Chemistry and Ecotoxicology* 3: 91-116. https://doi.org/https://doi.org/10.1016/j.enceco.2021.01.001. https://www.sciencedirect.com/science/article/pii/S2590182621000011.
Li, Dapeng, Rongkui Su, Xiancheng Ma, Zheng Zeng, Liqing Li, and Hanqing Wang. 2022. "Porous carbon for oxygenated and aromatic VOCs adsorption by molecular simulation and experimental study: Effect pore structure and functional groups." *Applied Surface*

Science 605: 154708. https://doi.org/https://doi.org/10.1016/j.apsusc.2022.154708. https://www.sciencedirect.com/science/article/pii/S0169433222022371.

Li, Feiyue, Andrew R. Zimmerman, Xin Hu, Zebin Yu, Jun Huang, and Bin Gao. 2020. "One-pot synthesis and characterization of engineered hydrochar by hydrothermal carbonization of biomass with ZnCl2." *Chemosphere* 254: 126866. https://doi.org/https://doi.org/10.1016/j.chemosphere.2020.126866. https://www.sciencedirect.com/science/article/pii/S0045653520310596.

Li, Hongbo, Xiaoling Dong, Evandro B da Silva, Letuzia M de Oliveira, Yanshan Chen, and Lena Q %J Chemosphere Ma. 2017. "Mechanisms of metal sorption by biochars: biochar characteristics and modifications." 178: 466-478.

Li, J., Q. Li, C. Qian, X. Wang, Y. Lan, B. Wang, and W. Yin. 2019. "Volatile organic compounds analysis and characterization on activated biochar prepared from rice husk." *International Journal of Environmental Science and Technology* 16 (12): 7653-7662. https://doi.org/10.1007/s13762-019-02219-4. https://doi.org/10.1007/s13762-019-02219-4.

Li, Jinfeng, Nan Zhang, Hongtao Zhao, Zhigang Li, Bo Tian, and Yunchen Du. 2021. "Cornstalk-derived macroporous carbon materials with enhanced microwave absorption." *Journal of Materials Science: Materials in Electronics* 32 (21): 25758-25768. https://doi.org/10.1007/s10854-020-04571-5. https://doi.org/10.1007/s10854-020-04571-5.

Li, Jinjin, Tangying Cheng, Xiuwei Ma, Xueyan Hou, Hao Wu, and Linjun Yang. 2022. "Effect of nitrogen functional groups on competitive adsorption between toluene and water vapor onto nitrogen-doped spherical resorcinol-formaldehyde resin-based activated carbon." *Environmental Science and Pollution Research* 29 (56): 85257-85270. https://doi.org/10.1007/s11356-022-21179-w. https://doi.org/10.1007/s11356-022-21179-w.

---. 2022. "Effect of nitrogen functional groups on competitive adsorption between toluene and water vapor onto nitrogen-doped spherical resorcinol-formaldehyde resin-based activated carbon." *Environmental Science and Pollution Research*. https://doi.org/10.1007/s11356-022-21179-w. https://doi.org/10.1007/s11356-022-21179-w.

Li, Jinjin, Tangying Cheng, Xiuwei Ma, Hao Wu, and Linjun Yang. 2022. "Toluene and water vapor adsorption characteristics and selectivity on hydrophobic resin-based activated carbon." *Colloids and Surfaces A: Physicochemical and Engineering Aspects* 642: 128604. https://doi.org/https://doi.org/10.1016/j.colsurfa.2022.128604. https://www.sciencedirect.com/science/article/pii/S0927775722003582.

---. 2023. "A hydrophobic and hierarchical porous resin-based activated carbon modified by g-C3N4 for toluene capture from humid conditions." *Separation and Purification Technology* 308: 122902. https://doi.org/https://doi.org/10.1016/j.seppur.2022.122902. https://www.sciencedirect.com/science/article/pii/S1383586622024595.

Li, Jinlong, Boxin Li, Guozhe Sui, Lijuan Du, Yan Zhuang, Yulin Zhang, and Yuanfang Zou. 2021. "Removal of volatile organic compounds from air using supported ionic liquid membrane containing ultraviolet-visible light-driven Nd-TiO2 nanoparticles." *Journal of Molecular Structure* 1231: 130023. https://doi.org/https://doi.org/10.1016/j.molstruc.2021.130023. https://www.sciencedirect.com/science/article/pii/S002228602100154X.

Li, Junfeng, Wei Zhou, Yanlin Su, Yang Zhao, Wenshuang Zhang, Liang Xie, Xiaoxiao Meng, Jihui Gao, Fei Sun, Pengxiang Wang, Guangbo Zhao, and Yukun Qin. 2022. "The enhancement mechanism of the microwave-assisted toluene desorption for activated carbon regeneration based on the constructive interference." *Journal of Cleaner Production* 378: 134542. https://doi.org/https://doi.org/10.1016/j.jclepro.2022.134542. https://www.sciencedirect.com/science/article/pii/S0959652622041142.

Li, Kai, Dongqing Zhang, Xiaojun Niu, Huafang Guo, Yuanyuan Yu, Zhihua Tang, Zhang Lin, and Mingli Fu. 2022. "Insights into CO2 adsorption on KOH-activated biochars derived from the mixed sewage sludge and pine sawdust." *Science of The Total Environment* 826: 154133. https://doi.org/https://doi.org/10.1016/j.scitotenv.2022.154133. https://www.sciencedirect.com/science/article/pii/S0048969722012256.

Li, Li-qing, Jian-fei Song, Xiao-long Yao, Gui-jie Huang, Zheng Liu, and Ling Tang. 2012. "Adsorption of volatile organic compounds on three activated carbon samples: Effect of pore structure." *Journal of Central South University* 19 (12): 3530-3539. https://doi.org/10.1007/s11771-012-1439-x. https://doi.org/10.1007/s11771-012-1439-x.

Li, Mei-syue, Siang Chen Wu, and Yang-hsin Shih. 2016. "Characterization of volatile organic compound adsorption on multiwall carbon nanotubes under different levels of relative humidity using linear solvation energy relationship." *Journal of Hazardous Materials* 315: 35-41. https://doi.org/https://doi.org/10.1016/j.jhazmat.2016.04.004. https://www.sciencedirect.com/science/article/pii/S030438941630334X.

Li, Ronghua, Yichen Zhang, Hongxia Deng, Zengqiang Zhang, Jim J. Wang, Sabry M. Shaheen, Ran Xiao, Jörg Rinklebe, Beidou Xi, Xiaosong He, and Juan Du. 2020. "Removing tetracycline and Hg(II) with ball-milled magnetic nanobiochar and its potential on polluted irrigation water reclamation." *Journal of Hazardous Materials* 384: 121095. https://doi.org/https://doi.org/10.1016/j.jhazmat.2019.121095. https://www.sciencedirect.com/science/article/pii/S0304389419310490.

Li, Xiangping, Jianguang Zhang, Bin Liu, and Zhenping Su. 2021. "A critical review on the application and recent developments of post-modified biochar in supercapacitors." *Journal of Cleaner Production* 310: 127428. https://doi.org/https://doi.org/10.1016/j.jclepro.2021.127428. https://www.sciencedirect.com/science/article/pii/S0959652621016474.

Li, Xin, Jie Ma, and Xiang Ling. 2020. "Design and dynamic behaviour investigation of a novel VOC recovery system based on a deep condensation process." *Cryogenics* 107: 103060. https://doi.org/https://doi.org/10.1016/j.cryogenics.2020.103060. https://www.sciencedirect.com/science/article/pii/S0011227519303212.

Li, Xiuquan, Li Zhang, Zhongqing Yang, Ziqiang He, Peng Wang, Yunfei Yan, and Jingyu Ran. 2020. "Hydrophobic modified activated carbon using PDMS for the adsorption of VOCs in humid condition." *Separation and Purification Technology* 239: 116517. https://doi.org/https://doi.org/10.1016/j.seppur.2020.116517. https://www.sciencedirect.com/science/article/pii/S1383586619347331.

Li, Xiuquan, Li Zhang, Zhongqing Yang, Ziqiang He, Peng Wang, Yunfei Yan, Jingyu %J Separation Ran, and Purification Technology. 2020. "Hydrophobic modified activated carbon using PDMS for the adsorption of VOCs in humid condition." 239: 116517.

Li, Xiuquan, Li Zhang, Zhongqing Yang, Peng Wang, Yunfei Yan, and Jingyu Ran. 2020. "Adsorption materials for volatile organic compounds (VOCs) and the key factors for VOCs adsorption process: A review." *Separation and Purification Technology* 235:

116213. https://doi.org/https://doi.org/10.1016/j.seppur.2019.116213. http://www.sciencedirect.com/science/article/pii/S1383586619328412.
Li, Yadong, Yuanhui Shen, Zhaoyang Niu, Junpeng Tian, Donghui Zhang, Zhongli Tang, and Wenbin Li. 2023. "Process analysis of temperature swing adsorption and temperature vacuum swing adsorption in VOCs recovery from activated carbon." *Chinese Journal of Chemical Engineering* 53: 346-360. https://doi.org/https://doi.org/10.1016/j.cjche.2022.01.029. https://www.sciencedirect.com/science/article/pii/S1004954122001070.
Li, Yao, Tao Zhang, Yage Wang, and Binbin Wang. 2021. "Transformation of waste cornstalk into versatile porous carbon adsorbent for selective CO2 capture and efficient methanol adsorption." *Journal of Environmental Chemical Engineering* 9 (5): 106149. https://doi.org/https://doi.org/10.1016/j.jece.2021.106149. https://www.sciencedirect.com/science/article/pii/S221334372101126X.
Li, Yingjie, Haiyu Chang, Hui Yan, Senlin Tian, and Philip G. Jessop. 2021. "Reversible Absorption of Volatile Organic Compounds by Switchable-Hydrophilicity Solvents: A Case Study of Toluene with N,N-Dimethylcyclohexylamine." *ACS Omega* 6 (1): 253-264. https://doi.org/10.1021/acsomega.0c04443. https://doi.org/10.1021/acsomega.0c04443.
Li, Zhikai, Tao Yang, Shaojun Yuan, Yongxiang Yin, Edwin J. Devid, Qiang Huang, Daniel Auerbach, and Aart W. Kleyn. 2020. "Boudouard reaction driven by thermal plasma for efficient CO2 conversion and energy storage." *Journal of Energy Chemistry* 45: 128-134. https://doi.org/https://doi.org/10.1016/j.jechem.2019.10.007. https://www.sciencedirect.com/science/article/pii/S209549561930854X.
Li, Zhirui, Yuqi Jin, Tong Chen, Feng Tang, Jie Cai, and Jiayu Ma. 2021. "Trimethylchlorosilane modified activated carbon for the adsorption of VOCs at high humidity." *Separation and Purification Technology* 272: 118659. https://doi.org/https://doi.org/10.1016/j.seppur.2021.118659. https://www.sciencedirect.com/science/article/pii/S1383586621003713.
Lian, Fei, Guannan Cui, Zhongqi Liu, Lian Duo, Guilong Zhang, and Baoshan Xing. 2016. "One-step synthesis of a novel N-doped microporous biochar derived from crop straws with high dye adsorption capacity." *Journal of Environmental Management* 176: 61-68. https://doi.org/https://doi.org/10.1016/j.jenvman.2016.03.043. https://www.sciencedirect.com/science/article/pii/S0301479716301487.
Liang, Xiaoming, Xiaofang Chen, Jiani Zhang, Tianli Shi, Xibo Sun, Liya Fan, Liming Wang, and Daiqi %J Atmospheric Environment Ye. 2017. "Reactivity-based industrial volatile organic compounds emission inventory and its implications for ozone control strategies in China." 162: 115-126.
Liang, Zhishu, Jijun Wang, Yuna Zhang, Cheng Han, Shengtao Ma, Jiangyao Chen, Guiying Li, and Taicheng An. 2020. "Removal of volatile organic compounds (VOCs) emitted from a textile dyeing wastewater treatment plant and the attenuation of respiratory health risks using a pilot-scale biofilter." *Journal of Cleaner Production* 253: 120019. https://doi.org/https://doi.org/10.1016/j.jclepro.2020.120019. https://www.sciencedirect.com/science/article/pii/S0959652620300664.
Lillo-Ródenas, M. A., D. Cazorla-Amorós, and A. Linares-Solano. 2011. "Benzene and toluene adsorption at low concentration on activated carbon fibres." *Adsorption* 17 (3): 473-481. https://doi.org/10.1007/s10450-010-9301-7. https://doi.org/10.1007/s10450-010-9301-7.

Lin, Fengfei, Xiaohao Liu, Meina Ma, Fenglei Qi, Yang Pan, Lu Wang, Peiyong Ma, and Ying Zhang. 2021. "Real-time monitoring the carbonization and activation process of activated carbon prepared from Chinese parasol via zinc chloride activation." *Journal of Analytical and Applied Pyrolysis* 155: 105089. https://doi.org/https://doi.org/10.1016/j.jaap.2021.105089. https://www.sciencedirect.com/science/article/pii/S0165237021000759.

Liu, Botao, Sherif A. Younis, and Ki-Hyun Kim. 2021. "The dynamic competition in adsorption between gaseous benzene and moisture on metal-organic frameworks across their varying concentration levels." *Chemical Engineering Journal* 421: 127813. https://doi.org/https://doi.org/10.1016/j.cej.2020.127813. https://www.sciencedirect.com/science/article/pii/S1385894720339334.

Liu, Chao, Jing Wang, Jingjing Wan, and Chengzhong Yu. 2021. "MOF-on-MOF hybrids: Synthesis and applications." *Coordination Chemistry Reviews* 432: 213743. https://doi.org/https://doi.org/10.1016/j.ccr.2020.213743. https://www.sciencedirect.com/science/article/pii/S0010854520311942.

Liu, Han-Bing, Bing Yang, and Nan-Dong Xue. 2016. "Enhanced adsorption of benzene vapor on granular activated carbon under humid conditions due to shifts in hydrophobicity and total micropore volume." *Journal of Hazardous Materials* 318: 425-432. https://doi.org/https://doi.org/10.1016/j.jhazmat.2016.07.026. https://www.sciencedirect.com/science/article/pii/S0304389416306471.

Liu, Han-Bing, Bing Yang, and Nan-Dong %J Journal of Hazardous Materials Xue. 2016. "Enhanced adsorption of benzene vapor on granular activated carbon under humid conditions due to shifts in hydrophobicity and total micropore volume." 318: 425-432.

Liu, Hongli, Ningyun Li, Mengying Feng, Guiying Li, Weiping Zhang, and Taicheng An. 2022. "Near-infrared light induced adsorption–desorption cycle for VOC recovery by integration of metal–organic frameworks with graphene oxide nanosheets." *Environmental Science: Nano* 9 (5): 1858-1868. https://doi.org/10.1039/D2EN00103A. http://dx.doi.org/10.1039/D2EN00103A.

Liu, Huidong, Guoren Xu, and Guibai Li. 2020. "The characteristics of pharmaceutical sludge-derived biochar and its application for the adsorption of tetracycline." *Science of The Total Environment* 747: 141492. https://doi.org/https://doi.org/10.1016/j.scitotenv.2020.141492. https://www.sciencedirect.com/science/article/pii/S004896972035021X.

Liu, Huijuan, Keyan Wei, and Chao Long. 2022. "Enhancing adsorption capacities of low-concentration VOCs under humid conditions using NaY@meso-SiO2 core–shell composite." *Chemical Engineering Journal* 442: 136108. https://doi.org/https://doi.org/10.1016/j.cej.2022.136108. https://www.sciencedirect.com/science/article/pii/S1385894722016060.

Liu, Huijuan, Yansong Yu, Qi Shao, and Chao Long. 2019. "Porous polymeric resin for adsorbing low concentration of VOCs: Unveiling adsorption mechanism and effect of VOCs' molecular properties." *Separation and Purification Technology* 228: 115755. https://doi.org/https://doi.org/10.1016/j.seppur.2019.115755. https://www.sciencedirect.com/science/article/pii/S138358661930749X.

Liu, Jie, Lijun Ye, Sanghyuk Wooh, Michael Kappl, Werner Steffen, and Hans-Jürgen Butt. 2019. "Optimizing Hydrophobicity and Photocatalytic Activity of PDMS-Coated

Titanium Dioxide." *ACS Applied Materials & Interfaces* 11 (30): 27422-27425. https://doi.org/10.1021/acsami.9b07490. https://doi.org/10.1021/acsami.9b07490.

Liu, Qingquan, Le Luo, and Luqing Zheng. 2018. "Lignins: Biosynthesis and Biological Functions in Plants." *International journal of molecular sciences* 19 (2): 335. https://doi.org/10.3390/ijms19020335. https://pubmed.ncbi.nlm.nih.gov/29364145

https://www.ncbi.nlm.nih.gov/pmc/articles/PMC5855557/.

Liu, Shuai, Yue Peng, Jianjun Chen, Tao Yan, Yani Zhang, Jun Liu, and Junhua Li. 2020. "A new insight into adsorption state and mechanism of adsorbates in porous materials." *Journal of Hazardous Materials* 382: 121103. https://doi.org/https://doi.org/10.1016/j.jhazmat.2019.121103. https://www.sciencedirect.com/science/article/pii/S030438941931057X.

Liu, Xingren, Yulong Shi, Qingwen Zhang, and Guichun Li. 2021. "Effects of biochar on nitrification and denitrification-mediated N2O emissions and the associated microbial community in an agricultural soil." *Environmental Science and Pollution Research* 28 (6): 6649-6663. https://doi.org/10.1007/s11356-020-10928-4. https://doi.org/10.1007/s11356-020-10928-4.

Liu, Yafei, Mengdi Song, Xingang Liu, Yuepeng Zhang, Lirong Hui, Liuwei Kong, Yingying Zhang, Chen Zhang, Yu Qu, Junling An, Depeng Ma, Qinwen Tan, and Miao Feng. 2020. "Characterization and sources of volatile organic compounds (VOCs) and their related changes during ozone pollution days in 2016 in Beijing, China." *Environmental Pollution* 257: 113599. https://doi.org/https://doi.org/10.1016/j.envpol.2019.113599. https://www.sciencedirect.com/science/article/pii/S0269749119333895.

Liu, Yingshu, Haiyang Tao, Xiong Yang, Xiaoyong Wu, Jinjuan Li, Chuanzhao Zhang, Ralph T. Yang, and Ziyi Li. 2023. "Adsorptive purification of NOx by HZSM-5 zeolites: Effects of Si/Al ratio, temperature, humidity, and gas composition." *Microporous and Mesoporous Materials* 348: 112331. https://doi.org/https://doi.org/10.1016/j.micromeso.2022.112331. https://www.sciencedirect.com/science/article/pii/S1387181122006497.

Liu, Yujing, X. Feng, and Darren Lawless. 2006. "Separation of gasoline vapor from nitrogen by hollow fiber composite membranes for VOC emission control." *Journal of Membrane Science* 271 (1): 114-124. https://doi.org/https://doi.org/10.1016/j.memsci.2005.07.012. https://www.sciencedirect.com/science/article/pii/S0376738805005375.

Liu, Yutong, and Tao %J Materials Tian. 2019. "Fabrication of diatomite/silicalite-1 composites and their property for VOCs adsorption." 12 (4): 551.

Lobato-Peralta, Diego Ramón, Estefanía Duque-Brito, Alejandro Ayala-Cortés, D. M. Arias, Adriana Longoria, Ana Karina Cuentas-Gallegos, P. J. Sebastian, and Patrick U. Okoye. 2021. "Advances in activated carbon modification, surface heteroatom configuration, reactor strategies, and regeneration methods for enhanced wastewater treatment." *Journal of Environmental Chemical Engineering* 9 (4): 105626. https://doi.org/https://doi.org/10.1016/j.jece.2021.105626. https://www.sciencedirect.com/science/article/pii/S2213343721006035.

Lomonaco, Tommaso, Enrico Manco, Andrea Corti, Jacopo La Nasa, Silvia Ghimenti, Denise Biagini, Fabio Di Francesco, Francesca Modugno, Alessio Ceccarini, Roger Fuoco, and Valter Castelvetro. 2020. "Release of harmful volatile organic compounds (VOCs) from photo-degraded plastic debris: A neglected source of environmental pollution." *Journal of Hazardous Materials* 394: 122596.

https://doi.org/https://doi.org/10.1016/j.jhazmat.2020.122596. https://www.sciencedirect.com/science/article/pii/S0304389420305859.
Lu, Pei-Jen, Hsin-Chieh Lin, Wen-Te Yu, and Jia-Ming %J Journal of the Taiwan institute of chemical engineers Chern. 2011. "Chemical regeneration of activated carbon used for dye adsorption." 42 (2): 305-311.
Lu, Shengyong, Xinlei Huang, Minghui Tang, Yaqi Peng, Shuchao Wang, and Chengetai Portia Makwarimba. 2021. "Synthesis of N-doped hierarchical porous carbon with excellent toluene adsorption properties and its activation mechanism." *Environmental Pollution* 284: 117113. https://doi.org/https://doi.org/10.1016/j.envpol.2021.117113. https://www.sciencedirect.com/science/article/pii/S0269749121006953.
Lu, Shuangchun, Qingling Liu, Rui Han, Jiaqi Shi, Miao Guo, Chunfeng Song, Na Ji, Xuebin Lu, and Degang Ma. 2021. "Core-shell structured Y zeolite/hydrophobic organic polymer with improved toluene adsorption capacity under dry and wet conditions." *Chemical Engineering Journal* 409: 128194. https://doi.org/https://doi.org/10.1016/j.cej.2020.128194. https://www.sciencedirect.com/science/article/pii/S1385894720343102.
Lu, Xiaohong, Fei Li, Xia Zhou, Jinrong Hu, and Ping Liu. 2022. "Biomass, lignocellulolytic enzyme production and lignocellulose degradation patterns by Auricularia auricula during solid state fermentation of corn stalk residues under different pretreatments." *Food Chemistry* 384: 132622. https://doi.org/https://doi.org/10.1016/j.foodchem.2022.132622. https://www.sciencedirect.com/science/article/pii/S0308814622005842.
Luengas, Angela, Astrid Barona, Cecile Hort, Gorka Gallastegui, Vincent Platel, and Ana Elias. 2015. "A review of indoor air treatment technologies." *Reviews in Environmental Science and Bio/Technology* 14 (3): 499-522. https://doi.org/10.1007/s11157-015-9363-9. https://doi.org/10.1007/s11157-015-9363-9.
Luo, Ling, Guolan Wang, Guozhong Shi, Mengting Zhang, Jing Zhang, Jinsong He, Yinlong Xiao, Dong Tian, Yanzong Zhang, Shihuai Deng, Wei Zhou, Ting Lan, and Ouping Deng. 2019. "The characterization of biochars derived from rice straw and swine manure, and their potential and risk in N and P removal from water." *Journal of Environmental Management* 245: 1-7. https://doi.org/https://doi.org/10.1016/j.jenvman.2019.05.072. https://www.sciencedirect.com/science/article/pii/S0301479719306930.
Lv, Yuting, Jing Sun, Guanqun Yu, Wenlong Wang, Zhanlong Song, Xiqiang Zhao, and Yanpeng Mao. 2020. "Hydrophobic design of adsorbent for VOC removal in humid environment and quick regeneration by microwave." *Microporous and Mesoporous Materials* 294: 109869. https://doi.org/https://doi.org/10.1016/j.micromeso.2019.109869. https://www.sciencedirect.com/science/article/pii/S1387181119307267.
Ma, Changchang, Hai Huang, Xin Gao, Tao Wang, Zhi Zhu, Pengwei Huo, Yang Liu, and Yongsheng %J Journal of the Taiwan Institute of Chemical Engineers Yan. 2018. "Honeycomb tubular biochar from fargesia leaves as an effective adsorbent for tetracyclines pollutants." 91: 299-308.
Ma, Hongfang, Juanjuan Yang, Xiang Gao, Zhibao Liu, Xinxin Liu, and Zhaogui Xu. 2019. "Removal of chromium (VI) from water by porous carbon derived from corn straw: Influencing factors, regeneration and mechanism." *Journal of Hazardous Materials* 369: 550-560. https://doi.org/https://doi.org/10.1016/j.jhazmat.2019.02.063. https://www.sciencedirect.com/science/article/pii/S0304389419301931.

Ma, Xiancheng, Liqing Li, Ruofei Chen, Chunhao Wang, Ke Zhou, and Hailong Li. 2018. "Porous carbon materials based on biomass for acetone adsorption: Effect of surface chemistry and porous structure." *Applied Surface Science* 459: 657-664. https://doi.org/https://doi.org/10.1016/j.apsusc.2018.07.170. https://www.sciencedirect.com/science/article/pii/S0169433218320671.

Ma, Xiancheng, Baogen Liu, Meihong Che, Qingding Wu, Ruofei Chen, Changqing Su, Xiang Xu, Zheng Zeng, and Liqing Li. 2021. "Biomass-based hierarchical porous carbon with ultrahigh surface area for super-efficient adsorption and separation of acetone and methanol." *Separation and Purification Technology* 269: 118690. https://doi.org/https://doi.org/10.1016/j.seppur.2021.118690. https://www.sciencedirect.com/science/article/pii/S1383586621004020.

Ma, Yongfei, Yong Qi, Lie Yang, Li Wu, Ping Li, Feng Gao, Xuebin Qi, and Zulin Zhang. 2021. "Adsorptive removal of imidacloprid by potassium hydroxide activated magnetic sugarcane bagasse biochar: Adsorption efficiency, mechanism and regeneration." *Journal of Cleaner Production* 292: 126005. https://doi.org/https://doi.org/10.1016/j.jclepro.2021.126005. https://www.sciencedirect.com/science/article/pii/S0959652621002250.

Mahmoud, Esawy, Ahmed El Baroudy, Nehal Ali, and Mahmoud Sleem. 2020. "Spectroscopic studies on the phosphorus adsorption in salt-affected soils with or without nano-biochar additions." *Environmental Research* 184: 109277. https://doi.org/https://doi.org/10.1016/j.envres.2020.109277. https://www.sciencedirect.com/science/article/pii/S0013935120301705.

Makoś-Chełstowska, Patrycja. 2023. "VOCs absorption from gas streams using deep eutectic solvents – A review." *Journal of Hazardous Materials* 448: 130957. https://doi.org/https://doi.org/10.1016/j.jhazmat.2023.130957. https://www.sciencedirect.com/science/article/pii/S030438942300239X.

Mallakpour, Shadpour, Fariba Sirous, and Chaudhery Mustansar Hussain. 2021. "Sawdust, a versatile, inexpensive, readily available bio-waste: From mother earth to valuable materials for sustainable remediation technologies." *Advances in Colloid and Interface Science* 295: 102492. https://doi.org/https://doi.org/10.1016/j.cis.2021.102492. https://www.sciencedirect.com/science/article/pii/S0001868621001330.

Manisalidis, Ioannis, Elisavet Stavropoulou, Agathangelos Stavropoulos, and Eugenia %J Frontiers in public health Bezirtzoglou. 2020. "Environmental and health impacts of air pollution: a review." 8.

Manyà, Joan J., David García-Morcate, and Belén González. 2020. Adsorption Performance of Physically Activated Biochars for Postcombustion CO2 Capture from Dry and Humid Flue Gas. *Applied Sciences* 10 (1). https://doi.org/10.3390/app10010376.

Marsh, Harry, and Francisco Rodríguez Reinoso. 2006. *Activated carbon*. Elsevier.

Mazlan, Mohammad Amir Firdaus, Yoshimitsu Uemura, Suzana Yusup, Fathelrahman Elhassan, Azhar Uddin, Ai Hiwada, and Mitsutaka Demiya. 2016. "Activated Carbon from Rubber Wood Sawdust by Carbon Dioxide Activation." *Procedia Engineering* 148: 530-537. https://doi.org/https://doi.org/10.1016/j.proeng.2016.06.549. https://www.sciencedirect.com/science/article/pii/S1877705816310165.

Megías-Sayago, Cristina, Irene Lara-Ibeas, Qiang Wang, Stephane Le Calvé, and Benoît Louis. 2020. "Volatile organic compounds (VOCs) removal capacity of ZSM-5 zeolite adsorbents for near real-time BTEX detection." *Journal of Environmental Chemical*

Engineering 8 (2): 103724. https://doi.org/https://doi.org/10.1016/j.jece.2020.103724. https://www.sciencedirect.com/science/article/pii/S2213343720300725.
Meng, Fanyue, Min Song, Yuexing Wei, and Yuling Wang. 2019. "The contribution of oxygen-containing functional groups to the gas-phase adsorption of volatile organic compounds with different polarities onto lignin-derived activated carbon fibers." *Environmental Science and Pollution Research* 26 (7): 7195-7204. https://doi.org/10.1007/s11356-019-04190-6. https://doi.org/10.1007/s11356-019-04190-6.
Meng, Qing Bo, Go-Su Yang, and Youn-Sik Lee. 2012. "Synthesis of 4-vinylpyridine–divinylbenzene copolymer adsorbents for microwave-assisted desorption of benzene." *Journal of Hazardous Materials* 205-206: 118-125. https://doi.org/https://doi.org/10.1016/j.jhazmat.2011.12.045. https://www.sciencedirect.com/science/article/pii/S0304389411015378.
---. 2013. "Preparation of highly porous hypercrosslinked polystyrene adsorbents: Effects of hydrophilicity on the adsorption and microwave-assisted desorption behavior toward benzene." *Microporous and Mesoporous Materials* 181: 222-227. https://doi.org/https://doi.org/10.1016/j.micromeso.2013.07.027. https://www.sciencedirect.com/science/article/pii/S1387181113003636.
Mohan, Velram Balaji, Kin-tak Lau, David Hui, and Debes Bhattacharyya. 2018. "Graphene-based materials and their composites: A review on production, applications and product limitations." *Composites Part B: Engineering* 142: 200-220. https://doi.org/https://doi.org/10.1016/j.compositesb.2018.01.013. https://www.sciencedirect.com/science/article/pii/S1359836817344426.
Mohd Azmi, Luqman Hakim, Pavani Cherukupally, Elwin Hunter-Sellars, Bradley P. Ladewig, and Daryl R. Williams. 2022. "Fabrication of MIL-101-polydimethylsiloxane composites for environmental toluene abatement from humid air." *Chemical Engineering Journal* 429: 132304. https://doi.org/https://doi.org/10.1016/j.cej.2021.132304. https://www.sciencedirect.com/science/article/pii/S1385894721038833.
Molés, Francisco, Joaquín Navarro-Esbrí, Bernardo Peris, Adrián Mota-Babiloni, and Ángel Barragán-Cervera. 2014. "Theoretical energy performance evaluation of different single stage vapour compression refrigeration configurations using R1234yf and R1234ze(E) as working fluids." *International Journal of Refrigeration* 44: 141-150. https://doi.org/https://doi.org/10.1016/j.ijrefrig.2014.04.025. https://www.sciencedirect.com/science/article/pii/S0140700714001017.
Mozaffar, Ahsan, and Yan-Lin Zhang. 2020. "Atmospheric Volatile Organic Compounds (VOCs) in China: a Review." *Current Pollution Reports* 6 (3): 250-263. https://doi.org/10.1007/s40726-020-00149-1. https://doi.org/10.1007/s40726-020-00149-1.
Mu, Xiaotian, Honglei Ding, Weiguo Pan, Qi Zhou, Wei Du, Kaina Qiu, Junchi Ma, and Kai Zhang. 2021. "Research progress in catalytic oxidation of volatile organic compound acetone." *Journal of Environmental Chemical Engineering* 9 (4): 105650. https://doi.org/https://doi.org/10.1016/j.jece.2021.105650. https://www.sciencedirect.com/science/article/pii/S2213343721006278.
Mujan, Igor, Aleksandar S. Anđelković, Vladimir Munćan, Miroslav Kljajić, and Dragan Ružić. 2019. "Influence of indoor environmental quality on human health and productivity - A review." *Journal of Cleaner Production* 217: 646-657.

https://doi.org/https://doi.org/10.1016/j.jclepro.2019.01.307. https://www.sciencedirect.com/science/article/pii/S0959652619303348.
Nascimento, Ícaro Vasconcelos do, Laís Gomes Fregolente, Arthur Prudêncio de Araújo Pereira, Carla Danielle Vasconcelos do Nascimento, Jaedson Cláudio Anunciato Mota, Odair Pastor Ferreira, Helon Hébano de Freitas Sousa, Débora Gonçala Gomes da Silva, Lucas Rodrigues Simões, A. G. Souza Filho, and Mirian Cristina Gomes Costa. 2023. "Biochar as a carbonaceous material to enhance soil quality in drylands ecosystems: A review." *Environmental Research* 233: 116489. https://doi.org/https://doi.org/10.1016/j.envres.2023.116489. https://www.sciencedirect.com/science/article/pii/S0013935123012938.
Neogi, Suvadip, Vikas Sharma, Nawaz Khan, Deepshi Chaurasia, Anees Ahmad, Shraddha Chauhan, Anuradha Singh, Siming You, Ashok Pandey, and Preeti Chaturvedi Bhargava. 2022. "Sustainable biochar: A facile strategy for soil and environmental restoration, energy generation, mitigation of global climate change and circular bioeconomy." *Chemosphere* 293: 133474. https://doi.org/https://doi.org/10.1016/j.chemosphere.2021.133474. https://www.sciencedirect.com/science/article/pii/S0045653521039485.
Nguyen, Thai Hoang, Van Vien Nguyen, Ngan Tuan Nguyen, Thien Nguyen, Tuong Vy T. Nguyen, Hoang Long Ngo, Le Thanh Nguyen Huynh, Thanh Nhut Tran, Thi Thanh Nguyen Ho, Thanh Tung Nguyen, and Viet Hai Le. 2023. "Preparation, characterization and CDI application of KOH-activated porous waste-corn-stalk-based carbon aerogel." *Journal of Porous Materials* 30 (4): 1183-1193. https://doi.org/10.1007/s10934-022-01411-1. https://doi.org/10.1007/s10934-022-01411-1.
Nigar, H., N. Navascués, O. de la Iglesia, R. Mallada, and J. Santamaría. 2015. "Removal of VOCs at trace concentration levels from humid air by Microwave Swing Adsorption, kinetics and proper sorbent selection." *Separation and Purification Technology* 151: 193-200. https://doi.org/https://doi.org/10.1016/j.seppur.2015.07.019. https://www.sciencedirect.com/science/article/pii/S1383586615300873.
Norbäck, Dan, Jamal Hisham Hashim, Zailina Hashim, and Faridah Ali. 2017. "Volatile organic compounds (VOC), formaldehyde and nitrogen dioxide (NO2) in schools in Johor Bahru, Malaysia: Associations with rhinitis, ocular, throat and dermal symptoms, headache and fatigue." *Science of The Total Environment* 592: 153-160. https://doi.org/https://doi.org/10.1016/j.scitotenv.2017.02.215. https://www.sciencedirect.com/science/article/pii/S0048969717304734.
Nzihou, Ange, Brian Stanmore, Nathalie Lyczko, and Doan Pham Minh. 2019. "The catalytic effect of inherent and adsorbed metals on the fast/flash pyrolysis of biomass: A review." *Energy* 170: 326-337. https://doi.org/https://doi.org/10.1016/j.energy.2018.12.174. https://www.sciencedirect.com/science/article/pii/S0360544218325489.
Ogungbenro, Adetola E., Dang V. Quang, Khalid A. Al-Ali, Lourdes F. Vega, and Mohammad R. M. Abu-Zahra. 2018. "Physical synthesis and characterization of activated carbon from date seeds for CO2 capture." *Journal of Environmental Chemical Engineering* 6 (4): 4245-4252. https://doi.org/https://doi.org/10.1016/j.jece.2018.06.030. https://www.sciencedirect.com/science/article/pii/S2213343718303385.
Oh, Ji-Young, Young-Woo You, Junbeam Park, Ji-Sook Hong, Iljeong Heo, Chang-Ha Lee, and Jeong-Kwon Suh. 2019. "Adsorption characteristics of benzene on resin-based activated carbon under humid conditions." *Journal of Industrial and Engineering Chemistry* 71:

242-249. https://doi.org/https://doi.org/10.1016/j.jiec.2018.11.032. https://www.sciencedirect.com/science/article/pii/S1226086X18314503.
Özhan, Abdurrahman, Ömer Şahin, Mehmet Maşuk Küçük, and Cafer Saka. 2014. "Preparation and characterization of activated carbon from pine cone by microwave-induced ZnCl2 activation and its effects on the adsorption of methylene blue." *Cellulose* 21 (4): 2457-2467. https://doi.org/10.1007/s10570-014-0299-y. https://doi.org/10.1007/s10570-014-0299-y.
Palliyarayil, A., H. Saini, K. Vinayakumar, P. Selvarajan, A. Vinu, N. S. Kumar, and S. Sil. 2021. "Advances in porous material research towards the management of air pollution." *Emergent Materials* 4 (3): 607-643. https://doi.org/10.1007/s42247-020-00151-9. https://doi.org/10.1007/s42247-020-00151-9.
Park, Eun Ji, Youn Kyoung Cho, Dae Han Kim, Myung-Geun Jeong, Yong Ho Kim, and Young Dok Kim. 2014. "Hydrophobic Polydimethylsiloxane (PDMS) Coating of Mesoporous Silica and Its Use as a Preconcentrating Agent of Gas Analytes." *Langmuir* 30 (34): 10256-10262. https://doi.org/10.1021/la502915r. https://doi.org/10.1021/la502915r.
Park, Soo-Jin, Yu-Sin Jang, Jae-Woon Shim, and Seung-Kon Ryu. 2003. "Studies on pore structures and surface functional groups of pitch-based activated carbon fibers." *Journal of Colloid and Interface Science* 260 (2): 259-264. https://doi.org/https://doi.org/10.1016/S0021-9797(02)00081-4. https://www.sciencedirect.com/science/article/pii/S0021979702000814.
Pei, Jingjing, and Jianshun S. Zhang. 2012. "Determination of adsorption isotherm and diffusion coefficient of toluene on activated carbon at low concentrations." *Building and Environment* 48: 66-76. https://doi.org/https://doi.org/10.1016/j.buildenv.2011.08.005. https://www.sciencedirect.com/science/article/pii/S0360132311002484.
Peyravi, Arman, Mohammad Feizbakhshan, Zaher Hashisho, David Crompton, and James E. Anderson. 2022. "Purge gas humidity improves microwave-assisted regeneration of polymeric and zeolite adsorbents." *Separation and Purification Technology* 288: 120640. https://doi.org/https://doi.org/10.1016/j.seppur.2022.120640. https://www.sciencedirect.com/science/article/pii/S1383586622002003.
Pi, Xinxin, Fei Sun, Jihui Gao, Yuwen Zhu, Lijie Wang, Zhibin Qu, Hui Liu, and Guangbo Zhao. 2017. "Microwave Irradiation Induced High-Efficiency Regeneration for Desulfurized Activated Coke: A Comparative Study with Conventional Thermal Regeneration." *Energy & Fuels* 31 (9): 9693-9702. https://doi.org/10.1021/acs.energyfuels.7b01260. https://doi.org/10.1021/acs.energyfuels.7b01260.
Pirola, Carlo, and Michela Mattia. 2021. "Purification of air from volatile organic compounds by countercurrent liquid gas mass transfer absorption process." *International Journal of Thermofluids* 9: 100060. https://doi.org/https://doi.org/10.1016/j.ijft.2020.100060. https://www.sciencedirect.com/science/article/pii/S2666202720300471.
Plata-Gryl, Maksymilian, Malwina Momotko, Sławomir Makowiec, and Grzegorz Boczkaj. 2022. "Characterization of diatomaceous earth coated with nitrated asphaltenes as superior adsorbent for removal of VOCs from gas phase in fixed bed column." *Chemical Engineering Journal* 427: 130653. https://doi.org/https://doi.org/10.1016/j.cej.2021.130653. https://www.sciencedirect.com/science/article/pii/S1385894721022397.

Qian, Qingli, Chenhao Gong, Zhongguo Zhang, and Guoqing Yuan. 2015. "Removal of VOCs by activated carbon microspheres derived from polymer: a comparative study." *Adsorption* 21 (4): 333-341. https://doi.org/10.1007/s10450-015-9673-9. https://doi.org/10.1007/s10450-015-9673-9.

Qiao, Kaili, Weijun Tian, Jie Bai, Jie Dong, Jing Zhao, Xiaoxi Gong, and Shuhui Liu. 2018. "Preparation of biochar from Enteromorpha prolifera and its use for the removal of polycyclic aromatic hydrocarbons (PAHs) from aqueous solution." *Ecotoxicology and Environmental Safety* 149: 80-87. https://doi.org/https://doi.org/10.1016/j.ecoenv.2017.11.027. https://www.sciencedirect.com/science/article/pii/S0147651317307790.

Qin, Chencheng, Hou Wang, Xingzhong Yuan, Ting Xiong, Jingjing Zhang, and Jin %J Chemical Engineering Journal Zhang. 2020. "Understanding structure-performance correlation of biochar materials in environmental remediation and electrochemical devices." 382: 122977.

Qin, Yuan, Yi Wang, Huiqiong Wang, Jinsuo Gao, and Zhenping Qu. 2013. "Effect of Morphology and Pore Structure of SBA-15 on Toluene Dynamic Adsorption/Desorption Performance." *Procedia Environmental Sciences* 18: 366-371. https://doi.org/https://doi.org/10.1016/j.proenv.2013.04.048. https://www.sciencedirect.com/science/article/pii/S1878029613001801.

Raganati, Federica, Michela Alfe, Valentina Gargiulo, Riccardo Chirone, and Paola Ammendola. 2019. "Kinetic study and breakthrough analysis of the hybrid physical/chemical CO2 adsorption/desorption behavior of a magnetite-based sorbent." *Chemical Engineering Journal* 372: 526-535. https://doi.org/https://doi.org/10.1016/j.cej.2019.04.165. https://www.sciencedirect.com/science/article/pii/S1385894719309520.

Rajabi, Hamid, Mojgan Hadi Mosleh, Tirto Prakoso, Negin Ghaemi, Parthasarathi Mandal, Amanda Lea-Langton, and Majid Sedighi. 2021. "Competitive adsorption of multicomponent volatile organic compounds on biochar." *Chemosphere* 283: 131288. https://doi.org/https://doi.org/10.1016/j.chemosphere.2021.131288. https://www.sciencedirect.com/science/article/pii/S0045653521017604.

Rajabi, Hamid, Mojgan Hadi Mosleh, Parthasarathi Mandal, Amanda Lea-Langton, and Majid Sedighi. 2021. "Sorption behaviour of xylene isomers on biochar from a range of feedstock." *Chemosphere* 268: 129310. https://doi.org/https://doi.org/10.1016/j.chemosphere.2020.129310. https://www.sciencedirect.com/science/article/pii/S0045653520335074.

Rajahmundry, Ganesh Kumar, Chandrasekhar Garlapati, Ponnusamy Senthil Kumar, Ratna Surya Alwi, and Dai-Viet N. Vo. 2021. "Statistical analysis of adsorption isotherm models and its appropriate selection." *Chemosphere* 276: 130176. https://doi.org/https://doi.org/10.1016/j.chemosphere.2021.130176. https://www.sciencedirect.com/science/article/pii/S0045653521006457.

Rashed, Ahmed O., Andrea Merenda, Takeshi Kondo, Marcio Lima, Joselito Razal, Lingxue Kong, Chi Huynh, and Ludovic F. Dumée. 2021. "Carbon nanotube membranes – Strategies and challenges towards scalable manufacturing and practical separation applications." *Separation and Purification Technology* 257: 117929. https://doi.org/https://doi.org/10.1016/j.seppur.2020.117929. https://www.sciencedirect.com/science/article/pii/S1383586620324023.

Rashidi, Nor Adilla, and Suzana Yusup. 2019. "Production of palm kernel shell-based activated carbon by direct physical activation for carbon dioxide adsorption." *Environmental Science and Pollution Research* 26 (33): 33732-33746. https://doi.org/10.1007/s11356-018-1903-8. https://doi.org/10.1007/s11356-018-1903-8.

Rathinavel, S., K. Priyadharshini, and Dhananjaya Panda. 2021. "A review on carbon nanotube: An overview of synthesis, properties, functionalization, characterization, and the application." *Materials Science and Engineering: B* 268: 115095. https://doi.org/https://doi.org/10.1016/j.mseb.2021.115095. https://www.sciencedirect.com/science/article/pii/S0921510721000556.

Reguyal, Febelyn, Ajit K. Sarmah, and Wei Gao. 2017. "Synthesis of magnetic biochar from pine sawdust via oxidative hydrolysis of FeCl2 for the removal sulfamethoxazole from aqueous solution." *Journal of Hazardous Materials* 321: 868-878. https://doi.org/https://doi.org/10.1016/j.jhazmat.2016.10.006. https://www.sciencedirect.com/science/article/pii/S0304389416309037.

Romero-Anaya, A. J., M. Ouzzine, M. A. Lillo-Ródenas, and A. Linares-Solano. 2014. "Spherical carbons: Synthesis, characterization and activation processes." *Carbon* 68: 296-307. https://doi.org/https://doi.org/10.1016/j.carbon.2013.11.006. https://www.sciencedirect.com/science/article/pii/S0008622313010543.

Romero-Anaya, Aroldo José, Mohammed Ouzzine, Maria Angeles Lillo-Rodenas, and Angel %J Carbon Linares-Solano. 2014. "Spherical carbons: Synthesis, characterization and activation processes." 68: 296-307.

Rong, Yang, Cong Pan, Kexin Song, Jong Chol Nam, Feng Wu, Zhixiong You, Zhengping Hao, Jinjun Li, and Zhongshen Zhang. 2023. "Bamboo-derived hydrophobic porous graphitized carbon for adsorption of volatile organic compounds." *Chemical Engineering Journal* 461: 141979. https://doi.org/https://doi.org/10.1016/j.cej.2023.141979. https://www.sciencedirect.com/science/article/pii/S1385894723007106.

Sajjadi, Seyed-Ali, Alireza Mohammadzadeh, Hai Nguyen Tran, Ioannis Anastopoulos, Guilherme L. Dotto, Zorica R. Lopičić, Selvaraju Sivamani, Abolfazl Rahmani-Sani, Andrei Ivanets, and Ahmad Hosseini-Bandegharaei. 2018. "Efficient mercury removal from wastewater by pistachio wood wastes-derived activated carbon prepared by chemical activation using a novel activating agent." *Journal of Environmental Management* 223: 1001-1009. https://doi.org/https://doi.org/10.1016/j.jenvman.2018.06.077. https://www.sciencedirect.com/science/article/pii/S0301479718307291.

Salehi, Ehsan, Mahdi Askari, and Yaser Darvishi. 2020. "Novel combinatorial extensions to breakthrough curve modeling of an adsorption column — Depth filtration hybrid process." *Journal of Industrial and Engineering Chemistry* 86: 232-243. https://doi.org/https://doi.org/10.1016/j.jiec.2020.03.015. https://www.sciencedirect.com/science/article/pii/S1226086X20301337.

Salvador, Francisco, Nicolas Martin-Sanchez, Ruth Sanchez-Hernandez, Maria Jesus Sanchez-Montero, and Carmen Izquierdo. 2015. "Regeneration of carbonaceous adsorbents. Part I: Thermal Regeneration." *Microporous and Mesoporous Materials* 202: 259-276. https://doi.org/https://doi.org/10.1016/j.micromeso.2014.02.045. https://www.sciencedirect.com/science/article/pii/S1387181114001218.

Salvador, Francisco, Nicolas Martin-Sanchez, Ruth Sanchez-Hernandez, Maria Jesus Sanchez-Montero, Carmen %J Microporous Izquierdo, and Mesoporous Materials. 2015. "Regeneration of carbonaceous adsorbents. Part I: thermal regeneration." 202: 259-276.

Sampieri, Alvaro, Gabriela Pérez-Osorio, Miguel Ángel Hernández-Espinosa, Irving Israel Ruiz-López, Mayra Ruiz-Reyes, Janette Arriola-Morales, and Rocío Iliana %J Nano Convergence Narváez-Fernández. 2018. "Sorption of BTEX on a nanoporous composite of SBA-15 and a calcined hydrotalcite." 5 (1): 1-17.

Saraga, Dikaia E, Xavier Querol, Regina M. B. O. Duarte, Noel J. Aquilina, Nuno Canha, Elena Gómez Alvarez, Milena Jovasevic-Stojanovic, Gabriel Bekö, Steigvilė Byčenkienė, Renata Kovacevic, Kristina Plauškaitė, and Nicola Carslaw. 2023. "Source apportionment for indoor air pollution: Current challenges and future directions." *Science of The Total Environment* 900: 165744. https://doi.org/https://doi.org/10.1016/j.scitotenv.2023.165744. https://www.sciencedirect.com/science/article/pii/S004896972304367X.

Scholten, Elke, Lev Bromberg, Gregory C. Rutledge, and T. Alan Hatton. 2011. "Electrospun Polyurethane Fibers for Absorption of Volatile Organic Compounds from Air." *ACS Applied Materials & Interfaces* 3 (10): 3902-3909. https://doi.org/10.1021/am200748y. https://doi.org/10.1021/am200748y.

Serafin, Jarosław, and Bartosz Dziejarski. 2023. "Application of isotherms models and error functions in activated carbon CO2 sorption processes." *Microporous and Mesoporous Materials* 354: 112513. https://doi.org/https://doi.org/10.1016/j.micromeso.2023.112513. https://www.sciencedirect.com/science/article/pii/S1387181123000847.

Sha, Qing'e, Manni Zhu, Hewen Huang, Yuzheng Wang, Zhijiong Huang, Xuechi Zhang, Mingshuang Tang, Menghua Lu, Cheng Chen, Bowen Shi, Zixi Chen, Lili Wu, Zhuangmin Zhong, Cheng Li, Yuanqian Xu, Fei Yu, Guanglin Jia, Songdi Liao, Xiaozhen Cui, Junwen Liu, and Junyu Zheng. 2021. "A newly integrated dataset of volatile organic compounds (VOCs) source profiles and implications for the future development of VOCs profiles in China." *Science of The Total Environment* 793: 148348. https://doi.org/https://doi.org/10.1016/j.scitotenv.2021.148348. https://www.sciencedirect.com/science/article/pii/S0048969721034197.

Shadkam, Ramin, Malek Naderi, Arash Ghazitabar, and Somaye Akbari. 2021. "Adsorption performance of reduced graphene-oxide/cellulose nano-crystal hybrid aerogels reinforced with waste-paper extracted cellulose-fibers for the removal of toluene pollution." *Materials Today Communications* 28: 102610. https://doi.org/https://doi.org/10.1016/j.mtcomm.2021.102610. https://www.sciencedirect.com/science/article/pii/S2352492821006024.

Shafawi, Anis Natasha, Abdul Rahman Mohamed, Pooya Lahijani, and Maedeh Mohammadi. 2021. "Recent advances in developing engineered biochar for CO2 capture: An insight into the biochar modification approaches." *Journal of Environmental Chemical Engineering* 9 (6): 106869. https://doi.org/https://doi.org/10.1016/j.jece.2021.106869. https://www.sciencedirect.com/science/article/pii/S2213343721018467.

Shah, Arth Jayesh, Bhavin Soni, and Sanjib Kumar Karmee. 2022. "Application of cotton stalk biochar as a biosorbent for the removal of malachite green and its microwave-assisted regeneration." *Energy, Ecology and Environment* 7 (1): 88-96. https://doi.org/10.1007/s40974-021-00217-2. https://doi.org/10.1007/s40974-021-00217-2.

Shah, Irfan Khursheed, Pascaline Pre, and B. J. Alappat. 2014. "Effect of thermal regeneration of spent activated carbon on volatile organic compound adsorption performances." *Journal of the Taiwan Institute of Chemical Engineers* 45 (4): 1733-1738. https://doi.org/https://doi.org/10.1016/j.jtice.2014.01.006. https://www.sciencedirect.com/science/article/pii/S1876107014000078.

Shen, Bowen, Shuai Zhao, Xiaoquan Yang, Mariolino Carta, Haoli Zhou, and Wanqin Jin. 2022. "Relation between permeate pressure and operational parameters in VOC/nitrogen separation by a PDMS composite membrane." *Separation and Purification Technology* 280: 119974. https://doi.org/https://doi.org/10.1016/j.seppur.2021.119974. https://www.sciencedirect.com/science/article/pii/S1383586621016804.

Shen, Xuhua, Rui Ou, Yutong Lu, Aihua Yuan, Jianfeng Liu, Jiayang Gu, Xiaocai Hu, Zhen Yang, and Fu Yang. 2020. "Record-high capture of volatile benzene and toluene enabled by activator implant-optimized banana peel-derived engineering carbonaceous adsorbents." *Environment International* 143: 105774. https://doi.org/https://doi.org/10.1016/j.envint.2020.105774. https://www.sciencedirect.com/science/article/pii/S0160412020308345.

Shen, Yan, Jian-Zhong Guo, Li-Qun Bai, Xiao-Qin Chen, and Bing Li. 2021. "High effective adsorption of Pb(II) from solution by biochar derived from torrefaction of ammonium persulphate pretreated bamboo." *Bioresource Technology* 323: 124616. https://doi.org/https://doi.org/10.1016/j.biortech.2020.124616. https://www.sciencedirect.com/science/article/pii/S0960852420318903.

Shi, Fengmei, Hongjiu Yu, Nan Zhang, Su Wang, Pengfei Li, Qiuyue Yu, Jie Liu, and Zhanjiang Pei. 2021. "Microbial succession of lignocellulose degrading bacteria during composting of corn stalk." *Bioengineered* 12 (2): 12372-12382. https://doi.org/10.1080/21655979.2021.2002622. https://doi.org/10.1080/21655979.2021.2002622.

Shi, Guibin, Song He, Guanyu Chen, Chichi Ruan, Yuansheng Ma, Qilin Chen, Xin Jin, Xinyu Liu, Chunxiang He, Chunhua Du, Huaming Dai, and Xiaobing Yang. 2021. "Crayfish shell-based micro-mesoporous activated carbon: Insight into preparation and gaseous benzene adsorption mechanism." *Chemical Engineering Journal*: 131148. https://doi.org/https://doi.org/10.1016/j.cej.2021.131148. https://www.sciencedirect.com/science/article/pii/S1385894721027297.

Shiue, Angus, Walter Den, Yu-Hao Kang, Shih-Cheng Hu, Gwo-tsuen Jou, C. H. Lin, Vincent Hu, and S. I. Lin. 2011. "Validation and application of adsorption breakthrough models for the chemical filters used in the make-up air unit (MAU) of a cleanroom." *Building and Environment* 46 (2): 468-477. https://doi.org/https://doi.org/10.1016/j.buildenv.2010.08.010. https://www.sciencedirect.com/science/article/pii/S0360132310002635.

Sips, Robert. 1948. "On the structure of a catalyst surface." *The journal of chemical physics* 16 (5): 490-495.

Soliman, N. K., and A. F. Moustafa. 2020. "Industrial solid waste for heavy metals adsorption features and challenges; a review." *Journal of Materials Research and Technology* 9 (5): 10235-10253. https://doi.org/https://doi.org/10.1016/j.jmrt.2020.07.045. https://www.sciencedirect.com/science/article/pii/S2238785420315441.

Song, Bingqing, Ming Chen, Ling Zhao, Hao Qiu, and Xinde Cao. 2019. "Physicochemical property and colloidal stability of micron- and nano-particle biochar derived from a

variety of feedstock sources." *Science of The Total Environment* 661: 685-695. https://doi.org/https://doi.org/10.1016/j.scitotenv.2019.01.193. https://www.sciencedirect.com/science/article/pii/S0048969719302128.

Song, Ming, Cheng Wang, Xianhui Chen, Jing Ma, and Weidong Xia. 2021. "Large-scale in-situ synthesis of nitrogen-doped graphene using magnetically rotating arc plasma." *Diamond and Related Materials* 116: 108417. https://doi.org/https://doi.org/10.1016/j.diamond.2021.108417. https://www.sciencedirect.com/science/article/pii/S0925963521001801.

Sonne, Christian, Changlei Xia, Payam Dadvand, Admir Créso Targino, and Su Shiung Lam. 2022. "Indoor volatile and semi-volatile organic toxic compounds: Need for global action." *Journal of Building Engineering* 62: 105344. https://doi.org/https://doi.org/10.1016/j.jobe.2022.105344. https://www.sciencedirect.com/science/article/pii/S235271022201350X.

Su, Changqing, Yang Guo, Hongyu Chen, Jianwu Zou, Zheng Zeng, and Liqing Li. 2020. "VOCs adsorption of resin-based activated carbon and bamboo char: Porous characterization and nitrogen-doped effect." *Colloids and Surfaces A: Physicochemical and Engineering Aspects* 601: 124983. https://doi.org/https://doi.org/10.1016/j.colsurfa.2020.124983. https://www.sciencedirect.com/science/article/pii/S0927775720305768.

Su, Zhiping, Yang Yang, Quanbo Huang, Ruwei Chen, Wenjiao Ge, Zhiqiang Fang, Fei Huang, and Xiaohui Wang. 2022. "Designed biomass materials for “green” electronics: A review of materials, fabrications, devices, and perspectives." *Progress in Materials Science* 125: 100917. https://doi.org/https://doi.org/10.1016/j.pmatsci.2021.100917. https://www.sciencedirect.com/science/article/pii/S0079642521001419.

Suliman, Waled, James B. Harsh, Nehal I. Abu-Lail, Ann-Marie Fortuna, Ian Dallmeyer, and Manuel Garcia-Perez. 2016. "Influence of feedstock source and pyrolysis temperature on biochar bulk and surface properties." *Biomass and Bioenergy* 84: 37-48. https://doi.org/https://doi.org/10.1016/j.biombioe.2015.11.010. https://www.sciencedirect.com/science/article/pii/S0961953415301501.

Sun, Jian, Zhenxing Shen, Yue Zhang, Zhou Zhang, Qian Zhang, Tian Zhang, Xinyi Niu, Yu Huang, Long Cui, Hongmei Xu, Hongxia Liu, Junji Cao, and Xuxiang Li. 2019. "Urban VOC profiles, possible sources, and its role in ozone formation for a summer campaign over Xi’an, China." *Environmental Science and Pollution Research* 26 (27): 27769-27782. https://doi.org/10.1007/s11356-019-05950-0. https://doi.org/10.1007/s11356-019-05950-0.

Sun, Jian, Jinhui Wang, Zhenxing Shen, Yu Huang, Yue Zhang, Xinyi Niu, Junji Cao, Qian Zhang, Hongmei Xu, Ningning Zhang, and Xuxiang Li. 2019. "Volatile organic compounds from residential solid fuel burning in Guanzhong Plain, China: Source-related profiles and risks." *Chemosphere* 221: 184-192. https://doi.org/https://doi.org/10.1016/j.chemosphere.2019.01.002. https://www.sciencedirect.com/science/article/pii/S0045653519300025.

Sun, Lei, Dan Yuan, Rurong Liu, Shungang Wan, and Xianju Lu. 2020. "Coadsorption of gaseous xylene, ethyl acetate and water onto porous biomass carbon foam pellets derived from liquefied Vallisneria natans waste." *Journal of Chemical Technology & Biotechnology* 95 (5): 1348-1360. https://doi.org/https://doi.org/10.1002/jctb.6319. https://doi.org/10.1002/jctb.6319.

Sun, Nannan, Chenggong Sun, Hao Liu, Jingjing Liu, Lee Stevens, Trevor Drage, Colin E. Snape, Kaixi Li, Wei Wei, and Yuhan Sun. 2013. "Synthesis, characterization and evaluation of activated spherical carbon materials for CO2 capture." *Fuel* 113: 854-862. https://doi.org/https://doi.org/10.1016/j.fuel.2013.03.047. https://www.sciencedirect.com/science/article/pii/S0016236113002354.

Sun, Yanlong, Bo Zhang, Tong Zheng, and Peng %J Chemical Engineering Journal Wang. 2017. "Regeneration of activated carbon saturated with chloramphenicol by microwave and ultraviolet irradiation." 320: 264-270.

Syarifah, Sharfina Mutia, Angzzas Sari Mohd Kassim, Ashuvila Mohd Aripin, Chee Ming Chan, Muhd Hafeez Zainulabidin, Nadiah Ishak, and Waluyo Adi Siswanto. 2021. "Brief Dataset on produced handsheet from oil palm residue lignocellulose treated with Bacillus cereus on mechanical and physical characterization." *Data in Brief* 36: 107030. https://doi.org/https://doi.org/10.1016/j.dib.2021.107030. https://www.sciencedirect.com/science/article/pii/S2352340921003140.

Tan, Li, Jiangen Wang, Bihai Cai, Chengyin Wang, Zhimin Ao, and Shaobin Wang. 2022. "Nitrogen-rich layered carbon for adsorption of typical volatile organic compounds and low-temperature thermal regeneration." *Journal of Hazardous Materials* 424: 127348. https://doi.org/https://doi.org/10.1016/j.jhazmat.2021.127348. https://www.sciencedirect.com/science/article/pii/S0304389421023165.

Tan, Xue-Fei, Shi-Shu Zhu, Ru-Peng Wang, Yi-Di Chen, Pau-Loke Show, Feng-Fa Zhang, and Shih-Hsin Ho. 2021. "Role of biochar surface characteristics in the adsorption of aromatic compounds: Pore structure and functional groups." *Chinese Chemical Letters* 32 (10): 2939-2946. https://doi.org/https://doi.org/10.1016/j.cclet.2021.04.059. https://www.sciencedirect.com/science/article/pii/S1001841721003016.

Tang, Minghui, Xinlei Huang, Yaqi Peng, and Shengyong Lu. 2020. "Hierarchical porous carbon as a highly efficient adsorbent for toluene and benzene." *Fuel* 270: 117478. https://doi.org/https://doi.org/10.1016/j.fuel.2020.117478. https://www.sciencedirect.com/science/article/pii/S0016236120304737.

Tao, Siyuan, Zhansheng Wu, Xiufang He, Bang-Ce Ye, and Chun %J Bioresources Li. 2018. "Characterization of biochar prepared from cotton stalks as efficient inoculum carriers for Bacillus subtilis SL-13." 13 (1): 1773-1786.

Thue, Pascal S., Eder C. Lima, Joseph M. Sieliechi, Caroline Saucier, Silvio L. P. Dias, Julio C. P. Vaghetti, Fabiano S. Rodembusch, and Flávio A. Pavan. 2017. "Effects of first-row transition metals and impregnation ratios on the physicochemical properties of microwave-assisted activated carbons from wood biomass." *Journal of Colloid and Interface Science* 486: 163-175. https://doi.org/https://doi.org/10.1016/j.jcis.2016.09.070. https://www.sciencedirect.com/science/article/pii/S0021979716307330.

Tian, Wenjie, Huayang Zhang, Xiaoguang Duan, Hongqi Sun, Guosheng Shao, and Shaobin Wang. 2020. "Porous Carbons: Structure-Oriented Design and Versatile Applications." *Advanced Functional Materials* 30 (17): 1909265. https://doi.org/https://doi.org/10.1002/adfm.201909265. https://doi.org/10.1002/adfm.201909265.

Tomin, Oleksii, Riku Vahala, and Maryam Roza Yazdani. 2021. "Tailoring metal-impregnated biochars for selective removal of natural organic matter and dissolved phosphorus from the aqueous phase." *Microporous and Mesoporous Materials* 328: 111499.

https://doi.org/https://doi.org/10.1016/j.micromeso.2021.111499. https://www.sciencedirect.com/science/article/pii/S1387181121006259.
Toyinbo, Oluyemi, Linda Hägerhed, Sani Dimitroulopoulou, Marzenna Dudzinska, Steven Emmerich, David Hemming, Ju-Hyeong Park, Ulla Haverinen-Shaughnessy, and Climate the Scientific Technical Committee 34 of the International Society of Indoor Air Quality. 2022. "Open database for international and national indoor environmental quality guidelines." *Indoor Air* 32 (4): e13028. https://doi.org/https://doi.org/10.1111/ina.13028. https://doi.org/10.1111/ina.13028.
Tran, Hai Nguyen, Chung-Kung Lee, Tien Vinh Nguyen, and Huan-Ping %J Environmental technology Chao. 2018. "Saccharide-derived microporous spherical biochar prepared from hydrothermal carbonization and different pyrolysis temperatures: synthesis, characterization, and application in water treatment." 39 (21): 2747-2760.
Tran, Hai Nguyen, Fatma Tomul, Nguyen Thi Hoang Ha, Dong Thanh Nguyen, Eder C. Lima, Giang Truong Le, Chang-Tang Chang, Vhahangwele Masindi, and Seung Han Woo. 2020. "Innovative spherical biochar for pharmaceutical removal from water: Insight into adsorption mechanism." *Journal of Hazardous Materials* 394: 122255. https://doi.org/https://doi.org/10.1016/j.jhazmat.2020.122255. https://www.sciencedirect.com/science/article/pii/S0304389420302430.
Uday, Vismaya, P. S. Harikrishnan, Kanchan Deoli, Faiza Zitouni, Jürgen Mahlknecht, and Manish Kumar. 2022. "Current trends in production, morphology, and real-world environmental applications of biochar for the promotion of sustainability." *Bioresource Technology* 359: 127467. https://doi.org/https://doi.org/10.1016/j.biortech.2022.127467. https://www.sciencedirect.com/science/article/pii/S0960852422007969.
Uddin, Kutub, Animesh Pal, and Bidyut Baran Saha. 2020. "Improved CO2 adsorption onto chemically activated spherical phenol resin." *Journal of CO2 Utilization* 41: 101255. https://doi.org/https://doi.org/10.1016/j.jcou.2020.101255. https://www.sciencedirect.com/science/article/pii/S2212982020305515.
Valdés, Héctor, Andrés L. Riquelme, Víctor A. Solar, Federico Azzolina-Jury, and Frédéric Thibault-Starzyk. 2021. "Removal of chlorinated volatile organic compounds onto natural and Cu-modified zeolite: The role of chemical surface characteristics in the adsorption mechanism." *Separation and Purification Technology* 258: 118080. https://doi.org/https://doi.org/10.1016/j.seppur.2020.118080. https://www.sciencedirect.com/science/article/pii/S1383586620325533.
Vardoulakis, Sotiris, Evanthia Giagloglou, Susanne Steinle, Alice Davis, Anne Sleeuwenhoek, Karen S. Galea, Ken Dixon, and Joanne O. Crawford. 2020. Indoor Exposure to Selected Air Pollutants in the Home Environment: A Systematic Review. *International Journal of Environmental Research and Public Health* 17 (23). https://doi.org/10.3390/ijerph17238972.
Vega, Esther, Jesús Lemus, Alba Anfruns, Rafael Gonzalez-Olmos, José Palomar, and María J. Martin. 2013. "Adsorption of volatile sulphur compounds onto modified activated carbons: Effect of oxygen functional groups." *Journal of Hazardous Materials* 258-259: 77-83. https://doi.org/https://doi.org/10.1016/j.jhazmat.2013.04.043. https://www.sciencedirect.com/science/article/pii/S0304389413002987.
Vellingiri, Kowsalya, Pawan Kumar, Akash Deep, and Ki-Hyun Kim. 2017. "Metal-organic frameworks for the adsorption of gaseous toluene under ambient temperature and pressure." *Chemical Engineering Journal* 307: 1116-1126.

https://doi.org/https://doi.org/10.1016/j.cej.2016.09.012. https://www.sciencedirect.com/science/article/pii/S1385894716312499.
Verma, Vishal Kumar, Senthilmurugan Subbiah, and Sri Harsha Kota. 2019. "Sericin-coated polyester based air-filter for removal of particulate matter and volatile organic compounds (BTEX) from indoor air." *Chemosphere* 237: 124462. https://doi.org/https://doi.org/10.1016/j.chemosphere.2019.124462. https://www.sciencedirect.com/science/article/pii/S0045653519316868.
Vikrant, Kumar, Ki-Hyun Kim, Wanxi Peng, Shengbo Ge, and Yong Sik Ok. 2020. "Adsorption performance of standard biochar materials against volatile organic compounds in air: A case study using benzene and methyl ethyl ketone." *Chemical Engineering Journal* 387: 123943. https://doi.org/https://doi.org/10.1016/j.cej.2019.123943. https://www.sciencedirect.com/science/article/pii/S1385894719333583.
Vilardi, Giorgio, Claudia Bassano, Paolo Deiana, and Nicola Verdone. 2020. "Exergy and energy analysis of biogas upgrading by pressure swing adsorption: Dynamic analysis of the process." *Energy Conversion and Management* 226: 113482. https://doi.org/https://doi.org/10.1016/j.enconman.2020.113482. https://www.sciencedirect.com/science/article/pii/S0196890420310141.
Virdis, Thomas, Christophe Walgraeve, Angelos Ioannidis, Herman Van Langenhove, and Joeri F. M. Denayer. 2021. "Multi-component ppm level adsorption of VOCs on the ZIF-8 and UiO-66 MOFs: Breakthrough analysis with selected ion flow tube mass spectrometry." *Journal of Environmental Chemical Engineering* 9 (6): 106568. https://doi.org/https://doi.org/10.1016/j.jece.2021.106568. https://www.sciencedirect.com/science/article/pii/S2213343721015451.
Wan, Jiang, Lin Liu, Khurram Shahzad Ayub, Wei Zhang, Genxiang Shen, Shuangqing Hu, and Xiaoyong Qian. 2020. "Characterization and adsorption performance of biochars derived from three key biomass constituents." *Fuel* 269: 117142. https://doi.org/https://doi.org/10.1016/j.fuel.2020.117142. https://www.sciencedirect.com/science/article/pii/S001623612030137X.
Wang, Chenpeng, Hang Yin, Pengjie Tian, Xuejiao Sun, Xiaoyang Pan, Kongfa Chen, Wen-Jie Chen, Qi-Hui Wu, and Shuiyuan Luo. 2020. "Remarkable adsorption performance of MOF-199 derived porous carbons for benzene vapor." *Environmental Research* 184: 109323. https://doi.org/https://doi.org/10.1016/j.envres.2020.109323. https://www.sciencedirect.com/science/article/pii/S0013935120302164.
Wang, Dongfang, Guiping Wu, Yufeng Zhao, Longzhe Cui, Chul-Ho Shin, Moon-Hee Ryu, Junxiong %J Environmental Science Cai, and Pollution Research. 2018. "Study on the copper (II)-doped MIL-101 (Cr) and its performance in VOCs adsorption." 25 (28): 28109-28119.
Wang, Jianlong, and Xuan Guo. 2020. "Adsorption isotherm models: Classification, physical meaning, application and solving method." *Chemosphere* 258: 127279. https://doi.org/https://doi.org/10.1016/j.chemosphere.2020.127279. https://www.sciencedirect.com/science/article/pii/S0045653520314727.
Wang, Jiaxing, Yaseen Muhammad, Zhu Gao, Syed Jalil Shah, Shuangxi Nie, Lihan Kuang, Zhongxing Zhao, Zhiwei Qiao, and Zhenxia Zhao. 2021. "Implanting polyethylene glycol into MIL-101(Cr) as hydrophobic barrier for enhancing toluene adsorption under highly humid environment." *Chemical Engineering Journal* 404: 126562.

https://doi.org/https://doi.org/10.1016/j.cej.2020.126562. https://www.sciencedirect.com/science/article/pii/S1385894720326905.
Wang, Jiong, Dominic Yellezuome, Zhiyi Zhang, Shengyong Liu, Jie Lu, Pin Zhang, Shuqing Zhang, Ping Wen, Md Maksudur Rahman, Chong Li, and Junmeng Cai. 2022. "Understanding pyrolysis mechanisms of pinewood sawdust and sugarcane bagasse from kinetics and thermodynamics." *Industrial Crops and Products* 177: 114378. https://doi.org/https://doi.org/10.1016/j.indcrop.2021.114378. https://www.sciencedirect.com/science/article/pii/S0926669021011432.
Wang, M., A. Lawal, P. Stephenson, J. Sidders, and C. Ramshaw. 2011. "Post-combustion CO2 capture with chemical absorption: A state-of-the-art review." *Chemical Engineering Research and Design* 89 (9): 1609-1624. https://doi.org/https://doi.org/10.1016/j.cherd.2010.11.005. https://www.sciencedirect.com/science/article/pii/S0263876210003345.
Wang, Ruimeng, Xinqi Luan, Jingyu Bao, Yaseen Muhammad, Syed Jalil Shah, Guanchen Wang, Jing Li, Guoyou Lin, Hongbing Ji, and Zhenxia Zhao. 2023. "Cr-N bridged MIL-101@tubular calcined N-doped polymer enhanced adsorption of vaporous toluene under high humidity." *Separation and Purification Technology* 305: 122540. https://doi.org/https://doi.org/10.1016/j.seppur.2022.122540. https://www.sciencedirect.com/science/article/pii/S1383586622020962.
Wang, Shanshan, Liangliang Huang, Yumeng Zhang, Licheng Li, and Xiaohua Lu. 2021. "A mini-review on the modeling of volatile organic compound adsorption in activated carbons: Equilibrium, dynamics, and heat effects." *Chinese Journal of Chemical Engineering* 31: 153-163. https://doi.org/https://doi.org/10.1016/j.cjche.2020.11.018. https://www.sciencedirect.com/science/article/pii/S100495412030690X.
Wang, Yi, Ya-Jie Hu, Xiang Hao, Pai Peng, Jun-You Shi, Feng Peng, and Run-Cang Sun. 2020. "Hydrothermal synthesis and applications of advanced carbonaceous materials from biomass: a review." *Advanced Composites and Hybrid Materials* 3 (3): 267-284. https://doi.org/10.1007/s42114-020-00158-0. https://doi.org/10.1007/s42114-020-00158-0.
Wang, Yunjia, Yanning Su, Lijuan Yang, Min Su, Ye Niu, Yin Liu, Hanxue Sun, Zhaoqi Zhu, Weidong Liang, and An Li. 2022. "Highly efficient removal of PM and VOCs from air by a self-supporting bifunctional conjugated microporous polymers membrane." *Journal of Membrane Science* 659: 120728. https://doi.org/https://doi.org/10.1016/j.memsci.2022.120728. https://www.sciencedirect.com/science/article/pii/S0376738822004732.
Wang, Ziheng, Majid Sedighi, and Amanda Lea-Langton. 2020. "Filtration of microplastic spheres by biochar: removal efficiency and immobilisation mechanisms." *Water Research* 184: 116165. https://doi.org/https://doi.org/10.1016/j.watres.2020.116165. https://www.sciencedirect.com/science/article/pii/S0043135420307028.
Wang, Zijian, Liying Liu, Guo Tian, Tingsheng Ren, Zhi Qi, and Gang Kevin Li. 2023. "Effect of isopropanol on CO2 capture by activated carbon: Adsorption performance and regeneration capacity." *Chemical Engineering Research and Design* 196: 632-641. https://doi.org/https://doi.org/10.1016/j.cherd.2023.06.056. https://www.sciencedirect.com/science/article/pii/S0263876223004173.

Wickramaratne, Nilantha P, and Mietek %J Journal of Materials Chemistry A Jaroniec. 2013. "Importance of small micropores in CO 2 capture by phenolic resin-based activated carbon spheres." 1 (1): 112-116.
Xian, Shikai, Ying Yu, Jing Xiao, Zhijuan Zhang, Qibin Xia, Haihui Wang, and Zhong Li. 2015. "Competitive adsorption of water vapor with VOCs dichloroethane, ethyl acetate and benzene on MIL-101(Cr) in humid atmosphere." *RSC Advances* 5 (3): 1827-1834. https://doi.org/10.1039/C4RA10463C. http://dx.doi.org/10.1039/C4RA10463C.
Xiang, Wei, Yongshan Wan, Xueyang Zhang, Zhenzhen Tan, Tongtong Xia, Yulin Zheng, and Bin Gao. 2020. "Adsorption of tetracycline hydrochloride onto ball-milled biochar: Governing factors and mechanisms." *Chemosphere* 255: 127057. https://doi.org/https://doi.org/10.1016/j.chemosphere.2020.127057. https://www.sciencedirect.com/science/article/pii/S0045653520312509.
Xiang, Wei, Xueyang Zhang, Kuiqing Chen, June Fang, Feng He, Xin Hu, Daniel C. W. Tsang, Yong Sik Ok, and Bin Gao. 2020. "Enhanced adsorption performance and governing mechanisms of ball-milled biochar for the removal of volatile organic compounds (VOCs)." *Chemical Engineering Journal* 385: 123842. https://doi.org/https://doi.org/10.1016/j.cej.2019.123842. https://www.sciencedirect.com/science/article/pii/S1385894719332577.
Xiang, Wei, Xueyang Zhang, Junpeng Luo, Ying Li, Tingting Guo, and Bin Gao. 2022. "Performance of lignin impregnated biochar on tetracycline hydrochloride adsorption: Governing factors and mechanisms." *Environmental Research* 215: 114339. https://doi.org/https://doi.org/10.1016/j.envres.2022.114339. https://www.sciencedirect.com/science/article/pii/S0013935122016668.
Xie, Tao, Krishna R. Reddy, Chengwen Wang, Erin Yargicoglu, and Kurt Spokas. 2015. "Characteristics and Applications of Biochar for Environmental Remediation: A Review." *Critical Reviews in Environmental Science and Technology* 45 (9): 939-969. https://doi.org/10.1080/10643389.2014.924180. https://doi.org/10.1080/10643389.2014.924180.
Xie, Zunyuan, Feng Wang, Ning Zhao, Wei Wei, and Yuhan Sun. 2011. "Hydrophobisation of activated carbon fiber and the influence on the adsorption selectivity towards carbon disulfide." *Applied Surface Science* 257 (8): 3596-3602. https://doi.org/https://doi.org/10.1016/j.apsusc.2010.11.085. https://www.sciencedirect.com/science/article/pii/S0169433210016089.
Xin-hui, Duan, C Srinivasakannan, and Liang %J Journal of the Taiwan Institute of chemical engineers Jin-sheng. 2014. "Process optimization of thermal regeneration of spent coal based activated carbon using steam and application to methylene blue dye adsorption." 45 (4): 1618-1627.
Xiong, Juan, Jinling Xu, Mengge Zhou, Wei Zhao, Chang Chen, Mingxia Wang, Wenfeng Tan, and Luuk Koopal. 2021. "Quantitative Characterization of the Site Density and the Charged State of Functional Groups on Biochar." *ACS Sustainable Chemistry & Engineering* 9 (6): 2600-2608. https://doi.org/10.1021/acssuschemeng.0c09051. https://doi.org/10.1021/acssuschemeng.0c09051.
Xiong, Zhang, Zhang Shihong, Yang Haiping, Shi Tao, Chen Yingquan, and Chen Hanping. 2013. "Influence of NH3/CO2 Modification on the Characteristic of Biochar and the CO2 Capture." *BioEnergy Research* 6 (4): 1147-1153. https://doi.org/10.1007/s12155-013-9304-9. https://doi.org/10.1007/s12155-013-9304-9.

Xu, Chao, Chang-Qing Ruan, Yunxiang Li, Jonas Lindh, and Maria Strømme. 2018. "High-Performance Activated Carbons Synthesized from Nanocellulose for CO2 Capture and Extremely Selective Removal of Volatile Organic Compounds." *Advanced Sustainable Systems* 2 (2): 1700147. https://doi.org/https://doi.org/10.1002/adsu.201700147. https://doi.org/10.1002/adsu.201700147.

Xu, Xiang, Yang Guo, Rui Shi, Hongyu Chen, Yankun Du, Baogen Liu, Zheng Zeng, Ziyu Yin, and Liqing Li. 2021. "Natural Honeycomb-like structure cork carbon with hierarchical Micro-Mesopores and N-containing functional groups for VOCs adsorption." *Applied Surface Science* 565: 150550. https://doi.org/https://doi.org/10.1016/j.apsusc.2021.150550. https://www.sciencedirect.com/science/article/pii/S0169433221016202.

Xu, Xiaoyun, Yulin Zheng, Bin Gao, and Xinde Cao. 2019. "N-doped biochar synthesized by a facile ball-milling method for enhanced sorption of CO2 and reactive red." *Chemical Engineering Journal* 368: 564-572. https://doi.org/https://doi.org/10.1016/j.cej.2019.02.165. https://www.sciencedirect.com/science/article/pii/S1385894719304139.

Xu, Zhihua, Yuwei Zhou, Zhenhua Sun, Daofang Zhang, Yuanxing Huang, Siyi Gu, and Weifang Chen. 2020. "Understanding reactions and pore-forming mechanisms between waste cotton woven and FeCl3 during the synthesis of magnetic activated carbon." *Chemosphere* 241: 125120. https://doi.org/https://doi.org/10.1016/j.chemosphere.2019.125120. https://www.sciencedirect.com/science/article/pii/S0045653519323598.

Yaashikaa, P. R., P. Senthil Kumar, Sunita Varjani, and A. Saravanan. 2020. "A critical review on the biochar production techniques, characterization, stability and applications for circular bioeconomy." *Biotechnology Reports* 28: e00570. https://doi.org/https://doi.org/10.1016/j.btre.2020.e00570. http://www.sciencedirect.com/science/article/pii/S2215017X20300023.

Yan, Lilong, Yue Liu, Yudan Zhang, Shuang Liu, Caixu Wang, Wanting Chen, Cong Liu, Zhonglin Chen, and Ying Zhang. 2020. "ZnCl2 modified biochar derived from aerobic granular sludge for developed microporosity and enhanced adsorption to tetracycline." *Bioresource Technology* 297: 122381. https://doi.org/https://doi.org/10.1016/j.biortech.2019.122381. https://www.sciencedirect.com/science/article/pii/S0960852419316116.

Yan, Qiangu, Jinghao Li, and Zhiyong Cai. 2021. "Preparation and characterization of chars and activated carbons from wood wastes." *Carbon Letters* 31 (5): 941-956. https://doi.org/10.1007/s42823-020-00205-2. https://doi.org/10.1007/s42823-020-00205-2.

Yan, Xueru, Stéphane Anguille, Marc Bendahan, and Philippe Moulin. 2019. "Ionic liquids combined with membrane separation processes: A review." *Separation and Purification Technology* 222: 230-253. https://doi.org/https://doi.org/10.1016/j.seppur.2019.03.103. https://www.sciencedirect.com/science/article/pii/S1383586618333938.

Yang, Cuiting, Guang Miao, Yunhong Pi, Qibin Xia, Junliang Wu, Zhong Li, and Jing Xiao. 2019. "Abatement of various types of VOCs by adsorption/catalytic oxidation: A review." *Chemical Engineering Journal* 370: 1128-1153. https://doi.org/https://doi.org/10.1016/j.cej.2019.03.232. https://www.sciencedirect.com/science/article/pii/S1385894719307041.

Yang, Fan, Shuaishuai Zhang, Yuqing Sun, Kui Cheng, Jiangshan Li, and Daniel C. W. Tsang. 2018. "Fabrication and characterization of hydrophilic corn stalk biochar-supported nanoscale zero-valent iron composites for efficient metal removal." *Bioresource Technology* 265: 490-497. https://doi.org/https://doi.org/10.1016/j.biortech.2018.06.029. https://www.sciencedirect.com/science/article/pii/S0960852418308083.

Yang, Tingting, Yingming Xu, Qingqing Huang, Yuebing Sun, Xuefeng Liang, Lin Wang, Xu Qin, and Lijie Zhao. 2021. "Adsorption characteristics and the removal mechanism of two novel Fe-Zn composite modified biochar for Cd(II) in water." *Bioresource Technology* 333: 125078. https://doi.org/https://doi.org/10.1016/j.biortech.2021.125078. https://www.sciencedirect.com/science/article/pii/S096085242100417X.

Yang, Xi, Honghong Yi, Xiaolong Tang, Shunzheng Zhao, Zhongyu Yang, Yueqiang Ma, Tiecheng Feng, and Xiaoxu Cui. 2018. "Behaviors and kinetics of toluene adsorption-desorption on activated carbons with varying pore structure." *Journal of Environmental Sciences* 67: 104-114. https://doi.org/https://doi.org/10.1016/j.jes.2017.06.032. https://www.sciencedirect.com/science/article/pii/S1001074217316108.

Yang, Xiaohu, Wenbin Wang, Shangsheng Feng, Linwen Jin, Tian Jian Lu, Yue Chai, and Qunli Zhang. 2016. "Thermal Analysis of Cold Storage: The Role of Porous Metal Foam." *Energy Procedia* 88: 566-573. https://doi.org/https://doi.org/10.1016/j.egypro.2016.06.079. https://www.sciencedirect.com/science/article/pii/S1876610216301436.

Yang, Yuxuan, Bingcheng Lin, Chen Sun, Minghui Tang, Shengyong Lu, Qunxing Huang, and Jianhua Yan. 2021. "Facile synthesis of tailored mesopore-enriched hierarchical porous carbon from food waste for rapid removal of aromatic VOCs." *Science of The Total Environment* 773: 145453. https://doi.org/https://doi.org/10.1016/j.scitotenv.2021.145453. https://www.sciencedirect.com/science/article/pii/S0048969721005210.

Yang, Yuxuan, Chen Sun, Qunxing Huang, and Jianhua Yan. 2022. "Hierarchical porous structure formation mechanism in food waste component derived N-doped biochar: Application in VOCs removal." *Chemosphere* 291: 132702. https://doi.org/https://doi.org/10.1016/j.chemosphere.2021.132702. https://www.sciencedirect.com/science/article/pii/S004565352103174X.

Yang, Yuxuan, Chen Sun, Bingcheng Lin, and Qunxing Huang. 2020. "Surface modified and activated waste bone char for rapid and efficient VOCs adsorption." *Chemosphere* 256: 127054. https://doi.org/https://doi.org/10.1016/j.chemosphere.2020.127054. https://www.sciencedirect.com/science/article/pii/S0045653520312479.

Yao, Xiaolong, Yao Liu, Tong Li, Tingting Zhang, Hailong Li, Wei Wang, Xianbao Shen, Feng Qian, and Zhiliang Yao. 2020. "Adsorption behavior of multicomponent volatile organic compounds on a citric acid residue waste-based activated carbon: Experiment and molecular simulation." *Journal of Hazardous Materials* 392: 122323. https://doi.org/https://doi.org/10.1016/j.jhazmat.2020.122323. https://www.sciencedirect.com/science/article/pii/S0304389420303113.

Yeboah, S. K., and J. Darkwa. 2016. "A critical review of thermal enhancement of packed beds for water vapour adsorption." *Renewable and Sustainable Energy Reviews* 58: 1500-1520. https://doi.org/https://doi.org/10.1016/j.rser.2015.12.134. https://www.sciencedirect.com/science/article/pii/S1364032115015178.

Yin, Tao, Xuan Meng, Linpeng Jin, Chao Yang, Naiwang Liu, and Li Shi. 2020. "Prepared hydrophobic Y zeolite for adsorbing toluene in humid environment." *Microporous and Mesoporous Materials* 305: 110327. https://doi.org/https://doi.org/10.1016/j.micromeso.2020.110327. https://www.sciencedirect.com/science/article/pii/S1387181120303309.

Yin, Tao, Xuan Meng, Sitan Wang, Xiaoyu Yao, Naiwang Liu, and Li Shi. 2022. "Study on the adsorption of low-concentration VOCs on zeolite composites based on chemisorption of metal-oxides under dry and wet conditions." *Separation and Purification Technology* 280: 119634. https://doi.org/https://doi.org/10.1016/j.seppur.2021.119634. https://www.sciencedirect.com/science/article/pii/S1383586621013423.

Yoon, Young Hee, and James H Nelson. 1984. "Application of gas adsorption kinetics I. A theoretical model for respirator cartridge service life." *American industrial hygiene association journal* 45 (8): 509-516.

Yu, Cheng-Hsiu, Chih-Hung Huang, Chung-Sung %J Aerosol Tan, and Air Quality Research. 2012. "A review of CO2 capture by absorption and adsorption." 12 (5): 745-769.

Yu, Kaifeng, Jingjing Wang, Xiaofeng Wang, Jicai Liang, and Ce Liang. 2020. "Sustainable application of biomass by-products: Corn straw-derived porous carbon nanospheres using as anode materials for lithium ion batteries." *Materials Chemistry and Physics* 243: 122644. https://doi.org/https://doi.org/10.1016/j.matchemphys.2020.122644. https://www.sciencedirect.com/science/article/pii/S0254058420300262.

Yu, Lian, Long Wang, Weicheng Xu, Limin Chen, Mingli Fu, Junliang Wu, and Daiqi Ye. 2018. "Adsorption of VOCs on reduced graphene oxide." *Journal of Environmental Sciences* 67: 171-178. https://doi.org/https://doi.org/10.1016/j.jes.2017.08.022. https://www.sciencedirect.com/science/article/pii/S1001074217309877.

Yu, Shujun, Xiangxue Wang, Yuejie Ai, Xiaoli Tan, Tasawar Hayat, Wenping Hu, and Xiangke Wang. 2016. "Experimental and theoretical studies on competitive adsorption of aromatic compounds on reduced graphene oxides." *Journal of Materials Chemistry A* 4 (15): 5654-5662. https://doi.org/10.1039/C6TA00890A. http://dx.doi.org/10.1039/C6TA00890A.

Yu, Wenchao, Fei Lian, Guannan Cui, and Zhongqi Liu. 2018. "N-doping effectively enhances the adsorption capacity of biochar for heavy metal ions from aqueous solution." *Chemosphere* 193: 8-16. https://doi.org/https://doi.org/10.1016/j.chemosphere.2017.10.134. https://www.sciencedirect.com/science/article/pii/S0045653517317125.

Yuan, Min, Meizhen Gao, Qi Shi, and Jinxiang Dong. 2020. "Understanding the characteristics of water adsorption in zeolitic imidazolate framework-derived porous carbon materials." *Chemical Engineering Journal* 379: 122412. https://doi.org/https://doi.org/10.1016/j.cej.2019.122412. https://www.sciencedirect.com/science/article/pii/S1385894719318157.

Zare, Karim, Vinod Kumar Gupta, Omid Moradi, Abdel Salam Hamdy Makhlouf, Mika Sillanpää, Mallikarjuna N. Nadagouda, Hamidreza Sadegh, Ramin Shahryari-Ghoshekandi, Angshuman Pal, and Zhou-jun Wang. 2015. "A comparative study on the basis of adsorption capacity between CNTs and activated carbon as adsorbents for removal of noxious synthetic dyes: a review." *Journal of nanostructure in chemistry* 5 (2): 227-236.

Zeng, Shengquan, Yong-Keun Choi, and Eunsung Kan. 2021. "Iron-activated bermudagrass-derived biochar for adsorption of aqueous sulfamethoxazole: Effects of iron impregnation

ratio on biochar properties, adsorption, and regeneration." *Science of The Total Environment* 750: 141691. https://doi.org/https://doi.org/10.1016/j.scitotenv.2020.141691. https://www.sciencedirect.com/science/article/pii/S0048969720352207.
Zeng, Shengquan, Yong-Keun Choi, and Eunsung %J Science of the Total Environment Kan. 2021. "Iron-activated bermudagrass-derived biochar for adsorption of aqueous sulfamethoxazole: effects of iron impregnation ratio on biochar properties, adsorption, and regeneration." 750: 141691.
Zhang, Dawei, Kejing Zhang, Xiaolan Hu, Qianqian He, Jinpeng Yan, and Yingwen Xue. 2021. "Cadmium removal by MgCl2 modified biochar derived from crayfish shell waste: Batch adsorption, response surface analysis and fixed bed filtration." *Journal of Hazardous Materials* 408: 124860. https://doi.org/https://doi.org/10.1016/j.jhazmat.2020.124860. https://www.sciencedirect.com/science/article/pii/S030438942032851X.
Zhang, Guangxin, Yangyu Liu, Shuilin Zheng, and Zaher Hashisho. 2019. "Adsorption of volatile organic compounds onto natural porous minerals." *Journal of Hazardous Materials* 364: 317-324. https://doi.org/https://doi.org/10.1016/j.jhazmat.2018.10.031. https://www.sciencedirect.com/science/article/pii/S0304389418309403.
Zhang, Ruihuan, Maosheng Zhong, Lin Jiang, Quankai Fu, Shijie Wang, Wenyu Zhang, Xiaoyan Li, and Lin Ma. 2022. "Effect of vapour-solid interfacial adsorption on benzene multiphase partition and its implication to vapour exposure assessment of contaminated soil in arid area." *Journal of Environmental Management* 315: 115182. https://doi.org/https://doi.org/10.1016/j.jenvman.2022.115182. https://www.sciencedirect.com/science/article/pii/S0301479722007551.
Zhang, Shaowen, Yilong Lin, Qing Li, Xiaoqi Jiang, Zhiwei Huang, Xiaomin Wu, Huawang Zhao, Guohua Jing, and Huazhen Shen. 2022. "Remarkable performance of N-doped carbonization modified MIL-101 for low-concentration benzene adsorption." *Separation and Purification Technology* 289: 120784. https://doi.org/https://doi.org/10.1016/j.seppur.2022.120784. https://www.sciencedirect.com/science/article/pii/S1383586622003434.
Zhang, Tengyan, Walter P. Walawender, L. T. Fan, Maohong Fan, Daren Daugaard, and R. C. Brown. 2004. "Preparation of activated carbon from forest and agricultural residues through CO2 activation." *Chemical Engineering Journal* 105 (1): 53-59. https://doi.org/https://doi.org/10.1016/j.cej.2004.06.011. https://www.sciencedirect.com/science/article/pii/S1385894704003080.
Zhang, Weiping, Guiying Li, Huajie Yin, Kun Zhao, Huijun Zhao, and Taicheng An. 2022. "Adsorption and desorption mechanism of aromatic VOCs onto porous carbon adsorbents for emission control and resource recovery: recent progress and challenges." *Environmental Science: Nano* 9 (1): 81-104. https://doi.org/10.1039/D1EN00929J. http://dx.doi.org/10.1039/D1EN00929J.
Zhang, Xiaodong, Yang Yang, Liang Song, Jinfeng Chen, Yiqiong Yang, and Yuxin Wang. 2019. "Enhanced adsorption performance of gaseous toluene on defective UiO-66 metal organic framework: Equilibrium and kinetic studies." *Journal of Hazardous Materials* 365: 597-605. https://doi.org/https://doi.org/10.1016/j.jhazmat.2018.11.049. https://www.sciencedirect.com/science/article/pii/S0304389418310689.
Zhang, Xinmin, Wenjuan Zhao, Lei Nie, Xia Shao, Hongyan Dang, Weiqi Zhang, and Di Wang. 2021. "A new classification approach to enhance future VOCs emission policies: Taking

solvent-consuming industry as an example." *Environmental Pollution* 268: 115868. https://doi.org/https://doi.org/10.1016/j.envpol.2020.115868. https://www.sciencedirect.com/science/article/pii/S026974912036557X.

Zhang, Xiong, Shihong Zhang, Haiping Yang, Ye Feng, Yingquan Chen, Xianhua Wang, and Hanping Chen. 2014. "Nitrogen enriched biochar modified by high temperature CO2–ammonia treatment: Characterization and adsorption of CO2." *Chemical Engineering Journal* 257: 20-27. https://doi.org/https://doi.org/10.1016/j.cej.2014.07.024. https://www.sciencedirect.com/science/article/pii/S1385894714009036.

Zhang, Xueyang, Lingyu Cao, Wei Xiang, Yue Xu, and Bin Gao. 2022. "Preparation and evaluation of fine-tuned micropore biochar by lignin impregnation for CO2 and VOCs adsorption." *Separation and Purification Technology* 295: 121295. https://doi.org/https://doi.org/10.1016/j.seppur.2022.121295. https://www.sciencedirect.com/science/article/pii/S1383586622008528.

Zhang, Xueyang, Bin Gao, Anne Elise Creamer, Chengcheng Cao, and Yuncong Li. 2017. "Adsorption of VOCs onto engineered carbon materials: A review." *Journal of Hazardous Materials* 338: 102-123. https://doi.org/https://doi.org/10.1016/j.jhazmat.2017.05.013. https://www.sciencedirect.com/science/article/pii/S0304389417303564.

Zhang, Xueyang, Bin Gao, Anne Elise Creamer, Chengcheng Cao, and Yuncong %J Journal of hazardous materials Li. 2017a. "Adsorption of VOCs onto engineered carbon materials: A review." 338: 102-123.

Zhang, Xueyang, Bin Gao, June Fang, Weixin Zou, Lin Dong, Chengcheng Cao, Jian Zhang, Yuncong Li, and Hailong Wang. 2019. "Chemically activated hydrochar as an effective adsorbent for volatile organic compounds (VOCs)." *Chemosphere* 218: 680-686. https://doi.org/https://doi.org/10.1016/j.chemosphere.2018.11.144. https://www.sciencedirect.com/science/article/pii/S0045653518322501.

Zhang, Xueyang, Xudong Miao, Wei Xiang, Jiankun Zhang, Chengcheng Cao, Hailong Wang, Xin Hu, and Bin Gao. 2021. "Ball milling biochar with ammonia hydroxide or hydrogen peroxide enhances its adsorption of phenyl volatile organic compounds (VOCs)." *Journal of Hazardous Materials* 403: 123540. https://doi.org/https://doi.org/10.1016/j.jhazmat.2020.123540. https://www.sciencedirect.com/science/article/pii/S0304389420315260.

Zhang, Yu, Zan Zhu, Wei-Ning Wang, and Sheng-Chieh Chen. 2022. "Mitigating the relative humidity effects on the simultaneous removal of VOCs and PM2.5 of a metal–organic framework coated electret filter." *Separation and Purification Technology* 285: 120309. https://doi.org/https://doi.org/10.1016/j.seppur.2021.120309. https://www.sciencedirect.com/science/article/pii/S138358662102013X.

Zhang, Yuxiu, Chaohai Wei, and Bo Yan. 2019. "Emission characteristics and associated health risk assessment of volatile organic compounds from a typical coking wastewater treatment plant." *Science of The Total Environment* 693: 133417. https://doi.org/https://doi.org/10.1016/j.scitotenv.2019.07.223. https://www.sciencedirect.com/science/article/pii/S0048969719333376.

Zhao, Bin, David O'Connor, Junli Zhang, Tianyue Peng, Zhengtao Shen, Daniel C. W. Tsang, and Deyi Hou. 2018. "Effect of pyrolysis temperature, heating rate, and residence time on rapeseed stem derived biochar." *Journal of Cleaner Production* 174: 977-987.

https://doi.org/https://doi.org/10.1016/j.jclepro.2017.11.013. https://www.sciencedirect.com/science/article/pii/S0959652617326641.
Zhao, Fengxiao, Rui Shan, Wenjian Li, Yuyuan Zhang, Haoran Yuan, and Yong Chen. 2021. "Synthesis, Characterization, and Dye Removal of ZnCl2-Modified Biochar Derived from Pulp and Paper Sludge." *ACS Omega* 6 (50): 34712-34723. https://doi.org/10.1021/acsomega.1c05142. https://doi.org/10.1021/acsomega.1c05142.
Zhao, Qiangyu, Quanxin Du, Yang Yang, Ziyu Zhao, Jie Cheng, Fukun Bi, Xiaoyu Shi, Jingcheng Xu, and Xiaodong Zhang. 2022. "Effects of regulator ratio and guest molecule diffusion on VOCs adsorption by defective UiO-67: Experimental and theoretical insights." *Chemical Engineering Journal* 433: 134510. https://doi.org/https://doi.org/10.1016/j.cej.2022.134510. https://www.sciencedirect.com/science/article/pii/S1385894722000183.
Zhao, Xiaoyan, Xiang Li, Tianle Zhu, and Xiaolong Tang. 2018. "Adsorption behavior of chloroform, carbon disulfide, and acetone on coconut shell-derived carbon: experimental investigation, simulation, and model study." *Environmental Science and Pollution Research* 25 (31): 31219-31229. https://doi.org/10.1007/s11356-018-3103-y. https://doi.org/10.1007/s11356-018-3103-y.
Zhao, Ya-Ting, Li-Qing Yu, Xin Xia, Xin-Yu Yang, Wei Hu, and Yun-Kai %J Analytical Methods Lv. 2018. "Evaluation of the adsorption and desorption properties of zeolitic imidazolate framework-7 for volatile organic compounds through thermal desorption-gas chromatography." 10 (40): 4894-4901.
Zhao, Zhipeng, Bing Wang, Benny K. G. Theng, Xinqing Lee, Xueyang Zhang, Miao Chen, and Peng Xu. 2022. "Removal performance, mechanisms, and influencing factors of biochar for air pollutants: a critical review." *Biochar* 4 (1): 30. https://doi.org/10.1007/s42773-022-00156-z. https://doi.org/10.1007/s42773-022-00156-z.
Zhen, Hanfei, Steven M. J. Jang, W. K. Teo, and K. Li. 2006. "Modified silicone–PVDF composite hollow-fiber membrane preparation and its application in VOC separation." *Journal of Applied Polymer Science* 99 (5): 2497-2503. https://doi.org/https://doi.org/10.1002/app.22860. https://doi.org/10.1002/app.22860.
Zheng, Chenghang, Jiali Shen, Yongxin Zhang, Weiwei Huang, Xinbo Zhu, Xuecheng Wu, Linghong Chen, Xiang Gao, and Kefa Cen. 2017. "Quantitative assessment of industrial VOC emissions in China: Historical trend, spatial distribution, uncertainties, and projection." *Atmospheric Environment* 150: 116-125. https://doi.org/https://doi.org/10.1016/j.atmosenv.2016.11.023. https://www.sciencedirect.com/science/article/pii/S1352231016308962.
Zheng, Xianming, Shuai Liu, Sadia Rehman, Zehui Li, and Pengyi Zhang. 2020. "Highly improved adsorption performance of metal-organic frameworks CAU-1 for trace toluene in humid air via sequential internal and external surface modification." *Chemical Engineering Journal* 389: 123424. https://doi.org/https://doi.org/10.1016/j.cej.2019.123424. https://www.sciencedirect.com/science/article/pii/S1385894719328372.
Zhou, Dong, Zeqing Lan, Wenzhu Cao, Yuzhou Chen, Shushen Zhang, Jianyang Hu, Jianyu Shang, Zenghui Peng, and Yongjun Liu. 2022. "Liquid crystal optical fiber sensor based on misaligned core configuration for temperature and mixed volatile organic compound detection." *Optics & Laser Technology* 156: 108545.

https://doi.org/https://doi.org/10.1016/j.optlastec.2022.108545. https://www.sciencedirect.com/science/article/pii/S0030399222006958.
Zhou, Qiying, Xia Jiang, Xi Li, Charles Qiang Jia, and Wenju Jiang. 2018. "Preparation of high-yield N-doped biochar from nitrogen-containing phosphate and its effective adsorption for toluene." *RSC advances* 8 (53): 30171-30179.
Zhou, Shangwen, Dongxiao Zhang, Hongyan Wang, and Xiaohan Li. 2019. "A modified BET equation to investigate supercritical methane adsorption mechanisms in shale." *Marine and Petroleum Geology* 105: 284-292. https://doi.org/https://doi.org/10.1016/j.marpetgeo.2019.04.036. https://www.sciencedirect.com/science/article/pii/S0264817219301862.
Zhu, Lina, Lingjun Meng, Jiaqi Shi, Jinhai Li, Xuesheng Zhang, and Mingbao %J Journal of environmental management Feng. 2019. "Metal-organic frameworks/carbon-based materials for environmental remediation: A state-of-the-art mini-review." 232: 964-977.
Zhu, Lingli, Dekui Shen, and Kai Hong Luo. 2020. "A critical review on VOCs adsorption by different porous materials: Species, mechanisms and modification methods." *Journal of Hazardous Materials* 389: 122102. https://doi.org/https://doi.org/10.1016/j.jhazmat.2020.122102. https://www.sciencedirect.com/science/article/pii/S0304389420300881.
Zhu, Lingli, Dekui Shen, and Kai Hong %J Journal of Hazardous Materials Luo. 2020. "A critical review on VOCs adsorption by different porous materials: Species, mechanisms and modification methods." 389: 122102.
Zhu, Meiping, Peng Hu, Zhangfa Tong, Zhongxing Zhao, and Zhenxia Zhao. 2017. "Enhanced hydrophobic MIL(Cr) metal-organic framework with high capacity and selectivity for benzene VOCs capture from high humid air." *Chemical Engineering Journal* 313: 1122-1131. https://doi.org/https://doi.org/10.1016/j.cej.2016.11.008. https://www.sciencedirect.com/science/article/pii/S1385894716315686.
Zhu, Rong, Qiongfen Yu, Ming Li, Hong Zhao, Shaoxuan Jin, Yaowei Huang, Jie Fan, and Jie Chen. 2021. "Analysis of factors influencing pore structure development of agricultural and forestry waste-derived activated carbon for adsorption application in gas and liquid phases: A review." *Journal of Environmental Chemical Engineering* 9 (5): 105905. https://doi.org/https://doi.org/10.1016/j.jece.2021.105905. https://www.sciencedirect.com/science/article/pii/S2213343721008824.
Zornoza, R., F. Moreno-Barriga, J. A. Acosta, M. A. Muñoz, and A. Faz. 2016. "Stability, nutrient availability and hydrophobicity of biochars derived from manure, crop residues, and municipal solid waste for their use as soil amendments." *Chemosphere* 144: 122-130. https://doi.org/https://doi.org/10.1016/j.chemosphere.2015.08.046. https://www.sciencedirect.com/science/article/pii/S0045653515300552.
Zou, Weixin, Bin Gao, Yong Sik Ok, and Lin Dong. 2019. "Integrated adsorption and photocatalytic degradation of volatile organic compounds (VOCs) using carbon-based nanocomposites: A critical review." *Chemosphere* 218: 845-859. https://doi.org/https://doi.org/10.1016/j.chemosphere.2018.11.175. https://www.sciencedirect.com/science/article/pii/S0045653518322823.
Zubbri, Nurul Azrin, Abdul Rahman Mohamed, Naoto Kamiuchi, and Maedeh Mohammadi. 2020. "Enhancement of CO2 adsorption on biochar sorbent modified by metal incorporation." *Environmental Science and Pollution Research* 27 (11): 11809-11829.

https://doi.org/10.1007/s11356-020-07734-3. https://doi.org/10.1007/s11356-020-07734-3.
Zubrik, Anton, Marek Matik, Eva Mačingová, Zuzana Danková, Dávid Jáger, Jaroslav Briančin, Libor Machala, Jiři Pechoušek, and Slavomír Hredzák. 2022. "The use of microwave irradiation for preparation and fast-acting regeneration of magnetic biochars." *Chemical Engineering and Processing - Process Intensification* 178: 109016. https://doi.org/https://doi.org/10.1016/j.cep.2022.109016. https://www.sciencedirect.com/science/article/pii/S0255270122002288.

ATTRIBUTION STATEMENT

We have made every reasonable attempt to acknowledge the copyright owners of the material used. If there are any copyright owners who have been unintentionally omitted or inaccurately acknowledged, we would appreciate hearing from you.

APPENDIX

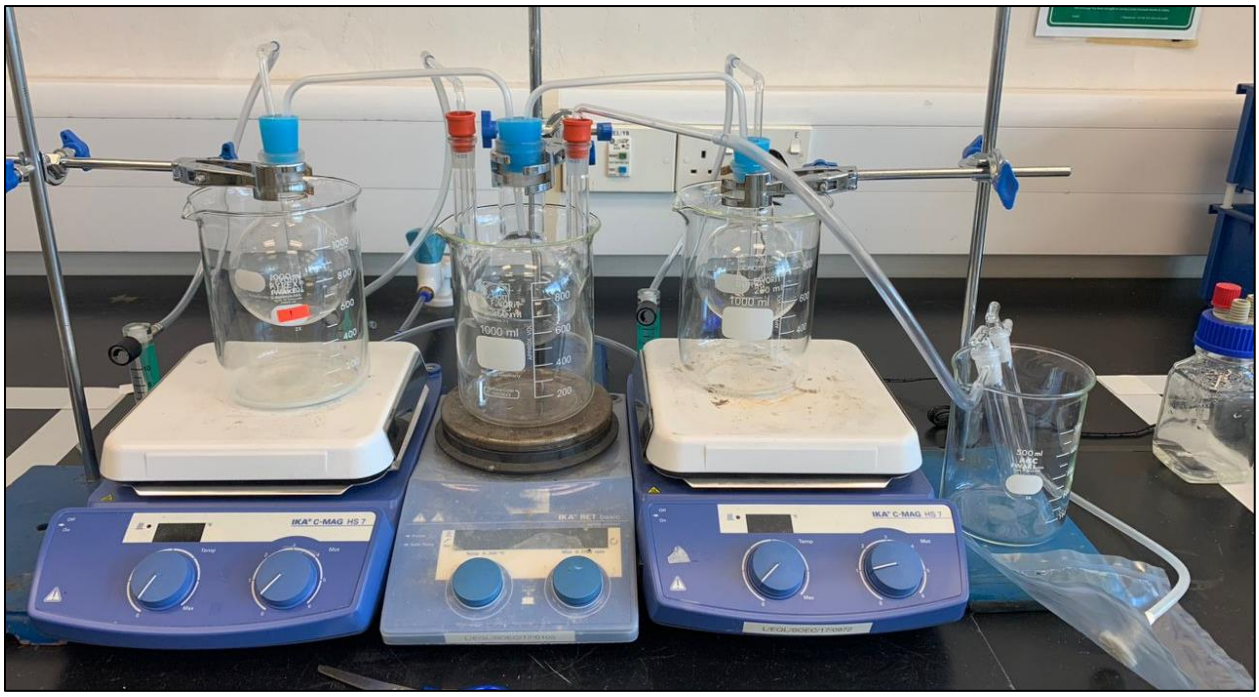

Figure 1: The actual photo of the acetone adsorption process.